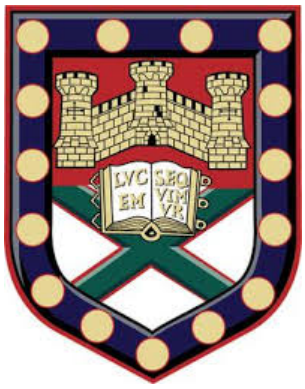

Resonant effects in weakly nonlinear geophysical fluid dynamics

Alexander Owen

January 7, 2019

Submitted by Alexander Owen, to the University of Exeter as a thesis for the degree of Doctor of Philosophy in Mathematics, January 2019.

Abstract

Many observed phenomena in geophysical systems, such as quasigeostrophy, and turbulence effects in rotating fluids, can be attributed to the resonances that emerge from multiple scale analysis. In this thesis the multiple scale method of asymptotic expansion is used to study resonant wave interactions in the context of quasigeostrophic geophysical systems, including and extending triad interactions. The one and two layer rotating shallow water equations and the equations for uniformly stratified fluid under the Boussinesq assumption are studied in detail, we evaluate their asymptotic expansions, and analyse their behaviour. Of particular interest is the expansion for the two layer equations, where we investigate a resonance not previously considered in the literature. We formulate general theory concerning the behaviour of the splitting of the dynamics into the fast and slow parts of the systems. We find that all layered shallow water type equations cannot have any interaction between a set of fast waves that produces a slow wave, regardless of whether they are resonant or non-resonant. In the stratified case we find that this is not true, although these interactions are constrained to a slow timescale.

Building on the resonant expansion, we then reformulate the expansions to allow the inclusion of near resonant interactions. We detail a new formulation of the near resonances as the representation of higher order interactions that are sufficiently fast acting to be included at the triad order of interaction. We then demonstrate the effectiveness of this near resonant expansion by direct numerical simulation and evaluation of the rotating shallow water equations. We derive qualitatively different behaviour, found analytically in the near resonant expansion of the stratified equations, showing that many higher order interactions not accessible in the layered equations are possible in the stratified case.

Finally we consider the expansions in the wavepacket framework, with the introduction of multiple spatial scales. We find that consideration of the magnitude of the difference between the group velocities of component wavepackets in a quartet interaction is sufficient to derive the higher order behaviour previously found by other methods in the literature. It then follows from this that the near resonant expansion can contain many types of interaction that are not possible between

wavepackets if only exact resonances are considered.

Contents

1 Introduction **17**

1.1 Historical background 23

1.2 Thesis outline 27

2 Equations of Motion **29**

2.1 Derivations of the fluid systems 30

2.1.1 Shallow water equations 30

2.1.2 Two layer shallow water equations 32

2.1.3 Uniformly stratified Equations 33

2.2 Conservation Laws 35

2.2.1 Ertel Potential Vorticity 35

2.2.2 Potential Vorticity and Enstrophy 39

2.2.3 Energy conservation 42

2.3 Eigenvector formulation 44

2.3.1 Rotating shallow water equations 44

2.3.2 Two layer rotating shallow water equations 47

2.3.3 Stratified equations 50

2.4 Chapter summary 53

3 Multiscale asymptotic expansion **55**

3.1 Weakly nonlinear limit 55

3.2 Expansion to triad order 56

3.3 Expansion to quartet order 59

3.4 Above quartet order 63

3.5 Chapter summary 66

4 Applications to rotating stratified flows **67**

4.1 The quasigeostrophic limit 68

4.1.1 Rotating shallow water equations 68

4.1.2 Two layer Rotating shallow water equations 69

4.1.3 Stratified equations 71

4.2 Rotating Shallow Water Equations 72

4.2.1 Nonlinear Interaction coefficient 73

4.2.2 Higher Order theory 75

4.3 Two Layer Rotating Shallow Water Equations 78

4.3.1 Interaction coefficients 79

4.3.2 Fast-fast-fast Resonances 81

4.3.3 Comparative strength of resonances 88

4.3.4 Discussion 89

4.3.5 Higher Order theory 92

4.4 Alternative method of expansion using conservation laws 92

4.4.1 Higher order expansion 94

4.5 Stratified Equations 96

4.5.1 Nonlinear Interaction Coefficient 97

4.6 Chapter summary 100

5 Near resonant expansion **103**

5.1 Triad order expansion 103

5.1.1 Slaved modes 106

5.1.2 Near resonances 107

5.1.3 Super-near resonances 108

5.2 Quartet Order expansion 109

5.2.1 Continuation of the near resonant part of the expansion 112

5.3 Expansion to arbitrary order 113

5.3.1 Near resonances 114

5.3.2 Splitting of n-tets in the near resonant part 115

5.4 Overview of expansion structure 115

5.4.1 Caveats 117

5.5 Chapter summary 118

6 Applications of the near resonant theory to rotating stratified flow **119**

6.1 One layer rotating shallow water equations 120

6.1.1 Numerical method 120

6.1.2 Initial conditions 120

6.1.3 Results 121

6.2 Stratified Equations 135

6.3 Chapter Summary 138

7 Wavepackets **141**

7.1 Derivation of a wavepacket 142

7.2 Multiple scale expansion in time and space 143

7.2.1 Structure of the wave envelope for a mode 145

7.3 Restrictions on wavepacket interactions between multiple packets 147

7.3.1 Slow mode input interactions 150

7.3.2 Mixed mode input interactions 150

7.3.3 Fast mode input interactions 151

7.3.4 A special case 151

7.4 Applications 153

7.4.1 Shallow water equations 153

7.4.2 Two layer rotating shallow water equations 153

7.4.3 Stratified equations 154

7.5 Chapter summary 154

8 Conclusions **155**

8.1 Summary 155

8.2 Discussion and Future work 157

A Appendix **159**

A.1 Big and Little O notation 159

A.2 Matrix Exponential 159

List of Tables

3.1 For given order of the equations, the timescale to which each order of the solution is considered is given. The timescales given in red are completely determined as they are simply derived from slaved modes and so their behaviour is inherited from the behaviour of $\boldsymbol{u}_0$ to the required timescale. 63

4.1 Size of the interaction coefficients for the given wavenumbers, chosen to form a resonant triad of fast-fast-fast modes and a near resonant triad for sets of fast-slow-fast modes. This shows that for the barotropic/baroclinic interactions the fast-fast-fast resonance is of similar magnitude to the fast-slow-fast one. However the dominant interactions will still be those occurring within a single vertical mode. Physical parameters used were as follows: $g = 10ms^{-2}$, $f = 0.0001s^{-1}$, $H_1 = 500m$, $H_2 = 4000m$, $L = 100/2\pi\ km$, the non-dimensional wavenumbers are quoted as $\boldsymbol{k}$ where the physical wavenumber is $\boldsymbol{k}/L$ and physical wavelength is $2\pi L/|\boldsymbol{k}|$. 90

List of Figures

1.1 The three cases: non-resonance (red), near resonance (green), and resonance (blue). For a timescale of around $t = 35s$ there is minor separation between the behaviours of the near and exact resonances, and so they can be treated similarly. 21

1.2 Wavenumber spacing affects the availability of near resonances. Here the dispersion relation linking k to ω is given by $\omega(k)$, which links the Δk spacing to the $\Delta\omega$ spacing. Dashed lines represent distinct ω values in the simulation, while the red area represents the area within which the near resonances lie, where the distance from a prescribed $\omega_1 + \omega_2$ is less than the given detuning. On the left with tighter spacing there are multiple near resonances, on the right with larger Δk there are no near resonances for the given detuning. 22

2.1 Diagram showing the set up of the one layer shallow water equations. 32

2.2 Diagram showing the set up of the two layer shallow water equations. 33

2.3 Diagram showing the direction of the group velocity (dashed) in the vertical plane of the wave vector but perpendicular to it due to the vertical component. 52

3.1 Quartet construction, as in Equation (3.31). The wave vector $\boldsymbol{k}_a$ takes the form of a slaved mode that can be projected onto our eigenbasis such that there are fast-like parts and a slow-like part. Each quartet has three possible sets of wavenumbers that can contribute to the quartet, ie $\boldsymbol{k}_a = \boldsymbol{k}_1 + \boldsymbol{k}_2$, $\boldsymbol{k}_b = \boldsymbol{k}_3 + \boldsymbol{k}_2$, and $\boldsymbol{k}_c = \boldsymbol{k}_1 + \boldsymbol{k}_3$. 62

3.2 Diagram of the n-tet construction, Two smaller N-tets, A&B of sizes $n - r + 2$ and $r + 1$ respectively, output the two modes a, and b that go into a connecting triad that returns the output mode with wavenumber $\boldsymbol{k}$. All possible combinations must be considered in a similar manner, summed, and then the coefficient symmetrised to give the equation in (3.34) 65

4.1 Graphical method to find possible resonant triads in the fast-fast-fast interactions. The dark hyperboloid is the manifold on which the ω_1 may lie (defined by the dispersion relation for $\boldsymbol{k}_1$), the light hyperboloid is centred around a chosen ω_1 in the first manifold. Any crossing point of the light and dark hyperboloids represents a possible resonance. 83

4.2 Projection onto wave space of the intersections of the surfaces in figure 4.1d showing the two sets of resonances. a) The non-rotating case equivalent to the diagram in Ball 1964, b) The case for large external Burgers number, and c) shows Burger number close to the critical value of the Burgers number such that the angle of incidence in the resonance must be small. 84

4.3 The quartic discriminant Δ for $R_2 = \{0, 0.25, 0.5, 0.75, 1, 1.25, 1.5, 1.75, 2\}$ represented as surfaces in parameter space $\{F^2, \theta\}$. Red shows values greater than 1, where there are 4 solutions and therefore the directional resonance (the resonance in figure 4.1d which can have limited angle of incidence between the waves) exists. 86

5.1 Diagram showing the definitions of the different terms. The size of Ω compared to ϵ determines the type of mode formed. When $\epsilon < \Omega_{min}$ the near resonances disappear and the non-resonances are identically slaved modes. 106

5.2 Diagram showing the super-near resonant splitting. All of the super-near resonant terms will be treated similarly to the exact resonances on the t_0 timescale. At the next timescale the largest of the super-near resonant terms will affect the motion, and so on for each timescale. 109

5.3 Quartet construction, as in equation (5.22). This figure is the same as figure 3.1, repeated here for convenience. The wavevector $\boldsymbol{k}_a$ takes the form of a slaved mode that can be projected onto our eigenbasis such that there are fast-like parts and a slow-like part. Each quartet has three possible slaved modes that can contribute to the quartet. 112

6.1 Distribution with time of the eigenmode amplitudes. Each graph shows the wavenumber $\boldsymbol{k}$ on the x and y axes, and the mode types α are $-, 0, +$ from left to right in the columns. Time increases downwards with graphs showing the distribution at 0s, 1s and 19s into the simulation. In the later times (on the triad timescale t_0) the output shows stimulated amplitudes in the zero modes close to $\boldsymbol{k} = (0, 0)$ that correspond to resonant interactions, and in the fast modes amplitudes increasing at $\boldsymbol{k} = (15n, 15n), n \in \mathbb{Z}$ that could only have been produced by near resonances as the fast-fast-fast interactions are never exactly resonant in the rotating shallow water equations. 122

6.2 Distribution with time of the log of the eigenmode amplitudes. The log scaling shows in much greater detail the distribution of energy amongst the different modes compared to fig 6.1. Many areas can be seen to have been stimulated, although on scales that correspond to the $\boldsymbol{u}_1$ parts of the expansion. With the log scaling in addition to what was visible in figure 6.1 the resonance between a slow mode and two fast modes with equal wavenumber modulus but different direction can be seen by the arcs of the circle forming close to $\boldsymbol{k} = (\pm 15, \pm 15)$ and $\boldsymbol{k} = (\pm 30, \pm 30)$. It is also clear that there is a complicated redistribution of a small amount of energy amongst the slow modes. 123

6.3 Distribution with time of specific eigenmode amplitudes. The amplitudes show how the energy of selected modes varies, with low wavenumber modes shown in the bottom row and higher wavenumbers in the top row. The left and right hand columns show the $\alpha = \pm$ fast modes respectively and the middle column shows the slow modes. In general the modes affected by the exact and near resonances show gradual changes on a slow timescale, whilst the amplitudes only involved in non-resonances show rapid oscillations but no sustained change. For example in the top right frame, the $\alpha = +$ modes, slow changes can be seen in mode $(15, 15, +)$, which is involved in a near resonant triad with several other modes, for example $(14, 16, +)$ and $(-1, 1, 0)$ (a close grid point to the exact resonance that forms the circular trace in figure 6.2), and $(15, 15, +)$ and $(30, 30, +)$ a near resonance that shows strong growth. In the bottom left frame the low wavenumber fast modes can be seen to oscillate rapidly with only minor sustained changes, a symptom of the lack of near or exact resonances affecting them. 124

6.4 Distribution with time of the log of specific eigenmode amplitudes. This figure follows the layout of fig 6.3 but on a log scale. On the log scale it can be seen clearly that rapidly oscillating amplitudes do not grow to the scales seen for the modes that do interact resonantly. 125

6.5 Diagram showing the regions referred to in the text, and the possible fast-slow-fast interactions of the input and double input wavelengths. 125

6.6 Distribution with time of the log of the eigenmode amplitudes. Time increases from top to bottom from $0s$, to $1s$, to $19s$. The central column shows the slow modes and the outside columns show the fast modes. In this simulation only the slow modes were included in the initial condition. In comparison to fig 6.2 there is no spread of energy to the higher wavenumber slow modes. It is clear that some energy has spread to the fast modes at low wavenumbers (the amplitudes close to the origin in the left and right columns). This is on a scale associated with the $\boldsymbol{u}_1$ part of the expansion, and can be associated with the $(0, 0, 0; 0)$ resonance of Reznik, Zeitlin, and Ben Jelloul 2001. Without the low energy fast modes providing a pathway via the slow-slow-fast and fast-slow-slow interactions this resonance would not be possible. 127

6.7 Graphs showing the relative strength of the real part of the interaction coefficients for different wavenumbers in each relevant case. The first wavenumber is fixed to (15,15), and the heat maps are given on axes corresponding to the output wavenumber $\boldsymbol{k}$, with $\boldsymbol{k}_2$ calculated from the other two wavenumbers. The top row shows the possible mode combinations outputting onto the slow mode. The middle row gives the output of mixed mode triads onto a fast mode, and the bottom row shows the possible fast mode only triads. From the differences in amplitude it is clear that some interactions will be weakened by the small size of the interaction coefficient. It should also be noted that these interactions are not necessarily resonant. For example from the central graph we can see that the fast-slow-fast interaction has O(1) interaction coefficient in the region of the resonance (the circular resonance seen in figure 6.2), this suggests that as well as forming a resonant interaction, the energy exchange between the modes will not be limited by the interaction coefficient, whereas from the centre top graph slow-fast-slow interactions between (15,15,+) and any other slow mode will not only be non-resonant, but limited by an interaction coefficient an order of magnitude smaller. 129

6.8 Distribution with time of the log of the eigenmode amplitudes. Time increases from top to bottom from $0s$, to $1s$, to $19s$. The central column shows the slow modes and the outside columns show the fast modes. In this simulation only the fast modes were included in the initial conditions. No energy is transferred to the slow modes, as expected from the proof in chapter 4 that the interaction coefficient for $(\pm, ..., \pm, 0)$ is always zero. It can be seen that both the self interaction and radial spreading of energy occur without the presence of slow modes, it follows that the radial spreading can be attributed to the near-resonant fast-fast-fast interactions such as mode (15,15,+) with mode (15,15,+) to form (30,30,+). It can also be seen that the spread of energy to low wavenumbers is very weak from fast mode only interactions, suggesting that the spread of energy to these modes will be mostly from interactions with slow modes. 132

6.9 Graphs showing the relative strength of the real part of the interaction coefficients for different wavenumbers in each relevant case. The first wavenumber is fixed to (0,1), and the heat maps are given on axes corresponding to the output wavenumber $\boldsymbol{k}$, with $\boldsymbol{k}_2$ calculated from the other two wavenumbers. The top row shows the possible mode combinations outputting onto the slow mode. The middle row gives the output of mixed mode triads onto a fast mode, and the bottom row shows the possible fast mode only triads. From the differences in amplitude it is clear that some interactions will be weakened by the small size of the interaction coefficient. It should also be noted that these interactions are not necessarily resonant. For the smaller wavenumber the complexity of the graphs is contained close to the origin, and the majority of the interaction coefficient follows a radial pattern, mostly dependent only on the angle of incidence between the modes. As an example the centre-right graph shows that the fast-slow-fast interaction that would cause energy to spread to wavenumbers close to (15,15,+) has an O(1) interaction coefficient, in this region there are resonances and near resonances, and the expected spreading of energy can be observed in figure 6.2 as the region of higher amplitudes around the (15,15,+) mode. 133

7.1 The wavepacket, in each field u, v, h for central wavenumber $\boldsymbol{k}^*$ for the case of $\alpha = 0$ in the shallow water equations with $c = 0.5$, $f = 1$ and $\epsilon = 0.35$. In the height field in the right hand frame a Gaussian wavepacket has been chosen, dictating the shape of the wavepackets in the other two fields given in the left hand and centre frames. The second row shows only the order ϵ correction term that adjusts the shape away from a simple Gaussian envelope. 146

Chapter 1

Introduction

The mathematical language of the oceans and atmosphere is that of partial differential equations. The nonlinearities involved in these are the major source of difficulty in the analysis; the linear problems would be analytically soluble, whereas those that are nonlinear are often not just difficult to solve, but non-integrable. However for analytic results extra assumptions can be made, a particularly common one being weak nonlinearity. Amplitude expansions are then used with multiple time, and sometimes space, scales. Defining $\epsilon \ll 1$, multiple times scales are represented in the mathematics: fast time t/ϵ, and slow times t, ϵt etc. Successive parts of the expansion can then be accounted for by different dynamical equations acting on each of the different timescales, depending on whether the effect is fast or slow acting.

Resonances emerge at each timescale of this expansion: particular nonlinear combinations that contribute to the dynamics on that timescale, while non-resonances can only contribute on a subsequent one. These resonances, to be introduced shortly, occur throughout the geophysical fluids literature: resonances give rise to the quasigeostrophy of Charney 1948, in turbulence studies resonances and the related near resonances have been linked to the formation of quasi-two-dimensional flows (Smith and Waleffe 1999), as well as being key to the theory of mesoscopic systems studied in the wave turbulence community (Kartashova and Mayrhofer 2007). Resonances are key to the understanding of many geophysical phenomena, many related to the splitting into the fast/slow and barotropic/baroclinic modes that arise naturally in the linear part of the systems. This thesis aims to explore some of the less trodden ground in the resonant literature: resonances at quartet order and beyond, as well as the extension of the theory to include near resonances. As well as this analysis, applications will be made to a few key rotating fluid systems, leading to some new results. In particular, new triad order results are found in the two layer rotating shallow water system, this work was originally detailed in Owen, Grimshaw, and

Wingate 2018.

All of the weakly nonlinear equations we will consider will take the general form:

$$\frac{\partial \boldsymbol{u}}{\partial t} + \frac{1}{\epsilon}\mathcal{L}\boldsymbol{u} = -\mathcal{N}(\boldsymbol{u}, \boldsymbol{u}), \tag{1.1}$$

where $\boldsymbol{u}$ is some state vector, $\mathcal{L}$ a linear operator acting on the spatial coordinates, and $\mathcal{N}$ is a bilinear operator, that represents a quadratic linearity.

For our initial discussion of the resonant behaviour that we will be investigating we will reduce the problem to the simpler but related form:

$$\frac{\partial \chi}{\partial t} + \mathcal{L}\chi = \epsilon f(t), \tag{1.2}$$

for some forcing function f that acts as a stand in for the nonlinear term. Although reducing to a linear system breaks the feedback mechanism by which the flow acts back on itself, it does provide a minimal model for resonance. We have changed to the scalar dependent variable χ for further simplicity, and implicitly rescaled so that the ϵ multiplies the forcing term.

The first stage of the analysis is to form an asymptotic expansion; we expand the dependent variable in the following manner:

$$\chi = \chi_0 + \epsilon\chi_1 + \epsilon^2\chi_2 + \dots . \tag{1.3}$$

We require that in all subsequent motion the asymptotic variables remain $O(1)$ (big-O notation is defined in appendix A.1). In other words, the separation between orders of the asymptotic series must be maintained. The phenomenon in which this fails is generally referred to as resonance: where parts of the solution are able to grow indefinitely. A basic example of resonance is the equation:

$$\frac{d\chi}{dt} + i\omega\chi = \epsilon e^{-i\lambda t}. \tag{1.4}$$

This equation can be considered the complex form of forced simple harmonic motion (by equating $\chi = dx/dt - \omega x i$), producing oscillating motion, with natural frequency ω. We will consider this example as a way of gaining intuition as to how the more complicated nonlinear resonances evolve - the focus of this thesis.

We start by solving equation (1.4) using basic techniques:

$$\chi = Ae^{-i\omega t} - \frac{i\epsilon}{\omega - \lambda}e^{-i\lambda t} \qquad \lambda \neq \omega, \tag{1.5}$$

$$\chi = Ae^{-i\omega t} + \epsilon t e^{-i\omega t} \qquad \lambda = \omega. \tag{1.6}$$

Here A is a complex constant of integration.

In the case of resonance where $\lambda = \omega$, as t increases the forced particular integral term $\epsilon t e^{-i\omega t}$ can become unacceptably large when $\epsilon t \sim O(1)$. However with our standard asymptotic expansion (1.3) we would have considered this term to relate to our smaller χ_1 part of the expansion, due to the presence of ϵ. To resolve this, we can introduce infinitely separated (and therefore independent) timescales. That is to say, we want to allow this change to take place over the 'slow timescale' $T = \epsilon t$. We make the change of variables $t \to t + T$ and use the chain rule to calculate the new time derivative:

$$\frac{d}{dt} \to \frac{d}{dt} + \epsilon \frac{d}{dT}.$$

To first order we now obtain the unforced equation in χ_0 resulting in the same complementary function as found in (1.5):

$$\frac{d\chi_0}{dt} + i\omega\chi_0 = 0, \tag{1.7}$$

$$\chi_0 = Ae^{-i\omega t}. \tag{1.8}$$

To next order we obtain:

$$\frac{d\chi_1}{dt} + i\omega\chi_1 = -\frac{d\chi_0}{dT} + e^{-i\omega t}.$$

Now, to avoid the resonance we must remove secular terms: in other words we remove the forcing on χ_1 responsible for the unhindered growth of the solution. We now want those terms that can become too large to be contained within the χ_0 variation and we achieve this by setting the right hand side to 0 so that these terms are cancelled out of the equation for χ_1:

$$\begin{aligned} -\frac{d\chi_0}{dT} + e^{-i\omega t} &= 0 \\ \Rightarrow \chi_0 &= Te^{-i\omega t} + g(t) \\ \Rightarrow \chi_0 &= Ae^{-i\omega t} + Te^{-i\omega t}. \end{aligned} \tag{1.9}$$

Here $g(t)$ appeared due to integration with respect to T and is the already known complementary function (1.8).

We have recovered the original non-asymptotic solution (1.6) but it is now in a valid asymptotic expansion to first order - due to the introduction of a slow timescale.

We now return to the full nonlinear equation (1.1). The role of the forcing from this example is returned to the nonlinear 'forcing' given by a quadratic nonlinear term $\mathcal{N}$. It is important that, although the resonance behaves in a similar manner to the oscillator example, the source of the resonance is in the flow itself. Parts of the flow are able to modulate each other such that the timescales on which the system evolves are intrinsic to the system itself.

The linear operator $\mathcal{L}$ on the left hand side of (1.1) will produce dynamics with some fundamental frequency ω (given by the dispersion relation, derived in chapter 2), in the same manner as before. This can be succinctly represented by terms of the form $\boldsymbol{u}_i = \hat{\boldsymbol{u}}_i e^{-i\omega_i t}$. The fundamental frequencies of the two inputs into the nonlinear term are then summed (because $e^{-i\omega_1 t}e^{-i\omega_2 t} = e^{-i(\omega_1+\omega_2)t}$) to give the 'forcing' frequency: $\lambda = \omega_1 + \omega_2$. We can then use this to update our resonance condition from (1.6) to the nonlinear resonance condition:

$$\omega = \lambda \qquad \Rightarrow \qquad \omega = \omega_1 + \omega_2. \tag{1.10}$$

For our nonlinear system, the integration with respect to T that was performed in (1.9) is not straightforward, and so this is simply left as a dynamical equation in slow time. As one progresses with the analysis this generates a hierarchy of equations defining the dynamics for each timescale. In chapter 3, the resonant expansion is formally derived for systems of equations, not just to this first slow timescale but to those beyond. This will be seen to generate what will be defined as triad, quartet and higher order resonances.

Returning to the example, we need to consider what happens close to a resonance, does the behaviour act like the non-resonant case (1.5) or like the resonant case (1.6)? The resonant detuning, defined as $\Omega = \omega - \lambda$, can be used to keep track of the proximity to resonance. It is small ($\sim \epsilon$) where the system is near to resonance. If we take the non-resonant solution (1.5) but with $\Omega = \epsilon$, we can use Taylor series to write the solution as:

$$\begin{aligned}
\chi &= Ae^{-i\omega t} - \frac{i\epsilon}{\epsilon}e^{-i(\omega-\epsilon)t} \\
&= Ae^{-i\omega t} + -ie^{-i\omega t}e^{i\epsilon t} \\
&= (A-i)e^{-i\omega t} + \epsilon t e^{i\omega t} + O(\epsilon^2 t^2) \\
&= A'e^{-i\omega t} + \epsilon t e^{i\omega t} + O(\epsilon^2 t^2),
\end{aligned} \tag{1.11}$$

which shows that for small ϵ the solution approximates the resonant one (1.6) until t becomes too large. Figure 1.1 shows (the real parts of) these three solutions: exactly resonant, near resonant

and non-resonant. The figure suggests how for some given timescale the near resonant solution behaves in the same secular manner as the exact resonance. Using the same reasoning as above where we derived (1.10) we arrive at the nonlinear near resonance condition:

$$\omega \sim \lambda \qquad \Rightarrow \qquad \omega - \omega_1 - \omega_2 \sim O(\epsilon).$$

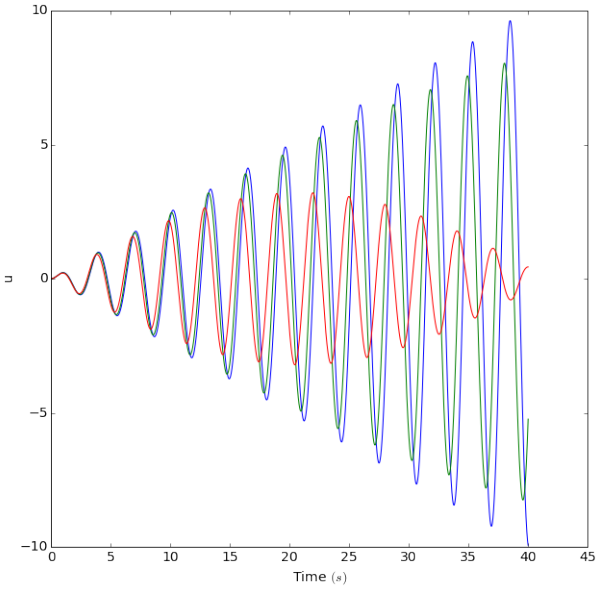

Figure 1.1: The three cases: non-resonance (red), near resonance (green), and resonance (blue). For a timescale of around $t = 35s$ there is minor separation between the behaviours of the near and exact resonances, and so they can be treated similarly.

In these cases one must be very careful about the balances between the various possible small parameters that are necessarily introduced, specifically the timescale, amplitude and the resonant detuning: all of these can potentially shift terms around within our asymptotic expansion.

Some detailed reasoning on when near resonances are important can be found in Nazarenko 2011, Kartashova, Nazarenko, and Rudenko 2008, Harper, Bustamante, and Nazarenko 2013 and other related papers. In these papers a scaling argument is made for when the near resonances will be of importance. It is assumed that the model being considered exists on a discrete grid of wavenumbers, spaced at intervals Δk. Then an approximate spacing between the intrinsic frequencies can be given by $\Delta\omega \sim \Delta k \; \partial\omega/\partial k$, where the derivative is derived from the dispersion relation of the system under consideration. This quantity is then compared to the detuning $\Omega = \omega - \omega_1 - \omega_2$. If $\Omega \gg \Delta\omega$, then it would be expected that many near resonances can be found in the system, and hence they must be considered in any expansion. This is shown in figure 1.2. The opposite case $\Omega \ll \Delta\omega$ would prerequisite exclusion of them. As we intend to investigate the effects of near resonances in a non-discrete domain, where $\Delta k \to 0$, we make the assumption throughout the later chapters that we are in the first regime: where near resonances are vital to the dynamics. The near resonant expansion will be derived in chapter 5, in a manner designed to

relate the near resonances back to the exact resonances we will have already explored.

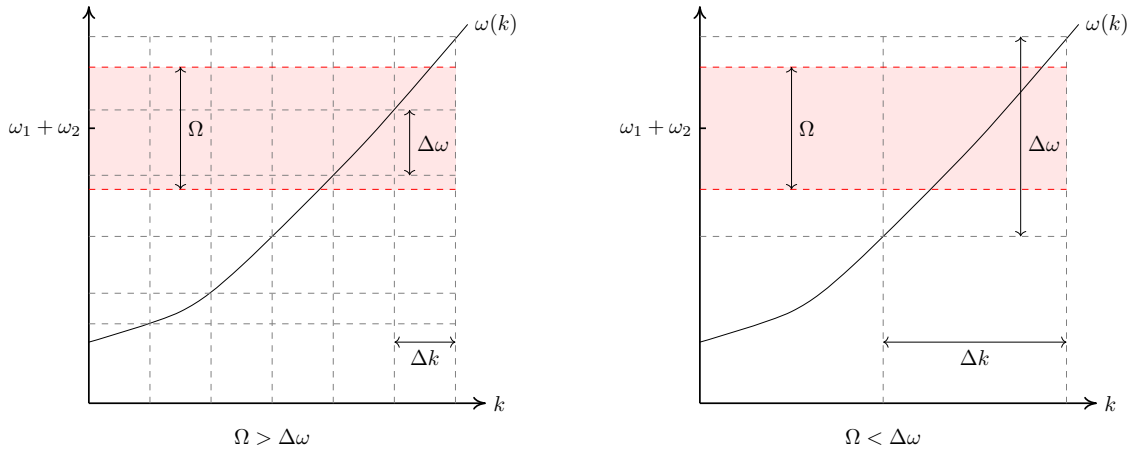

Figure 1.2: Wavenumber spacing affects the availability of near resonances. Here the dispersion relation linking k to ω is given by $\omega(k)$, which links the Δk spacing to the $\Delta\omega$ spacing. Dashed lines represent distinct ω values in the simulation, while the red area represents the area within which the near resonances lie, where the distance from a prescribed $\omega_1 + \omega_2$ is less than the given detuning. On the left with tighter spacing there are multiple near resonances, on the right with larger Δk there are no near resonances for the given detuning.

These ideas of near and exact resonances will be explored in the context of geophysical fluid dynamics. These types of flows often exhibit a particular characteristic that will be exploited in the subsequent work: fast-slow splitting. For weakly nonlinear systems the fastest part of the flow is the linear part, and in the linear part a balance can be found between the Coriolis and pressure terms such that at most only $O(\epsilon)$ time variation can occur. This balanced part can only evolve slowly due to the weak nonlinear terms. The phase speed (c_p) determines the velocity of the linear motion and it can be shown that $c_p = \omega/k \sim O(\epsilon)$ in these systems. Meanwhile any non-balanced part of the flow evolves due to the linear terms, and is the faster part of the flow, where $c_p \sim O(1)$. This is known as geostrophic balance, the systematic development of which is usually attributed to Charney 1948. In the cases studied in this thesis, with constant Coriolis parameter f, the assumption is slightly stronger such that for the balanced part $c_p = \omega = 0$. It is immediately clear that the resonance condition is always met by the balanced slow modes, whereas for the non-balanced fast modes resonance can be a very limiting constraint: the behaviour of the two modes in the nonlinear part is distinct and will be a central issue that we explore. This behaviour will be derived fully in chapter 2 in a very general context, so that it can be exploited to gain insight into a range of systems in the subsequent chapters.

This thesis has two major goals. The first goal is to explore the classical multiscale approach in the context of slow-fast systems, and the second main goal is to investigate the effect of resonant detuning on the amplitude equations. As well as presenting the theory, application to example systems will be included, some of which has been published in Owen, Grimshaw, and Wingate 2018. Some development of the theory in the context of wavepackets will also be discussed.

1.1 Historical background

All resonance theory starts by taking amplitude expansions, and not without reason these are sometimes referred to as Stokes' expansions: one of the early investigations into nonlinear wave behaviour in fluids was performed in Stokes 1847 (reprinted in Stokes 1880). For surface waves an approximate solution was found by linearisation of the equations, and going further than any previous work Stokes expanded up to third order in the nonlinear terms, to derive corrections caused by the wave interacting with itself. Although this is widely considered the classical work on water waves it was based on earlier works, in which single waves were considered, but nonlinearity neglected, by some of the most famous mathematicians of the eighteenth and nineteenth centuries, such as Laplace, Lagrange, and Cauchy - these contributions are detailed in the review of Craik 2004. A common approach in these times was to use the 'method of parallel sections': now normally termed columnar motion, the restriction that leads to the derivation of the shallow water equations, one of the core applications given in this thesis. To some extent Stokes set the precedent for the approach of the coming century, and so it is worth noting that this assumed a single wave; no wave interaction was considered, leading to some consternation later when interaction between different waves was introduced. As some of the work of this thesis will concentrate on two layer flow it is interesting that the same paper by Stokes seems to be the first place where two layer fluids were considered mathematically, although observations on the internal wave speed in these layered fluids can be found as far back as Franklin and Brownrigg 1774 (this observation is made even more impressive by how busy one would imagine Benjamin Franklin's schedule to have been in those years).

Later, theories were developed showing that in the linear approximations of many fluid systems there is a separation into fast and slow parts. Almost unnoticed at the time, Hough 1898 derived the Hough functions for the Laplace tidal equations (shallow water on the rotating sphere). These are the basis linear functions of the equations and received more attention after the papers of Rossby 1939b, Rossby 1939a, and Haurwitz 1937, Haurwitz 1940 where a specific form of slow mode was shown to have an important role in meteorology: the Rossby wave. Rossby and Haurwitz introduced the Rossby wave solutions on the beta-plane and sphere respectively and these became a pivotal part of early weather prediction and understanding. These ideas directly led to the development of quasigeostrophic theory, normally attributed to Charney 1948. The geostrophic part of the motion is exactly the Rossby wave for a beta-plane model (where Coriolis term is approximated such that it varies linearly with latitude), and synonymous with our slow modes for an f-plane (where Coriolis term is deemed constant). This was another nonlinear extension of the basic theory, however unlike that of Stokes in the previous century this was not limited to a single wave: the waves of different sizes were able to interact, and the nonlinearities

were between distinct waves, unlike Stoke's frequency correction terms. However, this still made a strong assumption, specifically geostrophic balance had to be assumed at first order, such that there was no possible interaction of fast and slow motions. Any of the fast components not in this balance were not considered in this theory, interactions of both components required mathematics that would come into play a decade later.

In the 60s the more general multiple scale method of asymptotic expansion started to find its place in geophysical fluids, indeed over the decade a large number of papers covered this topic. The first to use this concept was Phillips 1960 for the problem of surface wave interactions. However he was unknowingly reinventing the method already well known in other disciplines: Ziman 1960 used the theory in electron interactions for example. He found that sets of four waves could form resonances and allow nonlinear interactions to take place between waves. Interestingly, in his review paper, Phillips 1981 he recounts his initial presentation of his work at a meeting in 1962 where he received heavy criticism: despite solitary wave developments, the work of Stokes was still so dominant that the prevailing assumption for water waves was that no interactions could occur between different waves. However over the next decade several papers followed applying the new method to different situations: Ball 1964 applied the ideas to two layer non-rotating systems, and McGoldrick 1965 for capillary waves, both of which have a suitable dispersion relation for the interaction of three waves. Thorpe 1966 also studied interaction of external and internal waves for stably stratified fluid. Other related work that expanded knowledge of different time scales included: Hasselmann 1962 who furthered the surface wave work and generalised it from the special case of Phillips (although he originally started work on the problem independently), and Benney 1962 and Benney and Newell 1967 who further generalised the method, as well as Newell 1969 who applied it to Rossby wavepackets. One paper, Benney and Saffman 1966, received some further controversy with the publication of Hasselmann 1967 which cast doubt on the validity of the work in the absence of a statistical closure. A second version of the paper Hasselmann and Saffman 1967 was published, which included a rebuke from Saffmann suggesting that Hasselmann had simply made an error, and by the publication of Newell 1968 it would seem that it was accepted that the mathematics didn't require specific closure to be valid.

Many of the papers from this period included multiple spatial scales, giving rise to wavepackets. This was particularly important in the derivation of modulational instability theory, notably in Zakharov 1967 and Zakharov 1968 - the original Russian paper was published in 1967 and widely regarded as the original work on the subject. However almost simultaneously, and entirely separately, the derivation was also given by Benjamin and Feir 1967 and Benney and Newell 1967. Also the work of Lighthill 1965 indirectly derived the same phenomenon via averaged Lagrangian theory of Whitham 1965. Details of these developments can be found in Zakharov and

Ostrovsky 2009. In these papers it was shown that the expansions to quartet order led to the nonlinear Schrodinger equation, the focussing or defocussing version depending on the parameters. It followed that a long wave perturbation of the envelope could be unstable, an effect now widely known as modulational instability. In this period, simultaneous experimental work was performed to confirm the theory, some examples include two of the early confirmations of the theory: McGoldrick et al. 1966, and Longuet-Higgins and Smith 1966. The theoretical work would have included the second part of the work of Benjamin and Feir, which unfortunately never made it to print.

It should be mentioned that during this period there was much development of strongly nonlinear theory in the context of solitary wave solutions of the KdV equation (although it is itself derived from weakly nonlinear theory). This was famously initialised by the 1834 observations of of John Scott Russell in the Union canal near Edinburgh (published in Russell 1845). The equation then first appeared in a footnote and the solitary wave solution first written down in Boussinesq 1877, but then rediscovered with the solitary wave recalculated by Korteweg and De Vries 1895. However the real progress in this theory came with the development of soliton theory (Zabusky and Kruskal 1965) and the inverse scattering transform in Gardner et al. 1967 and Miura, Gardner, and Kruskal 1968, contemporaneously with the wave interaction theory. Indeed many of the key investigators were involved in both areas: soon after the discovery of the inverse scattering transform the papers by Shabat and Zakharov 1972 and Zakharov and Manakov 1976 extended the method in a manner that allowed solutions of the nonlinear Schrödinger and three wave equations respectively: equations that regularly occur during the type of resonance work discussed in the previous two paragraphs. More details can be found in Kaup, Reiman, and Bers 1979 where the three wave results are examined in detail, and another approach related to that of Zakharov and Shabat is that of Ablowitz et al. 1974.

Later the role of rotation in resonant interactions, initially for the shallow water equations, was studied by Warn 1986, and after by Babin, Mahalov, and Nicolaenko 1997, and Embid and Majda 1996. The approach of this last paper is used in parts of this thesis. In Embid and Majda 1996 the one layer shallow water equations were approached using the parameter limit from quasigeostrophy but retaining a fast time scale. It was found that the dynamics split into two equations: an equation of motion describing the well-known quasigeostrophic approximation for the geostrophically balanced part, and also a second equation, coupled to the first, describing the gravity waves (on the fast time scale) interacting with the geostrophic part. This interaction was shown to be one-way: the balanced part is unaffected by the gravity waves and acts as a catalyst to the gravity wave interactions (for detail see Ward and Dewar 2010).

A series of papers by Reznik, Zeitlin and collaborators have examined the wave interactions of

layered fluid models. We note especially Reznik, Zeitlin, and Ben Jelloul 2001 which explored different geostrophic limits in the one layer shallow water equations with compact support assumed for the initial conditions, and Zeitlin, Reznik, and Ben Jelloul 2003 who considered a two layer shallow water model in the rigid lid limit. They found that the long-time evolution of the slow part of the flow is unaffected by the fast part as the infinite domain allowed the fast modes to disperse. Recently Thomas 2016 re-examined the one layer model, and found that a restriction to a periodic domain might allow a continuing interaction between the fast and slow modes. We also note that Zeitlin 2013 investigated similarly a two layer model in the half-plane case where there is a boundary along which Kelvin waves can propagate.

Alongside the development of the multiple scales theory an important extension to include detuning of the resonance condition branched off towards the end of the sixties: near resonant interaction theory. Here the assumption that only exact resonances contribute to the nonlinear interaction is relaxed to the near resonant assumption by allowing the nonlinearity to be of comparable size to the detuning parameter for some triads. Several notable researchers working on near resonances attribute the original ideas of near resonance to the Newell 1969 paper, although it would perhaps be better to assign the origin of the idea to the earlier work of Bretherton 1964 where the three-wave equations (for periodic waves) with non-exact resonance were solved exactly. These equations regained some prominence recently when they were re-examined by Vanneste 2007, although work had been done on their solutions using geometric fluid mechanics ideas in Alber et al. 1998. Near resonance is a particularly important concept in numerical simulations, as the discretisation of the problem may actually render exact resonances inaccessible where they involve modes that lie off-grid. From the 1990's various numerical studies into near resonance were published such as Smith and Waleffe 1999, Smith and Lee 2005. Recent work has taken advantage of near resonant behaviour to create novel numerical integration methods including the parallel in time method described in the thesis of Peddle 2018, the specific scheme was first introduced by Haut and Wingate 2014 and Haut et al. 2015. These schemes rely on the averaging out of small oscillations for the non-near resonances to safely push these terms to the scale of the numerical error in the integration.

A major current research area that considers near resonances, but for a finite number of wavenumbers, such as are found in a numerical model, is considered in the field of wave turbulence. This is a similar topic to the one we discuss, except that the focus of the theory is on the behaviour of statistical properties of the fluid in question, rather than its dynamics. However many elements of the theory are relevant to our discussion throughout the thesis. Much of this theory is contained in the book by Nazarenko 2011. Here he quotes Peierls 1929 who he credits with the introduction of wave turbulence, including an equation of the joint probability density function,

a direction that the theory has now moved towards in the last few decades. Also intrinsically connected to the theory is Zakharov, who can be linked in his 'academic family tree' to almost every researcher in the subject area through supervisory roles in their early careers. Although the weakly nonlinear regime is only one area of wave turbulence, it is one of the major current areas of research on weakly nonlinear fluid dynamics as a whole.

An important issue that arises in wave turbulence theory is the finite box vs continuous limit that was illustrated in figure 1.2. This theorises the difference between a discrete and continuous wave spectrum, by considering the wavenumber spacing of a system. In discrete domains there can be an extremely limited set of exact resonances. Work on the number theory problem of finding these resonances has been done between Kartashova 1990, Kartashova 1998, summarised in her book Kartashova 2010. It is even possible, as for the resonance discussed in Owen, Grimshaw, and Wingate 2018, that entire branches of resonances are absent, removing behaviour from a simulation. At the other extreme, the importance of near resonances allows the 'modified dispersion relation' to take a large range of values - the near resonant traces become broad resulting in less constrained dynamics. As suggested by Kartashova, Nazarenko, and Rudenko 2008, because this allows large resonant clusters to exist, the motion moves into a chaotic regime, although no claims are made about the behaviour of this transition to chaos. In this thesis we mostly concern ourselves with this second case, where we have a continuous spectrum of wavenumbers, and near resonances are important to the motion.

This thesis will build upon the existing resonant and near resonant theory, avoiding the truncations of the system that are regularly made for simplification, in order to develop general theory for the behaviour of fast/slow systems, as well as then applying this to commonly used geophysical models.

1.2 Thesis outline

In this thesis we examine the theory of triad and higher order resonances, and the role that near resonances play, with a focus on fast-slow systems in geophysical fluid dynamics. These systems will be introduced in chapter 2. Some new results in the two layer equations are analysed in the exact resonant framework before moving on to near resonant theory. The intention is to give clear intuition as to where results on resonances and near resonances come from. The shallow water quartet resonances of Thomas 2016 that allow energy exchange between fast and slow parts of the flow are re-formed in a more general context and then discussed in a near resonant framework. General ideas about observations of qualitatively different behaviour in near resonant

simulations such as those in the simulations of Smith and Lee 2005 are discussed.

We start at the beginning: the derivation of key equations and quantities that will be used throughout the thesis, detailed in chapter 2. There are three main systems of interest in this thesis: the rotating shallow water equations, the two layer rotating shallow water equations, and the rotating stably stratified equations under the Boussinesq approximation. All of these systems are common rotating/stratified models in geophysical fluid dynamics and are derived from the incompressible Euler equations. A general derivation of Ertel potential vorticity is given, to be used later to draw conclusions common to all relevant systems.

In the next chapter we derive the resonant expansion (Chapter 3), to high order, by defining a new framework in which interaction coefficients are given in generalised form. We then move on to an expanded derivation in which we also include the near resonances (Chapter 5). This formulates the expansion so as to make clear the connections between the two forms, showing how near resonances can be considered a reordering of the asymptotic expansion to include the strongest parts of the higher order terms found in the exact resonant expansion.

Chapters are included after each of these sections giving results derived from the example systems (Chapters 4 and 6). For exact resonances these results are presented analytically. Some of the results in the literature are derived using the new framework, in order to showcase the clarity of the understanding given by the formulation. It can be seen where old results fit into a more general framework while giving added intuition. The results on the rotating two layer equations are a new application taken from the paper Owen, Grimshaw, and Wingate 2018. For the near resonant examples a case study is presented using the results of a full one layer shallow water numerical simulation. This demonstrates clearly how the near resonant expansion explains the dynamics much more accurately than the exact resonances, and gives the opportunity to pick out the pathways of energy exchange between modes.

Finally some observations are made of these results in the context of wavepackets in 7. The main takeaway from this chapter is how the wavepacket formulation adds another restriction to the possible resonant interactions, and has the potential to reduce the effectiveness of the interaction.

All the results are then summarised and concluded in chapter 8.

Chapter 2

Equations of Motion

In this chapter the main geophysical fluid systems in the thesis are derived from the incompressible Euler equations. The systems that will be analysed are the rotating shallow water equations, the two layer rotating shallow water equations and the uniformly stratified equations under the Boussinesq assumption. The rotating shallow water equations provide a simple example of a fluid system to analyse, while the other two represent two ways to introduce stratification into the system, an important property in geophysical contexts. Importantly all of them have a conserved enstrophy (defined in section 2.2.2) that is central to some of the generalisations of the thesis. The concept of a zero mode system is introduced and an argument made to suggest that this and quadratic nonlinearity are common properties that arise naturally out of fluid systems, specifically those without internal forces or internal energy exchange. These two features will be used in chapter 4 to pinpoint where properties of the asymptotic expansions come from. The systems are each decomposed into their fundamental eigenmode structure and other key properties such as potential vorticity are derived for use in the later analysis in chapters 4, 6 and 7. In these chapters exact resonant, near resonant, and wavepacket expansions are derived respectively for each example system.

2.1 Derivations of the fluid systems

All the systems considered in this thesis can be derived from the incompressible Euler equations with a constant rotational component (known as the f-plane assumption) and the action of gravity:

$$\rho \frac{D\boldsymbol{u}}{Dt} + \rho \boldsymbol{f} \times \boldsymbol{u} = -\nabla P - \rho g \hat{\boldsymbol{z}}, \tag{2.1}$$

$$\frac{D\rho}{Dt} = 0, \tag{2.2}$$

$$\nabla \cdot \boldsymbol{u} = 0. \tag{2.3}$$

Here $\rho(\boldsymbol{x}, t)$ is the fluid density, $p(\boldsymbol{x}, t)$ is the pressure, $\boldsymbol{u}(\boldsymbol{x}, t)$ the velocity, g the gravitational acceleration, and $\boldsymbol{f} = f\hat{\boldsymbol{z}}$. $D/Dt = \partial/\partial t + (\boldsymbol{u} \cdot \nabla)$ is the usual Lagrangian derivative, that accounts for advection of the flow. These equations are the momentum equation, conservation of mass, and incompressibility condition respectively. We note that all the nonlinear terms are quadratic.

The three simplifications that follow all modify the pressure part of the equations by making some assumption, namely the hydrostatic assumption, as well as different simplifying assumptions on the effect of gravity. A consequence of these simplifications is that the nonlinearities in the equations are always exactly quadratic. This will affect the formation of triads and quartets derived in chapter 3, allowing a general framework to be formulated.

2.1.1 Shallow water equations

The shallow water equations provide a common simplification used to study fluid where vertical motion is expected to be small in comparison to horizontal motion. It is also very useful from a theoretical perspective: the incompressibility condition is converted into an evolutionary equation, resulting in three evolutionary equations in three unknowns, reducing some of the complexity of the analysis. In section 4.2 the exact resonant expansion will be found to quartet order, and higher for specific cases. In section 6.1 a numerical simulation of the equations will be analysed in the context of the exact and near resonant frameworks set out over the following chapters.

The following derivation can be found for example in Salmon 1998 or Vallis 2006. We start from equations (2.1)-(2.3). We will consider only columnar motion and hence we will integrate over the vertical domain (in effect we replace the vertical variation with its average). We replace the density with an average density across the layer, ρ_0, eliminating the need for equation (2.2). By integrating the hydrostatic balance equation $\frac{\partial P}{\partial z} - \rho_0 g$ and assuming zero pressure at the top boundary we see that the pressure will be simply represented by a linear function of the layer

height:

$$P(x,y,z,t) = \rho_0 g(h(x,y,t) - z), \tag{2.4}$$

$$\Rightarrow \frac{D\boldsymbol{v}}{Dt} + \boldsymbol{f} \times \boldsymbol{v} = -g\nabla h, \tag{2.5}$$

where $\boldsymbol{v} = (u,v)^T$ are the horizontal components of the velocity.

We now consider the incompressibility condition (2.3). We can integrate for the vertical column in z:

$$\int_0^h \nabla \cdot \boldsymbol{v} + \frac{\partial w}{\partial z}\, dz = 0 \qquad \Rightarrow \qquad w|_{z=h} - w|_{z=0} = -h(\nabla \cdot \boldsymbol{v}). \tag{2.6}$$

But, by the definition of the free surface and the fixed base surface we can write:

$$w|_{z=h} = \frac{Dh}{Dt}, \tag{2.7}$$

$$w|_{z=0} = 0, \tag{2.8}$$

and so we can write the 'density' equation for the shallow water system as:

$$\frac{Dh}{Dt} + h(\nabla \cdot \boldsymbol{v}) = 0 \qquad \text{or} \qquad \frac{\partial h}{\partial t} + \nabla \cdot (h\boldsymbol{v}) = 0. \tag{2.9}$$

Our full system is determined by the 3 equations:

$$\frac{D\boldsymbol{v}}{Dt} + \boldsymbol{f} \times \boldsymbol{v} = -g\nabla h, \tag{2.10a}$$

$$\frac{\partial h}{\partial t} + \nabla \cdot (h\boldsymbol{v}) = 0. \tag{2.10b}$$

This forms a nonlinear hyperbolic system. With the inclusion of rotation, although these equations can form shocks, we expect his to only occur at small scale and hence we will not concern ourselves with the possibility in this thesis and continue on the assumption that only negligible shocks will occur.

Figure 2.1 shows the set up of this system. We will regularly use the surface displacement $\eta = h - H$ in calculations, as it is natural to assume the smallness of the quantity η/H, making it useful for scaling arguments.

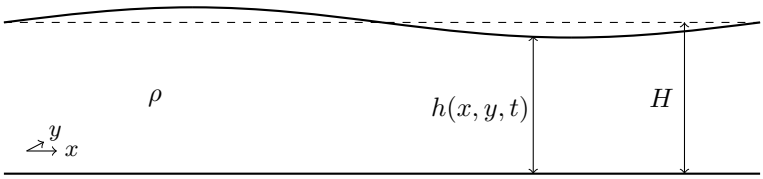

Figure 2.1: Diagram showing the set up of the one layer shallow water equations.

2.1.2 Two layer shallow water equations

The two layer version of the shallow water equations provide a basic system in which stratification can alter the flow, allowing one to maintain some of the advantages of the simplicity of the usual shallow water equations. It can be used as a minimal model of the interaction of the barotropic and baroclinic parts (defined later in section 2.3.2, an important concept in meteorology and oceanography) of the motion. Much of the work on two layer equations in this thesis is taken from Owen, Grimshaw, and Wingate 2018, the majority of which is contained in section 4.3.

Here we will make a similar columnar motion assumption to the single layer case. Now, however, we will assume that there is an interface, with separate fluid of different densities above and below, each part restricted individually to columnar motion. This is shown in figure 2.2. We calculate our pressure terms using these two layers and the boundary conditions $P(z = h_1 + h_2) = 0$, and $P_1(z = h_2) = P_2(z = h_2)$:

$$P_1(x, y, z, t) = \rho_1 g(h_1(x, y, t) + h_2(x, y, t) - z) \qquad z > h_2, \tag{2.11}$$

$$P_2(x, y, z, t) = \rho_1 g h_1(x, y, t) + \rho_2 g(h_2(x, y, t) - z) \qquad z < h_2. \tag{2.12}$$

Substitution into the momentum equation for each layer gives:

$$\frac{D_1 \boldsymbol{v}_1}{Dt} + \boldsymbol{f} \times \boldsymbol{v}_1 = -g\nabla(h_1 + h_2), \tag{2.13}$$

$$\frac{D_2 \boldsymbol{v}_2}{Dt} + \boldsymbol{f} \times \boldsymbol{v}_2 = -g\nabla(rh_1 + h_2), \tag{2.14}$$

where $r = \rho_1/\rho_2$ and $D_i/Dt = \partial/\partial t + (\boldsymbol{v}_i \cdot \nabla)$.

We now apply the same process to the incompressibility condition as was used in the one layer version:

$$w|_{z=h_1+h_2} - w|_{z=h_2} = -h_1(\nabla \cdot \boldsymbol{v}_1), \tag{2.15}$$

$$w|_{z=h_2} = -h_2(\nabla \cdot \boldsymbol{v}_2). \tag{2.16}$$

Using the definitions of the free surface layers we have:

$$\frac{D_1(h_1+h_2)}{Dt} - \frac{D_1 h_2}{Dt} = \frac{D_1 h_1}{Dt} = -h_1(\nabla \cdot \boldsymbol{v}_1), \tag{2.17}$$

$$\frac{D_2 h_2}{Dt} = -h_2(\nabla \cdot \boldsymbol{v}_2). \tag{2.18}$$

The mass conservation equations then take the same form as for the shallow water equations in each of the layers:

$$\frac{D_1 \boldsymbol{v}_1}{Dt} + \boldsymbol{f} \times \boldsymbol{v}_1 = -g\nabla(h_1+h_2), \tag{2.19a}$$

$$\frac{D_2 \boldsymbol{v}_2}{Dt} + \boldsymbol{f} \times \boldsymbol{v}_2 = -g\nabla(rh_1+h_2), \tag{2.19b}$$

$$\frac{D_1 h_1}{Dt} + h_1(\nabla \cdot \boldsymbol{v}_1) = 0, \tag{2.19c}$$

$$\frac{D_2 h_2}{Dt} + h_2(\nabla \cdot \boldsymbol{v}_2) = 0. \tag{2.19d}$$

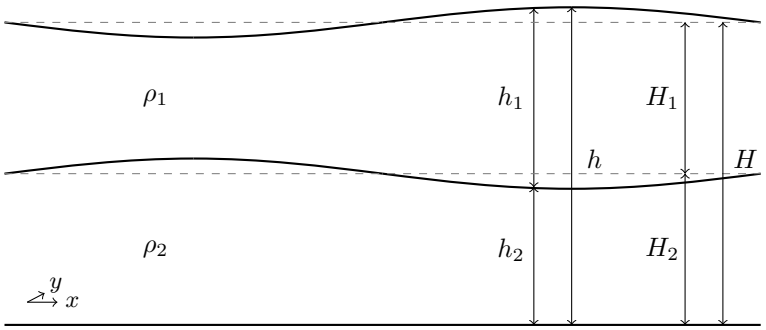

Figure 2.2: Diagram showing the set up of the two layer shallow water equations.

Similarly to the one layer equations the layer height perturbation will be used in many places: $\eta_i = h_i - H_i$.

2.1.3 Uniformly stratified Equations

In this thesis we will refer throughout to the stably-stratified incompressible rotating Euler equations under the Boussinesq approximation simply as the 'stratified equations'. The Boussinesq approximation is a commonly used assumption to avoid the complications arising from variable density, whilst maintaining the strongest effects it causes: those due to buoyancy.

For the stratified equations it is standard to assume that the changes in the density are small compared to a background variation in the vertical direction and are only important in the buoyancy term. There are assumed to be only small density changes horizontally. The density can therefore

be written as:

$$\rho = \bar{\rho} + \rho_0(z) + \rho'(x, y, z, t). \tag{2.20}$$

Where $\bar{\rho}$ is the mean value of the density, and $\rho'/\rho_0 \ll 1$ by the stated assumption, so that the greatest changes in density are in the vertical direction and accounted for in ρ_0. It is often assumed that ρ_0 is a linear function of z for simplicity, we will use this assumption as well to allow use of a periodic domain in the later analysis.

We substitute this form into the momentum equation (2.1) and neglect all but the mean value everywhere except for the gravity term. Dividing though by the density then making this assumption we get:

$$\frac{D\boldsymbol{u}}{Dt} + \boldsymbol{f} \times \boldsymbol{u} = -\nabla \frac{P}{\bar{\rho}} - \frac{\rho_0(z)}{\bar{\rho}} g\hat{\boldsymbol{z}} - \frac{\rho'(x, y, z, t)}{\bar{\rho}} g\hat{\boldsymbol{z}}. \tag{2.21}$$

We can absorb the $\rho_0 g\hat{\boldsymbol{z}}$ into the pressure term (referring to it as P_0) and can therefore eliminate the term from our momentum equation:

$$\frac{D\boldsymbol{u}}{Dt} + \boldsymbol{f} \times \boldsymbol{u} = -\nabla P' - \sigma\hat{\boldsymbol{z}}, \tag{2.22}$$

where $P' = (P - P_0)/\bar{\rho}$ and we have defined the negative buoyancy as $\sigma = \rho' g/\bar{\rho}$.

We now consider the conservation of mass equation (2.2) multiplied by $g/\bar{\rho}$:

$$\frac{g}{\bar{\rho}} \frac{\partial \rho'}{\partial t} + \frac{g}{\bar{\rho}} (\boldsymbol{u} \cdot \nabla)\rho' + \frac{gw}{\bar{\rho}} \frac{\partial \rho_0}{\partial z} = 0. \tag{2.23}$$

We define the Brunt-Väisälä frequency:

$$N^2 = -\frac{g}{\bar{\rho}} \frac{\partial \rho_0}{\partial z}, \tag{2.24}$$

and because of our assumption of a linear density gradient this is a constant. The remaining is our final equation:

$$\frac{\partial \sigma}{\partial t} + (\boldsymbol{u} \cdot \nabla)\sigma - N^2 w = 0. \tag{2.25}$$

We are left with the full equations:

$$\frac{D\boldsymbol{u}}{Dt} + \boldsymbol{f} \times \boldsymbol{u} = -\nabla P' - \sigma \hat{\boldsymbol{z}}, \tag{2.26}$$

$$\frac{\partial \sigma}{\partial t} + (\boldsymbol{u} \cdot \nabla)\sigma - N^2 w = 0, \tag{2.27}$$

$$\nabla \cdot \boldsymbol{u} = 0. \tag{2.28}$$

2.2 Conservation Laws

The following section contains derivations of the conservation laws for the systems. First we will derive Ertel potential vorticity, a general form of potential vorticity conservation in many fluid systems. This makes clear that the existence of this conservation is a common property that occurs provided there are no internal energy exchanges (entropy changes for example) or internal forces (magnetism for example). Linearisation of the potential vorticity property is then shown to underlie the slow-fast splitting of the fluid, leading to zero modes. The potential vorticity, enstrophy and energy conservation is then derived for each of the example systems.

2.2.1 Ertel Potential Vorticity

Here we derive a very general form of potential vorticity, known as Ertel potential vorticity (potential vorticity will be abbreviated to PV in the remainder of this work). This can be done starting from the compressible Euler equations, (2.1) and (2.2) (without (2.3)). Then given the existence of some materially (pointwise) conserved quantity in the specific equation set under consideration a potential vorticity can be derived. In all of our geophysical examples this conserved quantity corresponds to some proxy for buoyancy associated motions. The following proof is based closely on that given in Müller 1995.

Before we start we will briefly note that to generalise the momentum equation slightly further we will replace the gravitational force with the more general external force $\rho\nabla\Phi$, where Φ is some potential field. The gravitational case is recovered by setting $\Phi = gz$. For additional clarity we divide through by the density field to arrive at the form:

$$\frac{D\boldsymbol{u}}{Dt} + \boldsymbol{f} \times \boldsymbol{u} = -\frac{1}{\rho}\nabla P - \nabla\Phi. \tag{2.29}$$

We take the curl of the momentum equation (2.29):

$$\frac{D\boldsymbol{\zeta}}{Dt} - (\boldsymbol{\zeta}\cdot\nabla)\boldsymbol{u} + \boldsymbol{\zeta}(\nabla\cdot\boldsymbol{u}) = \frac{1}{\rho^2}\nabla\rho\times\nabla P, \tag{2.30}$$

where $\boldsymbol{\zeta} = \nabla\times\boldsymbol{u} + \boldsymbol{f}$ is the absolute vorticity and the right hand side benefited from the relation $\nabla\times\nabla = 0$.

Rearranging the mass equation (2.2) we write:

$$\nabla\cdot\boldsymbol{u} = -\frac{1}{\rho}\frac{D\rho}{Dt} = \rho\frac{D}{Dt}\frac{1}{\rho}, \tag{2.31}$$

which we can use to simplify (2.30) to:

$$\frac{D}{Dt}\frac{\boldsymbol{\zeta}}{\rho} - \frac{1}{\rho}(\boldsymbol{\zeta}\cdot\nabla)\boldsymbol{u} = \frac{1}{\rho^3}\nabla\rho\times\nabla P. \tag{2.32}$$

We now require a materially conserved quantity θ such that $D\theta/Dt = 0$. We take the scalar product of (2.32) with $\nabla\theta$:

$$\begin{aligned}\left(\frac{D}{Dt}\frac{\boldsymbol{\zeta}}{\rho}\right)\cdot\nabla\theta - \frac{1}{\rho}(\boldsymbol{\zeta}\cdot\nabla)\boldsymbol{u}\cdot\nabla\theta &= \frac{D}{Dt}\left(\frac{\boldsymbol{\zeta}\cdot\nabla\theta}{\rho}\right) - \frac{\boldsymbol{\zeta}}{\rho}\cdot\frac{D\nabla\theta}{Dt} - \frac{1}{\rho}(\boldsymbol{\zeta}\cdot\nabla)\boldsymbol{u}\cdot\nabla\theta \\ &= \frac{D}{Dt}\left(\frac{\boldsymbol{\zeta}\cdot\nabla\theta}{\rho}\right) - \frac{\boldsymbol{\zeta}}{\rho}\cdot\nabla\frac{D\theta}{Dt} = \frac{D}{Dt}\left(\frac{\boldsymbol{\zeta}\cdot\nabla\theta}{\rho}\right)\end{aligned}$$

$$\Rightarrow \frac{D}{Dt}\left(\frac{\boldsymbol{\zeta}\cdot\nabla\theta}{\rho}\right) = \frac{1}{\rho^3}\left(\nabla\rho\times\nabla P\right)\cdot\nabla\theta. \tag{2.33}$$

We now require one more constraint to have complete conservation of the bracketed term, that the right hand side is zero. This occurs in many situations (see Vallis 2006 for discussion). In our examples this comes from relations of the form $\theta = \theta(\rho)$, such that $\nabla\rho$ and $\nabla\theta$ are parallel.

This gives the Ertel conservation relation:

$$\frac{Dq}{Dt} = 0, \tag{2.34}$$

$$q = \frac{(\nabla\times\boldsymbol{u} + \boldsymbol{f})\cdot\nabla\theta}{\rho}. \tag{2.35}$$

All other PV conservation laws can be derived from this, and so we can draw general conclusions from this conservation law.

As an aside, another alternative derivation is via a Casimir conserved quantity in the Hamiltonian framework. For more information the reader is referred to Morrison 1998 and Shepherd 1990 for example. This derivation is particularly powerful in revealing that the conservation can

be considered to be due to the null space of the non-canonical transformation from Lagrangian to Eulerian frames that underlies all fluid systems.

From potential vorticity to zero modes

We will now use the potential vorticity conservation to directly prove the existence of non-propagating linear modes of the equations, such that they have a zero eigenvalue: the zero modes. Slow modes can refer to any mode with phase speed of $O(\epsilon)$, and the zero modes form a subset of these. Because we use examples in an f-plane throughout, the phase speeds are exactly 0 and so we interchange the terms slow and zero modes. Discussion of the situation where the phase speed is small but non-zero is included in chapter 8.

The next step is to linearise the conservation law, then from the linearised version we will show how the existence of the conservation law automatically leads to the existence of linear modes that do not propagate in the linear solution - zero modes. This will form the justification for the generalisation of the theory in the later chapters to zero mode systems as a common form of fluid systems.

If we assume that the variables can be written in the forms:

$$\boldsymbol{u} = \boldsymbol{U} + \boldsymbol{u}', \qquad \rho = P + \rho', \qquad \theta = \Theta + \theta' \qquad u', \rho', \theta' \sim O(\epsilon), \tag{2.36}$$

for ϵ small, then we can approximate to first order the linearised version of the conservation law:

$$\left(\frac{\partial}{\partial t} + (\boldsymbol{U}\cdot\nabla)\right)\left(\frac{(\nabla\times\boldsymbol{u}')\cdot\nabla\Theta + (\nabla\times\boldsymbol{U}+\boldsymbol{f})\cdot\nabla\theta'}{P} - \rho'\frac{(\nabla\times\boldsymbol{U}+\boldsymbol{f})\cdot\nabla\Theta}{P^2}\right) + (\boldsymbol{u}'\cdot\nabla)\left(\frac{(\nabla\times\boldsymbol{u}')\cdot\nabla\Theta + (\nabla\times\boldsymbol{U}+\boldsymbol{f})\cdot\nabla\Theta}{P}\right) = 0. \tag{2.37}$$

Here we have made the assumption that the Coriolis force is constant and $O(1)$.

If we assume that the first order of the velocity is 0, and that the rotation parameter is independent of the spatial variables this reduces to the simple form:

$$\frac{\partial Q}{\partial t} = 0, \tag{2.38}$$

$$Q = \frac{(P\nabla\times\boldsymbol{u}' - \rho'\boldsymbol{f})\cdot\nabla\Theta + P\boldsymbol{f}\cdot\nabla\theta'}{P^2}. \tag{2.39}$$

This is a general definition for the linearised PV. As this equation is dependent on all of the linearised equations of motion, it is equally valid to substitute this equation for any other in the linearised set, as the resultant set will still be a set of n independent equations in n variables. This

immediately defines a splitting in the eigenmodes of the linear system: there must be a mode with eigenvalue 0, that contains all of the linearised conserved quantity. The remainder of the eigenmodes will not 'carry' any of the linearised quantity and will have non zero eigenvalue.

We write this process out explicitly for a linearised three variable equation set. In the original equations we have variables u, v, p representing two components of velocity and some measure of pressure respectively. We define the state vector $\boldsymbol{u} = (u, v, p)^T$. We invert the definition of the linearly conserved quantity Q so that $p = p(u, v, Q)$ and substitute this into the momentum equations defining a new state vector $\hat{\boldsymbol{u}} = (u, v, Q)^T$:

$$\frac{\partial \boldsymbol{u}}{\partial t} = \mathcal{L}\boldsymbol{u} \rightarrow \frac{\partial \hat{\boldsymbol{u}}}{\partial t} = \hat{\mathcal{L}}\hat{\boldsymbol{u}} \qquad \text{or} \qquad \frac{\partial}{\partial t}\begin{pmatrix} u \\ v \\ Q \end{pmatrix} = \hat{\mathcal{L}}\begin{pmatrix} u \\ v \\ Q \end{pmatrix}, \tag{2.40}$$

where $\mathcal{L}$ is the linear part of the equations in variables u, v, p and $\hat{\mathcal{L}}$ is the linear part in u, v, Q.

We consider the situation $u = 0$, $v = 0$, then due to our conservation law:

$$\frac{\partial}{\partial t}\begin{pmatrix} 0 \\ 0 \\ Q \end{pmatrix} = \hat{\mathcal{L}}\begin{pmatrix} 0 \\ 0 \\ Q \end{pmatrix} = 0. \tag{2.41}$$

We recognise this as the statement of an eigenfunction of $\hat{\mathcal{L}}$ with eigenvalue 0: a zero mode. We can convert back to the original coordinates simply by using the relation $p = p(u, v, Q)$. In a real conservative system (with constant parameters) a first order linear operator will be antisymmetric, with an eigenfunction basis that forms an orthogonal set. It follows that the other eigenfunctions must have $Q = 0$, and so we have a neat partitioning with all of the linearly conserved quantity in a single eigenmode that does not evolve linearly.

The Lagrangian to Eulerian transform ubiquitous in fluid dynamics is responsible for introducing the conserved potential vorticity quantity, as well as introducing quadratic interaction terms. These two qualities together form the basis of the generalisations made in this thesis. This definition deliberately made less assumptions than in any of the example systems investigated, to demonstrate how the theory extends beyond the given examples. One slightly more specific conclusion will now be drawn to differentiate the attributes of layered and continuously stratified equations.

Layered vs continuous PV

The Ertel PV given by:

$$q = \frac{(\nabla \times \boldsymbol{u} + \boldsymbol{f}) \cdot \nabla \theta}{\rho}, \tag{2.42}$$

can be found for the layered equations using the conservation with the flow of the ratio $\theta = z/h_i$ (see Vallis 2006). This leads to a PV of the form:

$$q = \frac{(\nabla \times \boldsymbol{v} + \boldsymbol{f}) \cdot \hat{\boldsymbol{z}}}{h}. \tag{2.43}$$

Here the z component is the only that is non-zero, and hence we consider only the scalar value. Additionally it can be noted that a constant term can be removed from this that will not be relevant to the evolution of the quantity: f/H. We define the PV perturbation $q_{pert} = q - f/H$.

The pointwise enstrophy perturbation (defined shortly in section 2.2.2) is then given by $\frac{1}{2}hq_{pert}^2$, which can be written:

$$Z = \frac{1}{2}hq_{pert}^2 = \frac{Q^2}{2h}, \tag{2.44}$$

where Q is again the linearised PV. More details will be given in section 2.2.2. As we have just shown that all linearised PV is contained in the zero modes, if the contributions to the Q^2 term in the enstrophy only come from fast modes, the enstrophy is exactly zero to all orders. This will be used in chapter 4 to prove that certain mode interactions are impossible at all orders of expansion for layered systems. This distinguishes the layered-type equations from the stratified equations, and will be shown to be an important difference between the behaviours of the asymptotic expansions.

2.2.2 Potential Vorticity and Enstrophy

The potential vorticity and enstrophy conservation laws will be used in section 4.4. They will give a direct method of showing that two fast modes cannot interact to form a slow mode due to the splitting of linear PV into the slow modes as shown in (2.34), which is otherwise a time consuming algebra exercise.

Enstrophy

Enstrophy is an integral conserved quantity that can be derived from the potential vorticity. We multiply the Ertel PV conservation equation (2.34) by ρq:

$$\rho q \frac{Dq}{Dt} = \frac{\partial}{\partial t}\left(\frac{1}{2}\rho q^2\right) + \nabla \cdot \left(\frac{1}{2}\rho q^2 \boldsymbol{u}\right) - \frac{1}{2}\left(\frac{\partial \rho}{\partial t} + \nabla \cdot (\rho \boldsymbol{u})\right) q^2 = 0. \tag{2.45}$$

The last term is 0 by conservation of mass (2.2), and we define the pointwise enstrophy $Z = \rho q^2/2$ so that:

$$\frac{\partial Z}{\partial t} + \nabla \cdot (Z\boldsymbol{u}) = 0. \tag{2.46}$$

Integrating this over a volume V moving with the fluid and using the divergence theorem we obtain the integral conservation law for enstrophy:

$$\frac{\partial \mathcal{Z}}{\partial t} = 0, \tag{2.47}$$

$$\mathcal{Z} = \int_V Z dV. \tag{2.48}$$

We have also assumed that there are no sources or sinks, as we are considering conservative systems.

In individual systems the form of Z can vary based on the density ρ in each system. In the Boussinesq system this is a constant mean value and so can be omitted so that $Z = q^2/2$. In the shallow water equations the layer height h acts as a proxy for the density and so this replaces it in the enstrophy definition to give $Z = hq^2/2$. It can also be noted that the derivation follows exactly the same for the PV perturbation q_{pert}, giving an enstrophy perturbation $\rho q_{pert}/2$, and equivalent specific forms for a given equation set.

In the following sections we define the form of the potential vorticity and enstrophy for each system.

Shallow water equations

The potential vorticity is formed by taking the curl of the momentum equation and using the conservation of mass equation to put into the conservation form:

$$\frac{Dq}{Dt} = 0, \qquad q = \frac{\zeta + f}{h}, \tag{2.49}$$

where $\zeta = (\nabla \times \boldsymbol{v})_z$ is the relative vorticity. As discussed in section 2.2.1, we normally wish to consider the perturbation to this, $q_{pert} = q - f/H$. At next order, in the linear part of the problem, we have:

$$\frac{\partial Q}{\partial t} = 0, \qquad Q = \zeta - \frac{f\eta}{H}. \tag{2.50}$$

As previously proved in section 2.2.1, the linear PV will always be exactly zero for a fast mode.

The (pointwise) enstrophy perturbation is given by:

$$\frac{\partial Z}{\partial t} + \nabla \cdot (Z\boldsymbol{v}) = 0, \qquad Z = \frac{1}{2} h q_{pert}^2. \tag{2.51}$$

It will be useful to write this in the form:

$$Z = \frac{1}{2} h q_{pert}^2 = \frac{Q^2}{2h}. \tag{2.52}$$

Which is derived by a Taylor expansion in η/H. As explained in section 2.2.1, this form is important as it will be shown in section 4.4.1 that for many configurations the enstrophy is then 0 to all orders, leading to conclusions about the interactions of different modes.

Two layer shallow water equations

The only coupling between layers is in the pressure part, which is lost when the curl is considered, and so by the same derivation:

$$\frac{D_i q_i}{Dt} = 0, \qquad q_i = \frac{\zeta_i + f}{h_i}, \tag{2.53}$$

where D_i/Dt is the Lagrangian derivative for the flow in the ith layer and $\zeta_i = (\nabla \times \boldsymbol{v}_i)_z$ is the relative vorticity. For the linear part of the problem we have:

$$\frac{\partial Q_i}{\partial t} = 0, \qquad Q_i = \zeta_i - \frac{f\eta_i}{H_i}. \tag{2.54}$$

The (pointwise) enstrophy perturbation is given by:

$$\frac{\partial Z_i}{\partial t} + \nabla \cdot (Z_i \boldsymbol{v}_i) = 0, \qquad Z_i = \frac{1}{2} h_i q_i^2. \tag{2.55}$$

Here we have assumed that q_i is the perturbation of the PV. We write this in the form:

$$Z = \frac{1}{2} h_i q_i^2 = \frac{Q_i^2}{2h_i}. \tag{2.56}$$

Again, this is similar to the form given for the one layer case and will be referred to in section 4.4.1. It can also be shown that the n-layer equations will take this exact same form of conservation, as each layer will have its independent conservation law.

Stratified Equations

The potential vorticity is defined as:

$$\frac{Dq}{Dt} = 0, \qquad q = (\boldsymbol{\zeta} + \boldsymbol{f}) \cdot \nabla(\sigma + N^2 z), \tag{2.57}$$

with $\boldsymbol{\zeta} = \nabla \times \boldsymbol{u}$. The linear potential vorticity is then defined as:

$$\frac{\partial Q}{\partial t} = 0, \qquad Q = N^2 \zeta_h + f \frac{\partial \sigma}{\partial z}, \tag{2.58}$$

where ζ_h is the vertical component of vorticity and it can be checked that this is again 0 for the fast linear modes. The (pointwise) enstrophy is given by:

$$\frac{\partial Z}{\partial t} + \nabla \cdot (Z \boldsymbol{u}) = 0, \qquad Z = \frac{1}{2} q^2. \tag{2.59}$$

We can write this:

$$Z = \frac{1}{2} (Q + \boldsymbol{\zeta} \cdot \nabla \sigma)^2. \tag{2.60}$$

2.2.3 Energy conservation

The energy conservation law is now stated for each system, to be used in section 4.4 as a way to derive the asymptotic expansion of a system.

Rotating shallow water equations

The pointwise energy of the rotating shallow water equations is derived by taking the scalar product of the momentum equation with $\boldsymbol{u}$ and then manipulating into flux form using the conservation

of mass. This gives:

$$\frac{\partial E}{\partial t} + \nabla \cdot \boldsymbol{F} = 0, \tag{2.61}$$

$$E = \frac{1}{2} h |\boldsymbol{u}|^2 + \frac{1}{2} g h^2, \tag{2.62}$$

$$\boldsymbol{F} = \frac{1}{2} h |\boldsymbol{u}|^2 \boldsymbol{u} + g h^2 \boldsymbol{u}. \tag{2.63}$$

Integrating over a volume moving with the flow we obtain the integral form:

$$\frac{\partial \mathcal{E}}{\partial t} = 0, \tag{2.64}$$

$$\mathcal{E} = \int_D \frac{1}{2} h |\boldsymbol{u}|^2 + \frac{1}{2} g h^2 \, d\boldsymbol{x}. \tag{2.65}$$

Two layer rotating shallow water equations

By taking scalar products per layer, the pointwise energy of the two layer system is given by:

$$\frac{\partial E}{\partial t} + \nabla \cdot \boldsymbol{F} = 0, \tag{2.66}$$

$$E = \frac{1}{2} r h_1 |\boldsymbol{u}_1|^2 + \frac{1}{2} h_2 |\boldsymbol{u}_2|^2 + \frac{1}{2} r g h_1^2 + r g h_1 h_2 + \frac{1}{2} g h_2^2, \tag{2.67}$$

$$\boldsymbol{F} = \frac{1}{2} (r h_1 |\boldsymbol{u}_1|^2 \boldsymbol{u}_1 + h_2 |\boldsymbol{u}_2|^2 \boldsymbol{u}_2 + r P_1 h_1 \boldsymbol{u}_1 + P_2 h_2 \boldsymbol{u}_2). \tag{2.68}$$

Here $P_1 = g(h_1 + h_2)$ and $P_2 = g(r h_1 + h_2)$.

Or in integral form:

$$\frac{\partial \mathcal{E}}{\partial t} = 0, \tag{2.69}$$

$$\mathcal{E} = \int_D \frac{1}{2} r h_1 |\boldsymbol{u}_1|^2 + \frac{1}{2} h_2 |\boldsymbol{u}_2|^2 + \frac{1}{2} r g h_1^2 + r g h_1 h_2 + \frac{1}{2} g h_2^2 \, d\boldsymbol{x}. \tag{2.70}$$

Stratified equations

In the same manner as the other two equation sets, the energy is given by:

$$\frac{\partial E}{\partial t} + \nabla \cdot \boldsymbol{F} = 0, \tag{2.71}$$

$$E = \frac{1}{2} |\boldsymbol{u}|^2 + \frac{\sigma^2}{2N^2}, \tag{2.72}$$

$$\boldsymbol{F} = \left(\frac{1}{2} |\boldsymbol{u}|^2 + P' + \frac{\sigma^2}{2N^2} \right) \boldsymbol{u}, \tag{2.73}$$

and so:

$$\frac{\partial \mathcal{E}}{\partial t} = 0, \tag{2.74}$$

$$\mathcal{E} = \int_D \frac{1}{2}|\boldsymbol{u}|^2 + \frac{\sigma^2}{2N^2}\, d\boldsymbol{x}. \tag{2.75}$$

2.3 Eigenvector formulation

It will be useful to consider the linearised form of all of the equations, as this naturally forms the first stage of weakly nonlinear calculations. The linear part of the equations can then be transformed to its eigenbasis, each component of which will evolve according to its eigenvalue. These are also commonly known as modal functions, in oceanography for instance, but here we shall use the term eigenfunctions.

The eigenmodes will interact with each other in sets of 3, 4, 5 etc to form triad, quartet, and higher order interactions that will be derived in chapter 3. These modes each have an intrinsic frequency given by the eigenvalue. This is the fundamental frequency referred to in the exposition of chapter 1, that forms the components of the resonance condition. As shown in section 2.2.1 there will be a fast-slow splitting, with the eigenvalues of the slow modes equal to zero so that they only evolve nonlinearly. In all of our examples the slow modes will physically correspond to PV modes, those that obey geostrophic balance. The fast modes correspond to gravity waves.

We shall assume boundary conditions that admit Fourier transforms (this will apply throughout this thesis from this point onwards) and then derive the eigenfunctions in spectral space for each equation set.

2.3.1 Rotating shallow water equations

We now explicitly derive the fast/slow modes for the linear part of the shallow water system. To linearise we assume the following scaling:

$$\boldsymbol{v} \sim \epsilon, \qquad H \sim 1, \qquad \eta \sim \epsilon.$$

The viscosity has been assumed to be 0 from the start and so the system will be conservative. This scaling will remove all nonlinear terms at first order leaving the linearised equations:

$$\frac{\partial \boldsymbol{v}}{\partial t} + \boldsymbol{f} \times \boldsymbol{v} = -g\nabla\eta, \tag{2.76}$$

$$\frac{\partial \eta}{\partial t} + H\nabla \cdot \boldsymbol{v} = 0. \tag{2.77}$$

We define $c = \sqrt{gH}$ and $\phi = g\eta/c$, this will simplify the later calculations by introducing symmetry in the linear part. This c scales like a velocity and, as will be seen, corresponds to the phase velocity of gravity waves in the system with small enough wavelength to neglect the Coriolis effect. With these substitutions the equations now read:

$$\frac{\partial \boldsymbol{v}}{\partial t} + \boldsymbol{f} \times \boldsymbol{v} = -c\nabla\phi, \tag{2.78}$$

$$\frac{\partial \phi}{\partial t} + c\nabla \cdot \boldsymbol{v} = 0. \tag{2.79}$$

We proceed by assuming that the solutions will take a Fourier form:

$$\boldsymbol{v} = \sum_{\boldsymbol{k}} \hat{\boldsymbol{v}}_{\boldsymbol{k}} e^{i(\boldsymbol{k}\cdot\boldsymbol{x} - \omega t)}, \tag{2.80}$$

$$\phi = \sum_{\boldsymbol{k}} \hat{\phi}_{\boldsymbol{k}} e^{i(\boldsymbol{k}\cdot\boldsymbol{x} - \omega t)}. \tag{2.81}$$

For a given wavenumber this gives the simple mapping for the derivatives:

$$\nabla \to i\boldsymbol{k}, \qquad \frac{\partial}{\partial t} \to -i\omega. \tag{2.82}$$

Substitution into the equations gives the following system of equations written in vector form:

$$-i\omega \begin{pmatrix} \hat{u} \\ \hat{v} \\ \hat{\phi} \end{pmatrix} = \begin{pmatrix} 0 & -f & ick \\ f & 0 & icl \\ ick & icl & 0 \end{pmatrix} \begin{pmatrix} \hat{u} \\ \hat{v} \\ \hat{\phi} \end{pmatrix}. \tag{2.83}$$

This is a skew-Hermitian matrix (inherited from the skew-symmetry property of the Poisson bracket: this is a conservative system). In a skew-Hermitian matrix the eigenvectors form an orthogonal set, whilst the eigenvalues are pure imaginary values.

From the form of equation (2.83) the eigenvalues of the right hand side are by definition the

wave frequency, $-i\omega$, on the left. We solve for the eigenvalues and eigenvectors and obtain:

$$\omega_{\boldsymbol{k}}^{\alpha} = -\sqrt{c^2|\boldsymbol{k}|^2 + f^2}, \qquad 0, \qquad \sqrt{c^2|\boldsymbol{k}|^2 + f^2}, \tag{2.84}$$

$$\boldsymbol{r}_{\boldsymbol{k}}^{\alpha} = \begin{pmatrix} \frac{(-k\omega + ifl)}{\sqrt{2}|k|\omega} \\ \frac{(-ifk - l\omega)}{\sqrt{2}|k|\omega} \\ \frac{|k|c}{\sqrt{2}\omega} \end{pmatrix}, \begin{pmatrix} -\frac{ilc}{\omega} \\ \frac{ikc}{\omega} \\ \frac{f}{\omega} \end{pmatrix}, \begin{pmatrix} \frac{(k\omega + ifl)}{\sqrt{2}|k|\omega} \\ \frac{(-ifk + l\omega)}{\sqrt{2}|k|\omega} \\ \frac{|k|c}{\sqrt{2}\omega} \end{pmatrix}. \tag{2.85}$$

Here is the unsigned wave frequency: $\omega = \sqrt{c^2|\boldsymbol{k}|^2 + f^2}$ in the construction of each eigenvector, it should be noted that this is still non-zero for the slow modes. The superscript $\alpha = -,\ 0,\ +$ will be used to refer to each mode respectively, while $\boldsymbol{k}$ defines the wavenumber of the Fourier mode. The eigenvectors have been normalised and form an orthonormal basis.

These eigenvectors correspond to two gravity waves (one travelling in each direction, the fast modes) and the slow mode that contains the linear part of the potential vorticity of the system and doesn't move at all in the linear system due to the 0 eigenvalue.

To decompose the system into eigenvectors we use the matrix $T = (\boldsymbol{r}_{\boldsymbol{k}}^{-}, \boldsymbol{r}_{\boldsymbol{k}}^{0}, \boldsymbol{r}_{\boldsymbol{k}}^{+})^T$. Due to the orthonormality of the eigenvectors, left multiplication of the vector $(u, v, \phi)^T$ by T will return the amplitude of each eigenvector in the system for the given wavenumber.

The full Fourier modes will now take the form:

$$\boldsymbol{u} = \sum_{\boldsymbol{k},\alpha} a_{\boldsymbol{k}}^{\alpha} \boldsymbol{r}_{\boldsymbol{k}}^{\alpha} e^{i(\boldsymbol{k}\cdot\boldsymbol{x} - \omega t)}, \tag{2.86}$$

where $\boldsymbol{u}$ combines all three variables into a state vector $(u, v, \phi)^T$, and $a_{\boldsymbol{k}}^{\alpha}$ is the amplitude of the particular eigenmode at that wavenumber.

Group velocity

The group velocity is defined as:

$$\boldsymbol{c}_g = \frac{\partial \omega}{\partial \boldsymbol{k}}. \tag{2.87}$$

By differentiation of the three branches of the dispersion relation solutions (2.84) we obtain:

$$\boldsymbol{c}_g^0 = \boldsymbol{0}, \tag{2.88}$$

$$\boldsymbol{c}_g^{\pm} = \pm \frac{c^2}{\sqrt{c^2|\boldsymbol{k}|^2 + f^2}} \boldsymbol{k}. \tag{2.89}$$

The group velocity is in the direction of propagation, and in the case of the zero modes wavepackets will be stationary.

2.3.2 Two layer rotating shallow water equations

We now extend the derivation of the fast/slow modes for the linear part, but this time in the two layer shallow water system.

The process for two layers is similar except for the initial scaling step to put the resulting matrix into skew-hermitian form. The two layers are coupled by the gravity terms and so some way of combining the two layers into linearly independent modes must be found. This is in fact the well known barotropic/baroclinic decomposition (see for example Gill 1982). These are also referred to as external and internal modes respectively. Similarly to the one layer equations, the linearised form of the two layer equations is:

$$\frac{\partial \boldsymbol{v}_1}{\partial t} + \boldsymbol{f} \times \boldsymbol{v}_1 = -g\nabla(\eta_1 + \eta_2), \tag{2.90}$$

$$\frac{\partial \boldsymbol{v}_2}{\partial t} + \boldsymbol{f} \times \boldsymbol{v}_2 = -g\nabla(r\eta_1 + \eta_2), \tag{2.91}$$

$$\frac{\partial \eta_1}{\partial t} + H_1(\nabla \cdot \boldsymbol{v}_1) = 0, \tag{2.92}$$

$$\frac{\partial \eta_2}{\partial t} + H_2(\nabla \cdot \boldsymbol{v}_2) = 0. \tag{2.93}$$

We wish to find some scaling such that these form a decoupled system. We write:

$$\boldsymbol{v}_m = L_m H_1 \boldsymbol{v}_1 + H_2 \boldsymbol{v}_2, \tag{2.94}$$

where the subscript m will indicate the vertical mode of the variable. To define the transformation we need to calculate L_m.

Applying (2.94) to the conservation of mass equations:

$$\frac{\partial}{\partial t}(L_m\eta_1 + \eta_2) + \nabla \cdot \boldsymbol{v}_m = 0, \tag{2.95}$$

and so to maintain the decoupling we define:

$$p_m = c_m(L_m\eta_1 + \eta_2), \tag{2.96}$$

so that:

$$\frac{\partial}{\partial t}p_m + c_m \nabla \cdot \boldsymbol{v}_m = 0. \tag{2.97}$$

We now apply the transformation to the momentum equations:

$$\frac{\partial \boldsymbol{v}_m}{\partial t} + \boldsymbol{f} \times \boldsymbol{v}_m = -\nabla((L_m H_1 + rH_2)g\eta_1 + (L_m H_1 + H_2)g\eta_2) \tag{2.98}$$

$$= -\nabla\left(g(L_m H_1 + H_2)\left(\frac{L_m H_1 + rH_2}{L_m H_1 + H_2}\eta_1 + \eta_2\right)\right), \tag{2.99}$$

and so to maintain decoupling we enforce the form (2.96) in a RHS that will equal $c_m \nabla p_m$ giving the following relations:

$$\frac{L_m H_1 + rH_2}{L_m H_1 + H_2} = L_m, \tag{2.100}$$

$$L_m H_1 + H_2 = \frac{c_m^2}{g}. \tag{2.101}$$

Equation (2.100) is a quadratic equation in L_m, and c_m can then be calculated from (2.101) for each root. Solving these equations defines the required transformation:

$$L_m H_1 = \frac{H_1 - H_2}{2} + m\sqrt{\left(\frac{H_1 - H_2}{2}\right)^2 + H_1 H_2 r}, \tag{2.102}$$

$$c_m^2 = g\frac{H_1 + H_2}{2} + mg\sqrt{\left(\frac{H_1 - H_2}{2}\right)^2 + H_1 H_2 r}, \tag{2.103}$$

$$m = \pm.$$

Writing the transformed equations in Fourier space we get:

$$i\omega \begin{pmatrix} \hat{u}_+ \\ \hat{v}_+ \\ \hat{p}_+ \\ \hat{u}_- \\ \hat{v}_- \\ \hat{p}_- \end{pmatrix} = \begin{pmatrix} 0 & -f & c_+ki & 0 & 0 & 0 \\ f & 0 & c_+li & 0 & 0 & 0 \\ c_+ki & c_+li & 0 & 0 & 0 & 0 \\ 0 & 0 & 0 & 0 & -f & c_-ki \\ 0 & 0 & 0 & f & 0 & c_-li \\ 0 & 0 & 0 & c_-ki & c_-li & 0 \end{pmatrix} \begin{pmatrix} \hat{u}_+ \\ \hat{v}_+ \\ \hat{p}_+ \\ \hat{u}_- \\ \hat{v}_- \\ \hat{p}_- \end{pmatrix}. \tag{2.104}$$

Solving the eigenproblem to find ω goes as before:

$$\omega = -\sqrt{c_+^2|\boldsymbol{k}|^2 + f^2},\ \ 0,\ \ \sqrt{c_+^2|\boldsymbol{k}|^2 + f^2},\ \ -\sqrt{c_-^2|\boldsymbol{k}|^2 + f^2},\ \ 0,\ \ \sqrt{c_-^2|\boldsymbol{k}|^2 + f^2}, \tag{2.105}$$

with corresponding (orthonormalised) modal functions respectively:

$$\begin{pmatrix} \frac{(-k\omega_+ + ifl)}{\sqrt{2}|k|\omega_+} \\ \frac{(-ifk - l\omega_+)}{\sqrt{2}|k|\omega_+} \\ \frac{|k|c_+}{\sqrt{2}\omega_+} \\ 0 \\ 0 \\ 0 \end{pmatrix}, \begin{pmatrix} -\frac{ilc_+}{\omega_+} \\ \frac{ikc_+}{\omega_+} \\ \frac{f}{\omega_+} \\ 0 \\ 0 \\ 0 \end{pmatrix}, \begin{pmatrix} \frac{(k\omega_+ + ifl)}{\sqrt{2}|k|\omega_+} \\ \frac{(-ifk + l\omega_+)}{\sqrt{2}|k|\omega_+} \\ \frac{|k|c_+}{\sqrt{2}\omega_+} \\ 0 \\ 0 \\ 0 \end{pmatrix}, \begin{pmatrix} 0 \\ 0 \\ 0 \\ \frac{(-k\omega_- + ifl)}{\sqrt{2}|k|\omega_-} \\ \frac{(-ifk - l\omega_-)}{\sqrt{2}|k|\omega_-} \\ \frac{|k|c_-}{\sqrt{2}\omega_-} \end{pmatrix}, \begin{pmatrix} 0 \\ 0 \\ 0 \\ -\frac{ilc_-}{\omega_-} \\ \frac{ikc_-}{\omega_-} \\ \frac{f}{\omega_-} \end{pmatrix}, \begin{pmatrix} 0 \\ 0 \\ 0 \\ \frac{(k\omega_- + ifl)}{\sqrt{2}|k|\omega_-} \\ \frac{(-ifk + l\omega_-)}{\sqrt{2}|k|\omega_-} \\ \frac{|k|c_-}{\sqrt{2}\omega_-} \end{pmatrix}. \tag{2.106}$$

Where $\omega_\pm = \sqrt{c_\pm^2 |\boldsymbol{k}|^2 + f^2}$. The physical explanation of the eigenvectors is similar to in the one layer equations, but now mode-wise: each vertical mode has its own distinct fast and slow modes.

It should be noted that the transform (2.94) changes the form of the nonlinear terms. These now look like:

$$N_u^m = \sum_{m_1, m_2} A^m_{m_1 m_2} (\boldsymbol{v}_{m_1} \cdot \nabla) \boldsymbol{v}_{m_2}, \tag{2.107}$$

$$N_p^m = \sum_{m_1, m_2} \frac{c_m}{c_{m_1}} A^m_{m_1 m_2} \nabla \cdot (p_{m_1} \boldsymbol{v}_{m_2}). \tag{2.108}$$

Where:

$$A^m_{m_1 m_2} = \frac{m_1 m_2}{(L_+ - L_-)^2} \left[\frac{L_m}{H_1} + \frac{L_{-m_1} L_{-m_2}}{H_2} \right], \tag{2.109}$$

and the the terms N_u^m and N_p^m are the nonlinear part of the new momentum and pressure equations respectively, for vertical mode m.

Group velocities

From (2.105) we obtain:

$$\boldsymbol{c}_g^{0m} = \boldsymbol{0}, \tag{2.110}$$

$$\boldsymbol{c}_g^{\pm m} = \pm \frac{c_m^2}{\sqrt{c_m^2 |\boldsymbol{k}|^2 + f^2}} \boldsymbol{k}. \tag{2.111}$$

2.3.3 Stratified equations

The derivation of the eigenmodes in the stratified equations is slightly different, as we must deal with the non-evolving incompressibility condition.

Linearising the equations we get:

$$\frac{\partial \boldsymbol{u}}{\partial t} + \boldsymbol{f} \times \boldsymbol{u} = -\nabla P' - \sigma \hat{\boldsymbol{z}}, \tag{2.112}$$

$$\frac{\partial \sigma}{\partial t} - N^2 w = 0, \tag{2.113}$$

$$\nabla \cdot \boldsymbol{u} = 0. \tag{2.114}$$

We can remove the pressure dependence by using the incompressibility condition. Taking the divergence of the momentum equation and using incompressibility we get:

$$P' = \Delta^{-1}(\boldsymbol{f} \cdot \nabla \times \boldsymbol{u} - \frac{\partial \sigma}{\partial z}). \tag{2.115}$$

Our remaining linearised equations then become:

$$\frac{\partial \boldsymbol{u}}{\partial t} + \boldsymbol{f} \times \boldsymbol{u} + \nabla \Delta^{-1}(\boldsymbol{f} \cdot \nabla \times \boldsymbol{u} - N\frac{\partial \hat{\sigma}}{\partial z}) + N\hat{\sigma}\hat{\boldsymbol{z}} = 0, \tag{2.116}$$

$$\frac{\partial \hat{\sigma}}{\partial t} - Nw = 0, \tag{2.117}$$

where we have scaled $\hat{\sigma} = \sigma/N$ for convenience.

We now proceed as with the layered equations, taking Fourier transforms and putting into vector form:

$$-i\omega \begin{pmatrix} \hat{u} \\ \hat{v} \\ \hat{w} \\ \hat{\sigma} \end{pmatrix} + \begin{pmatrix} -\frac{fkl}{|\boldsymbol{k}|^2} & -\frac{f(l^2+m^2)}{|\boldsymbol{k}|^2} & 0 & -N\frac{mk}{|\boldsymbol{k}|^2} \\ \frac{f(k^2+m^2)}{|\boldsymbol{k}|^2} & \frac{fkl}{|\boldsymbol{k}|^2} & 0 & -N\frac{ml}{|\boldsymbol{k}|^2} \\ -\frac{fml}{|\boldsymbol{k}|^2} & \frac{fmk}{|\boldsymbol{k}|^2} & 0 & N\frac{k^2+l^2}{|\boldsymbol{k}|^2} \\ 0 & 0 & -N & 0 \end{pmatrix} \begin{pmatrix} \hat{u} \\ \hat{v} \\ \hat{w} \\ \hat{\sigma} \end{pmatrix} = 0. \tag{2.118}$$

This system has the characteristic polynomial:

$$\omega^2 \left(\omega^2 - \frac{m^2 f^2 + N^2(k^2+l^2)}{|\boldsymbol{k}|^2} \right) = 0. \tag{2.119}$$

The eigenvalues are then:

$$\omega_{\boldsymbol{k}}^- = -\frac{\sqrt{m^2 f^2 + N^2(k^2+l^2)}}{|\boldsymbol{k}|}, \qquad \omega_{\boldsymbol{k}}^0 = 0, \qquad \omega_{\boldsymbol{k}}^+ = \frac{\sqrt{m^2 f^2 + N^2(k^2+l^2)}}{|\boldsymbol{k}|}, \tag{2.120}$$

with associated eigenvectors:

$$\boldsymbol{r}_{\boldsymbol{k}}^{-} = \begin{pmatrix} \frac{-flm - i\omega km}{\sqrt{2}\omega|\boldsymbol{k}|\sqrt{k^2+l^2}} \\ \frac{fkm - i\omega lm}{\sqrt{2}\omega|\boldsymbol{k}|\sqrt{k^2+l^2}} \\ \frac{i\sqrt{k^2+l^2}}{\sqrt{2}|\boldsymbol{k}|} \\ \frac{N\sqrt{k^2+l^2}}{\sqrt{2}\omega|\boldsymbol{k}|} \end{pmatrix}, \qquad \boldsymbol{r}_{\boldsymbol{k}}^{0} = \begin{pmatrix} \frac{Nl}{\omega|\boldsymbol{k}|} \\ -\frac{Nk}{\omega|\boldsymbol{k}|} \\ 0 \\ \frac{fm}{\omega|\boldsymbol{k}|} \end{pmatrix}, \qquad \boldsymbol{r}_{\boldsymbol{k}}^{+} = \begin{pmatrix} \frac{-flm + i\omega km}{\sqrt{2}\omega|\boldsymbol{k}|\sqrt{k^2+l^2}} \\ \frac{fkm + i\omega lm}{\sqrt{2}\omega|\boldsymbol{k}|\sqrt{k^2+l^2}} \\ -\frac{i\sqrt{k^2+l^2}}{\sqrt{2}|\boldsymbol{k}|} \\ \frac{N\sqrt{k^2+l^2}}{\sqrt{2}\omega|\boldsymbol{k}|} \end{pmatrix}, \tag{2.121}$$

where $\omega = \omega_{\boldsymbol{k}}^{+} = \frac{\sqrt{m^2 f^2 + N^2(k^2+l^2)}}{|\boldsymbol{k}|}$.

The repeated 0 root also leads to another generalised eigenvector that is only accessible by breaking the incompressibility condition (see Embid and Majda 1996) and so we will ignore it.

In all the following we will use the same notation as the layered equations for the state vector $\boldsymbol{u}$ which consists of the velocities and the negative buoyancy variable: $(u, v, w, \sigma)^T$.

Group Velocities

From (2.120) we obtain:

$$\boldsymbol{c}_g^0 = \boldsymbol{0}, \tag{2.122}$$

$$\boldsymbol{c}_g^{\pm} = \pm \frac{(N^2 - f^2)m}{|\boldsymbol{k}|^3 \sqrt{f^2 m^2 + N^2(k^2+l^2)}} \begin{pmatrix} mk \\ ml \\ -(k^2+l^2) \end{pmatrix}. \tag{2.123}$$

Taking the dot product with the wavenumber vector $(k, l, m)^T$ gives a zero result: the group velocity is perpendicular to the wave vector. However by inspection the horizontal parts are parallel. This means the energy will propagate vertically in the opposite direction to the vertical wave vector component. The relation of wavenumber and group velocity direction is illustrated in figure 2.3.

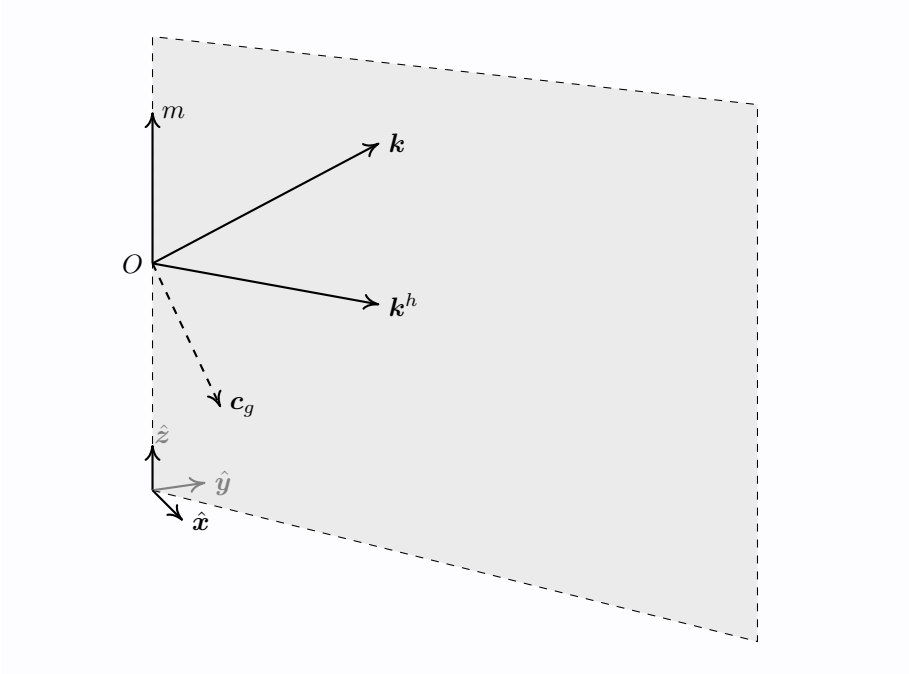

Figure 2.3: Diagram showing the direction of the group velocity (dashed) in the vertical plane of the wave vector but perpendicular to it due to the vertical component.

2.4 Chapter summary

In this chapter the following main points were covered:

- The specific systems that will be considered through the thesis were derived, to be referred to in chapters 4 and 6 where exact and near resonant asymptotic expansions are formed respectively, and then analysed.
- It was demonstrated that systems that support zero modes and quadratic nonlinearity occur naturally in fluid systems in the absence of internal forces and energy changes, this will help generalise some of the conclusions in chapter 4. Explicit forms of potential vorticity, enstrophy and energy were given for each system, also for use in chapter 4.
- The eigenstructure of each system was established. This determines the behaviour of the modes in the linear part of each system. These modes will be seen to form the building blocks of the triads, quartets etc from chapter 3 onwards, and their frequencies, given by the eigenvalues, will be those of the resonance condition stated in chapter 1.
- Group velocity was stated, for later use in chapter 7 where wavepackets will be considered.

Chapter 3

Multiscale asymptotic expansion

In this chapter we derive the full resonant expansion in the context of a system of equations with quadratic nonlinearity. This is the formal derivation of the ideas discussed in chapter 1 corresponding to the situations where a resonance leads to a secular growth and parts of the system are able to grow on a slow timescale.

Initially the expansion is calculated up to triad order as in Owen, Grimshaw, and Wingate 2018, however the expansion is then continued beyond the usual triad/quartet orders to establish a general formula for high order interaction coefficients. We develop the theory here so that in chapter 4 we can apply the techniques to the geophysical systems described in chapter 2, leading to conclusions about the nonlinear interactions that occur in each case. This chapter can be compared to chapter 5, where a similar process will be performed but to form the near resonant expansion.

3.1 Weakly nonlinear limit

We are interested in taking the weakly nonlinear limit in our equations, so that a valid asymptotic expansion can be formed. Weak nonlinearity is defined as a scaling such that the linear part of the equation takes the prominent role with all nonlinear terms considered to be ϵ smaller in amplitude. In systems with no parameters this is achieved by taking the size of the variables to be $\sim \epsilon$. This automatically gifts linear terms $\sim \epsilon$ and quadratic terms $\sim \epsilon^2$ (in the cases we consider, and many idealised fluid models the nonlinear term is exactly quadratic). In systems with parameters the scalings can be made in relation to the physical parameters, and in this thesis we use the quasigeostrophic scaling which will be described in chapter 4, for each system before the theory

is applied.

By taking the weakly nonlinear limit we are able to form an asymptotic expansion, where we approximate the exact solution with a series of increasingly small terms, such that truncating the series at any term will leave the remainder (or the error) that is smaller than everything that has come before. Defined formally we write an asymptotic series for $\boldsymbol{u}$ as:

$$\begin{aligned} \boldsymbol{u} &= \boldsymbol{u}_0 + \epsilon \boldsymbol{u}_1 + \epsilon^2 \boldsymbol{u}_2 + O(\epsilon^3), \\ \boldsymbol{u}_0, \boldsymbol{u}_1, \boldsymbol{u}_2 &\sim O(1), \end{aligned} \tag{3.1}$$

where we have used big-O notation, described in appendix A.1.

3.2 Expansion to triad order

When we form the asymptotic expansion, the first order at which the nonlinearity is involved allows the formation of triads. We now perform these calculations to derive the triads.

We take a completely general dynamical equation with quadratic nonlinearity, scaling such that it is weakly nonlinear:

$$\frac{\partial \boldsymbol{u}}{\partial t} + \frac{1}{\epsilon}\mathcal{L}\boldsymbol{u} + \mathcal{N}(\boldsymbol{u}, \boldsymbol{u}) = 0. \tag{3.2}$$

Here we follow Embid and Majda 1996 by expressing the weakly nonlinear scaling so that the linear part scales like $1/\epsilon$ instead of the more common scaling with $\mathcal{N} \sim \epsilon$. This shifts our fastest timescale to a $1/\epsilon$ scaling but other than this shift the process follows as normal.

The nonlinear terms are represented by the bilinear operator $\mathcal{N}$. This operator has two arguments, but only one input, $\boldsymbol{u}$, and hence we have some freedom in its definition. We choose to define it symmetrically, so that it operates equivalently on the first and second arguments. We write:

$$\mathcal{N}(\boldsymbol{a}, \boldsymbol{b}) = \frac{1}{2}\left(\mathcal{N}(\boldsymbol{a}, \boldsymbol{b}) + \mathcal{N}(\boldsymbol{b}, \boldsymbol{a})\right). \tag{3.3}$$

We define the fast time scale $\tau = t/\epsilon$ as in Embid and Majda 1996 and slow timescales $t_n = \epsilon^n t$, $n \in \mathbb{Z}^+$ and write $\boldsymbol{u} = \boldsymbol{u}(\boldsymbol{x}, \tau, t_0, t_1, ...)$ as a function of multiple time scales. Then (3.2) becomes:

$$\frac{1}{\epsilon}\left(\frac{\partial \boldsymbol{u}}{\partial \tau} + \mathcal{L}\boldsymbol{u}\right) = -\left(\frac{\partial \boldsymbol{u}}{\partial t_0} + \mathcal{N}(\boldsymbol{u}, \boldsymbol{u})\right) - \left(\sum_{n=1}^{\infty} \epsilon^n \frac{\partial \boldsymbol{u}}{\partial t_n}\right). \tag{3.4}$$

We expand the variable $\boldsymbol{u}$ as follows:

$$\boldsymbol{u}(\boldsymbol{x},\tau,t_0,t_1,...) = \boldsymbol{u}_0(\boldsymbol{x},\tau,t_0,t_1,...) + \epsilon\boldsymbol{u}_1(\boldsymbol{x},\tau,t_0,t_1,...) + ... \,. \tag{3.5}$$

Substitution into equation (3.4) gives the following at each order:

$$O(\epsilon^{-1}) \qquad \frac{\partial \boldsymbol{u}_0}{\partial \tau} + \mathcal{L}\boldsymbol{u}_0 = 0, \tag{3.6}$$

$$O(1) \qquad \frac{\partial \boldsymbol{u}_1}{\partial \tau} + \mathcal{L}\boldsymbol{u}_1 = -\left(\frac{\partial \boldsymbol{u}_0}{\partial t_0} + \mathcal{N}(\boldsymbol{u}_0,\boldsymbol{u}_0)\right), \tag{3.7}$$

$$O(\epsilon) \qquad \frac{\partial \boldsymbol{u}_2}{\partial \tau} + \mathcal{L}\boldsymbol{u}_2 = -\left(\frac{\partial \boldsymbol{u}_1}{\partial t_0} + \frac{\partial \boldsymbol{u}_0}{\partial t_1} + \mathcal{N}(\boldsymbol{u}_0,\boldsymbol{u}_1) + \mathcal{N}(\boldsymbol{u}_1,\boldsymbol{u}_0)\right). \tag{3.8}$$

It can be noted here that because our nonlinearity is quadratic (3.8) can only contain nonlinear terms that are combinations of the previous $\boldsymbol{u}_i$. If there were a cubic nonlinearity this would appear directly here as a combination of the $\boldsymbol{u}_0$ modes. In this thesis we will deliberately concentrate on quadratic nonlinearities and so the following all assumes this.

At first order the equation is linear and so we can solve using linear theory. We assume that the appropriate conditions are met such that Fourier transforms can be taken on the domain, then using the exponential operator (defined in appendix A.2) and the integrating factor technique we write:

$$\frac{\partial}{\partial \tau}\left(e^{\tau\mathcal{L}}\boldsymbol{u}_0\right) = 0. \tag{3.9}$$

Solving this:

$$\boldsymbol{u}_0(\boldsymbol{x},\tau,t_0,t_1,...) = e^{-\tau\mathcal{L}}\bar{\boldsymbol{u}}(\boldsymbol{x},t_0,t_1,...), \tag{3.10}$$

$$\bar{\boldsymbol{u}} = \boldsymbol{u}_0(\boldsymbol{x},0,t_0,t_1,...). \tag{3.11}$$

At next order we perform the same integration factor technique on the left hand side and integrate to get:

$$\boldsymbol{u}_1 e^{\tau\mathcal{L}} = \boldsymbol{u}_1|_{\tau=0} - \left(\tau\frac{\partial \bar{\boldsymbol{u}}}{\partial t_0} + \int_0^\tau e^{s\mathcal{L}}\mathcal{N}(e^{-s\mathcal{L}}\bar{\boldsymbol{u}}, e^{-s\mathcal{L}}\bar{\boldsymbol{u}})ds\right). \tag{3.12}$$

With the equation in this form we can identify possible secular terms as any of $O(\tau)$ or higher: those in the round brackets. This mirrors the process taken in the introductory example in chapter 1. To maintain the separation of scales for the velocities/pressures as defined in (3.5) these terms must be $o(\tau)$ in the limit $\tau \to \infty$. This is the 'cancellation of oscillations' concept, used by Schochet 1994, where he used the concept to prove convergence for general hyperbolic equations. To make

clearer the specific wave components that lead to resonances we will also write the vector $\bar{\boldsymbol{u}}$ as a sum over its (complete) eigenbasis. Written in the eigenbasis the matrix exponential is just the exponential of the frequency of the corresponding eigenvalue ($e^{-i\omega\tau}$) for each component of the sum, and we have:

$$e^{-s\mathcal{L}}\bar{\boldsymbol{u}} = \sum_{\boldsymbol{k},\alpha} a^{\alpha}_{\boldsymbol{k}} \boldsymbol{r}^{\alpha}_{\boldsymbol{k}} e^{i(\boldsymbol{k}\cdot\boldsymbol{x}-\omega^{\alpha}_{\boldsymbol{k}}s)}. \tag{3.13}$$

Using this substitution gives the following:

$$\begin{aligned}\left\{\frac{\partial \bar{\boldsymbol{u}}}{\partial t_0}\right\}^{\alpha}_{\boldsymbol{k}} &= -\lim_{\tau\to\infty}\frac{1}{\tau}\int_0^{\tau} e^{s\mathcal{L}}\mathcal{N}(e^{-s\mathcal{L}}\bar{\boldsymbol{u}}, e^{-s\mathcal{L}}\bar{\boldsymbol{u}})ds \\ &= -\lim_{\tau\to\infty}\frac{1}{\tau}\int_0^{\tau} \sum_{\substack{\boldsymbol{k},\boldsymbol{k}_1,\boldsymbol{k}_2\\ \alpha,\alpha_1,\alpha_2\\ \boldsymbol{k}=\boldsymbol{k}_1+\boldsymbol{k}_2}} C^{\alpha_1\alpha_2\alpha}_{\boldsymbol{k}_1\boldsymbol{k}_2\boldsymbol{k}} a^{\alpha_1}_{\boldsymbol{k}_1} a^{\alpha_2}_{\boldsymbol{k}_2} \boldsymbol{r}^{\alpha}_{\boldsymbol{k}} e^{i\boldsymbol{k}\cdot\boldsymbol{x}} e^{-i(\omega^{\alpha_1}_{\boldsymbol{k}_1}+\omega^{\alpha_2}_{\boldsymbol{k}_2}-\omega^{\alpha}_{\boldsymbol{k}})s} ds,\end{aligned} \tag{3.14}$$

where $a^{\alpha_i}_{\boldsymbol{k}_i}$ represents the wave amplitude of each eigenfunction which varies on all slower timescales t_n but is fixed over fast timescale τ such that all fast motion is accounted for in the structure of the eigenbasis. Similarly, the notation $\{...\}^{\alpha}_{\boldsymbol{k}}$ represents the part of the expression in the bracket formed of waves with wavenumber $\boldsymbol{k}$ of eigenmodes α.The interaction coefficient is defined as:

$$C^{\alpha_1\alpha_2\alpha}_{\boldsymbol{k}_1\boldsymbol{k}_2\boldsymbol{k}} = \left\langle \mathcal{N}(\boldsymbol{r}^{\alpha_1}_{\boldsymbol{k}_1}, \boldsymbol{r}^{\alpha_2}_{\boldsymbol{k}_2}), \boldsymbol{r}^{\alpha}_{\boldsymbol{k}} \right\rangle, \tag{3.15}$$

where $\langle\cdot,\cdot\rangle$ is the scalar product of the system and derivatives in the operator $\mathcal{N}$ are expressed in the spectral space. In the case of Fourier transforms this uses the mapping:

$$\frac{\partial}{\partial \boldsymbol{x}} \to i\boldsymbol{k}. \tag{3.16}$$

The integral (3.14) can be computed exactly. In the limit, the integral of all oscillatory contributions exactly cancel to 0 and so the only contributions come from the non-oscillatory constant contributions where $\Omega = \omega^{\alpha}_{\boldsymbol{k}} - \omega^{\alpha_1}_{\boldsymbol{k}_1} - \omega^{\alpha_2}_{\boldsymbol{k}_2} = 0$: the resonant triads. These are exactly equivalent to the situation in which $\omega = \lambda$ in the forced simple harmonic motion example in chapter 1.

This allows the integral to be performed simply such that the integrand is constant in fast time τ:

$$\begin{aligned}\frac{\partial \bar{\boldsymbol{u}}}{\partial t_0} &= \lim_{\tau\to\infty}\frac{1}{\tau}\int_0^{\tau} ds \sum_{\substack{\boldsymbol{k},\boldsymbol{k}_1,\boldsymbol{k}_2\\ \alpha,\alpha_1,\alpha_2}} C^{\alpha_1\alpha_2\alpha}_{\boldsymbol{k}_1\boldsymbol{k}_2\boldsymbol{k}} a^{\alpha_1 m_1}_{\boldsymbol{k}_1} a^{\alpha_2}_{\boldsymbol{k}_2} \boldsymbol{r}^{\alpha}_{\boldsymbol{k}} e^{i\boldsymbol{k}\cdot\boldsymbol{x}} \delta_{\boldsymbol{k}-\boldsymbol{k}_1-\boldsymbol{k}_2}\delta_{\omega-\omega_1-\omega_2} \\ &= \sum_{\substack{\boldsymbol{k},\boldsymbol{k}_1,\boldsymbol{k}_2\\ \alpha,\alpha_1,\alpha_2}} C^{\alpha_1\alpha_2\alpha}_{\boldsymbol{k}_1\boldsymbol{k}_2\boldsymbol{k}} a^{\alpha_1 m_1}_{\boldsymbol{k}_1} a^{\alpha_2}_{\boldsymbol{k}_2} \boldsymbol{r}^{\alpha}_{\boldsymbol{k}} e^{i\boldsymbol{k}\cdot\boldsymbol{x}} \delta_{\boldsymbol{k}-\boldsymbol{k}_1-\boldsymbol{k}_2}\delta_{\omega-\omega_1-\omega_2}\ ,\end{aligned} \tag{3.17}$$

or in terms of only wave amplitudes:

$$\frac{\partial a^{\alpha}_{\boldsymbol{k}}}{\partial t_0} = \sum_{\substack{\boldsymbol{k},\boldsymbol{k}_1,\boldsymbol{k}_2 \\ \alpha,\alpha_1,\alpha_2}} C^{\alpha_1\alpha_2\alpha}_{\boldsymbol{k}_1\boldsymbol{k}_2\boldsymbol{k}} a^{\alpha_1}_{\boldsymbol{k}_1} a^{\alpha_2}_{\boldsymbol{k}_2} \delta_{\boldsymbol{k}-\boldsymbol{k}_1-\boldsymbol{k}_2} \delta_{\omega-\omega_1-\omega_2} \ . \tag{3.18}$$

This defines the dynamics of the $\boldsymbol{u}_0$ modes up to this timescale. This asymptotic representation is correct for times up to $O(1)$, the t_0 timescale.

3.3 Expansion to quartet order

Having formed the triads we continue with the calculations to form quartets. It will be seen that due to the quadratic nonlinearity no direct quartets can be found, quartets will instead be formed of the non-resonant triads from the previous order of interaction. These must first be calculated to continue the analysis.

We now calculate the $\boldsymbol{u}_1$ terms. We return to (3.7):

$$\frac{\partial \boldsymbol{u}_1}{\partial \tau} + \mathcal{L}\boldsymbol{u}_1 = -\left(\frac{\partial \boldsymbol{u}_0}{\partial t} + \mathcal{N}(\boldsymbol{u}_0, \boldsymbol{u}_0)\right). \tag{3.19}$$

We remove the secular terms that we have just fixed to zero (using equation (3.14)):

$$\frac{\partial \boldsymbol{u}_1}{\partial \tau} + \mathcal{L}\boldsymbol{u}_1 = -\mathcal{N}^{nr}(\boldsymbol{u}_0, \boldsymbol{u}_0). \tag{3.20}$$

Here we have written $\mathcal{N}^{nr}$ to indicate that only the non-resonant parts, where $\omega - \omega_1 - \omega_2 \neq 0$, of the nonlinear term are included. We now solve for $\boldsymbol{u}_1$. As the left hand side has the same form as (3.6) the complementary function would find linear modes of the same form as for $\boldsymbol{u}_0$. We can assume that these contributions to the solution are accounted for in the $\boldsymbol{u}_0$ terms (this is possible as $O(1+\epsilon) = O(1)$; the entire initial condition can be accounted for at the previous order, see Ablowitz 2011). Hence we set the complementary function to be identically 0 at this (and all subsequent orders). Now we simply need to find the particular integral for our right hand side:

$$\boldsymbol{u}_1 = -e^{-\tau\mathcal{L}} \int_0^{\tau} e^{s\mathcal{L}} \mathcal{N}^{nr}(e^{-s\mathcal{L}}\bar{\boldsymbol{u}}, e^{-s\mathcal{L}}\bar{\boldsymbol{u}}) ds, \tag{3.21}$$

or in the eigenmode basis:

$$\{\boldsymbol{u}_1\}^{\alpha_a}_{\boldsymbol{k}_a} = -\sum_{\substack{\boldsymbol{k}_1,\boldsymbol{k}_2\\ \alpha_1,\alpha_2}} C^{\alpha_1\alpha_2\alpha_a}_{\boldsymbol{k}_1\boldsymbol{k}_2\boldsymbol{k}_a}\big|_{nr}\, a^{\alpha_1}_{\boldsymbol{k}_1} a^{\alpha_2}_{\boldsymbol{k}_2} \boldsymbol{r}^{\alpha_a}_{\boldsymbol{k}_a} e^{-\omega_a \tau} \int_0^\tau e^{i(-\omega_1-\omega_2+\omega_a)s} ds\ \delta_{\boldsymbol{k}_a-\boldsymbol{k}_1-\boldsymbol{k}_2}$$
$$= \sum_{\substack{\boldsymbol{k}_1,\boldsymbol{k}_2\\ \alpha_1,\alpha_2}} \frac{C^{\alpha_1\alpha_2\alpha_a}_{\boldsymbol{k}_1\boldsymbol{k}_2\boldsymbol{k}_a}\big|_{nr}\, a^{\alpha_1}_{\boldsymbol{k}_1} a^{\alpha_2}_{\boldsymbol{k}_2}}{i(\omega_a-\omega_1-\omega_2)} \boldsymbol{r}^{\alpha_a}_{\boldsymbol{k}_a} e^{-i(\omega_1+\omega_2)\tau}\ \delta_{\boldsymbol{k}_a-\boldsymbol{k}_1-\boldsymbol{k}_2}. \tag{3.22}$$

Note that $\boldsymbol{u}_1$ (the slaved modes) does **not** evolve according to the dispersion relation: by the definition of non-resonance $\omega_a \neq \omega_1+\omega_2$. This means that it is not a solution to the linear problem, it is distinct from the $\boldsymbol{u}_0$ linear solutions, although we have a complete spatial basis and so we can break $\boldsymbol{u}_1$ into 'mode-like' parts (fast-like and slow-like parts), allowing us to use the same nonlinear interaction coefficient as for the usual linear modes. It is also important to note that the motion of this mode is entirely determined by the $a^\alpha_{\boldsymbol{k}}$s and so it does not evolve independently: the modes are slaved to the zeroth order approximation. We have also assumed that $\boldsymbol{u}_1|_{\tau=0} = 0$; there are no slaved modes in the initial condition, because the initial condition is assumed to be entirely accounted for in the $\boldsymbol{u}_0$ part.

Now that we have the form of $\boldsymbol{u}_1$ we can continue to the next order of expansion in (3.8):

$$\frac{\partial \boldsymbol{u}_2}{\partial \tau} + \mathcal{L}\boldsymbol{u}_2 = -\left(\frac{\partial \boldsymbol{u}_1}{\partial t_0} + \frac{\partial \boldsymbol{u}_0}{\partial t_1} + \mathcal{N}(\boldsymbol{u}_0,\boldsymbol{u}_1) + \mathcal{N}(\boldsymbol{u}_1,\boldsymbol{u}_0)\right). \tag{3.23}$$

Following the same process of removing secular terms that we used to derive equation (3.14) we have the equation:

$$\frac{\partial \bar{\boldsymbol{u}}}{\partial t_1} = -\lim_{\tau\to\infty}\frac{1}{\tau}\int_0^\tau e^{s\mathcal{L}}\left(e^{-s\mathcal{L}'}\frac{\partial \bar{\boldsymbol{u}}_1}{\partial t_0} + \mathcal{N}(e^{-s\mathcal{L}}\bar{\boldsymbol{u}}, e^{-s\mathcal{L}'}\bar{\boldsymbol{u}}_1) + \mathcal{N}(e^{-s\mathcal{L}'}\bar{\boldsymbol{u}}_1, e^{-s\mathcal{L}}\bar{\boldsymbol{u}})\right) ds, \tag{3.24}$$

where $\boldsymbol{u}_1 = e^{-\tau\mathcal{L}'}\bar{\boldsymbol{u}}_1$, expressed as $\{\bar{\boldsymbol{u}}_1\}^\alpha_{\boldsymbol{k}} e^{-i(\omega_1+\omega_2)\tau}$ in the eigenmode basis for some input modes subscripted 1 and 2. We now consider each term individually. Taking the first term on the right hand side:

$$-\lim_{\tau\to\infty}\frac{1}{\tau}\int_0^\tau \left\{e^{s(\mathcal{L}-\mathcal{L}')}\frac{\partial \bar{\boldsymbol{u}}_1}{\partial t_0}\right\}^\alpha_{\boldsymbol{k}} ds$$
$$= -\sum_{\substack{\boldsymbol{k}_1,\boldsymbol{k}_2\\ \alpha_1,\alpha_2}} \frac{C^{\alpha_1\alpha_2\alpha}_{\boldsymbol{k}_1\boldsymbol{k}_2\boldsymbol{k}}\big|_{nr}}{i(\omega-\omega_1-\omega_2)}\ \delta_{\boldsymbol{k}-\boldsymbol{k}_1-\boldsymbol{k}_2} \lim_{\tau\to\infty}\frac{1}{\tau}\int_0^\tau \frac{\partial}{\partial t_0}(a^{\alpha_1}_{\boldsymbol{k}_1} a^{\alpha_2}_{\boldsymbol{k}_2})\boldsymbol{r}^\alpha_{\boldsymbol{k}} e^{i(\omega-\omega_1-\omega_2)s} ds. \tag{3.25}$$

Now from (3.18) the derivative in the integrand can be expanded:

$$\begin{aligned}\frac{\partial}{\partial t_0}(a_{\boldsymbol{k}_1}^{\alpha_1}a_{\boldsymbol{k}_2}^{\alpha_2}) =& a_{\boldsymbol{k}_1}^{\alpha_1}\frac{\partial}{\partial t_0}(a_{\boldsymbol{k}_2}^{\alpha_2}) + a_{\boldsymbol{k}_2}^{\alpha_2}\frac{\partial}{\partial t_0}(a_{\boldsymbol{k}_1}^{\alpha_1}) \\ &= a_{\boldsymbol{k}_1}^{\alpha_1}\sum_{\substack{\boldsymbol{k}_a,\boldsymbol{k}_b\\ \alpha_2,\alpha_a,\alpha_b\\ \boldsymbol{k}_2=\boldsymbol{k}_a+\boldsymbol{k}_b}} C_{\boldsymbol{k}_a\boldsymbol{k}_b\boldsymbol{k}_2}^{\alpha_a\alpha_b\alpha_2}a_{\boldsymbol{k}_a}^{\alpha_a}a_{\boldsymbol{k}_b}^{\alpha_b} \;+\; a_{\boldsymbol{k}_2}^{\alpha_2}\sum_{\substack{\boldsymbol{k}_a,\boldsymbol{k}_b\\ \alpha_a,\alpha_b\\ \boldsymbol{k}_1=\boldsymbol{k}_a+\boldsymbol{k}_b}} C_{\boldsymbol{k}_a\boldsymbol{k}_b\boldsymbol{k}_1}^{\alpha_a\alpha_b\alpha_1}a_{\boldsymbol{k}_a}^{\alpha_a}a_{\boldsymbol{k}_b}^{\alpha_b}. \end{aligned} \tag{3.26}$$

None of these terms have any τ dependence, and so the derivative can be moved outside the integral and the limit:

$$\begin{aligned}&-\lim_{\tau\to\infty}\frac{1}{\tau}\int_0^\tau\left\{e^{s(\mathcal{L}-\mathcal{L}')}\frac{\partial\bar{\boldsymbol{u}}_1}{\partial t_0}\right\}_{\boldsymbol{k}}^{\alpha} ds \\ &\quad= -\sum_{\substack{\boldsymbol{k}_1,\boldsymbol{k}_2\\ \alpha_1,\alpha_2}}\frac{C_{\boldsymbol{k}_1\boldsymbol{k}_2\boldsymbol{k}}^{\alpha_1\alpha_2\alpha}\big|_{nr}}{i(\omega-\omega_1-\omega_2)}\,\delta_{\boldsymbol{k}-\boldsymbol{k}_1-\boldsymbol{k}_2}\frac{\partial}{\partial t_0}(a_{\boldsymbol{k}_1}^{\alpha_1}a_{\boldsymbol{k}_2}^{\alpha_2})\boldsymbol{r}_{\boldsymbol{k}}^{\alpha}\lim_{\tau\to\infty}\frac{1}{\tau}\int_0^\tau e^{i(\omega-\omega_1-\omega_2)s}ds. \end{aligned} \tag{3.27}$$

We now have, similarly to the treatment of equation (3.14) at the triad order, that the limit:

$$\lim_{\tau\to\infty}\frac{1}{\tau}\int_0^\tau e^{i(\omega-\omega_1-\omega_2)s}ds, \tag{3.28}$$

will send every term to 0 by cancellation of oscillations, unless $\omega-\omega_1-\omega_2=0$. We know that no terms have this form as we required the triad to be non-resonant and hence this term must be 0.

We now consider the second term of (3.24). Writing in the eigenmode basis we see that upon substitution of (3.22) we form various quartet resonances from the terms within the integral:

$$\begin{aligned}&-\lim_{\tau\to\infty}\frac{1}{\tau}\int_0^\tau\left\{e^{s\mathcal{L}}\mathcal{N}(e^{-s\mathcal{L}}\bar{\boldsymbol{u}},e^{-s\mathcal{L}'}\bar{\boldsymbol{u}}_1)\right\}_{\boldsymbol{k}}^{\alpha}ds \\ &=-\lim_{\tau\to\infty}\frac{1}{\tau}\int_0^\tau\sum_{\substack{\boldsymbol{k}_a,\boldsymbol{k}_3\\ \alpha_a,\alpha_3}}C_{\boldsymbol{k}_a\boldsymbol{k}_3\boldsymbol{k}}^{\alpha_a\alpha_3\alpha}\boldsymbol{r}_{\boldsymbol{k}}^{\alpha}a_{\boldsymbol{k}_3}^{\alpha_3}e^{-i\omega_3 s}\delta_{\boldsymbol{k}-\boldsymbol{k}_a-\boldsymbol{k}_3}\sum_{\substack{\boldsymbol{k}_1,\boldsymbol{k}_2\\ \alpha_1,\alpha_2}}\frac{C_{\boldsymbol{k}_1\boldsymbol{k}_2\boldsymbol{k}_a}^{\alpha_1\alpha_2\alpha_a}\big|_{nr}a_{\boldsymbol{k}_1}^{\alpha_1}a_{\boldsymbol{k}_2}^{\alpha_2}}{i(\omega_a-\omega_1-\omega_2)}e^{-i(\omega_1+\omega_2)s}\;\delta_{\boldsymbol{k}_a-\boldsymbol{k}_1-\boldsymbol{k}_2}e^{i\omega s}ds \\ &=-\sum_{\substack{\boldsymbol{k}_a,\boldsymbol{k}_3\\ \alpha_a,\alpha_3}}\sum_{\substack{\boldsymbol{k}_1,\boldsymbol{k}_2\\ \alpha_1,\alpha_2}}\lim_{\tau\to\infty}\frac{1}{\tau}\int_0^\tau\frac{C_{\boldsymbol{k}_a\boldsymbol{k}_3\boldsymbol{k}}^{\alpha_a\alpha_3\alpha}\;C_{\boldsymbol{k}_1\boldsymbol{k}_2\boldsymbol{k}_a}^{\alpha_1\alpha_2\alpha_a}\big|_{nr}}{i(\omega_a-\omega_1-\omega_2)}a_{\boldsymbol{k}_1}^{\alpha_1}a_{\boldsymbol{k}_2}^{\alpha_2}a_{\boldsymbol{k}_3}^{\alpha_3}\boldsymbol{r}_{\boldsymbol{k}}^{\alpha}e^{i(\omega-\omega_1-\omega_2-\omega_3)s}\;\delta_{\boldsymbol{k}-\boldsymbol{k}_1-\boldsymbol{k}_2-\boldsymbol{k}_3}ds \\ &=-\sum_{\substack{\boldsymbol{k}_1,\boldsymbol{k}_2,\boldsymbol{k}_3\\ \alpha_a,\alpha_1,\alpha_2,\alpha_3}}\frac{C_{\boldsymbol{k}_a\boldsymbol{k}_3\boldsymbol{k}}^{\alpha_a\alpha_3\alpha}\;C_{\boldsymbol{k}_1\boldsymbol{k}_2\boldsymbol{k}_a}^{\alpha_1\alpha_2\alpha_a}\big|_{nr}}{i(\omega_a-\omega_1-\omega_2)}a_{\boldsymbol{k}_1}^{\alpha_1}a_{\boldsymbol{k}_2}^{\alpha_2}a_{\boldsymbol{k}_3}^{\alpha_3}\boldsymbol{r}_{\boldsymbol{k}}^{\alpha}\delta_{\omega-\omega_1-\omega_2-\omega_3}\;\delta_{\boldsymbol{k}-\boldsymbol{k}_1-\boldsymbol{k}_2-\boldsymbol{k}_3}. \end{aligned} \tag{3.29}$$

By the symmetry of the nonlinear interaction coefficient the third term of (3.24) is identical to the second and so we can now write the whole equation as:

$$\frac{\partial}{\partial t_1}\{\bar{\boldsymbol{u}}\}_{\boldsymbol{k}}^{\alpha} = -\sum_{\substack{\boldsymbol{k}_1,\boldsymbol{k}_2,\boldsymbol{k}_3\\ \alpha_1,\alpha_2,\alpha_3}}Q_{\boldsymbol{k}_1\boldsymbol{k}_2\boldsymbol{k}_3\boldsymbol{k}}^{\alpha_1\alpha_2\alpha_3\alpha}a_{\boldsymbol{k}_1}^{\alpha_1}a_{\boldsymbol{k}_2}^{\alpha_2}a_{\boldsymbol{k}_3}^{\alpha_3}\boldsymbol{r}_{\boldsymbol{k}}^{\alpha}\delta_{\omega-\omega_1-\omega_2-\omega_3}\;\delta_{\boldsymbol{k}-\boldsymbol{k}_1-\boldsymbol{k}_2-\boldsymbol{k}_3}, \tag{3.30}$$

where:

$$Q^{\alpha_1\alpha_2\alpha_3\alpha}_{\boldsymbol{k}_1\boldsymbol{k}_2\boldsymbol{k}_3\boldsymbol{k}} = \sum_{\alpha_a} \frac{2C^{\alpha_a\alpha_3\alpha}_{\boldsymbol{k}_a\boldsymbol{k}_3\boldsymbol{k}}\, C^{\alpha_1\alpha_2\alpha_a}_{\boldsymbol{k}_1\boldsymbol{k}_2\boldsymbol{k}_a}\big|_{nr}}{i(\omega_a - \omega_1 - \omega_2)}, \tag{3.31}$$

and $\boldsymbol{k_a} = \boldsymbol{k_1} + \boldsymbol{k_2}$ and $\boldsymbol{k_a} = \boldsymbol{k} - \boldsymbol{k_3}$.

Similarly to the triad case it is useful to symmetrise this in the input coefficients (1,2,3) as follows:

$$Q^{\alpha_1\alpha_2\alpha_3\alpha}_{\boldsymbol{k}_1\boldsymbol{k}_2\boldsymbol{k}_3\boldsymbol{k}} = \frac{2}{3}\left[\sum_{\alpha_a} \frac{C^{\alpha_a\alpha_3\alpha}_{\boldsymbol{k}_a\boldsymbol{k}_3\boldsymbol{k}}\, C^{\alpha_1\alpha_2\alpha_a}_{\boldsymbol{k}_1\boldsymbol{k}_2\boldsymbol{k}_a}\big|_{nr}}{i(\omega_a - \omega_1 - \omega_2)} + \sum_{\alpha_b} \frac{C^{\alpha_b\alpha_1\alpha}_{\boldsymbol{k}_b\boldsymbol{k}_1\boldsymbol{k}}\, C^{\alpha_2\alpha_3\alpha_b}_{\boldsymbol{k}_2\boldsymbol{k}_3\boldsymbol{k}_b}\big|_{nr}}{i(\omega_b - \omega_2 - \omega_3)} + \sum_{\alpha_c} \frac{C^{\alpha_c\alpha_2\alpha}_{\boldsymbol{k}_c\boldsymbol{k}_2\boldsymbol{k}}\, C^{\alpha_3\alpha_1\alpha_c}_{\boldsymbol{k}_3\boldsymbol{k}_1\boldsymbol{k}_c}\big|_{nr}}{i(\omega_c - \omega_3 - \omega_1)}\right]. \tag{3.32}$$

Here each of the three permutations of waves $1, 2, 3$ has been summed,and then divided by 3, such that the interaction coefficient is identical no matter the ordering of the input waves.

Figure 3.1 shows diagrammatically how the non-resonant triads combine to form a quartet.

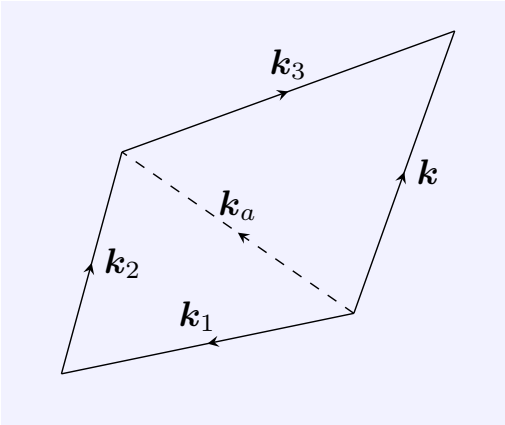

Figure 3.1: Quartet construction, as in Equation (3.31). The wave vector $\boldsymbol{k}_a$ takes the form of a slaved mode that can be projected onto our eigenbasis such that there are fast-like parts and a slow-like part. Each quartet has three possible sets of wavenumbers that can contribute to the quartet, ie $\boldsymbol{k}_a = \boldsymbol{k}_1 + \boldsymbol{k}_2$, $\boldsymbol{k}_b = \boldsymbol{k}_3 + \boldsymbol{k}_2$, and $\boldsymbol{k}_c = \boldsymbol{k}_1 + \boldsymbol{k}_3$.

This completes the asymptotic expansion up to the quartet order of expansion, defining all dynamics up to the t_1 timescale. We can now move on to the higher orders of expansion.

3.4 Above quartet order

In a similar manner of linking triads together one can form 'n-tets', a term we introduce as the generalisation of triads, quartets, quintets, sextets etc, for combinations of n modes. In the following we establish a general form for the mathematics of these interactions, from which we can deduce results that hold to all orders of expansion.

The n-tets are defined by the pth order equation:

$$O(\epsilon^p) \qquad \frac{\partial \boldsymbol{u}_{p+1}}{\partial \tau} + \mathcal{L}\boldsymbol{u}_{p+1} = -\sum_{m=0}^{p}\left(\frac{\partial \boldsymbol{u}_{p-m}}{\partial t_m} + \mathcal{N}(\boldsymbol{u}_m, \boldsymbol{u}_{p-m})\right), \tag{3.33}$$

the general form of equations (3.6)-(3.8), where $p = n - 3$.

	$\boldsymbol{u}_0$	$\boldsymbol{u}_1$	$\boldsymbol{u}_2$	$\boldsymbol{u}_3$	$\boldsymbol{u}_4$	...
$O(1/\epsilon)$	τ	-	-	-	-	...
$O(1)$	t_0	τ	-	-	-	...
$O(\epsilon)$	t_1	t_0	τ	-	-	...
$O(\epsilon^2)$	t_2	t_1	t_0	τ	-	...
$O(\epsilon^3)$	t_3	t_2	t_1	t_0	τ	...
$\vdots$	$\vdots$	$\vdots$	$\vdots$	$\vdots$	$\vdots$	$\ddots$

Table 3.1: For given order of the equations, the timescale to which each order of the solution is considered is given. The timescales given in red are completely determined as they are simply derived from slaved modes and so their behaviour is inherited from the behaviour of $\boldsymbol{u}_0$ to the required timescale.

Consider table 3.1, which breaks down the dependence of each order of the asymptotic series in terms of its dependence on the various timescales. The terms in red are those which are already determined by the behaviour of $\boldsymbol{u}_0$, ie slaved. Hence, in the same manner with which we justified that the left hand term in (3.24) was negligible, our secularity condition will never contain any of the time derivatives in (3.33) other than that of $\partial \boldsymbol{u}_0/\partial t_p$. Crucially, this means that the terms defining the evolution on the t_p timescale will always reduce to just the nonlinear combinations $\mathcal{N}(\boldsymbol{u}_a, \boldsymbol{u}_b)$ for all non-negative integers a, b such that $p = a + b$. The dynamics of each of the contributing components $\boldsymbol{u}_a, \boldsymbol{u}_b$ can be calculated as a function of those at lower orders which in turn behave in the same way, until all motion is determined by the $\boldsymbol{u}_0$ terms. We can therefore calculate a general higher order interaction coefficient as a recurrence relation.

We start by calculating the different possible combinations a, b available for the nonlinear part $\mathcal{N}(\boldsymbol{u}_a, \boldsymbol{u}_b)$. Given some input $\boldsymbol{u}_a$ this must be formed of $a+1$ $\boldsymbol{u}_0$ modes in an $a+2$-tet, and similarly for $\boldsymbol{u}_b$. In the output triad we have $a + b + 2$ input $\boldsymbol{u}_0$ modes that must be split into the two groups of sizes $a + 1,\ b + 1$. Define $n = a + b + 1$ so that n is the order of interaction ($n = 1$ corresponds to triads), and $r = b + 1$, the number of input modes into the second triad, the first triad then has $n - r + 1 = a + 1$ input modes. The number of possible mode permutations then corresponds to

$(n+1)!$ where these are shared between the two input n-tets in the division determined by the value of r.

To symmetrise the interaction coefficient we must add all permutations of the input wavenumbers and then divide by the number of them, $(n+1)!$. Due to symmetries in the input interaction coefficients there will be repeated contributions ie $C^{\alpha_1\alpha_2\alpha_a}_{\boldsymbol{k}_1\boldsymbol{k}_2\boldsymbol{k}_a}$ and $C^{\alpha_2\alpha_1\alpha_a}_{\boldsymbol{k}_2\boldsymbol{k}_1\boldsymbol{k}_a}$ will both appear in different terms of the relation, although both are equal. However the relation is most simply stated in the form given below.

For each of the permutations the quantity required will be the multiplication of the two input n-tet coefficients with a triad coefficient that takes these two outputs as its inputs and returns the output. This manner of combining smaller n-tets is displayed diagrammatically in figure 3.2. We then need to sum over each possible r, to give all possible splittings into two n-tets.

Combining these components we get the interaction coefficients, to any desired order, defined inductively as follows:

$$\{C^{(n)}\}^{\alpha_1\ldots\alpha_{n+2}\alpha}_{\boldsymbol{k}_1\ldots\boldsymbol{k}_{n+1}\boldsymbol{k}} = \frac{1}{(n+1)!}\sum_{r=1}^{n}\left[\sum_{\alpha_a,\alpha_b}\frac{\{C^{(1)}\}^{\alpha_a\alpha_b\alpha}_{\boldsymbol{k}_a\boldsymbol{k}_b\boldsymbol{k}}\ \{C^{(r-1)}\}^{\alpha_{n-r+2}\ldots\alpha_{n+1}\alpha_b}_{\boldsymbol{k}_{n-r+2}\ldots\boldsymbol{k}_{n+1}\boldsymbol{k}_b}\Big|_{nr}\ \{C^{(n-r)}\}^{\alpha_1\ldots\alpha_{n-r+1}\alpha_a}_{\boldsymbol{k}_1\ldots\boldsymbol{k}_{n-r+1}\boldsymbol{k}_a}\Big|_{nr}}{-\{\Omega^{(n-r)}\}^{a}_{1,\ldots,n-r+1}\{\Omega^{(r-1)}\}^{b}_{n-r+2,\ldots,n+1}} + \textit{input wavenumber permutations}\right], \tag{3.34}$$

where: $\{\Omega^{(n)}\}^{a}_{b,\ldots,c} = \omega_a - \omega_b - \ldots - \omega_c$.

Where $C^{(n)}$ is the nonlinear interaction coefficient at the nth closure (ie $n=1$ would be triad interactions at the first closure). We need to define the particular case of $\{C^{(0)}\}^{\alpha_i\alpha}_{\boldsymbol{k}_i\boldsymbol{k}} = 1$ such that it is simply an identity mapping with $\boldsymbol{k}_i = \boldsymbol{k}$, $\alpha_i = \alpha$. We also define separately $\Omega^{(0)} = -i$. These special cases are necessary terms corresponding to $\mathcal{N}(\boldsymbol{u}_0, \boldsymbol{u}_{n-1})$ where an $n-1$-tet is combined with a mode, not another n-tet.

This allows one to algorithmically compute a given interaction coefficient to any order, making higher order resonant simulations feasible. Although the coefficients are very computationally intensive to calculate (exponential complexity in the order n of the coefficent), they are fixed quantities of a system and can be calculated and stored before the simulation is run. Symmetries may allow for a more efficient calculation although they will not be explored here.

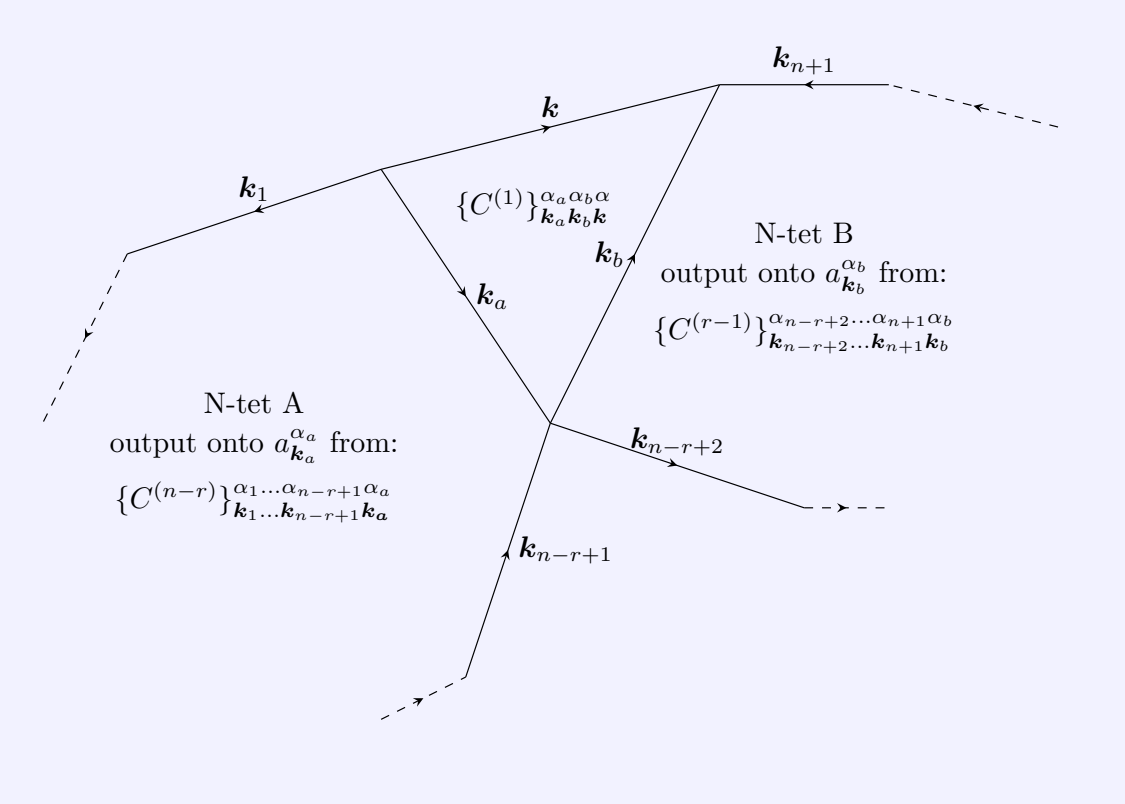

n-tet construction.

Figure 3.2: Diagram of the n-tet construction, Two smaller N-tets, A&B of sizes $n-r+2$ and $r+1$ respectively, output the two modes a, and b that go into a connecting triad that returns the output mode with wavenumber $\boldsymbol{k}$. All possible combinations must be considered in a similar manner, summed, and then the coefficient symmetrised to give the equation in (3.34)

3.5 Chapter summary

The following constitute the key points of the chapter:

- The method of multiple scales as a valid asymptotic approximation for weakly nonlinear equations was derived.
- The resonances that describe the key contributing components at each timescale of the equations were derived.
- It was shown how higher order resonances are formed by combination of non-resonant triads.
- A new generalised higher order interaction coefficient was defined by recurrence relation for any system with quadratic nonlinearity (3.34).

Chapter 4

Applications to rotating stratified flows

The geophysical fluid systems introduced in chapter 2 are now investigated using the theory of the previous chapter to form an expansion up to triad order and then beyond. This allows several conclusions to be drawn about the behaviour of each system, specifically new conclusions are drawn on the fast wave interactions in the two layer rotating shallow water equations, and generalisations are made about the higher order behaviour of all the examples.

We start, in section 4.1 by defining the quasigeostrophic limit in each system by showing how the equations can be put in non-dimensional form. Then in sections 4.2, 4.3 and 4.5 we perform the multiscale expansion to each equation set. Section 4.4 gives an alternative method of deriving the asymptotic series from which we can use conservation laws to derive interaction coefficients of the equations, and from this we can draw conclusions general to layered equations. The existing literature on the shallow water equations is recovered up to triad order, and to higher orders the literature is reconfirmed in the new general setting, and extends to arbitrary order using the new framework. For the two layer shallow water equations (with the analysis based on that of Owen, Grimshaw, and Wingate 2018) we find new behaviour, with interactions between fast modes in the barotropic and baroclinic parts of the flow, which we discuss in detail. The strength of these new interactions is considered against the others present in the flow, and it is discussed how the new interaction could be entirely neglected in a discrete domain, unless near resonances are taken into account. This motivates the following chapters where near resonant expansions will be derived and applied to the systems, and it will be found that a subset of the higher order interactions can occur on the triad timescale. The stratified equations are briefly discussed in a general manner to show the difference in some of the conclusions of the higher order theory to

the layered systems.

4.1 The quasigeostrophic limit

In the following sections the specific weakly nonlinear limit that will be taken for the example systems is derived in each case.

4.1.1 Rotating shallow water equations

We non-dimensionalise the variables as follows:

$$\begin{aligned} &x, y \sim L, \qquad u, v \sim U, \qquad t \sim L/U, \\ &H \sim H, \qquad \eta \sim D, \end{aligned} \tag{4.1}$$

where L, D and U are appropriate scales for each quantity, and hence:

$$\nabla \sim \frac{1}{L}, \qquad (\boldsymbol{u} \cdot \nabla)\boldsymbol{u} \sim \frac{U^2}{L}, \qquad \frac{\partial}{\partial t} \sim \frac{U}{L}. \tag{4.2}$$

We reduce the parameters to the standard non-dimensional set of Rossby, Froude, and amplitude ratio respectively:

$$Ro = \frac{U}{fL}, \qquad Fr = \frac{U}{\sqrt{gH}}, \qquad \theta = \frac{D}{H}. \tag{4.3}$$

The resulting non-dimensional equations are:

$$\frac{D\boldsymbol{u}'}{Dt'} + Ro^{-1}\hat{\boldsymbol{z}} \times \boldsymbol{u}' = -Fr^{-2}\theta\nabla\eta', \tag{4.4}$$

$$\frac{\partial \eta'}{\partial t'} + \theta^{-1}\nabla \cdot \boldsymbol{u}' + \nabla \cdot (\eta'\boldsymbol{u}') = 0, \tag{4.5}$$

where $'$ indicates the non-dimensionalised variables.

We consider the linear terms in the expression, those where we have gathered the non-dimensional parameters. We want these to be an order greater than the nonlinear terms which we have now scaled to $O(1)$, and hence we require:

$$Ro^{-1} \sim \epsilon^{-1}, \qquad Fr^{-2}\theta \sim \epsilon^{-1}, \qquad \theta^{-1} \sim \epsilon^{-1}. \tag{4.6}$$

From which we read off $Ro \sim \epsilon$, $Fr \sim \epsilon$, $\theta \sim \epsilon$, which we note is just a more precise version of the statement all variables scale like ϵ, where the sizes have been defined with reference to the parameters and length scales. We also define at this point the Burger number $Bu = Ro^2/Fr^2 \sim O(1)$.

This is the standard quasigeostrophic limit, originally used by Charney 1948. In order to consider different physical scenarios when we continue the analysis, the original dimensional variables will be used. However there is an underlying assumption that implicitly this is an asymptotic limit as $\epsilon \to 0$.

4.1.2 Two layer Rotating shallow water equations

The quasigeostrophic scaling for the two layer case follows similarly.

We non-dimensionalise (assuming that the variables in each layer are the same order of magnitude) as follows:

$$\begin{aligned} &x, y \sim L, \qquad u_i, v_i \sim U, \qquad t \sim L/U, \\ &H_i \sim H, \qquad \eta_i \sim D, \qquad p_i \sim gD. \end{aligned} \tag{4.7}$$

The length scale L can be chosen to be one of the two deformation scales c_m/f where c_m is the linear long wave phase speed defined above in (2.103). We reduce to Rossby, Froude, and amplitude ratio as with the one layer equations in section 4.1.1 above, and the resulting non-dimensional equations are similar but now layer-wise:

$$\frac{D\boldsymbol{u}_i'}{Dt'} + Ro^{-1}\hat{\boldsymbol{z}} \times \boldsymbol{u}_i' = -Fr^{-2}\theta \nabla p_i', \tag{4.8}$$

$$\frac{\partial \eta_i'}{\partial t'} + \theta^{-1}\nabla \cdot \boldsymbol{u}_i' + \nabla \cdot (\eta_i' \boldsymbol{u}_i') = 0, \tag{4.9}$$

where $'$ indicates the non-dimensionalised variables.

It should be noted that the assumption that the scalings are the same in each layer automatically leads to the same assumption in each vertical mode (as defined above in (2.106)). However we have said nothing about the relative density or height scaling between the layers. Two common possible scalings are the rigid lid limit and the thin layer limit which we shall define here (taken from Owen, Grimshaw, and Wingate 2018) for completeness. However later results will be provided for the more pedestrian limit where both densities are assumed to be $O(1)$.

Rigid lid limit

The rigid lid approximation is a specific case of the two layer equations used in geophysical applications. The rigid lid equations are only physically realised when the top layer is at a fixed solid boundary, otherwise they are an approximation based on the (unphysical) assumptions that the gravitational force is large compared to the Coriolis force and the densities of the two layers are close. In this parameter regime the sizes of waves on the external boundary are negligible compared to the size of the waves on the internal layer. The limit $g \to \infty$ is used to force rigidity in the upper layer when no physical boundary actually exists. This limit is taken separately to the asymptotic limit we are taking; this defines the basic system before any other assumptions are made.

We start the derivation (see Salmon 1998) by taking $r \to 1$ and defining the reduced gravity $g' = g(1-r)$ which we then require to be finite in the limit. The transformation to external and internal modes then becomes:

$$L_m = \begin{cases} 1 & m = +, \\ -\frac{H_2}{H_1} & m = -, \end{cases} \tag{4.10}$$

$$c_m^2 = \begin{cases} g(H_1 + H_2) & m = +, \\ \frac{g' H_1 H_2}{H_1 + H_2} & m = -, \end{cases} \tag{4.11}$$

by setting $r = 1 - \delta$, $g' = g\delta$, $\delta \ll 1$ and taking Taylor series in δ.

Because in this limit we take $g \to \infty$, the external wave speed becomes infinite ($c_+ \to \infty$) and the corresponding external Rossby radius of deformation $\lambda_+ = c_+/f \to \infty$ as well. By definition, below the Rossby radius of deformation the surface displacement, and hence fast modes, are negligible and so for an infinite radius all fast modes must be neglected. This corresponds to the external boundary becoming fixed in the long wave limit. Effectively waves cannot propagate on the external boundary and so it becomes 'rigid'.

Another consequence of this limit is that the pressure in the external mode becomes undefined, changing the structure of the equations: this pressure can no longer evolve in time. This means that if the external mode is initially defined as motionless the equations only describe the internal mode in a one layer system similar to the usual one.

When we subsequently consider the two layer equations we are interested in the interactions between the layers, and hence the rigid rid limit will not be imposed so as not to reduce the degrees of freedom of the two layers.

Thin layer limit

Another application relevant to the ocean is to make the upper layer thin compared to the lower layer. However this would change the analysis completely: the thin layer/internal mode will be pushed to the next order of the expansion and so the leading order effects will be equivalent to the one layer case, with corrections at higher order. Effectively this would violate the weakly nonlinear assumption we have just made, we wish to maintain amplitude separation of the linear and nonlinear parts.

To see this consider the amplitude ratio $D/H \sim \epsilon$. If we choose one of our layer depths to be asymptotically small, to avoid violation of this condition we require $D \sim \epsilon^2$ and so all of the dynamics of this layer can only affect the $O(\epsilon^2)$ terms and higher in the non-triad interactions.

Equivalently setting $H_1 = H$, $H_2 = H\epsilon$ in (2.103):

$$c_m^2 = gH \begin{cases} 1 + \frac{r_\rho}{4}\epsilon \quad + O(\epsilon^2) & m = +, \\ (1 - \frac{r_\rho}{4})\epsilon \; + O(\epsilon^2) & m = -, \end{cases}$$

$$L_m = \begin{cases} 1 - (\frac{r_\rho}{4} - 1)\epsilon \; + O(\epsilon^2) & m = +, \\ -\frac{r_\rho}{4}\epsilon \qquad\qquad\quad + O(\epsilon^2) & m = -, \end{cases}$$

which shows that the internal mode will be asymptotically small and asymptotically slow in our calculations.

4.1.3 Stratified equations

To form the quasigeostrophic limit for the stratified equations we start by non-dimensionalising (similarly to Embid and Majda 1996 for example) as follows:

$$\begin{aligned} &x, y, z \sim L, \qquad u, v, w \sim U, \qquad t \sim L/U, \\ &\sigma \sim S, \qquad \eta \sim D, \qquad P \sim P. \end{aligned} \tag{4.12}$$

We reduce the parameters to the Rossby, Froude, and Euler numbers and a ratio of buoyancy to velocity, now defined as:

$$Ro = \frac{U}{fL}, \qquad Fr = \frac{U}{LN}, \qquad Eu = \frac{P}{U^2}, \qquad \Gamma = \frac{SL}{U^2}. \tag{4.13}$$

The resulting non-dimensional equations are:

$$\frac{D\boldsymbol{u}'}{Dt'} + Ro^{-1}\hat{\boldsymbol{z}} \times \boldsymbol{u}' = -Eu\nabla' P' - \Gamma\sigma\hat{\boldsymbol{z}}, \tag{4.14}$$

$$\frac{\partial\sigma'}{\partial t'} + (\boldsymbol{u}' \cdot \nabla')\sigma' - Fr^{-2}\Gamma^{-1}w' = 0, \tag{4.15}$$

$$\nabla' \cdot \boldsymbol{u}' = 0, \tag{4.16}$$

where $'$ indicates the non-dimensionalised variables.

As for the layered equations we need the linear part to scale like ϵ^{-1} and so we have the following scalings:

$$Ro,\ Fr \sim \epsilon, \qquad Eu,\ \Gamma \sim \epsilon^{-1}. \tag{4.17}$$

This defines the quasigeostrophic scaling for the stratified equations.

The geostrophic limit will be assumed in all of the following examples, rendering them weakly nonlinear, and therefore appropriate for multiple scale theory.

4.2 Rotating Shallow Water Equations

We now derive the multiscale expansion for the rotating shallow water equations, the simplest of the geophysical applications presented in this thesis.

There are many sources for the multiple scales theory on the rotating shallow water equations. A few relevant examples amongst the many are Warn 1986, and Embid and Majda 1996, and examples that expand up to the quartet order include Reznik, Zeitlin, and Ben Jelloul 2001 and Thomas 2016. We will use the theory of Chapter 3 to rederive this expansion up to triad order, and then to deduce the higher order results, recovering some of their work and extending it further. The aim is to try to show that the specific quartet results of these authors are easily explained in the context of zero mode systems, using the framework set out in the previous chapter.

4.2.1 Nonlinear Interaction coefficient

From (3.15) the interaction coefficient takes the form:

$$C^{\alpha_1\alpha_2\alpha}_{\boldsymbol{k}_1\boldsymbol{k}_2\boldsymbol{k}} = \frac{i}{2}\Big[(\boldsymbol{v}^{\alpha_1}_{\boldsymbol{k}_1}\cdot\boldsymbol{k}_2)(\boldsymbol{v}^{\alpha_2}_{\boldsymbol{k}_2}\cdot\boldsymbol{v}^{\alpha}_{\boldsymbol{k}}) + (\boldsymbol{v}^{\alpha_2}_{\boldsymbol{k}_2}\cdot\boldsymbol{k}_1)(\boldsymbol{v}^{\alpha_1}_{\boldsymbol{k}_1}\cdot\boldsymbol{v}^{\alpha}_{\boldsymbol{k}}) + (\boldsymbol{v}^{\alpha_1}_{\boldsymbol{k}_1}\cdot(\boldsymbol{k}_1+\boldsymbol{k}_2))\phi^{\alpha_2}_{\boldsymbol{k}_2}\phi^{\alpha m*}_{\boldsymbol{k}} + (\boldsymbol{v}^{\alpha_2}_{\boldsymbol{k}_2}\cdot(\boldsymbol{k}_1+\boldsymbol{k}_2))\phi^{\alpha_1}_{\boldsymbol{k}_1}\phi^{\alpha *}_{\boldsymbol{k}}\Big], \tag{4.18}$$

where $\boldsymbol{v} = (u, v)^T$, $\boldsymbol{r}^{\alpha}_{\boldsymbol{k}} = (\boldsymbol{v}^{\alpha}_{\boldsymbol{k}}, \phi^{\alpha}_{\boldsymbol{k}})^T$ and * denotes the complex conjugate.

We then calculate the interaction coefficients explicitly by substitution of the system's eigenvectors (2.85) into (4.18): For the slow modes:

$$C^{0,0,0}_{\boldsymbol{k}_1\boldsymbol{k}_2\boldsymbol{k}} = \frac{c(\boldsymbol{k}_2\times\boldsymbol{k}_1)}{2\omega\omega_1\omega_2}\left(\omega_2^2-\omega_1^2\right). \tag{4.19}$$

Here ω_i is the unsigned frequency for the wave with wavenumber $\boldsymbol{k}_i$.

For two slow and one fast mode:

$$C^{\alpha_1,0,0}_{\boldsymbol{k}_1\boldsymbol{k}_2\boldsymbol{k}} = \frac{i\omega_2}{2\sqrt{2}\omega\omega_1|\boldsymbol{k}_1|}\Big[if(\boldsymbol{k}_2\times\boldsymbol{k}_1)_z + \alpha_1\omega_1(\boldsymbol{k}_1\cdot\boldsymbol{k})\Big], \tag{4.20}$$

$$C^{0,0,\alpha}_{\boldsymbol{k}_1\boldsymbol{k}_2\boldsymbol{k}} = \frac{i(\boldsymbol{k}_1\times\boldsymbol{k}_2)_z}{2\sqrt{2}\omega\omega_1\omega_2c^2|\boldsymbol{k}|}\Big[2\alpha\omega(\boldsymbol{k}_2\times\boldsymbol{k}_1)_z + ifc^2\left(\omega_1^2-\omega_2^2\right)\Big]. \tag{4.21}$$

For two fast and a slow mode:

$$C^{\alpha_1\alpha_20}_{\boldsymbol{k}_1\boldsymbol{k}_2\boldsymbol{k}} = \quad 0, \tag{4.22}$$

$$C^{\alpha_10\alpha}_{\boldsymbol{k}_1\boldsymbol{k}_2\boldsymbol{k}} = \frac{i}{4c\omega\omega_1\omega_2|\boldsymbol{k}||\boldsymbol{k}_1|}\Big[2i(\alpha\alpha_1\omega_1\omega - f^2)c^2(\boldsymbol{k}\cdot\boldsymbol{k_1})(\boldsymbol{k}_1\times\boldsymbol{k})_z) - i\alpha\alpha_1\omega_1\omega c^2(\boldsymbol{k}_1\times\boldsymbol{k})_z|\boldsymbol{k}_1|^2 + \alpha_1\omega_1fc^2(\boldsymbol{k}\cdot\boldsymbol{k_1})|\boldsymbol{k}_1|^2) + 2\alpha\omega c^2f(\boldsymbol{k}\times\boldsymbol{k}_1)_z^2 + ic^4|\boldsymbol{k}_1|^2|\boldsymbol{k}|^2(\boldsymbol{k}\times\boldsymbol{k}_1)_z\Big]. \tag{4.23}$$

For three fast modes:

$$C^{\alpha_1\alpha_2\alpha}_{\boldsymbol{k}_1\boldsymbol{k}_2\boldsymbol{k}} = \frac{i}{4\sqrt{2}\omega\omega_1\omega_2|\boldsymbol{k}||\boldsymbol{k}_1||\boldsymbol{k}_2|}\Big[$$
$$\big(\alpha_1\omega_1\alpha_2\alpha\omega\omega_2(|\boldsymbol{k}_1|^2+|\boldsymbol{k}_2|^2)+(\alpha_1\omega_1|\boldsymbol{k}_1|^2+\alpha_2\omega_2|\boldsymbol{k}_2|^2)f^2\big)(\boldsymbol{k}_1\cdot\boldsymbol{k}_2)$$
$$+(2\alpha_1\omega_1\alpha_2\alpha\omega\omega_2+(\alpha_1\omega_1+\alpha_2\omega_2)f^2)(\boldsymbol{k}_1\cdot\boldsymbol{k}_2)^2+f^2(\alpha_2\omega_2-\alpha_1\omega_1)(\boldsymbol{k}_1\times\boldsymbol{k}_2)_z^2$$
$$+if(\alpha_2\alpha\omega\omega_2+f^2)|\boldsymbol{k}_2|^2(\boldsymbol{k}_2\times\boldsymbol{k}_1)_z-if(\alpha_1\alpha\omega\omega_1+f^2)|\boldsymbol{k}_1|^2(\boldsymbol{k}_2\times\boldsymbol{k}_1)_z$$
$$+c^2(\omega_1\alpha_1+\omega_2\alpha_2)|\boldsymbol{k}_2|^2|\boldsymbol{k}|^2|\boldsymbol{k}_1|^2+c^2(\omega_1\alpha_1|\boldsymbol{k}_2|^2+\omega_2\alpha_2|\boldsymbol{k}_1|^2)|\boldsymbol{k}|^2(\boldsymbol{k}_1\cdot\boldsymbol{k}_2)$$
$$+if c^2(|\boldsymbol{k}_2|^2-|\boldsymbol{k}_1|^2)|\boldsymbol{k}|^2(\boldsymbol{k}_2\times\boldsymbol{k}_1)_z\Big]. \tag{4.24}$$

These interaction coefficients were previously found in, and agree with those calculated in Ward and Dewar 2010 for example.

Throughout the thesis triads will be referred to in the format: type-type-type, so for example: slow-slow-fast triads. This should be understood to be two input slow modes acting to alter a fast mode: the right hand mode type will always represent the 'output' of the interaction. A second equivalent notation is used as well: $(\alpha_1,\alpha_2;\alpha)$, which for this example is written $(0,0;\pm)$. Both notations extend to higher order interactions, with the output mode on the far right hand side.

Trivially there can be no resonances between a fast mode and two slow ones. It can also be shown (see fast-fast-fast resonances subsection below) that there are no possible fast-only resonances. The only remaining interactions are the slow-slow-slow and the fast-slow-fast interactions. This gives a set of coupled equations, one for the slow mode evolution and the second to describe the evolution of the fast mode due to interaction with the slow mode (referred to as scattering by Ward and Dewar 2010 for example, also sometimes called the catalytic interaction). This is a key result in the fast-slow splitting of a system: the slow part of the flow is unaffected by the fast, and as only scattering of fast waves occurs there is no energy transfer between the two parts to triad order. It can be shown (for instance in the aforementioned references) that the slow mode evolution is exactly the usual barotropic quasigeostrophic equations.

Fast-fast-fast resonances

Here we prove that no resonances are possible between triads of three fast waves in this system. Other proofs can be found in Embid and Majda 1996 and Ward and Dewar 2010 for example. A graphical proof is also possible, as is done in the similar case of the two layer rotating shallow water equations in section 4.3.2.

We combine the triad and resonance conditions and write them explicitly as follows:

$$\pm\sqrt{c^2|\boldsymbol{k}_1+\boldsymbol{k}_2|^2+f^2}=\pm\sqrt{c^2|\boldsymbol{k}_1|^2+f^2}\pm\sqrt{c^2|\boldsymbol{k}_2|^2+f^2}. \tag{4.25}$$

We write $F=f/(c|\boldsymbol{k}_2|)$, $\cos\theta=(\boldsymbol{k}_1\cdot\boldsymbol{k}_2)/|\boldsymbol{k}_1||\boldsymbol{k}_2|$ and $K=|\boldsymbol{k}_1|/|\boldsymbol{k}_2|$, transforming the equation to:

$$\pm\sqrt{1+K^2+2K\cos\theta+F^2}=\pm\sqrt{K^2+F^2}\pm\sqrt{1+F^2}. \tag{4.26}$$

We square both sides rearrange and square again:

$$2K\cos\theta-F^2=\pm2\sqrt{K^2+F^2}\sqrt{1+F^2}, \tag{4.27}$$

$$K^2(F^2+\sin^2\theta)-F^2K\cos\theta+F^2+\frac{3}{4}F^4=0. \tag{4.28}$$

Equation (4.28) is quadratic in K and has no solutions as shown by the negative discriminant:

$$\begin{aligned}&F^4\cos^2\theta-(3F^4+4F^2)(F^2+\sin^2\theta)=\\&\quad-3F^4-4F^4\sin^2\theta-3F^6-4F^2\sin^2\theta)\leq0,\end{aligned} \tag{4.29}$$

where equality is only achieved by $F=0$, which requires 0 rotation. Approximate solutions can exist where $F=f/(c|\boldsymbol{k}_2|)$ is small (this is highly relevant to the near resonant expansion of the later chapters).

4.2.2 Higher Order theory

We have shown that the possible triad interactions are very limited, only two possible sets of modes can interact. We continue to higher order to see what other interactions can take place, and whether the unused triad combinations can act as building blocks to form a resonant pathway for quartet and higher order interactions.

We continue by using the theory from chapter 3 to write the quartets as combinations of non-resonant triads. The possible quartets (minus permutations) are:

1. $(0,0,0;0)$,
2. $(0,0,0;\pm)$,
3. $(\pm,0,0;0)$,
4. $(0,0,\pm;\pm)$,
5. $(0,\pm,\pm;0)$,
6. $(0,\pm,\pm;\pm)$,
7. $(\pm,\pm,\pm;0)$,
8. $(\pm,\pm,\pm;\pm)$,

where the notation $(a, b, c; d)$ is understood to mean mode types a, b, and c acting on the output mode of type d, similarly to the triad notation defined above.

Of these, 2 and 3 can trivially never resonate. Quartet 1 is the next order of interaction between the zero modes, found by both Reznik, Zeitlin, and Ben Jelloul 2001 and Thomas 2016. 4 and 5 belong to the quartet given in the Thomas paper, referred to there as 'wave dragging'. Quartet 6 can be shown to be exchanges between triads of fast modes catalysed by a zero mode and 7 will shortly be shown to have an interaction coefficient of zero (this is due to conservation of linear PV). Quartet 8 is formed of combinations of fast modes, and this includes self interaction, which leads to modulational instability given by the nonlinear Schrödinger equation (see Zakharov and Ostrovsky 2009 for example). We now consider each possible non-trivial quartet one by one.

For quartet 1, from the general form (3.32) we write the interaction coefficient as follows:

$$Q^{0\ 0\ 0\ 0}_{\boldsymbol{k}_1\boldsymbol{k}_2\boldsymbol{k}_3\boldsymbol{k}} = \frac{2}{3}\left[\sum_{\alpha_a=\pm}\frac{C^{\alpha_a\ 0\ 0}_{\boldsymbol{k}_a\boldsymbol{k}_3\boldsymbol{k}}\,C^{0\ \ 0\ \alpha_a}_{\boldsymbol{k}_1\boldsymbol{k}_2\boldsymbol{k}_a}\big|_{nr}}{i(\omega_a-\omega_1-\omega_2)}+\sum_{\alpha_b=\pm}\frac{C^{\alpha_b 0\ 0}_{\boldsymbol{k}_b\boldsymbol{k}_1\boldsymbol{k}}\,C^{0\ \ 0\ \alpha_b}_{\boldsymbol{k}_2\boldsymbol{k}_3\boldsymbol{k}_b}\big|_{nr}}{i(\omega_b-\omega_2-\omega_3)}+\sum_{\alpha_c=\pm}\frac{C^{\alpha_c\ 0\ 0}_{\boldsymbol{k}_c\boldsymbol{k}_2\boldsymbol{k}}\,C^{0\ 0\ \alpha_c}_{\boldsymbol{k}_3\boldsymbol{k}_1\boldsymbol{k}_c}\big|_{nr}}{i(\omega_c-\omega_3-\omega_1)}\right].$$

The point of interest to highlight here is that, because we require that the component triads cannot themselves be resonant, the interactions must be mediated via a fast-like slaved mode (α_a, α_b, or α_c). In the standard derivation of the barotropic quasigeostrophic equations where the motion is limited to the balanced zero modes from the outset, there can be no quartet interaction, despite the appearance of zero-only quartet interactions in the full equations. This is due to the omission of fast wave motions that occurs during the derivation.

We now consider resonance 5 (the type of which Thomas 2016 gives an example):

$$Q^{0\ \pm\ \mp\ 0}_{\boldsymbol{k}_1\boldsymbol{k}_2\boldsymbol{k}_3\boldsymbol{k}} = \frac{2}{3}\left[\sum_{\alpha_a}\frac{C^{\alpha_a\mp\ 0}_{\boldsymbol{k}_a\boldsymbol{k}_3\boldsymbol{k}}\,C^{0\ \pm\ \alpha_a}_{\boldsymbol{k}_1\boldsymbol{k}_2\boldsymbol{k}_a}\big|_{nr}}{i(\omega_a-\omega_1-\omega_2)}+\sum_{\alpha_b}\frac{C^{\alpha_b 0\ 0}_{\boldsymbol{k}_b\boldsymbol{k}_1\boldsymbol{k}}\,C^{\pm\ \mp\ \alpha_b}_{\boldsymbol{k}_2\boldsymbol{k}_3\boldsymbol{k}_b}\big|_{nr}}{i(\omega_b-\omega_2-\omega_3)}+\sum_{\alpha_c}\frac{C^{\alpha_c\pm\ 0}_{\boldsymbol{k}_c\boldsymbol{k}_2\boldsymbol{k}}\,C^{\mp\ 0\ \alpha_c}_{\boldsymbol{k}_3\boldsymbol{k}_1\boldsymbol{k}_c}\big|_{nr}}{i(\omega_c-\omega_3-\omega_1)}\right].$$

Now using the resonance conditions and the fact that $C^{\pm\ \mp\ 0}_{\boldsymbol{k}_1\boldsymbol{k}_2\boldsymbol{k}} = 0$ we can reduce the possible combinations to $\alpha_a = 0$, $\alpha_b = \pm$, and $\alpha_c = 0$:

$$Q^{0\ \pm\ \mp\ 0}_{\boldsymbol{k}_1\boldsymbol{k}_2\boldsymbol{k}_3\boldsymbol{k}} = \frac{2}{3}\left[\frac{C^{0\mp\ 0}_{\boldsymbol{k}_a\boldsymbol{k}_3\boldsymbol{k}}\,C^{0\ \pm\ 0}_{\boldsymbol{k}_1\boldsymbol{k}_2\boldsymbol{k}_a}\big|_{nr}}{i(\omega_a-\omega_1-\omega_2)}+\sum_{\alpha_b=\pm}\frac{C^{\pm 0\ 0}_{\boldsymbol{k}_b\boldsymbol{k}_1\boldsymbol{k}}\,C^{\pm\ \mp\ \pm}_{\boldsymbol{k}_2\boldsymbol{k}_3\boldsymbol{k}_b}\big|_{nr}}{i(\omega_b-\omega_2-\omega_3)}+\frac{C^{0\pm\ 0}_{\boldsymbol{k}_c\boldsymbol{k}_2\boldsymbol{k}}\,C^{\mp\ 0\ 0}_{\boldsymbol{k}_3\boldsymbol{k}_1\boldsymbol{k}_c}\big|_{nr}}{i(\omega_c-\omega_3-\omega_1)}\right].$$

Our quartets include combinations of slow-fast-slow triads and fast-fast-fast triads: the two possible triad interactions that did not occur to first approximation due to the resonance condition. We can therefore expect that any physical behaviour of the full system that these triads cause, by moving energy between these modes, is captured at second order in the asymptotic expansion, as a two stage movement of energy between modes. By considering the quartets as combinations of triads, the physical interactions are less obscured in the mathematics. Technically it remains to

prove that this particular combination of triads does not have zero interaction coefficient, but as a specific example is included in the appendix of Thomas 2016 this is sufficient to show that this resonance is present in the expansion.

We now consider resonance 7. In this case we can draw a more general conclusion about all orders of the expansion for resonances of the form $(\pm, ..., \pm; 0)$ and so we move straight to the more general form of the interaction coefficient given by (3.34). We write:

$$\{C^{(n)}\}^{\pm... \pm 0}_{\boldsymbol{k}_1...\boldsymbol{k}_{n+1}\boldsymbol{k}} = \sum_{r=1}^{n} \frac{1}{(n+1)!} \left[\sum_{\alpha_a,\alpha_b} \frac{\{C^{(1)}\}^{\alpha_a\alpha_b 0}_{\boldsymbol{k}_a\boldsymbol{k}_b\boldsymbol{k}} \{C^{(r-1)}\}^{\pm...\pm\alpha_b}_{\boldsymbol{k}_{n-r+2}...\boldsymbol{k}_{n+1}\boldsymbol{k}_b}\Big|_{nr} \{C^{(n-r)}\}^{\pm...\pm\alpha_a}_{\boldsymbol{k}_1...\boldsymbol{k}_{n-r+1}\boldsymbol{k}_a}\Big|_{nr}}{\{\Omega^{(n-r)}\}^{a}_{1,...,n-r+1}\{\Omega^{(r-1)}\}^{b}_{n-r+2,...,n+1}} + perm. \right].$$

We will use an inductive argument. We assume that $\{C^{(p)}\}^{\pm...\pm\ 0}_{\boldsymbol{k}_1...\boldsymbol{k}_{p+1}\boldsymbol{k}_a} = 0$ for all $p < n$. The contribution for $\alpha_a = 0$ will cause the right hand coefficient ($C^{(n-r)}$) to be 0. Similarly $\alpha_b = 0$ will cause the middle coefficient ($C^{(r-1)}$) to be 0. But for the only remaining option, $\alpha_a, \alpha_b = \pm$, the left hand interaction coefficient ($C^{(1)}$) has the same form and so that is also 0. All possible combinations contribute 0 to the interaction coefficient and so the output is always 0. We note also that all permutations have the same form in this case. Hence we have an inductive step, and can conclude that because a set of only fast modes cannot affect slow modes at first order ($C^{\pm\pm 0} = 0$), this is true for all orders. This higher order expansion has not been calculated before to the best of the author's knowledge. Although it was somewhat apparent from conservation of linear PV that conservation of this form might be expected, this derivation shows that the higher orders terms in the PV will not introduce higher order alterations to the PV in the rotating shallow water equations.

As noted in section 4.2.1, we also cannot have a resonant interaction between a single fast mode and the slow modes such as resonances 2 and 3 (because $\omega + 0 + ... + 0 \neq 0$). This limits our interactions with a zero mode output so that for the nth closure with resonance between $n + 2$ modes the number of fast modes ($n_f \in \mathbb{N}$) must be in the range $1 < n_f < n + 1$ (hence at first closure there is no possible value of n_f). This is our generalisation of the conclusion in Thomas 2016 that there exist energy exchanges between fast and slow modes at closures above first order.

The conclusions of this example are in fact general to any system with zero modes, that has $C^{\pm\pm 0} = 0$. Section 4.4 will provide a different method of establishing the relation $C^{\pm\pm 0} = 0$ that will deepen our understanding, and is simply generalised to all layered zero mode systems. It is generally accepted that the first order of expansion is dominant (for example: for rotating shallow water equations this is triad order, for surface waves quartet order) however for systems with

distinguished zero modes there will always be interactions that are never present at triad order, and hence the full physics is not in the model unless both triad and quartets are considered. We suggest that above this order, but not before, there is no particular benefit to greater expansion, as all physics is included and higher orders will simply be weaker interactions important only on longer timescales.

To summarise, we have shown that the only possible resonant quartets with slow mode output are the $(0,0,0;0)$ quartet, that can only exist due to small $\boldsymbol{u}_1$ fast-like modes, and $(0,\pm,\mp;0)$ quartets, an example of which was given in Thomas 2016. We also generalise the finding of zero interaction coefficient for the triad $(\pm,\mp;0)$ to all n-tets of the form $(\pm,...,\pm;0)$

4.3 Two Layer Rotating Shallow Water Equations

The work in this section is based on Owen, Grimshaw, and Wingate 2018, and is an example of the expansion up to triad order of the multiple scales expansion. We take the eigenfunction decomposition into vertical and wave modes from chapter 2 and continue to explicitly define the nonlinear effects in this specific case. Extra detail is presented where the behaviour diverges significantly from that of the one layer case.

The interaction coefficient is defined using (2.107) and (2.108) as:

$$C^{\alpha_1\alpha_2\alpha}_{\boldsymbol{k}_1\boldsymbol{k}_2\boldsymbol{k}m_1m_2m} = \frac{iA^m_{m_1m_2}}{2}\Big[(\boldsymbol{v}^{\alpha_1m_1}_{\boldsymbol{k}_1}\cdot\boldsymbol{k}_2)(\boldsymbol{v}^{\alpha_2m_2}_{\boldsymbol{k}_2}\cdot\boldsymbol{v}^{\alpha m}_{\boldsymbol{k}}) + (\boldsymbol{v}^{\alpha_2m_2}_{\boldsymbol{k}_2}\cdot\boldsymbol{k}_1)(\boldsymbol{v}^{\alpha_1m_1}_{\boldsymbol{k}_1}\cdot\boldsymbol{v}^{\alpha m}_{\boldsymbol{k}}) + \frac{c_m}{c_{m_2}}(\boldsymbol{v}^{\alpha_1m_1}_{\boldsymbol{k}_1}\cdot(\boldsymbol{k}_1+\boldsymbol{k}_2))p^{\alpha_2m_2}_{\boldsymbol{k}_2}p^{\alpha m*}_{\boldsymbol{k}} + \frac{c_m}{c_{m_1}}(\boldsymbol{v}^{\alpha_2m_2}_{\boldsymbol{k}_2}\cdot(\boldsymbol{k}_1+\boldsymbol{k}_2))p^{\alpha_1m_1}_{\boldsymbol{k}_1}p^{\alpha m*}_{\boldsymbol{k}}\Big]. \tag{4.30}$$

Here $\boldsymbol{v}=(u,v)^T$, and for clarity in distinguishing between the vertical modes in the following, the mode information is encoded into two superscripts α and m. This gives the following explicit triad resonance condition and t_0 evolution equation:

$$\omega^{\alpha m}_{\boldsymbol{k}} - \omega^{\alpha_1m_1}_{\boldsymbol{k}_1} - \omega^{\alpha_2m_2}_{\boldsymbol{k}_2} = 0, \tag{4.31}$$

$$\frac{\partial}{\partial t_0}a^{\alpha m}_{\boldsymbol{k}} = \sum_{\substack{\boldsymbol{k},\boldsymbol{k}_1,\boldsymbol{k}_2\\ \alpha,\alpha_1,\alpha_2}} C^{\alpha_1\alpha_2\alpha}_{\boldsymbol{k}_1\boldsymbol{k}_2\boldsymbol{k}m_1m_2m}a^{\alpha_1m_1}_{\boldsymbol{k}_1}(t)a^{\alpha_2m_2}_{\boldsymbol{k}_2}(t)\delta_{\boldsymbol{k}-\boldsymbol{k}_1-\boldsymbol{k}_2}\delta_{\omega-\omega_1-\omega_2}\,. \tag{4.32}$$

The only possible resonances are the combinations of modes in the form $(\alpha_1, \alpha_2; \alpha)$:

$$\begin{aligned} &\text{a) } (0, \pm; \pm),\ (\pm, 0; \pm), \\ &\text{b) } (\pm, \pm; 0), \\ &\text{c) } (\pm, \pm; \pm), \\ &\text{d) } (0, 0; 0). \end{aligned} \tag{4.33}$$

The first and second in (4.33a) are treated as equivalent due to the symmetry of the input modes chosen in the interaction coefficient C. Combination (4.33b) leads to an interaction term of zero as will be shown presently in section 4.3.1 by direct substitution of the eigenvectors into C in (4.30).

There are only three types of interactions remaining. Slow-slow-slow (4.33d) that define the development of the PV modes over the longer time scale t, and fast-slow-fast (4.33a), and fast-fast-fast (4.33c) that define the scattering of fast modes off a slow mode and interactions of fast modes amongst themselves respectively.

For the one layer equations it was shown in section 4.2.1 that there are no fast-fast-fast resonances, and further, that the equations for the slow part have no dependence on the fast modes. In the following it is shown that in the two layer case the slow part again evolves independently of the fast, giving the quasigeostrophic equation. However unlike the one layer case it can be shown that there are interactions amongst the fast waves for the two layer system, provided they are between different vertical modes.

4.3.1 Interaction coefficients

To begin the analysis of the evolution equation (4.32) we calculate the interaction coefficients, after which we will look at the resonance condition. When these two parts are defined the full evolution of the equations to triad order will be known.

The interaction coefficients are worked out explicitly for the different possible mode combinations. This is achieved by substitution of the specific mode forms given in (2.106) into the general form given in (4.30). This allows us to examine in detail and categorise the different possible nonlinear interactions in this system. The vertical mode parameter m_i is left general and setting $m = m_1 = m_2$ returns a comparable expression to the one derived in section 4.2.1 for the one layer case.

For the slow modes:

$$C^{0,0,0}_{\boldsymbol{k}_1\boldsymbol{k}_2\boldsymbol{k}m_1m_2m} = \frac{A^m_{m_1m_2}c_m(\boldsymbol{k}_2\times\boldsymbol{k}_1)}{2\omega\omega_1\omega_2}\left(c_{m_1}\frac{\omega_2^2}{c_{m_2}} - c_{m_2}\frac{\omega_1^2}{c_{m_1}}\right) \tag{4.34a}$$

$$= \frac{iA^m_{m_1m_2}}{2}\frac{c_m}{\omega}\left(\frac{\omega_2}{c_{m_2}}(\boldsymbol{v}_1\cdot\boldsymbol{k}_2) + \frac{\omega_1}{c_{m_1}}(\boldsymbol{v}_2\cdot\boldsymbol{k}_1)\right). \tag{4.34b}$$

For two slow and a fast mode:

$$C^{\alpha_1,0,0}_{\boldsymbol{k}_1\boldsymbol{k}_2\boldsymbol{k}m_1m_2m} = \frac{ic_m\omega_2A^m_{m_1m_2}}{2\sqrt{2}\omega\omega_1c_{m_2}|\boldsymbol{k}_1|}\Big[if(\boldsymbol{k}_2\times\boldsymbol{k}_1)_z + \alpha_1\omega_1(\boldsymbol{k}_1\cdot\boldsymbol{k})\Big], \tag{4.35}$$

$$C^{0,0,\alpha}_{\boldsymbol{k}_1\boldsymbol{k}_2\boldsymbol{k}m_1m_2m} = \frac{iA^m_{m_1m_2}(\boldsymbol{k}_1\times\boldsymbol{k}_2)_z}{2\sqrt{2}\omega\omega_1\omega_2c_{m_1}c_{m_2}|\boldsymbol{k}|}\Big[2\alpha\omega(\boldsymbol{k}_2\times\boldsymbol{k}_1)_z + if\left(c^2_{m_2}(\omega_1^2+\omega^2) - c^2_{m_1}(\omega_2^2+\omega^2)\right)\Big]. \tag{4.36}$$

For two fast and a slow mode (no resonance possible):

$$C^{\alpha_1\alpha_20}_{\boldsymbol{k}_1\boldsymbol{k}_2\boldsymbol{k}m_1m_2m} = \quad 0, \tag{4.37}$$

$$\begin{aligned}C^{\alpha_10\alpha}_{\boldsymbol{k}_1\boldsymbol{k}_2\boldsymbol{k}m_1m_2m} =& \frac{iA^m_{m_1m_2}}{4c_{m_2}\omega\omega_1\omega_2|\boldsymbol{k}||\boldsymbol{k}_1|}\Big[(if^2(c_m^2-c_{m_2}^2)|\boldsymbol{k}|^2(\boldsymbol{k}\times\boldsymbol{k}_1)_z + 2if^2c^2_{m_2}(\boldsymbol{k}\cdot\boldsymbol{k_1})(\boldsymbol{k}\times\boldsymbol{k}_1)_z)\\ &+\alpha_1\omega_1f(c_m^2-c_{m_2}^2)|\boldsymbol{k}|^2(\boldsymbol{k}_1\cdot\boldsymbol{k}) - i\alpha\alpha_1\omega_1\omega c^2_{m_2}(\boldsymbol{k}_1\times\boldsymbol{k})_z|\boldsymbol{k}_1|^2\\ &+\alpha_1\omega_1fc^2_{m_2}(\boldsymbol{k}\cdot\boldsymbol{k_1})|\boldsymbol{k}_1|^2 + 2i\alpha\alpha_1\omega_1\omega c^2_{m_2}(\boldsymbol{k}_1\times\boldsymbol{k})_z(\boldsymbol{k}_1\cdot\boldsymbol{k})\\ &+2\alpha\omega c^2_{m_2}f(\boldsymbol{k}\times\boldsymbol{k}_1)_z^2 + ic^2_{m_2}c^2_m|\boldsymbol{k}_1|^2|\boldsymbol{k}|^2(\boldsymbol{k}\times\boldsymbol{k}_1)_z\Big].\end{aligned} \tag{4.38}$$

For three fast modes:

$$\begin{aligned}C^{\alpha_1\alpha_2\alpha}_{\boldsymbol{k}_1\boldsymbol{k}_2\boldsymbol{k}m_1m_2m} =& \frac{iA^m_{m_1m_2}}{4\sqrt{2}\omega\omega_1\omega_2|\boldsymbol{k}||\boldsymbol{k}_1||\boldsymbol{k}_2|}\Big[\\ &+\big(\alpha_1\omega_1\alpha_2\alpha\omega\omega_2(|\boldsymbol{k}_1|^2+|\boldsymbol{k}_2|^2) + (\alpha_1\omega_1|\boldsymbol{k}_1|^2+\alpha_2\omega_2|\boldsymbol{k}_2|^2)f^2\big)(\boldsymbol{k}_1\cdot\boldsymbol{k}_2)\\ &+(2\alpha_1\omega_1\alpha_2\alpha\omega\omega_2 + (\alpha_1\omega_1+\alpha_2\omega_2)f^2)(\boldsymbol{k}_1\cdot\boldsymbol{k}_2)^2 + f^2(\alpha_2\omega_2-\alpha_1\omega_1)(\boldsymbol{k}_1\times\boldsymbol{k}_2)_z^2\\ &+if(\alpha_2\alpha\omega\omega_2+f^2)|\boldsymbol{k}_2|^2(\boldsymbol{k}_2\times\boldsymbol{k}_1)_z - if(\alpha_1\alpha\omega\omega_1+f^2)|\boldsymbol{k}_1|^2(\boldsymbol{k}_2\times\boldsymbol{k}_1)_z\\ &+c_m^2(\omega_1\alpha_1+\omega_2\alpha_2)|\boldsymbol{k}_2|^2|\boldsymbol{k}|^2|\boldsymbol{k}_1|^2 + c_m^2(\omega_1\alpha_1|\boldsymbol{k}_2|^2+\omega_2\alpha_2|\boldsymbol{k}_1|^2)|\boldsymbol{k}|^2(\boldsymbol{k}_1\cdot\boldsymbol{k}_2)\\ &+ifc_m^2(|\boldsymbol{k}_2|^2-|\boldsymbol{k}_1|^2)|\boldsymbol{k}|^2(\boldsymbol{k}_2\times\boldsymbol{k}_1)_z\Big].\end{aligned} \tag{4.39}$$

We recover the second version of the slow-slow-slow interactions (4.34b) from the usual quasi-geostrophic equations, as will now be demonstrated.

As the fast modes have zero linear PV the restriction to slow modes is equivalent to the as-

sumption that the flow, to first approximation, is solely the geostrophic part. The second part of the quasigeostrophic approximation is to assume the advection of the flow is due only to this geostrophic part (the slow mode interaction), and hence we would expect that the equation for the slow part:

$$\frac{\partial a_{\boldsymbol{k}}^{0m}}{\partial t} + \sum_{1,2} C_{\boldsymbol{k}_1\boldsymbol{k}_2\boldsymbol{k}}^{0,0,0\,m_1m_2m} a_{\boldsymbol{k}_1}^{0m_1} a_{\boldsymbol{k}_2}^{0m_2}\ \delta_{\boldsymbol{k}-\boldsymbol{k}_1+\boldsymbol{k}_2} = 0, \tag{4.40}$$

is equivalent to the quasigeostrophic equations:

$$\frac{\partial Q_i}{\partial t} + ((\boldsymbol{u}_g)_i \cdot \nabla) Q_i = 0. \tag{4.41}$$

To prove this equivalence between (4.40) and (4.41), we start by transforming (4.41) into the mode basis:

$$\frac{\partial Q_m}{\partial t} + \sum_{m_1 m_2} A_{m_1 m_2}^{m} ((\boldsymbol{u}_g)_{m_1} \cdot \nabla) Q_{m_2} = 0. \tag{4.42}$$

For a general slow eigenvector $\boldsymbol{r}_{\boldsymbol{k}}^{0m}$ we now consider the linear potential vorticity: $Q_{\boldsymbol{k}}^{m} = -\omega_{\boldsymbol{k}}^{m} a_{\boldsymbol{k}}^{0m}/c_m$ calculated directly from the form in (2.106) using the linear PV relation $Q_m = \zeta_m - f p_m/c_m$. With this we then write the quasigeostrophic equation symmetrically in Fourier space to see:

$$\begin{aligned}\frac{\partial a_{\boldsymbol{k}}^{0m}}{\partial t} + \sum_{1,2} \frac{i A_{m_1 m_2}^{m}}{2} \frac{c_m}{\omega} \left(\frac{\omega_2}{c_{m_2}} (\boldsymbol{v}_1 \cdot \boldsymbol{k}_2) + \frac{\omega_1}{c_{m_1}} (\boldsymbol{v}_2 \cdot \boldsymbol{k}_1) \right) a_{\boldsymbol{k}_1}^{0m_1} a_{\boldsymbol{k}_2}^{0m_2}\ \delta_{\boldsymbol{k}-\boldsymbol{k}_1-\boldsymbol{k}_2} \\ = \frac{\partial a_{\boldsymbol{k}}^{0m}}{\partial t} + \sum_{1,2} C_{\boldsymbol{k}_1\boldsymbol{k}_2\boldsymbol{k}}^{0,0,0\,m_1m_2m} a_{\boldsymbol{k}_1}^{0m_1} a_{\boldsymbol{k}_2}^{0m_2}\ \delta_{\boldsymbol{k}-\boldsymbol{k}_1-\boldsymbol{k}_2} = 0.\end{aligned} \tag{4.43}$$

This confirms that the two layer quasigeostrophic equations are recovered as they were in the one layer case (see Embid and Majda 1996). These are still the usual quasigeostrophic equations in our limit, even though we have included a fast time scale.

4.3.2 Fast-fast-fast Resonances

Of particular interest in the two-layer equations are the fast-fast-fast resonances. These are a clear difference to the single layer version of the shallow water equations, where they cannot occur. We now consider where these resonances are permitted by the dispersion relations. The fast-fast-fast resonances were originally considered by Ball 1964 for the simpler case with no Coriolis force. The following subsection shows graphically how these resonances can exist (this graphical method was discovered independently by researchers in different fields, for example Ziman 1960 and Ball 1964). In addition to the graphical method, the full derivation of the resonances

is given in the next subsection.

Graphical method

Figure 4.1 shows possible resonances using the graphical method of finding resonances (cf Ball 1964). The method involves drawing all the branches of the dispersion relation twice, once centred around the origin and the second time around a chosen point on any of the surfaces representing a possible frequency $\omega_1(\boldsymbol{k}_1)$. This second set of resonances then give all possible solutions to $\omega_1 + \omega_2 (= \omega)$ on coordinates given by $\boldsymbol{k}_1 + \boldsymbol{k}_2 (= \boldsymbol{k})$. Therefore any point that lies on both of the dispersion relation sets must solve the triad and resonance conditions. Due to the large number of branches of the dispersion relation we here restrict each diagram to specific branches, drawing only the leaves relevant for discussion.

Case (a) in the diagram shows that there are no resonances between waves of the same vertical mode, equivalent to the one layer case. However we find that the resonances always exist for any combination of fast modes with different vertical modes: cases (b), (c), and (d) in figure 4.1. In addition there is another more unusual resonance (seen in the lower sheet of the light hyperboloid in case (d) in figure 4.1) where the ratio of the input and output wave speeds is less than 1 ($c_{m_2}/c_m < 1$). Where the output wave is an external wave and one of the inputs is internal if we then consider sufficiently large values of the Burger number for the external mode ($Bu = c_+^2 |\boldsymbol{k}_1|^2 / f^2 = L_r^2 / L^2$) this resonance will exist. This condition corresponds to wavelengths at least $\sqrt{3}$ times smaller than the radius of deformation (see below). It should be noted that the apparent simplicity of this bound is due to the limiting assumptions made to get an absolute bound, namely the angle of incidence between the waves is 0, and the ratio of baroclinic to barotropic wave speeds is 0 (clearly this is non-physical, but provides a good approximation where the ratio is small).

Alternatively the equivalent resonance also exists where the two input waves are of different type to the output. Here the ratio of input to output wave speeds needs to be greater than 1 and so the input waves are both external modes. We then require that the wavelength of one input mode is such that the external Burger number is sufficiently large: $Bu = c_+^2 |\boldsymbol{k}_1|^2 / f^2 > 3$.

These resonances are unusual in that they only exist for angles of incidence within a range around $\pm\pi$. Figure 4.2 shows the intersections of the surfaces from figure 4.1d projected into the (k, l) plane and shows more clearly the angle dependence of the resonance. It can be seen that without the Coriolis force the angle of incidence is in a range ($-\pi/2$, $\pi/2$) but as the Coriolis force becomes more dominant the range of angles is limited to be closer to $-\pi$.

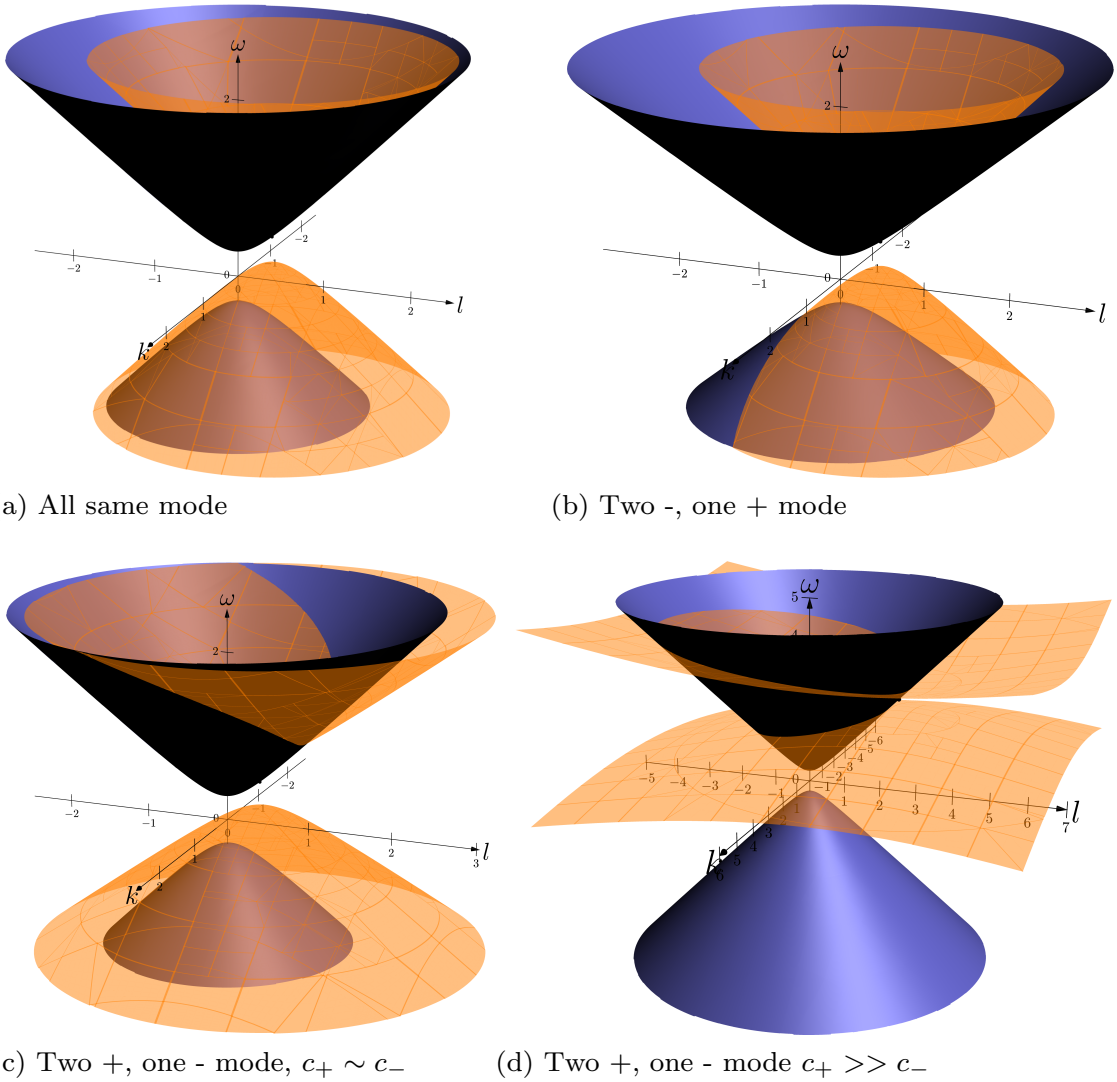

(a) All same mode

(b) Two -, one + mode

(c) Two +, one - mode, $c_+ \sim c_-$

(d) Two +, one - mode $c_+ >> c_-$

Figure 4.1: Graphical method to find possible resonant triads in the fast-fast-fast interactions. The dark hyperboloid is the manifold on which the ω_1 may lie (defined by the dispersion relation for $\boldsymbol{k}_1$), the light hyperboloid is centred around a chosen ω_1 in the first manifold. Any crossing point of the light and dark hyperboloids represents a possible resonance.

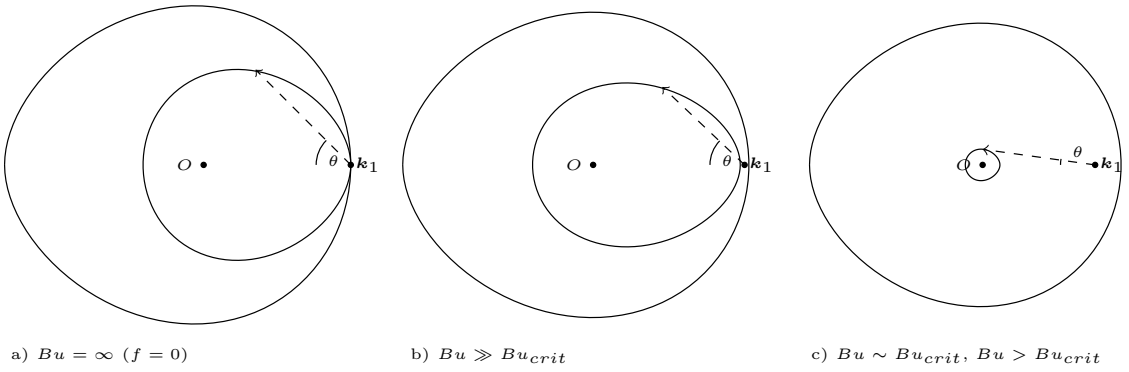

Figure 4.2: Projection onto wave space of the intersections of the surfaces in figure 4.1d showing the two sets of resonances. a) The non-rotating case equivalent to the diagram in Ball 1964, b) The case for large external Burgers number, and c) shows Burger number close to the critical value of the Burgers number such that the angle of incidence in the resonance must be small.

Algebraic method

The following is the exact method to find the resonances discussed with reference to the graphical method. This is taken from the appendix of Owen, Grimshaw, and Wingate 2018.

We seek to solve:

$$\alpha\omega = \alpha_1\omega_1 + \alpha_2\omega_2, \tag{4.44}$$

where $\alpha_i = \pm 1$. We substitute the relevant branches of the dispersion relation:

$$\alpha\sqrt{c_m^2|\boldsymbol{k}|^2 + f^2} = \alpha_1\sqrt{c_{m_1}^2|\boldsymbol{k}_1|^2 + f^2} + \alpha_2\sqrt{c_{m_2}^2|\boldsymbol{k}_2|^2 + f^2}, \tag{4.45}$$

we square both sides and rearrange:

$$c_m^2|\boldsymbol{k}|^2 - c_{m_1}^2|\boldsymbol{k}_1|^2 - c_{m_2}^2|\boldsymbol{k}_2|^2 - f^2 = 2\alpha_1\alpha_2\sqrt{c_{m_1}^2|\boldsymbol{k}_1|^2 + f^2}\sqrt{c_{m_2}^2|\boldsymbol{k}_2|^2 + f^2}, \tag{4.46}$$

we square again:

$$(c_m^2(|\boldsymbol{k}_1|^2 + 2(\boldsymbol{k}_1\cdot\boldsymbol{k}_2) + |\boldsymbol{k}_2|^2) - c_{m_1}^2|\boldsymbol{k}_1|^2 - c_{m_2}^2|\boldsymbol{k}_2|^2 - f^2)^2 = 4(c_{m_1}^2|\boldsymbol{k}_1|^2 + f^2)(c_{m_2}^2|\boldsymbol{k}_2|^2 + f^2), \tag{4.47}$$

we expand and gather terms:

$$
\begin{aligned}
&(c_m^2 - c_{m_1}^2)^2|\boldsymbol{k}_1|^4 + (c_m^2 - c_{m_2}^2)^2|\boldsymbol{k}_2|^4 \\
&+4c_m^2(c_m^2 - c_{m_1}^2)(\boldsymbol{k}_1 \cdot \boldsymbol{k}_2)|\boldsymbol{k}_1|^2 + 4c_m^2(c_m^2 - c_{m_2}^2)(\boldsymbol{k}_1 \cdot \boldsymbol{k}_2)|\boldsymbol{k}_2|^2 \\
&+4c_m^4(\boldsymbol{k}_1 \cdot \boldsymbol{k}_2)^2 + 2(-c_{m_2}^2 c_{m_1}^2 + c_m^4 - c_m^2 c_{m_1}^2 - c_{m_2}^2 c_m^2)|\boldsymbol{k}_1|^2|\boldsymbol{k}_2|^2 \\
&-2(c_m^2 + c_{m_1}^2)|\boldsymbol{k}_1|^2 f^2 - 2(c_m^2 + c_{m_2}^2)|\boldsymbol{k}_2|^2 f^2 - 4c_m^2(\boldsymbol{k}_1 \cdot \boldsymbol{k}_2)f^2 - 3f^4 = 0.
\end{aligned} \tag{4.48}
$$

We define $K = |\boldsymbol{k}_2|/|\boldsymbol{k}_1|$, $R_1 = c_{m_1}^2/c_m^2$, $R_2 = c_{m_2}^2/c_m^2$ and $F = f/c_m|\boldsymbol{k}_1|$ with θ as the angle between the two input wave vectors. Writing the equation as a quartic in K:

$$
\begin{aligned}
&AK^4 + BK^3 + CK^2 + DK + E = 0, \\
&A = (1 - R_2)^2, \\
&B = 4(1 - R_2)\cos\theta, \\
&C = 4\cos^2\theta + 2(1 - R_2)(1 - R_1) - 4R_1R_2 - 2(1 + R_2)F^2, \\
&D = 4((1 - R_1) - F^2)\cos\theta, \\
&E = (1 - R_1)^2 - 2(1 + R_1)F^2 - 3F^4.
\end{aligned} \tag{4.49}
$$

There are three distinct cases to consider:

1. $R_1 = R_2 = 1$ (Reduces to the one layer case - no solution).
2. $R_1 = 1 \neq R_2$.
3. $R_1 = R_2 \neq 1$.

Within each of these cases $R_i > 1$ $R_i < 1$ need to be considered.

Considering the second case $R_1 = 1$, equations (4.49) become:

$$
\begin{aligned}
&AK^4 + BK^3 + CK^2 + DK + E = 0, \\
&A = (1 - R_2)^2, \\
&B = 4(1 - R_2)\cos\theta, \\
&C = 4\cos^2\theta - 4R_2 - 4F^2, \\
&D = -4F^2\cos\theta, \\
&E = -4F^2 - 3F^4.
\end{aligned} \tag{4.50}
$$

Following Rees 1922, we define p, q, s as the coefficients of the reduced quartic, then for all

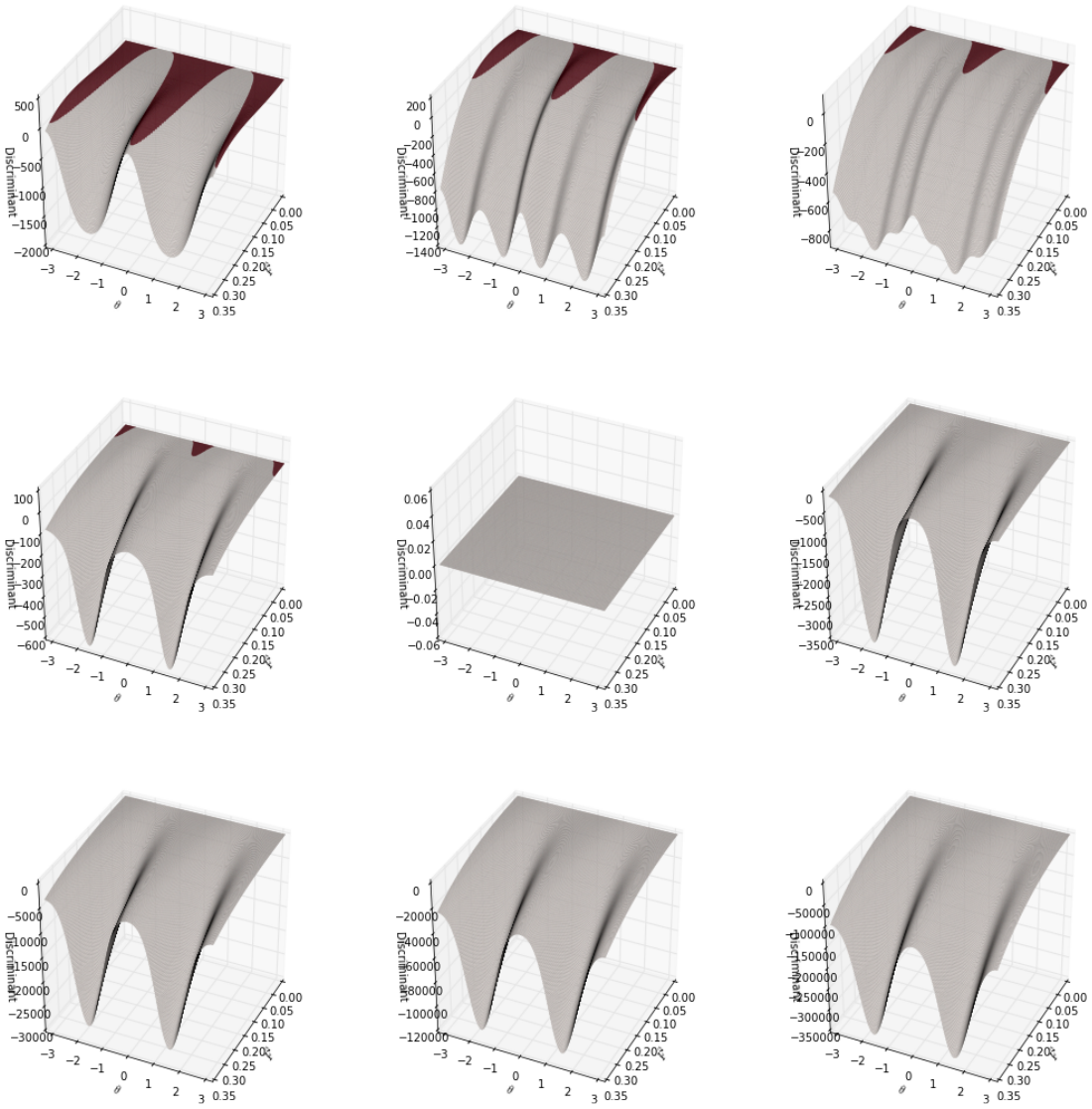

Figure 4.3: The quartic discriminant Δ for $R_2 = \{0, 0.25, 0.5, 0.75, 1, 1.25, 1.5, 1.75, 2\}$ represented as surfaces in parameter space $\{F^2, \theta\}$. Red shows values greater than 1, where there are 4 solutions and therefore the directional resonance (the resonance in figure 4.1d which can have limited angle of incidence between the waves) exists.

parameter values our equation has: $q < 0$, $p = s - q^2/4 < 0$. This means that there are either 2 or 4 real solutions when the quartic discriminant Δ is less than or greater than 0 respectively. This is plotted in figure 4.3. The areas of 4 solutions correspond to the second crossing point shown in the hyperboloid diagrams in figure 4.1.

The definitions of Δ, q and p are:

$$q = 8AC - 3B^2, \tag{4.51}$$

$$p = 64A^3E - 16A^2C^2 + 16AB^2C - 16A^2BD - 3B^4, \tag{4.52}$$

$$\begin{aligned}\Delta = {} & 256A^3E^3 - 192A^2BDE^2 - 128A^2C^2E^2 + 144A^2CD^2E \\ & - 27A^2D^4 + 144AB^2CE^2 - 6AB^2D^2E - 80ABC^2DE \\ & + 18ABCD^3 + 16AC^4E - 4AC^3D^2 - 27B^4E^2 + 18B^3CDE \\ & - 4B^3D^3 - 4B^2C^3E + B^2C^2D^2.\end{aligned} \tag{4.53}$$

In full:

$$q = -16(R_2-1)^2(F^2(R_2+1) + 2R_2 + \cos^2\theta) \leq 0, \tag{4.54}$$

$$p = -256(F^2+1)(R_2-1)^4(F^2(R_2^2 - R_2 + 1) + R_2^2 + 2R_2\cos^2\theta) \leq 0, \tag{4.55}$$

$$\begin{aligned}\Delta = {} & -4096F^2(1+F^2)^2(R_2-1)^2\Big[4R_2(R_2 - \cos^2\theta)^3 \\ & + (R_2^2(11R_2^2 - 8R_2 + 8) - 2R_2(R_2+10)(2R_2-1)\cos^2\theta + (2R_2-1)(10R_2+1)\cos^4\theta)F^2 \\ & + (2(R_2^2 - R_2 + 1)(5R_2^2 - 2R_2 + 2) + 2(2R_2-1)(R_2^2 - 7R_2 + 1)\cos^2\theta)F^4 \\ & + 3(R_2^2 - R_2 + 1)^2F^6\Big].\end{aligned} \tag{4.56}$$

The largest value of F^2 with 4 solutions occurs at $R_2 = 0$, $\cos^2\theta = 1$. In this case the discriminant is as follows:

$$\Delta = -4096F^4(1+F^2)^2\left[-1 + 2F^2 + 3F^4\right], \tag{4.57}$$

and so the point from which the resonance occurs, where there is a bifurcation from 2 to 4 solutions of the quartic, is given by the solutions to:

$$-1 + 2F^2 + 3F^4 = 0, \tag{4.58}$$

$$F^2 = -1 \text{ or } \frac{1}{3}. \tag{4.59}$$

As F is real this only occurs at the solution $F^2 = 1/3$. For values greater than this $\Delta < 0$ and so the directional resonance (that of figure 4.1d) doesn't occur. This means $1/F^2 = c_m^2|\boldsymbol{k}_1|^2/f^2 = Bu > 3$ is the range of values for which this resonance can exist.

So with reference to the original resonance equation (4.44) to recover α values we find that there are three distinct types of resonances:

1. $R_2 > 1$: where $\alpha = \alpha_2 = -\alpha_1$.

2. $R_2 < 1$: where $\alpha = \alpha_2 = \alpha_1$.

3. $R_2 < 1$, $\Delta > 0$: where $\alpha = \alpha_1 = -\alpha_2$.

It is then possible to map these resonances onto those with $R_1 = R_2 \neq 1$ by rearranging the input and output waves and relabelling:

$$\alpha_1\omega_1(\boldsymbol{k}_1) + \alpha_2\omega_2(\boldsymbol{k}_2) = \alpha\omega(\boldsymbol{k}), \tag{4.60}$$

$$\Rightarrow \alpha_1\omega_1(\boldsymbol{k}_1) - \alpha\omega(\boldsymbol{k}) = -\alpha_2\omega_2(\boldsymbol{k}_2), \tag{4.61}$$

$$\Rightarrow \alpha_a\omega_a(\boldsymbol{k}_a) + \alpha_b\omega_b(\boldsymbol{k}_b) = \alpha_c\omega_c(\boldsymbol{k}_c), \tag{4.62}$$

where $\alpha_a = \alpha_1$, $\alpha_b = -\alpha$, $\alpha_c = -\alpha_2$ and the wavenumber vectors are $\boldsymbol{k}_a = -\boldsymbol{k}_1$, $\boldsymbol{k}_b = \boldsymbol{k} = \boldsymbol{k}_1 + \boldsymbol{k}_2$, $\boldsymbol{k}_c = \boldsymbol{k}_2$. In the new set of resonances $R_a = c^2_{m_1}/c^2_{m_2}$, $R_b = c^2_m/c^2_{m_2}$ $\left(= R_2^{-1}\right)$, $F = f/c_m|\boldsymbol{k}_1|$. We then have the equivalent set of 3 resonances:

1. $R_a = R_b < 1$: where $\alpha_b = \alpha_c = \alpha_a$.

2. $R_a = R_b > 1$: where $\alpha_b = \alpha_c = -\alpha_a$.

3. $R_a = R_b > 1$, $\Delta > 0$: where $-\alpha_b = \alpha_a = \alpha_c$.

It should be noted that the angle θ is now the angle between the first input wave and the output wave.

To conclude we add the fast-fast-fast resonances into the equations describing the first closure to form:

$$\frac{\partial a^{0m}_{\boldsymbol{k}}}{\partial t} + \sum_{1,2} C^{0,0,0}_{\boldsymbol{k}_1\boldsymbol{k}_2\boldsymbol{k}}{}^{m_1m_2m} a^{0m_1}_{\boldsymbol{k}_1} a^{0m_2}_{\boldsymbol{k}_2}\ \delta_{\boldsymbol{k}-\boldsymbol{k}_1-\boldsymbol{k}_2} = 0, \tag{4.63}$$

$$\begin{aligned}\frac{\partial a^{\alpha m}_{\boldsymbol{k}}}{\partial t} + \sum_{1,2} C^{0,\alpha_2,\alpha}_{\boldsymbol{k}_1\boldsymbol{k}_2\boldsymbol{k}}{}^{m_1m_2m} a^{0m_1}_{\boldsymbol{k}_1} a^{\alpha_2 m_2}_{\boldsymbol{k}_2}\ \delta_{\boldsymbol{k}-\boldsymbol{k}_1-\boldsymbol{k}_2}\delta_{\omega-\omega_2} \\ + \sum_{1,2} C^{\alpha_1,\alpha_2,\alpha}_{\boldsymbol{k}_1\boldsymbol{k}_2\boldsymbol{k}}{}^{m_1m_2m} a^{\alpha_1 m_1}_{\boldsymbol{k}_1} a^{\alpha_2 m_2}_{\boldsymbol{k}_2}\ \delta_{\boldsymbol{k}-\boldsymbol{k}_1-\boldsymbol{k}_2}\delta_{\omega-\omega_1-\omega_2} = 0,\end{aligned} \tag{4.64}$$

with the interaction coefficients from section (4.3.1).

4.3.3 Comparative strength of resonances

In order to examine the strength of the new resonance within the full equation 3.49 we position the fast-fast-fast resonance against the fast-slow-fast resonance by numerical evaluation of the size of

the interaction coefficient in the case of each triad for the same given wavelengths. The parameters were chosen to be physically applicable in an oceanic context with typical wave speeds of orders $\sim 100ms^{-1}, 10ms^{-1}$ for the barotropic and baroclinic parts respectively. Wavenumbers were then chosen such that the fast-fast-fast triad is exactly at resonance and the fast-slow-fast triad it is close to resonance. Sets of wavenumbers are chosen with $\theta \sim 1°$, $\theta \sim 45°$ and $\theta \sim 176°$ where θ is the angle between the input and output barotropic modes. This is to check that this angle does not affect the size of the interaction, to pick out an interaction lying on each of the two branches of the traces previously sketched in figure 4.2, and to have examples with barotropic wavelengths larger and smaller than the baroclinic. For reference the wavelength of the wavenumber $(500, 0)$ barotropic mode would be ~ 200m, the $(-15.21, 10)$ baroclinic/barotropic mode ~ 5.5km, and the $(-967.25, 30)$ mode is ~ 100m.

In table 4.1 the maximum absolute value of the different interaction coefficients in any permutation of mixed vertical modes is given, for mixed vertical modes on lines 1, 3 and 5 and for a single vertical mode on lines 2, 4, 6. The α parts of the modes correspond respectively with the wavenumbers given in the left hand column with the vertical mode information m quoted with the wavenumber. Fast-fast-fast interactions within a single vertical mode are not displayed as this interaction doesn't occur. Assuming that all mode amplitudes are within an order of magnitude of each other, this should scale like the change in time of each part of the reduced equations (4.64). We find that both interactions have a similar order of magnitude. However it should be noted that if we choose a single vertical mode for all of the constituent modes (lines 2, 4, and 8) a larger interaction coefficient can occur for the catalytic scattering case. This suggests that although the overall dynamics may be dominated by the same resonances present in the one layer case, the new resonance is important in evaluating energy exchange between the baroclinic and barotropic modes. The difference in amplitude between the single and mixed mode cases is almost entirely due to the $A^m_{m_1 m_2}$ term (defined in (2.109)), and for this parameter set the coupling between the modes is weak due to density ratio $r \sim 1$. This relates to the rigid lid limit: from section 4.1.2 we see that for similar densities $L_- \sim -H_2/H_1$ and so for the mixed mode layers substitution into $A^m_{m_1 m_2}$ leads to almost exact cancellation. For applications with a smaller density ratio it would be expected that the mixed mode terms would become a more significant part of the overall flow, however in general the barotropic part of the flow could be expected to dominate the dynamics.

4.3.4 Discussion

These resonances are equivalent to those found by Ball 1964 but now extended to the rotating case. Unlike those found by Ball, for certain parameter regimes some of these triads showed

Wavenumbers and vertical mode	Max $\lvert C^{\pm 0 \pm}\rvert$	Max $\lvert C^{\pm \pm \pm}\rvert$
$(500, 0, +)$, $(-15.21, 10, -)$, $(484.79, 10, +)$	3.02×10^{-10}	8.04×10^{-10}
$(500, 0, +)$, $(-15.21, 10, +)$, $(484.79, 10, +)$	3.05×10^{-7}	-
$(500, 0, +)$, $(-122.49, 300, -)$, $(377.51, 300, +)$	3.99×10^{-10}	6.07×10^{-10}
$(500, 0, +)$, $(-122.49, 300, +)$, $(377.51, 300, +)$	4.03×10^{-7}	-
$(500, 0, +)$, $(-967.25, 30, -)$, $(-467.25, 30, +)$	1.07×10^{-10}	4.51×10^{-10}
$(500, 0, +)$, $(-967.25, 30, +)$, $(-467.25, 30, +)$	1.93×10^{-7}	-

Table 4.1: Size of the interaction coefficients for the given wavenumbers, chosen to form a resonant triad of fast-fast-fast modes and a near resonant triad for sets of fast-slow-fast modes. This shows that for the barotropic/baroclinic interactions the fast-fast-fast resonance is of similar magnitude to the fast-slow-fast one. However the dominant interactions will still be those occurring within a single vertical mode. Physical parameters used were as follows: $g = 10ms^{-2}$, $f = 0.0001s^{-1}$, $H_1 = 500m$, $H_2 = 4000m$, $L = 100/2\pi\ km$, the non-dimensional wavenumbers are quoted as $\boldsymbol{k}$ where the physical wavenumber is $\boldsymbol{k}/L$ and physical wavelength is $2\pi L/|\boldsymbol{k}|$.

unusual behaviour with waves interacting preferentially with waves of a small angle of incidence. In addition this resonance ceases to exist for wavelengths more than some factor greater than the Rossby deformation radius. This resonance is very likely to always be present in applications to real oceanic or atmospheric conditions with large deformation radii. However in other planets where the length scales and planetary rotation rates may be different, it could be possible to have parameter regimes such that certain resonances exist for different wavenumbers at different latitudes. Particularly interesting are the cases with parameters such that this resonance affects very small wavenumbers. In these cases the resonance is almost entirely between waves with angles of incidence close to zero. In addition this resonance can be arbitrarily strong, dependent on the size of the other waves, due to the $|\boldsymbol{k}|$, $|\boldsymbol{k}_2|$ terms in the interaction coefficient (4.39). This describes a possible mechanism for energy to be transferred to low wavenumbers.

Similarly to the one layer case, in section 4.3.1 the slow modes were shown to behave exactly as the quasigeostrophic equations for two layers. The weakly nonlinear approximation to this order allows the motion to be split into two equations, the quasigeostrophic equation for the slow part and equations describing the interactions of the fast modes with the slow modes and amongst themselves.

Our 'critical Burger number' condition can be interpreted as a maximum wavenumber at which this particular resonance will exist. However we can also show that a more general, minimum wavenumber at which fast-fast-fast resonances occur must exist. For this we simply take the limit $|\boldsymbol{k}| \to 0$ in the resonance condition:

$$\omega = f + \frac{c_m^2}{2f}|\boldsymbol{k}|^2 + ... \sim f,$$

and this clearly shows that no resonances can exist, provided the Burger number of each wave involved is sufficiently small to make this approximation. In most applications we might expect that this limit will not be reached due to the large size of the Burger number, although it might arise for large fast-rotating planets.

A fundamental issue arises when considering numerical simulations of the equations (4.63-4.64), using discrete wavenumbers. The dispersion relation is a function of $\boldsymbol{k}$ which takes all real values. When we have discrete values of $\boldsymbol{k}$ such as in a numerical simulation of the equations, or when there is a periodic domain, it is possible for the loci of the dispersion relation (such as in figure 4.2) to lie 'off-grid', never crossing any of the grid points corresponding to the discrete wavenumbers. More precisely: we have a countable set of frequencies ω in our model, forming a countable subset of the reals. Adding any pair of this subset doesn't necessarily return a member of the subset (an analogy would be that no integer a exists such that $\sqrt{2}+\sqrt{3}=\sqrt{a}$). There is no guarantee that the frequencies will ever exactly resonate and in general only near resonances may appear. We find that even if we explicitly choose parameter values to ensure that some particular triad is exactly resonant, it does not automatically follow that any other exact resonant triad appears in the discrete set of wavenumbers (barring the trivial permutations where $\boldsymbol{k}\rightarrow-\boldsymbol{k}$). The entire resonance may be absent, removing its physical effect from the model.

This observation has been previously made in Smith and Waleffe 1999. Investigations of this nature into the existence of resonant sets in discrete domains have been carried out, details of which can be found in Kartashova 2010 for example. However the progress made with this number theoretic issue is mostly restricted to problems in which the dispersion relation is proportional to a rational power of $\boldsymbol{k}$. This is not the case here, and we cannot establish the existence of resonant sets in this way. This is an interesting problem that seems to be due to the interplay between resonances and a periodic domain. This is a good example of the limits of exact resonances compared to near resonances: with any exactly resonant theory it may not be possible to simulate on a periodic domain without losing physical effects. Near resonant interactions (as in for example Smith and Lee 2005) would reintroduce missing resonances, and hence missing physics into the simulations.

At higher orders of the expansion one might expect that terms will appear in which the fast wave modes influence the slow, as found in the one layer system by Thomas 2016. If we consider only the set of modes in one vertical mode the dynamics behaves identically to a single layer. Because of this, in terms of wave interactions, we don't expect to lose behaviours within the two layer model: all the dynamics from the one layer model will be present plus any additional interactions.

4.3.5 Higher Order theory

The higher order theory actually requires very little extension from the one layer theory. All the results will pass in the same way, such is the strength of using the generalised higher order interaction coefficient. We expect all combinations of fast waves acting on a slow wave to have an interaction coefficient of zero as given in (4.37). Then, by the same inductive argument as given for the one layer equations in section 4.2.2, it follows that all combinations of fast modes cannot output a slow mode.

All possible triad mode combinations will take part in the triad or quartet interactions (except the fast-fast-slow interactions, as explained) the main difference being that some fast-fast-fast interactions had been promoted to triad order as shown in the triad order analysis.

4.4 Alternative method of expansion using conservation laws

In this section before continuing onto the stratified equations, we explore a different manner of calculating the expansion, based on conservation laws. The aim is to provide insight into the physical cause of the results of the previous section. The analysis follows closely that contained in Owen, Grimshaw, and Wingate 2018, which is based on that of Vanneste 2007, extending it to special cases, and to the quartet order of the expansion. It gives a general proof that fast modes alone cannot combine to create a zero mode in layered equations.

Before we continue we define some more compact notation. This method requires less consideration of wavenumbers and so the necessity to write everything explicitly in subscripts and superscripts is reduced. We therefore reduce (slightly) the number of coefficients by defining notation that combines information into a reduced form. The C and a are now defined as:

$$C_p^{qr} = C_{\boldsymbol{k}_1\boldsymbol{k}_2\boldsymbol{k}}^{\alpha_1\alpha_2\alpha}, \qquad a_p = a_{\boldsymbol{k}}^{\alpha},$$
$$p = \{\boldsymbol{k}, \alpha\}, \qquad q = \{\boldsymbol{k}_1, \alpha_1\}, \qquad r = \{\boldsymbol{k}_2, \alpha_2\}.$$

The subscript now defines the output mode with the superscripts denoting the inputs. Mode information has been conglomerated into a single identifier. This will hopefully make the content of the section more readable, and worth the expense of introducing a second notation.

We will extend the argument in Vanneste 2007 (more details in Vanneste and Vial 1994, and Ripa 1981). We start by defining the nonlinear interaction coefficient in terms of the quadratic part

of the energy and/or enstrophy. This is done by defining quadratic forms that, as well as giving the first terms of the conservation laws, form an orthogonality condition over the different modes.

First we consider the linearised problem. The dispersion relation is derived where the different branches give rise to different modes, as given in chapter 2. We now write the quadratic part of the energy (or enstrophy) in the form:

$$\mathcal{E}^{(2)} = \frac{1}{2}\int_D \boldsymbol{u}^\dagger \boldsymbol{E}\boldsymbol{u}\, d\boldsymbol{x}, \tag{4.65}$$

where $\boldsymbol{u}$ is the state vector, $\boldsymbol{u}^\dagger$ is its conjugate transpose and $\boldsymbol{E}$ is a Hermitian matrix. It can be proven Vanneste 2007 that this must obey the following orthogonality relation:

$$\boldsymbol{u}_p^\dagger \boldsymbol{E}\boldsymbol{u}_q = E_p^{(2)}\delta_{pq}. \tag{4.66}$$

This relation defines the constants $E_p^{(2)}$.

We now solve the nonlinear problem by taking Fourier transforms and splitting into the eigenmodes from the linear problem. We can use this orthogonality relation to isolate the effect on the amplitude of each mode:

$$\dot{a}_p = \frac{1}{2}\sum_{qr} C_p^{qr} a_q^* a_r^* e^{i\Omega_{pqr}t}\delta_{\boldsymbol{k}_p+\boldsymbol{k}_q+\boldsymbol{k}_r}, \tag{4.67}$$

$$C_p^{qr} = \boldsymbol{u}_p^\dagger \boldsymbol{E}[\boldsymbol{N}(\boldsymbol{u}_q,\boldsymbol{u}_r)+\boldsymbol{N}(\boldsymbol{u}_r,\boldsymbol{u}_q)]^*/E_p^{(2)}, \tag{4.68}$$

$$\Omega_{pqr} = \omega_p+\omega_q+\omega_r, \tag{4.69}$$

where $\dot{a}$ denotes differentiation of a with respect to time. The slightly different form of Ω is due to using the conjugates of the modes, and using the reality condition $a_p^* = a_{-p}$.

So far equations (4.67)-(4.69) are identical to Vanneste's work, but also equivalent to the multiscale analysis in this and the preceding chapters; the selection of the orthonormal basis simply chooses the basis in which $\boldsymbol{E} = \boldsymbol{I}$ and $E_p^{(2)} = 1$.

Using the conservation of energy and enstrophy laws: the energy (or enstrophy) can be expanded as:

$$\mathcal{E} = \mathcal{E}^{(2)}+\mathcal{E}^{(3)}+... = \frac{1}{2}\sum_p E_p^{(2)}|a_p|^2 + \frac{1}{6}\sum_{pqr} E_{pqr}^{(3)} a_p^* a_q^* a_r^* e^{i\Omega_{pqr}t}+... . \tag{4.70}$$

Here the coefficient $E_{pqr}^{(3)}$ is symmetric in it's arguments and can be derived from the form of the enstrophy and energy for the equation set being studied. However, the exact form of the cubic

energy is not needed for our purpose and we omit it here, the form of the enstrophy is given and used shortly in section 4.4.1. We differentiate (4.70) in time and, because it is a conserved quantity, this derivative must be equal to zero at each order. The lowest order terms are:

$$\dot{\mathcal{E}}^{(2)} = \frac{1}{2}\sum_{pqr} E_p^{(2)} C_p^{qr} a_p^* a_q^* a_r^* e^{i\Omega_{pqr}t}\delta_{\boldsymbol{k}_p+\boldsymbol{k}_q+\boldsymbol{k}_r} \quad + \quad \text{c.c} \quad + ..., \tag{4.71}$$

$$\dot{\mathcal{E}}^{(3)} = \frac{1}{6}\sum_{pqr} i\Omega_{pqr} E_{pqr}^{(3)} a_p^* a_q^* a_r^* e^{i\Omega_{pqr}t} + ..., \tag{4.72}$$

where these terms are both approximately 0. Here we have used equation (4.67) to express the time derivative as a terms. This equality will hold for arbitrary amplitudes and so we choose to consider the case where every wave amplitude is 0 apart from three that form a resonant triad.

Summing the different permutations over a chosen triad (a, b, c) and then repeating the method for enstrophy:

$$E_a^{(2)} C_a^{bc} + E_b^{(2)} C_b^{ac} + E_c^{(2)} C_c^{ba} = -i\Omega_{abc} E_{abc}^{(3)}, \tag{4.73}$$

$$Z_a^{(2)} C_a^{bc} + Z_b^{(2)} C_b^{ac} + Z_c^{(2)} C_c^{ba} = -i\Omega_{abc} Z_{abc}^{(3)}. \tag{4.74}$$

Here $Z_{abc}^{(3)}$ is defined equivalently to $E_{abc}^{(3)}$ but represents instead the cubic enstrophy. We consider the resonant cases $\Omega_{abc} = 0$, to the first order time scale.

From section 2.2.1, fast modes have zero quadratic enstrophy contribution: $Z_i = 0$ and so in the case of two fast modes (b, c) combining to make a slow mode (a) all that remains in (4.74) is: $C_a^{bc} = 0$.

4.4.1 Higher order expansion

In section 4.2.2 we found that to all orders sets of fast modes cannot output a zero mode. Here we repeat that finding using this alternative derivation. This is new work, extending the previous literature to higher order. It is assumed, and necessary for the following manipulations, that the nonlinearity is quadratic with no cubic or higher order terms present, as is the case in all the applications we consider.

We continue to higher order for the enstrophy. Expanding the enstrophy to 4th order in ampli-

tude:

$$\mathcal{Z} = \mathcal{Z}^{(2)} + \mathcal{Z}^{(3)} + ... = \sum_p Z_p^{(2)} |a_p|^2 + \sum_{pqr} Z_{pqr}^{(3)} a_p^* a_q^* a_r^* e^{i\Omega_{pqr}t} + \sum_{pqrs} Z_{pqrs}^{(4)} a_p^* a_q^* a_s^* a_r^* e^{i\Omega_{pqrs}t} + ... \,. \tag{4.75}$$

We then take derivatives in time:

$$\begin{aligned}\frac{\partial \mathcal{Z}}{\partial t} &= \frac{\partial \mathcal{Z}^{(2)}}{\partial t} + \frac{\partial \mathcal{Z}^{(3)}}{\partial t} + ... \\ &= \sum_{pqr} Z_p^{(2)} C_p^{qr} a_p^* a_q^* a_r^* e^{i\Omega_{pqr}t} + \sum_{pqr} i\Omega_{pqr} Z_{pqr}^{(3)} a_p^* a_q^* a_r^* e^{i\Omega_{pqr}t} \\ &\quad + \sum_{pqrs} C_m^{rs} Z_{pqm}^{(3)} a_p^* a_q^* a_s^* a_r^* e^{i\Omega_{pqrs}t} + \sum_{pqrs} i\Omega_{pqrs} Z_{pqrs}^{(4)} a_p^* a_q^* a_s^* a_r^* e^{i\Omega_{pqrs}t} + ... \,.\end{aligned} \tag{4.76}$$

We choose to consider only the terms that are 4th order in amplitude:

$$\frac{\partial \mathcal{Z}^{(3)}}{\partial t} + ... = \sum_{pqrs} (C_m^{rs} Z_{pqm}^{(3)} + i\Omega_{pqrs} Z_{pqrs}^{(4)}) a_p^* a_q^* a_s^* a_r^* e^{i\Omega_{pqrs}t} = 0. \tag{4.77}$$

We consider an isolated quartet, as before we are free to do this due to the arbitrariness of the wave amplitudes. We are left with the following:

$$C_a^{12} Z_{34a}^{(3)} + C_b^{23} Z_{41b}^{(3)} + C_c^{34} Z_{12c}^{(3)} + C_d^{41} Z_{23d}^{(3)} = -i\Omega_{1234} Z_{1234}^{(4)}. \tag{4.78}$$

Here a, b, c, d are modes such that the wavenumber is $\boldsymbol{k}_a = \boldsymbol{k}_1 + \boldsymbol{k}_2$ etc. From section 2.2.2 we have the form of $Z^{(3)}$ for the one and two layer equations:

$$Z_i^{(3)} = -\eta_i Q_i^2, \tag{4.79}$$

and so after symmetrisation:

$$Z_{123}^{(3)} = \frac{1}{3} \left(\eta_1 Q_2 Q_3 + \eta_3 Q_1 Q_2 + \eta_2 Q_3 Q_1 \right), \tag{4.80}$$

where Q is the linear PV of the mode. We see that if two or three of the modes in the $Z_{123}^{(3)}$ are fast modes, say $Q_1 = Q_2 = 0$ for example, then $Z_{123}^{(3)} = 0$. We now consider equation (4.78) for modes 2, 3, 4 fast and mode 1 slow. We first consider the 1st and 4th terms on the left hand side. If modes a and d are fast or slow then we have the situation described above: $Z_{34a}^{(3)} = Z_{23d}^{(3)} = 0$. For the 2nd and 3rd terms this occurs for b and c fast. However if b, and c are slow we can then consider the interaction coefficients. However from the previous order for fast modes interacting to form a slow mode we have: $C_b^{23} = C_c^{34} = 0$. Every term must be identically zero either due to the quadratic enstrophy conservation, or due to the zero interaction coefficient from the previous

order.

It follows that enstrophy is conserved to 3rd order. This did not require any new constraints: the first order behaviour automatically caused fast mode combinations to be unable to impact an output zero mode. This is the same situation as we found in the inductive argument made above in section 4.2.2 on the interaction coefficient. This will repeat similarly at every order for the layered equations due to the form of the enstrophy given in (2.52) and (2.56).

This analysis shows that conservation of enstrophy in interactions of many fast modes with a single slow mode is entirely fulfilled where the triad interaction coefficient $C_1^{23} = 0$. It is also irrelevant to this construction that the detuning needs to be zero as the $Z^{(n)}$ term in layered equations is always 0 for less than 2 slow mode combinations. The key point is that this is independent of resonances, and the analysis is completely generalisable for all zero mode systems with a similar form of potential vorticity (ie layered type equations).

In contrast the stratified equations have the weaker condition that $C_1^{23} = 0$ only for an exact resonance. This breaks the logic of the preceding paragraphs; it doesn't follow that the interactions will be 0 to every order. This is observed in the following section in the form of the interaction coefficient. We note that as this is due to the linearised structure of the potential vorticity, if the investigation were performed using the full nonlinearised PV to define the slow mode then one would expect the conservation to hold once more, and indeed the full PV mode would be obtained from our slow mode by a near-identity transform. However, as linearisation and asymptotic expansion in the manner presented here is ubiquitous in the field it is of importance that the behaviour is qualitatively different in this paradigm and so we will contrast the layered and stratified equations in this way in the remainder of the work.

4.5 Stratified Equations

Work on stratified flow using the Boussinesq approximation exists in McComas and Bretherton 1977 where a triad similar to the mixed mode fast-fast-fast triad, the interactions between gravity waves, was investigated. In that and related subsequent work by Bartello 1995 amongst others, the inclusion of vertical wavenumbers means that the form of the triads are fundamentally different from the layered cases just considered. One would expect that interaction between gravity waves of different vertical modes in the two layer equations mimics transfer of gravity wave energy vertically, and that there is an equivalent process in the stratified case. This correlates with the observation that in the continuously stratified equations there are no interactions between gravity waves lying in the same horizontal plane (Lelong and Riley 1991), but that for non-horizontal

gravity waves resonant interactions do exist. This suggests that the asymptotically expanded two layer equations may act as a proxy for understanding of the fully stratified case.

We now examine the stratified equations using the framework from chapter 3 to continue to higher orders, not previously investigated in this manner. We will then compare this to the layered equations. We find that whilst the gravity waves will interact in the manner described, similarly to the layered equations, the fast-fast-slow modes have a fundamentally different character to those of the shallow water systems.

4.5.1 Nonlinear Interaction Coefficient

Here we derive the form of the nonlinear interaction coefficient for this equation set in each triad type. The main difference from the layered equations is the coefficient for the $(\pm,\pm;0)$ interaction, which is no longer identically 0, as indicated by the form of the enstrophy and the theory of section 4.4.1.

The interaction coefficient for these equations takes the form:

$$C^{\alpha_1\alpha_2\alpha}_{\boldsymbol{k}_1\boldsymbol{k}_2\boldsymbol{k}} = \frac{i}{2}\Big[(\boldsymbol{u}^{\alpha_1}_{\boldsymbol{k}_1}\cdot\boldsymbol{k}_2)(\boldsymbol{r}^{\alpha_2}_{\boldsymbol{k}_2}\cdot\boldsymbol{r}^{\alpha}_{\boldsymbol{k}}) + (\boldsymbol{u}^{\alpha_2}_{\boldsymbol{k}_2}\cdot\boldsymbol{k}_1)(\boldsymbol{r}^{\alpha_1}_{\boldsymbol{k}_1}\cdot\boldsymbol{r}^{\alpha}_{\boldsymbol{k}})\Big]. \tag{4.81}$$

This was calculated in each individual case. For brevity we define the horizontal part of the wavenumber $\boldsymbol{k}^h = (k,l)^T$, so that $|\boldsymbol{k}^h|^2 + m^2 = |\boldsymbol{k}|^2$.

For the slow modes:

$$\begin{aligned} C^{0,0,0}_{\boldsymbol{k}_1\boldsymbol{k}_2\boldsymbol{k}} &= \frac{iN(\boldsymbol{k}_1\times\boldsymbol{k}_2)_z}{2\omega\omega_1\omega_2|\boldsymbol{k}||\boldsymbol{k}_1||\boldsymbol{k}_2|}\left[N^2(|\boldsymbol{k}^h_1|^2-|\boldsymbol{k}^h_2|^2)+f^2(m_1^2-m_2^2)\right] \\ &= \frac{iN(\boldsymbol{k}_1\times\boldsymbol{k}_2)_z}{2\omega\omega_1\omega_2|\boldsymbol{k}||\boldsymbol{k}_1||\boldsymbol{k}_2|}\left[\omega_1^2|\boldsymbol{k}_1|^2-\omega_2^2|\boldsymbol{k}_2|^2\right]. \end{aligned} \tag{4.82}$$

For two slow and one fast mode:

$$\begin{aligned} C^{\alpha_1,0,0}_{\boldsymbol{k}_1\boldsymbol{k}_2\boldsymbol{k}} =& \frac{i}{2\sqrt{2}\omega_1\omega_2\omega|\boldsymbol{k}_2||\boldsymbol{k}||\boldsymbol{k}_1||\boldsymbol{k}^h_1|}\Big[(f(\boldsymbol{k}\times\boldsymbol{k}_2)_z - i\alpha_1\omega_1(\boldsymbol{k}^h\cdot\boldsymbol{k}^h_2))N^2(m_1|\boldsymbol{k}^h_2|^2+m_2|\boldsymbol{k}^h_1|^2) \\ &+i\alpha_1\omega_1 m_1 N^2|\boldsymbol{k}^h|^2|\boldsymbol{k}^h_2|^2 + \left[fm_1(\boldsymbol{k}\times\boldsymbol{k}_2)_z + i\alpha_1\omega_1 m_1(\boldsymbol{k}^h_1\cdot\boldsymbol{k}^h_2) - i\alpha_1\omega_1 m_2|\boldsymbol{k}^h_1|^2\right]f^2(mm_2)\Big], \end{aligned} \tag{4.83}$$

$$C^{0,0,\alpha}_{\boldsymbol{k}_1\boldsymbol{k}_2\boldsymbol{k}} = \frac{iN^2(\boldsymbol{k}_2\times\boldsymbol{k}_1)_z}{\sqrt{2}\omega\omega_1\omega_2|\boldsymbol{k}||\boldsymbol{k}_1||\boldsymbol{k}_2||\boldsymbol{k}^h|}\Big[f(m_2-m_1)|\boldsymbol{k}^h|^2 + fm(|\boldsymbol{k}^h_1|^2-|\boldsymbol{k}^h_2|^2) + 2i\alpha\omega m(\boldsymbol{k}_2\times\boldsymbol{k}_1)_z\Big]. \tag{4.84}$$

For two fast and a slow mode:

$$C^{\alpha_1\alpha_2 0}_{\boldsymbol{k}_1\boldsymbol{k}_2\boldsymbol{k}} = \frac{iN}{2\omega\omega_1\omega_2|\boldsymbol{k}||\boldsymbol{k}_1||\boldsymbol{k}_2||\boldsymbol{k}_1^h||\boldsymbol{k}_2^h|}\Big[i(\alpha_1\omega_1+\alpha_2\omega_2)f(\boldsymbol{k}_1^h\cdot\boldsymbol{k}_2^h)(m_1^2|\boldsymbol{k}_2^h|^2+m_2^2|\boldsymbol{k}_1^h|^2) \\ -2i(\alpha_1\omega_1+\alpha_2\omega_2)fm_2m_1|\boldsymbol{k}_1^h|^2|\boldsymbol{k}_2^h|^2+(\alpha_1\alpha_2\omega_2\omega_1+f^2)(m_2^2|\boldsymbol{k}_1^h|^2-m_1^2|\boldsymbol{k}_2^h|^2)(\boldsymbol{k}_2\times\boldsymbol{k}_1)_z\Big]. \tag{4.85}$$

For this interaction coefficient we can simplify further. Using the dispersion relation (2.120), we write:

$$(\alpha_1\omega_1-\alpha_2\omega_2)(\alpha_1\omega_1+\alpha_2\omega_2)=\omega_1^2-\omega_2^2=\frac{(N^2-f^2)(m_2^2|\boldsymbol{k}_1^h|^2-m_1^2|\boldsymbol{k}_2^h|^2)}{|\boldsymbol{k}_1|^2|\boldsymbol{k}_2|^2}. \tag{4.86}$$

This can then be used to rewrite the last term of the interaction coefficient, and hence:

$$C^{\alpha_1\alpha_2 0}_{\boldsymbol{k}_1\boldsymbol{k}_2\boldsymbol{k}} = \frac{iN(\alpha_1\omega_1+\alpha_2\omega_2)}{2\omega\omega_1\omega_2|\boldsymbol{k}||\boldsymbol{k}_1||\boldsymbol{k}_2||\boldsymbol{k}_1^h||\boldsymbol{k}_2^h|}\Big[if(\boldsymbol{k}_1^h\cdot\boldsymbol{k}_2^h)(m_1^2|\boldsymbol{k}_2^h|^2+m_2^2|\boldsymbol{k}_1^h|^2) \\ -2ifm_2m_1|\boldsymbol{k}_1^h|^2|\boldsymbol{k}_2^h|^2+\frac{1}{N^2-f^2}(\alpha_1\omega_1-\alpha_2\omega_2)(\alpha_1\alpha_2\omega_2\omega_1+f^2)|\boldsymbol{k}_1|^2|\boldsymbol{k}_2|^2(\boldsymbol{k}_2\times\boldsymbol{k}_1)_z\Big]. \tag{4.87}$$

The resonance condition in this case is given by:

$$\alpha_1\omega_1+\alpha_2\omega_2=0, \tag{4.88}$$

and so for a resonant triad $C^{\alpha_1\alpha_2 0}_{\boldsymbol{k}_1\boldsymbol{k}_2\boldsymbol{k}}=0$. This coefficient will be commented on further in chapter 6, when this resonance is explored in a near resonant framework. Here significant differences are found from the layered equations in the previous sections. For the triad order expansion there is no such difference as the term is 0.

$$C^{\alpha_1 0\alpha}_{\boldsymbol{k}_1\boldsymbol{k}_2\boldsymbol{k}} = \frac{iN}{4\omega\omega_1\omega_2|\boldsymbol{k}||\boldsymbol{k}_1||\boldsymbol{k}_2||\boldsymbol{k}_1^h||\boldsymbol{k}^h|} \\ \Big[\big[fm_i(\boldsymbol{k}\times\boldsymbol{k}_j)_z+i\alpha_i\omega_i m_i(\boldsymbol{k}_i^h\cdot\boldsymbol{k}_j^h) \\ -i\alpha_i\omega_i m_j|\boldsymbol{k}_i^h|^2\big]\big[fm(\boldsymbol{k}^h\cdot\boldsymbol{k}_i^h)+i\alpha\omega m(\boldsymbol{k}_j\times\boldsymbol{k})_z-fm_i(\boldsymbol{k}^h\cdot\boldsymbol{k}_j^h)\big] \\ +(\boldsymbol{k}_j\times\boldsymbol{k}_i)_z\big[f^2mm_j((N^2+\omega\omega_j)|\boldsymbol{k}_j^h|^2|\boldsymbol{k}^h|^2 \\ +(\alpha\alpha_j\omega\omega_j+f^2)mm_j(\boldsymbol{k}^h\cdot\boldsymbol{k}_j^h)+ifmm_j(\alpha\omega+\alpha_j\omega_j)(\boldsymbol{k}\times\boldsymbol{k}_j)_z\big]\Big]. \tag{4.89}$$

For three fast modes:

$$C^{\alpha_1\alpha_2\alpha}_{\boldsymbol{k}_1\boldsymbol{k}_2\boldsymbol{k}} = \frac{i}{4\sqrt{2}\omega_1\omega\omega_2|\boldsymbol{k}||\boldsymbol{k}_1||\boldsymbol{k}_2||\boldsymbol{k}^h_1||\boldsymbol{k}^h_2||\boldsymbol{k}^h|}$$
$$\Bigg[\Big[fm_1(\boldsymbol{k}\times\boldsymbol{k}_2)_z + i\alpha_1\omega_1 m_1(\boldsymbol{k}^h_1\cdot\boldsymbol{k}^h_2) - i\alpha_1\omega_1 m_2|\boldsymbol{k}^h_1|^2\Big]\Big[f^2 mm_2((N^2+\omega\omega_2)|\boldsymbol{k}^h_2|^2|\boldsymbol{k}^h|^2$$
$$+(\alpha\alpha_2\omega\omega_2+f^2)mm_2(\boldsymbol{k}^h\cdot\boldsymbol{k}^h_2) + ifmm_2(\alpha\omega+\alpha_2\omega_2)(\boldsymbol{k}\times\boldsymbol{k}_2)_z\Big]$$
$$+\Big[fm_2(\boldsymbol{k}\times\boldsymbol{k}_1)_z + i\alpha_2\omega_2 m_2(\boldsymbol{k}^h_2\cdot\boldsymbol{k}^h_1) - i\alpha_2\omega_2 m_1|\boldsymbol{k}^h_2|^2\Big]\Big[f^2 mm_1((N^2+\omega\omega_1)|\boldsymbol{k}^h_1|^2|\boldsymbol{k}^h|^2$$
$$+(\alpha\alpha_1\omega\omega_1+f^2)mm_1(\boldsymbol{k}^h\cdot\boldsymbol{k}^h_1) + ifmm_1(\alpha\omega+\alpha_1\omega_1)(\boldsymbol{k}\times\boldsymbol{k}_1)_z\Big]\Bigg]. \tag{4.90}$$

The implementation of the theory to triad order is very similar to the layered equations of the previous sections. No resonant interactions are possible between two fast modes to return a slow mode, but the three fast modes can interact provided that the modes are not all travelling horizontally or all vertically. If they are all horizontal/vertical the resonance condition becomes the following:

$$\pm N \pm N \pm N = 0, \qquad \text{or} \qquad \pm f \pm f \pm f = 0, \tag{4.91}$$

which can never be satisfied for non-zero stratification/rotation. This was previously found in Lelong and Riley 1991 and complements the finding that in the one layer equations such resonances cannot exist, while in the two layer mixed vertical mode interactions (akin to non-horizontal motion) are permitted.

One key difference from the layered equations is due to the fast-fast-slow interaction. In the layered equations this interaction coefficient was identically zero, however in the stratified equations it is only identically zero in the case of exact resonant triads. At the higher orders of interaction where the non-resonant triads form building blocks of the quartets, and larger n-tets, these resonances are able to participate in energy exchanges. This is reflected in the theory of the previous section. For the stratified equations the cubic part of the enstrophy is given in (2.60):

$$\mathcal{Z}_3 = \left(N(\nabla\times\boldsymbol{u})_z + f\frac{\partial\sigma}{\partial z}\right)(\nabla\sigma\cdot\nabla\times\boldsymbol{u})\,. \tag{4.92}$$

Unlike the layered equations the cubic order of an enstrophy expansion won't be 0 for combinations containing only one slow mode. The slow-fast splitting separates the modes based on linear PV content. This means that although we still expect the interaction coefficient $C^{\alpha_1\alpha_2 0}_{\boldsymbol{k}_1\boldsymbol{k}_2\boldsymbol{k}}$ to be zero for a resonant triad, it should not be identically zero for the non-resonant triads, as in the case of the layered equations (this is commented on in Lelong and Riley 1991). To see this

we consider equation (4.74). It is now not true that $Z^{(3)}_{abc} = 0$ and so the result $C^{\alpha_1\alpha_2 0}_{\boldsymbol{k}_1\boldsymbol{k}_2\boldsymbol{k}} = 0$ is dependent on the condition $\Omega_{abc} = 0$, that the triad is resonant. This breaks the reasoning applied to equation (4.78) for the layered cases in which we concluded that $\{C^{(n)}\}^{\alpha_1\ldots\alpha_{n+1}0}_{\boldsymbol{k}_1\ldots\boldsymbol{k}_{n+1}\boldsymbol{k}} = 0$. For the stratified equations these interactions are viable and in comparison to the layered equations the constraint on the number of fast modes in a mixed mode resonant interaction at nth order becomes the slightly more lenient $1 < n_f \leq n + 1$ for $n \geq 2$. More will be concluded about these particular resonances in the following chapters in the near resonant context.

Although we found that the barotropic/baroclinic fast mode interactions in the two layer rotating shallow water equations appear to mirror the vertically propagating mode interactions in the stratified equations, it doesn't appear that the same can be said for the slow modes of the system. This isolates a key difference between the layered and stratified equations. The restriction to layers removes many higher order resonant pathways from the system. To quartet order there is a fundamental difference in the interactions due to the spontaneous creation of slow modes from the fast modes. However the change in total enstrophy would be unaffected if the contributions from the $\boldsymbol{u}_1$ part were to be considered. We investigate this further in the near resonant case in chapter 6, where some $\boldsymbol{u}_1$ terms can be promoted up an order in the asymptotic expansion, due to faster growth.

4.6 Chapter summary

The key points in this chapter were:

- We applied the theory of chapter 3 to the one layer equations. This confirmed existing work and generalised the higher order resonant theory.
- We presented new work from the application of the theory to the two layer rotating shallow water equations, evaluating the contribution to vertical energy movement in the fast modes. We discussed how this resonance may be completely absent in a discrete domain without consideration of near resonant modes.
- We demonstrated an alternative method extending that of Vanneste 2007 for deriving interaction coefficients from conserved quantities. This demonstrated directly how the conservation laws lead to behaviour of the interaction coefficients.
- We derived general theory during the application of the conservation laws that applies to all layered zero mode quadratic systems (and hence many fluid applications) and this was contrasted to the situation in the stratified equations.

In each of the applications considered, examples of where the theory requires extension to near resonant expansions were identified: in the one layer equations it was seen that fast only interactions can be arbitrarily close to resonance but never exactly, in the two layer equations the fast-fast-fast resonance discussed was such that it might not appear at all in a discrete domain, and in the stratified equations it was seen that conservation of enstrophy may appear to be broken if one is not able to consider the evolution of some slaved mode $\boldsymbol{u}_1$ parts of the dynamics on the same timescale as the triads. All of these reasons point towards the necessity of a near resonant expansion. This will now be explored in the subsequent chapters.

Chapter 5

Near resonant expansion

As discussed in chapter 1, where resonant detuning is sufficiently small we expect the behaviour to approximate the exact resonances. In the development of the asymptotic expansion near resonances become relevant due to bad ordering of the series: slaved modes that we assumed to be $O(\epsilon)$ may in fact grow large enough that they need to be included in the larger part of the expansion. If the description of the possible issue sounds like the description of secular terms in the original multiple scale expansion of chapter 3, that is because that is exactly the issue which arises; the set of secular terms must be expanded to take into account all of the terms that grow on the timescale $t_0 \sim \epsilon t$: the near resonances.

These small changes to the expansion cause a step change in the behaviour of the expanded system. Numerical examples of this physically different behaviour can be found in for instance Smith and Lee 2005 and related papers. The effects in numerical examples can be particularly noticeable, where the wavenumber spacing can decimate the number of available exact resonances. Here we will describe a new framework that can quantify how the near resonant system links to the exact resonant system of the previous chapters by effectively 'promoting' higher order resonances to the triad timescale. We will then apply the framework to the example geophysical systems in chapter 6 where we will see that it gives a much better approximation of the true solution.

5.1 Triad order expansion

The theory in the subsequent sections is presented in a similar manner to the theory in chapter 3. This is by design, to reflect that the method is derived similarly but now extends the exact

expansion. In this vein, we start with the triad derivation as in section 3.2, but we will now include the broader range of secular terms represented by the near resonances.

We set up the expansion similarly to the exact resonant case and begin with the equivalent equations, those of (3.6-3.8), restated here:

$$O(\epsilon^{-1}) \qquad \frac{\partial \boldsymbol{u}_0}{\partial \tau} + \mathcal{L}\boldsymbol{u}_0 = 0, \tag{5.1}$$

$$O(1) \qquad \frac{\partial \boldsymbol{u}_1}{\partial \tau} + \mathcal{L}\boldsymbol{u}_1 = -\left(\frac{\partial \boldsymbol{u}_0}{\partial t_0} + \mathcal{N}(\boldsymbol{u}_0, \boldsymbol{u}_0)\right), \tag{5.2}$$

$$O(\epsilon) \qquad \frac{\partial \boldsymbol{u}_2}{\partial \tau} + \mathcal{L}\boldsymbol{u}_2 = -\left(\frac{\partial \boldsymbol{u}_1}{\partial t_0} + \frac{\partial \boldsymbol{u}_0}{\partial t_1} + \mathcal{N}(\boldsymbol{u}_0, \boldsymbol{u}_1) + \mathcal{N}(\boldsymbol{u}_1, \boldsymbol{u}_0)\right). \tag{5.3}$$

If we were to continue as in section 3.2, at first order the equation is linear and we can write the solution in terms of the exponential operator and $\bar{\boldsymbol{u}}$, constant in fast time:

$$\begin{aligned} \boldsymbol{u}_0(\boldsymbol{x}, \tau, t_0, t_1) &= e^{-\tau\mathcal{L}}\bar{\boldsymbol{u}}(\boldsymbol{x}, t_0, t_1), \\ \bar{\boldsymbol{u}} &= \boldsymbol{u}_0(\boldsymbol{x}, 0, t_0, t_1). \end{aligned} \tag{5.4}$$

Then solving at the next order:

$$e^{\tau\mathcal{L}}\boldsymbol{u}_1 = \boldsymbol{u}_1|_{\tau=0} - \left(\tau\frac{\partial \bar{\boldsymbol{u}}}{\partial t_0} + \int_0^\tau e^{s\mathcal{L}}\mathcal{N}(e^{-s\mathcal{L}}\bar{\boldsymbol{u}}, e^{-s\mathcal{L}}\bar{\boldsymbol{u}})ds\right). \tag{5.5}$$

We need to make sure that, as previously in (3.18), the $\boldsymbol{u}_1$ terms are the leading order error to the expansion in $\boldsymbol{u}_0$ and that they do not grow to $O(1)$ size. We equate the secular terms:

$$\begin{aligned} \frac{\partial \bar{\boldsymbol{u}}}{\partial t_0} &= -\frac{1}{\tau}\int_0^\tau e^{s\mathcal{L}}\mathcal{N}(e^{-s\mathcal{L}}\bar{\boldsymbol{u}}, e^{-s\mathcal{L}}\bar{\boldsymbol{u}})ds \\ &= -\frac{1}{\tau}\int_0^\tau \sum_{\substack{\boldsymbol{k},\boldsymbol{k}_1,\boldsymbol{k}_2 \\ \alpha,\alpha_1,\alpha_2 \\ \boldsymbol{k}=\boldsymbol{k}_1+\boldsymbol{k}_2}} C^{\alpha_1\alpha_2\alpha}_{\boldsymbol{k}_1\boldsymbol{k}_2\boldsymbol{k}} a^{\alpha_1}_{\boldsymbol{k}_1} a^{\alpha_2}_{\boldsymbol{k}_2} \boldsymbol{r}^{\alpha}_{\boldsymbol{k}} e^{i\boldsymbol{k}\cdot\boldsymbol{x}} e^{-i(\omega^{\alpha_1}_{\boldsymbol{k}_1} + \omega^{\alpha_2}_{\boldsymbol{k}_2} - \omega^{\alpha}_{\boldsymbol{k}})s} ds. \end{aligned} \tag{5.6}$$

This is almost equivalent to equation (3.14) except that we take more care in the limit to identify the secular terms. This will allow the near resonances to remain in our expansion.

We can bound the size of the integral to determine the size of the contribution to the series, to ensure that $\boldsymbol{u}_1$ is not going to contain modes that grow too large. A maximum bound on the integral can be given by:

$$\begin{aligned} &\left|\frac{1}{\tau}\int_0^\tau e^{i\Omega s}ds\right| = \left|\frac{e^{i\Omega\tau}-1}{\tau\Omega}\right| \leq \frac{2}{\tau|\Omega|} \sim O\left(\frac{\epsilon}{\Omega}\right), \\ &\text{where:} \qquad \Omega = \omega^{\alpha}_{\boldsymbol{k}} - \omega^{\alpha_1}_{\boldsymbol{k}_1} - \omega^{\alpha_2}_{\boldsymbol{k}_2}. \end{aligned} \tag{5.7}$$

It is apparent that in the case of near resonances ($\Omega \sim \epsilon$) we cannot bound the contributions to

$O(\epsilon)$ and so they cannot be pushed to the next order in the expansion: they are secular. We define Ω_{lim} as the maximum detuning size at which we consider there to be resonance. In the weakly nonlinear limit $\epsilon \to 0$, it follows that the appropriate maximum resonant detuning $\Omega_{lim} \to 0$ and so there are no near resonances to contribute, and the exact expansion would be appropriate. Because the sizes of the possible Ω's of each triad grouping are determined by the system, but the nonlinearity size ϵ has been imposed, we always expect near resonances in the system for small but finite ϵ. Therefore, in the pursuit of a practical limit, we maintain near resonances in our expansion. For the remainder of the work we will fix $\Omega_{lim} = O(\epsilon)$.

We contrast the two cases of near and exact resonance in terms of the minimum non-zero detuning in the system Ω_{min} (also shown in Figure 5.1):

- $\epsilon < \Omega_{min}$
  - Exact resonances - $\Omega = 0$, formed by the terms that remain secular in the limit.
  - Non-resonances - All non-exact resonances. These behave as slaved modes, shown in chapter 3
- $\epsilon > \Omega_{min}$
  - Near resonances - $\Omega \sim O(\epsilon)$, these terms with sufficiently small Ω vary at the same rate as exact resonances; they are secular terms.
  - Non-resonances - $\Omega = O(1)$ formed by all non-near resonances, these behave as slaved modes

When $\epsilon > \Omega_{min}$, the non-exact resonances are distributed such that some belong to the near resonant group. As will be seen the near resonances cause similar behaviour to the non-resonances and are only differentiated by the timescale on which they act.

The exact resonances can be considered a special case (or a subset) of the near resonances. For use later, to explicitly avoid division by small terms, we must define the concept of a super-near resonance: a subset of the near resonances with $\Omega \sim O(\epsilon^n)$, $n \geq 2$. This notion is explored in section 5.1.3.

Sections 5.1.1, 5.1.2, and 5.1.3 perform essentially the same process as one another: calculating the output from a triad interaction and placing it at the appropriate timescale, in the cases of non-resonance, near resonance, and super-near resonance respectively.

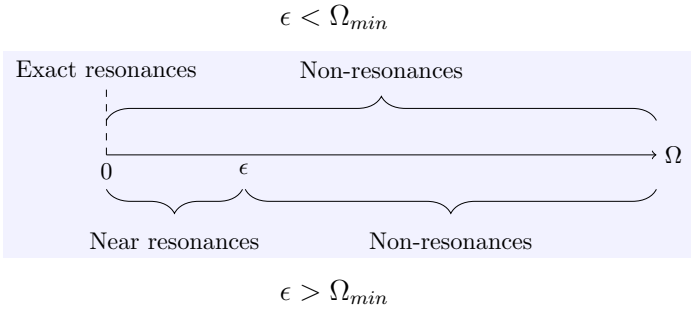

Figure 5.1: Diagram showing the definitions of the different terms. The size of Ω compared to ϵ determines the type of mode formed. When $\epsilon < \Omega_{min}$ the near resonances disappear and the non-resonances are identically slaved modes.

5.1.1 Slaved modes

Where the triads have Ω large, such that no resonance occurs, we simply cannot consider them on the t_0 timescale. We proceed as we did for exact resonances in section 3.3, solving to calculate their behaviour, as slaved modes that contribute to the next order in the term $\boldsymbol{u}_1$. These will then be passed back into the quadratic nonlinearity as before to form a 'pseudo' cubic interaction. We return to (5.2):

$$\frac{\partial \boldsymbol{u}_1}{\partial \tau} + \mathcal{L}\boldsymbol{u}_1 = -\left(\frac{\partial \boldsymbol{u}_0}{\partial t_0} + \mathcal{N}(\boldsymbol{u}_0, \boldsymbol{u}_0)\right). \tag{5.8}$$

We remove the exact and near resonant secular terms, that will instead contribute to the motion as a slow change to the $\boldsymbol{u}_0$ term as part of equation (5.12). These remaining non-resonant terms will be equated with the τ derivative and linear operator from the left hand side:

$$\frac{\partial \boldsymbol{u}_1}{\partial \tau} + \mathcal{L}\boldsymbol{u}_1 = -\mathcal{N}^{nnr}(\boldsymbol{u}_0, \boldsymbol{u}_0). \tag{5.9}$$

Here we have written $\mathcal{N}^{nnr}$ to indicate that only the non-near resonant parts of the nonlinear term are included, this constitutes the main difference from the exactly resonant case. We now solve for $\boldsymbol{u}_1$. The complementary function would find linear modes of the same form as for $\boldsymbol{u}_0$ and hence we can assume they are identically 0 as the solution in this form is accounted for in those first order terms (see Craik 1988 for instance). Now we simply need to find the particular integral for our right hand side. This is given by:

$$\boldsymbol{u}_1 = -e^{-\tau\mathcal{L}} \int_0^\tau e^{s\mathcal{L}} \mathcal{N}^{nnr}(e^{-s\mathcal{L}}\bar{\boldsymbol{u}}, e^{-s\mathcal{L}}\bar{\boldsymbol{u}}) ds, \tag{5.10}$$

or in the eigenmode basis:

$$\{\boldsymbol{u}_1\}^{\alpha_a}_{\boldsymbol{k}_a} = -\sum_{\substack{\boldsymbol{k}_1,\boldsymbol{k}_2\\ \alpha_1,\alpha_2}} C^{\alpha_1\alpha_2\alpha_a}_{\boldsymbol{k}_1\boldsymbol{k}_2\boldsymbol{k}_a}\big|_{nnr}\, a^{\alpha_1}_{\boldsymbol{k}_1} a^{\alpha_2}_{\boldsymbol{k}_2} \boldsymbol{r}^{\alpha_a}_{\boldsymbol{k}_a} e^{i\boldsymbol{k}\cdot\boldsymbol{x}} e^{-i\omega_a\tau} \int_0^\tau e^{i(-\omega_1-\omega_2+\omega_a)s} ds\; \delta_{\boldsymbol{k}_a-\boldsymbol{k}_1-\boldsymbol{k}_2}$$
$$= \sum_{\substack{\boldsymbol{k}_1,\boldsymbol{k}_2\\ \alpha_1,\alpha_2}} \frac{C^{\alpha_1\alpha_2\alpha_a}_{\boldsymbol{k}_1\boldsymbol{k}_2\boldsymbol{k}_a}\big|_{nnr}\, a^{\alpha_1}_{\boldsymbol{k}_1} a^{\alpha_2}_{\boldsymbol{k}_2}}{i(\omega_a-\omega_1-\omega_2)} \boldsymbol{r}^{\alpha_a}_{\boldsymbol{k}_a} e^{i\boldsymbol{k}\cdot\boldsymbol{x}} e^{-i(\omega_1+\omega_2)\tau}\; \delta_{\boldsymbol{k}_a-\boldsymbol{k}_1-\boldsymbol{k}_2}. \tag{5.11}$$

In the integration we used $\boldsymbol{u}_1(\tau=0)=0$, because the initial conditions are entirely accounted for in the $\boldsymbol{u}_0$ terms. We see that $\boldsymbol{u}_1$ does **not** evolve according to the dispersion relation: by the definition of non-resonance $\omega_a \neq \omega_1+\omega_2$. These are the slaved modes: they evolve only through the change to the two underlying modes $a^{\alpha_1}_{\boldsymbol{k}_1}$, $a^{\alpha_2}_{\boldsymbol{k}_2}$.

5.1.2 Near resonances

Literature describing isolated near resonant triads can be found starting originally in Bretherton 1964 and more recently in Vanneste 2007. In the isolated case not much is changed from exact resonant interactions, the detuning can only affect the phase by an $O(1)$ amount and changes to the behaviour of the amplitude can only be $O(\epsilon)$. Here we consider the triads in a non-isolated manner, such that they may interact with one another as permitted by the triad condition $\boldsymbol{k}=\boldsymbol{k}_1+\boldsymbol{k}_2$. This will lead to qualitatively different behaviour compared to the exact resonant expansion.

To see this, we first return to (5.6):

$$\frac{\partial \bar{\boldsymbol{u}}}{\partial t_0} = -\frac{1}{\tau}\int_0^\tau \sum_{\substack{\boldsymbol{k},\boldsymbol{k}_1,\boldsymbol{k}_2\\ \alpha,\alpha_1,\alpha_2\\ \boldsymbol{k}=\boldsymbol{k}_1+\boldsymbol{k}_2}} C^{\alpha_1\alpha_2\alpha}_{\boldsymbol{k}_1\boldsymbol{k}_2\boldsymbol{k}} a^{\alpha_1}_{\boldsymbol{k}_1}(t_0,t_1) a^{\alpha_2}_{\boldsymbol{k}_2}(t_0,t_1) \boldsymbol{r}^{\alpha}_{\boldsymbol{k}} e^{i\boldsymbol{k}\cdot\boldsymbol{x}} e^{i\Omega^{\alpha_1\alpha_2\alpha}_{\boldsymbol{k}_1\boldsymbol{k}_2\boldsymbol{k}} s} ds.$$

However we now explicitly write the ϵ scaling of Ω such that $\tau\Omega = \tau\epsilon\Delta = t_0\Delta$, with $\Delta = O(1)$ which slows the dependence of the exponential to the t_0 timescale:

$$\frac{\partial a^{\alpha}_{\boldsymbol{k}}}{\partial t_0} = -\sum_{\substack{\boldsymbol{k}_1,\boldsymbol{k}_2\\ \alpha_1,\alpha_2\\ \boldsymbol{k}=\boldsymbol{k}_1+\boldsymbol{k}_2}} C^{\alpha_1\alpha_2\alpha}_{\boldsymbol{k}_1\boldsymbol{k}_2\boldsymbol{k}} a^{\alpha_1}_{\boldsymbol{k}_1}(t_0,t_1) a^{\alpha_2}_{\boldsymbol{k}_2}(t_0,t_1) e^{i\Delta^{\alpha_1\alpha_2\alpha}_{\boldsymbol{k}_1\boldsymbol{k}_2\boldsymbol{k}} t_0} \frac{1}{\tau}\int_0^\tau ds$$
$$= -\sum_{\substack{\boldsymbol{k}_1,\boldsymbol{k}_2\\ \alpha_1,\alpha_2\\ \boldsymbol{k}=\boldsymbol{k}_1+\boldsymbol{k}_2}} C^{\alpha_1\alpha_2\alpha}_{\boldsymbol{k}_1\boldsymbol{k}_2\boldsymbol{k}} a^{\alpha_1}_{\boldsymbol{k}_1}(t_0,t_1) a^{\alpha_2}_{\boldsymbol{k}_2}(t_0,t_1) e^{i\Delta^{\alpha_1\alpha_2\alpha}_{\boldsymbol{k}_1\boldsymbol{k}_2\boldsymbol{k}} t_0}. \tag{5.12}$$

This dynamical equation is similar to that of the exact resonances (3.18), except for the exponential term. It defines evolution on the t_0 timescale, as before.

For use later we now also perform the integration in t_0. This is similar to finding the particular integral for the slaved modes in the previous section (equation (5.10)), except on the slower

timescale t_0 (and larger $\boldsymbol{u}_0$). This is done by parts:

$$a^{\alpha}_{\boldsymbol{k}} = -\sum_{\substack{\boldsymbol{k}_1,\boldsymbol{k}_2\\ \alpha_1,\alpha_2\\ \boldsymbol{k}=\boldsymbol{k}_1+\boldsymbol{k}_2}} C^{\alpha_1\alpha_2\alpha}_{\boldsymbol{k}_1\boldsymbol{k}_2\boldsymbol{k}} \left(\frac{a^{\alpha_1}_{\boldsymbol{k}_1}(t_0,t_1)a^{\alpha_2}_{\boldsymbol{k}_2}(t_0,t_1)}{i\Delta^{\alpha_1\alpha_2\alpha}_{\boldsymbol{k}_1\boldsymbol{k}_2\boldsymbol{k}}} e^{i\Delta^{\alpha_1\alpha_2\alpha}_{\boldsymbol{k}_1\boldsymbol{k}_2\boldsymbol{k}}t_0} \right.$$
$$\left. - \int_0^{t_0} \frac{\frac{\partial}{\partial s}(a^{\alpha_1}_{\boldsymbol{k}_1}(s,t_1))a^{\alpha_2}_{\boldsymbol{k}_2}(s,t_1) + a^{\alpha_1}_{\boldsymbol{k}_1}(s,t_1)\frac{\partial}{\partial s}(a^{\alpha_2}_{\boldsymbol{k}_2}(s,t_1))}{i\Delta^{\alpha_1\alpha_2\alpha}_{\boldsymbol{k}_1\boldsymbol{k}_2\boldsymbol{k}}} e^{i\Delta^{\alpha_1\alpha_2\alpha}_{\boldsymbol{k}_1\boldsymbol{k}_2\boldsymbol{k}}s} ds \right). \quad (5.13)$$

We will pause this analysis here until we have completed the derivation of the quartets, save to mention two things. Firstly, the left hand term in the sum has the same form as the slaved modes, except for the timescale of the exponential. Secondly the right hand term can be integrated again in the same manner, which we will see mirrors the quartet expansion process. For this reason the t_1 dependence has been explicitly written in the arguments of the amplitudes.

The key observation is that the near resonances behave exactly as the slaved mode interactions, except that instead of affecting the $\boldsymbol{u}_1$ part on timescale τ they affect the $\boldsymbol{u}_0$ part on timescale t_0. This allows them to evolve independently; they are not behaving in the slaved manner of the $\boldsymbol{u}_1$ part.

5.1.3 Super-near resonances

In this section we will introduce new terminology, super-near resonance, to describe near resonances that are extra close to being exactly resonant, such that $\Omega \sim O(\epsilon^2)$. This is necessary to avoid division by a small quantity in (5.13). It is seen that super-near resonances will behave like exact resonances until quartet order or higher.

In the previous section we assumed a scaling on Ω of $O(\epsilon)$ so that $\Delta \sim O(1)$. This is necessary to avoid problems arising from division by ϵ - a form of secularity. We therefore need to treat differently any super-near resonance, which we define as those with $\Omega \sim O(\epsilon^n)$, $n \geq 2$. This is illustrated in figure 5.2. Similarly to section 5.1.2 we will change the timescale over which these resonances act. We change:

$$\Omega\tau \to \Delta_{(n)} t_n \qquad \text{for} \qquad \Omega \sim O(\epsilon^{n+1}),$$
$$\Delta_{(n)} \sim O(1), \quad (5.14)$$

where we can identify $\Delta = \Delta_{(0)}$.

In these cases the exponential has no t_0 dependence, and so these expansion terms will behave in the same manner as the exact resonances, albeit with extra slow time exponential

terms modulating their behaviour:

$$\frac{\partial}{\partial t_0} a_{\boldsymbol{k}}^{\alpha} = \sum exact\ resonances + \sum near\ resonances + \sum_{\substack{\boldsymbol{k}_1,\boldsymbol{k}_2 \\ \alpha_1,\alpha_2}} C_{\boldsymbol{k}_1\boldsymbol{k}_2\boldsymbol{k}}^{\alpha_1\alpha_2\alpha} a_{\boldsymbol{k}_1}^{\alpha_1}(t_0,t_1) a_{\boldsymbol{k}_2}^{\alpha_2}(t_0,t_1) e^{i\Delta_{(n)}t_n} \delta_{\boldsymbol{k}-\boldsymbol{k}_1-\boldsymbol{k}_2} \,. \tag{5.15}$$

These terms do not require different treatment to the exact resonances, although on the longer timescales they will cause a shift to the wave phases of any amplitude affected by them. Figure 5.2 shows this splitting of the different super-near resonant parts.

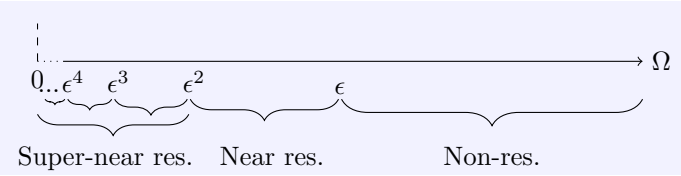

Figure 5.2: Diagram showing the super-near resonant splitting. All of the super-near resonant terms will be treated similarly to the exact resonances on the t_0 timescale. At the next timescale the largest of the super-near resonant terms will affect the motion, and so on for each timescale.

5.2 Quartet Order expansion

We have the form of $\boldsymbol{u}_1$ from section 5.1.1 we can continue to the next order of expansion given by (5.3):

$$\frac{\partial \boldsymbol{u}_2}{\partial \tau} + \mathcal{L}\boldsymbol{u}_2 = -\left(\frac{\partial \boldsymbol{u}_1}{\partial t_0} + \frac{\partial \boldsymbol{u}_0}{\partial t_1} + \mathcal{N}(\boldsymbol{u}_0,\boldsymbol{u}_1) + \mathcal{N}(\boldsymbol{u}_1,\boldsymbol{u}_0)\right). \tag{5.16}$$

We are able to write the nonlinear part in this manner as we are only considering systems with quadratic nonlinearity; if there were cubic nonlinearity it's effects would appear in the equations here. Because of this the only manner in which quartet terms can arise is by interaction of slaved modes with the basic modes. The following is almost identical to the expansion for the resonant case, the key difference being that **the $\boldsymbol{u}_1$ terms are now only formed by the non-near resonant interactions**, those formed by the near resonances belong in the $\boldsymbol{u}_0$ part and are no longer considered slaved.

Following the same process of removing secular terms we have the equation:

$$\frac{\partial \bar{\boldsymbol{u}}}{\partial t_1} = -\frac{1}{\tau}\int_0^{\tau} e^{s(\mathcal{L}-\mathcal{L}')}\frac{\partial \bar{\boldsymbol{u}}_1}{\partial t_0} + e^{s\mathcal{L}}\left(\mathcal{N}(e^{-s\mathcal{L}}\bar{\boldsymbol{u}}, e^{-s\mathcal{L}'}\bar{\boldsymbol{u}}_1) + \mathcal{N}(e^{-s\mathcal{L}'}\bar{\boldsymbol{u}}_1, e^{-s\mathcal{L}}\bar{\boldsymbol{u}})\right) ds, \tag{5.17}$$

where $\boldsymbol{u}_1 = \bar{\boldsymbol{u}}_1 e^{-\tau\mathcal{L}'}$, shorthand for $\{\bar{\boldsymbol{u}}_1\}_{\boldsymbol{k}}^{\alpha} e^{-i(\omega_1+\omega_2)\tau}$ in the eigenbasis. Writing in the eigenmode

basis we see that we form various quartet resonances from the terms within the integral. We will analyse each term on the right hand side of (5.17) individually. Taking the first term:

$$-\frac{1}{\tau}\int_0^\tau \left\{e^{s(\mathcal{L}-\mathcal{L}')}\frac{\partial \bar{\boldsymbol{u}}_1}{\partial t_0}\right\}_{\boldsymbol{k}}^{\alpha} ds = -\sum_{\substack{\boldsymbol{k}_1,\boldsymbol{k}_2\\ \alpha_1,\alpha_2}} \frac{C^{\alpha_1\alpha_2\alpha}_{\boldsymbol{k}_1\boldsymbol{k}_2\boldsymbol{k}}\big|_{nnr}}{i(\omega-\omega_1-\omega_2)}\,\delta_{\boldsymbol{k}-\boldsymbol{k}_1-\boldsymbol{k}_2}\frac{1}{\tau}\int_0^\tau \frac{\partial}{\partial t_0}(a^{\alpha_1}_{\boldsymbol{k}_1}a^{\alpha_2}_{\boldsymbol{k}_2})\boldsymbol{r}^{\alpha}_{\boldsymbol{k}}e^{i(\omega-\omega_1-\omega_2)s}ds. \tag{5.18}$$

At this point if we were to expand the derivatives in t_0 using (5.12) we will not alter the dependence of the exponential term on τ, which is the important component of the integral. We now have, similarly to at the triad order, that:

$$\frac{1}{\tau}\int_0^\tau e^{i(\omega-\omega_1-\omega_2)s}ds,$$

will send every term to $O(\epsilon)$ by cancellation of oscillations, unless $\omega-\omega_1-\omega_2\sim O(\epsilon)$. We know that no terms have this form as we required the triad to be non-near resonant, and hence this term must be 0. This is in effect the statement that slaved modes do not evolve on the t_0 timescale.

We now consider the second term, substituting into it (5.11):

$$\begin{aligned}
&-\frac{1}{\tau}\int_0^\tau \left\{e^{s\mathcal{L}}\mathcal{N}(e^{-s\mathcal{L}}\bar{\boldsymbol{u}},e^{-s\mathcal{L}'}\bar{\boldsymbol{u}}_1)\right\}_{\boldsymbol{k}}^{\alpha} ds\\
&=-\frac{1}{\tau}\int_0^\tau \sum_{\substack{\boldsymbol{k}_a,\boldsymbol{k}_3\\ \alpha_a,\alpha_3}} C^{\alpha_a\alpha_3\alpha}_{\boldsymbol{k}_a\boldsymbol{k}_3\boldsymbol{k}}\boldsymbol{r}^{\alpha}_{\boldsymbol{k}}a^{\alpha_3}_{\boldsymbol{k}_3}e^{-i\omega_3 s}\delta_{\boldsymbol{k}-\boldsymbol{k}_a-\boldsymbol{k}_3}\sum_{\substack{\boldsymbol{k}_1,\boldsymbol{k}_2\\ \alpha_1,\alpha_2}}\frac{C^{\alpha_1\alpha_2\alpha_a}_{\boldsymbol{k}_1\boldsymbol{k}_2\boldsymbol{k}_a}\big|_{nnr}a^{\alpha_1}_{\boldsymbol{k}_1}a^{\alpha_2}_{\boldsymbol{k}_2}}{i(\omega_a-\omega_1-\omega_2)}e^{-i(\omega_1+\omega_2)s}\,e^{i\omega s}\delta_{\boldsymbol{k}_a-\boldsymbol{k}_1-\boldsymbol{k}_2}ds\\
&=-\sum_{\substack{\boldsymbol{k}_a,\boldsymbol{k}_3\\ \alpha_a,\alpha_3}}\sum_{\substack{\boldsymbol{k}_1,\boldsymbol{k}_2\\ \alpha_1,\alpha_2}}\frac{1}{\tau}\int_0^\tau \frac{C^{\alpha_a\alpha_3\alpha}_{\boldsymbol{k}_a\boldsymbol{k}_3\boldsymbol{k}}\,C^{\alpha_1\alpha_2\alpha_a}_{\boldsymbol{k}_1\boldsymbol{k}_2\boldsymbol{k}_a}\big|_{nnr}}{i(\omega_a-\omega_1-\omega_2)}a^{\alpha_1}_{\boldsymbol{k}_1}a^{\alpha_2}_{\boldsymbol{k}_2}a^{\alpha_3}_{\boldsymbol{k}_3}\boldsymbol{r}^{\alpha}_{\boldsymbol{k}}e^{i(\omega-\omega_1-\omega_2-\omega_3)s}\,\delta_{\boldsymbol{k}-\boldsymbol{k}_1-\boldsymbol{k}_2-\boldsymbol{k}_3}ds\\
&=-\sum_{\substack{\boldsymbol{k}_1,\boldsymbol{k}_2,\boldsymbol{k}_3\\ \alpha_a,\alpha_1,\alpha_2,\alpha_3}}\frac{C^{\alpha_a\alpha_3\alpha}_{\boldsymbol{k}_a\boldsymbol{k}_3\boldsymbol{k}}\,C^{\alpha_1\alpha_2\alpha_a}_{\boldsymbol{k}_1\boldsymbol{k}_2\boldsymbol{k}_a}\big|_{nnr}}{i(\omega_a-\omega_1-\omega_2)}a^{\alpha_1}_{\boldsymbol{k}_1}a^{\alpha_2}_{\boldsymbol{k}_2}a^{\alpha_3}_{\boldsymbol{k}_3}\boldsymbol{r}^{\alpha}_{\boldsymbol{k}}\delta_{\omega-\omega_1-\omega_2-\omega_3}\,\delta_{\boldsymbol{k}-\boldsymbol{k}_1-\boldsymbol{k}_2-\boldsymbol{k}_3}.
\end{aligned}\tag{5.19}$$

Here we have only considered the exact quartet resonances, although the quartet near resonances follow similarly to the previous order. We will briefly reproduce the scaling argument from (5.7) for the quartet near resonances. Because we now want to consider timescales up to t_1, our τ must reach a size $\sim 1/\epsilon^2$. This also means that we should consider the t_0 variation in the amplitudes, which we write as $\epsilon\tau$. We write, using integration by parts and chain rule:

$$\begin{aligned}
&\left|\frac{1}{\tau}\int_0^\tau \frac{C^{\alpha_a\alpha_3\alpha}_{\boldsymbol{k}_a\boldsymbol{k}_3\boldsymbol{k}}\,C^{\alpha_1\alpha_2\alpha_a}_{\boldsymbol{k}_1\boldsymbol{k}_2\boldsymbol{k}_a}\big|_{nnr}}{i(\omega_a-\omega_1-\omega_2)}a^{\alpha_1}_{\boldsymbol{k}_1}(\epsilon\tau)a^{\alpha_2}_{\boldsymbol{k}_2}(\epsilon\tau)a^{\alpha_3}_{\boldsymbol{k}_3}(\epsilon\tau)\boldsymbol{r}^{\alpha}_{\boldsymbol{k}}e^{i\Omega^{(2)}s}\,ds\right|\\
&=\frac{1}{\tau}\left|\frac{C^{\alpha_a\alpha_3\alpha}_{\boldsymbol{k}_a\boldsymbol{k}_3\boldsymbol{k}}\,C^{\alpha_1\alpha_2\alpha_a}_{\boldsymbol{k}_1\boldsymbol{k}_2\boldsymbol{k}_a}\big|_{nnr}}{i(\omega_a-\omega_1-\omega_2)}\boldsymbol{r}^{\alpha}_{\boldsymbol{k}}\right|\left|a^{\alpha_1}_{\boldsymbol{k}_1}a^{\alpha_2}_{\boldsymbol{k}_2}a^{\alpha_3}_{\boldsymbol{k}_3}\frac{e^{i\Omega^{(2)}s}-1}{i\Omega^{(2)}}+\epsilon\int_0^\tau\frac{\partial}{\partial t_0}\left(a^{\alpha_1}_{\boldsymbol{k}_1}(t_0)a^{\alpha_2}_{\boldsymbol{k}_2}(t_0)a^{\alpha_3}_{\boldsymbol{k}_3}(t_0)\right)\frac{e^{i\Omega^{(2)}s}}{\Omega^{(2)}}\,ds\right|\\
&\lesssim\frac{1}{\tau}\left|\frac{C^{\alpha_a\alpha_3\alpha}_{\boldsymbol{k}_a\boldsymbol{k}_3\boldsymbol{k}}\,C^{\alpha_1\alpha_2\alpha_a}_{\boldsymbol{k}_1\boldsymbol{k}_2\boldsymbol{k}_a}\big|_{nnr}}{i(\omega_a-\omega_1-\omega_2)}\boldsymbol{r}^{\alpha}_{\boldsymbol{k}}\right|\left|a^{\alpha_1}_{\boldsymbol{k}_1}a^{\alpha_2}_{\boldsymbol{k}_2}a^{\alpha_3}_{\boldsymbol{k}_3}\frac{e^{i\Omega^{(2)}s}-1}{i\Omega^{(2)}}\right|\sim\frac{\epsilon^2}{\Omega^{(2)}}.
\end{aligned}\tag{5.20}$$

Here we used the notation $\Omega^{(2)}$ for the quartet detuning: $\omega - \omega_1 - \omega_2 - \omega_3$. In the same manner as the near resonant triads, the near resonant quartets require $\Omega^{(2)} \sim \epsilon^2$. In effect, we are averaging over the t_0 timescale when solving for this order of the dynamics. We know all variation of the amplitudes for timescale t_0 from the triad near resonances and so this can be computed by equation (5.12), although unlike the averaging over τ there is not necessarily any well behaved oscillating behaviour to simplify the expression. Some work has been done to try to investigate resonances that might occur in situations where well behaved oscillating behaviour can be assumed of the nonlinear evolution in t_0 for example in Bustamante, Quinn, and Lucas 2014, however these mechanisms appear to depend on contrived situations in which a triad is assumed to simultaneously evolve independently from all other modes, to give a regular nonlinear oscillation, and act on another mode, which contradicts the assumption of independence. In (5.20) we have made the assumption that variation of the amplitudes will not produce coherent growth, and so we could push the second part of the integral to $O(\epsilon^3)$ and ignore it in our scaling argument.

One main point of note is that any possible quartet can only be formed of non-near resonant slaved modes in this expansion. The requirement is that $\Omega^{\alpha_a \alpha_3 \alpha}_{\boldsymbol{k}_a \boldsymbol{k}_3 \boldsymbol{k}} \sim O(1)$ as well as $\Omega^{\alpha_1 \alpha_2 \alpha_3 \alpha}_{\boldsymbol{k}_1 \boldsymbol{k}_2 \boldsymbol{k}_3 \boldsymbol{k}} \sim O(\epsilon^2)$. Some corollaries of this are given in section 5.4.1, and section 5.3.2.

By the symmetry of the nonlinear interaction coefficient the third term in (5.17) is identical to the second and so we have:

$$\frac{\partial}{\partial t_1} a^{\alpha}_{\boldsymbol{k}} = - \sum_{\substack{\boldsymbol{k}_1, \boldsymbol{k}_2, \boldsymbol{k}_3 \\ \alpha_1, \alpha_2, \alpha_3 \\ \Omega^{(2)} \leq \epsilon^2}} Q^{\alpha_1 \alpha_2 \alpha_3 \alpha}_{\boldsymbol{k}_1 \boldsymbol{k}_2 \boldsymbol{k}_3 \boldsymbol{k}} a^{\alpha_1}_{\boldsymbol{k}_1} a^{\alpha_2}_{\boldsymbol{k}_2} a^{\alpha_3}_{\boldsymbol{k}_3} \delta_{\boldsymbol{k} - \boldsymbol{k}_1 - \boldsymbol{k}_2 - \boldsymbol{k}_3}, \tag{5.21}$$

where:

$$Q^{\alpha_1 \alpha_2 \alpha_3 \alpha}_{\boldsymbol{k}_1 \boldsymbol{k}_2 \boldsymbol{k}_3 \boldsymbol{k}} = \sum_{\alpha_a} \frac{2 C^{\alpha_a \alpha_3 \alpha}_{\boldsymbol{k}_a \boldsymbol{k}_3 \boldsymbol{k}} \, C^{\alpha_1 \alpha_2 \alpha_a}_{\boldsymbol{k}_1 \boldsymbol{k}_2 \boldsymbol{k}_a} \big|_{nnr}}{i(\omega_a - \omega_1 - \omega_2)}, \tag{5.22}$$

with $\boldsymbol{k}_a = \boldsymbol{k}_1 + \boldsymbol{k}_2$, $\boldsymbol{k}_a = \boldsymbol{k} - \boldsymbol{k}_3$, and $\Omega^{(2)} \leq \epsilon^2$.

Similarly to the triad case it is useful to symmetrise this in the input coefficients (1,2,3) as follows:

$$Q^{\alpha_1 \alpha_2 \alpha_3 \alpha}_{\boldsymbol{k}_1 \boldsymbol{k}_2 \boldsymbol{k}_3 \boldsymbol{k}} = \frac{2}{3} \left[\sum_{\alpha_a} \frac{C^{\alpha_a \alpha_3 \alpha}_{\boldsymbol{k}_a \boldsymbol{k}_3 \boldsymbol{k}} \, C^{\alpha_1 \alpha_2 \alpha_a} _{\boldsymbol{k}_1 \boldsymbol{k}_2 \boldsymbol{k}_a} \big|_{nnr}}{i(\omega_a - \omega_1 - \omega_2)} + \sum_{\alpha_b} \frac{C^{\alpha_b \alpha_1 \alpha}_{\boldsymbol{k}_b \boldsymbol{k}_1 \boldsymbol{k}} \, C^{\alpha_2 \alpha_3 \alpha_b}_{\boldsymbol{k}_2 \boldsymbol{k}_3 \boldsymbol{k}_b} \big|_{nnr}}{i(\omega_b - \omega_2 - \omega_3)} + \sum_{\alpha_c} \frac{C^{\alpha_c \alpha_2 \alpha}_{\boldsymbol{k}_c \boldsymbol{k}_2 \boldsymbol{k}} \, C^{\alpha_3 \alpha_1 \alpha_c}_{\boldsymbol{k}_3 \boldsymbol{k}_1 \boldsymbol{k}_c} \big|_{nnr}}{i(\omega_c - \omega_3 - \omega_1)} \right]. \tag{5.23}$$

It should be noted that this symmetrisation might not be possible: some of the combinations of triads may be near resonant, and so do not form slaved modes, and hence cannot be considered in the same manner. These are dealt with in the next section.

We can visualise this construction as in figure 5.3, where two non-near resonant triads form the quartet.

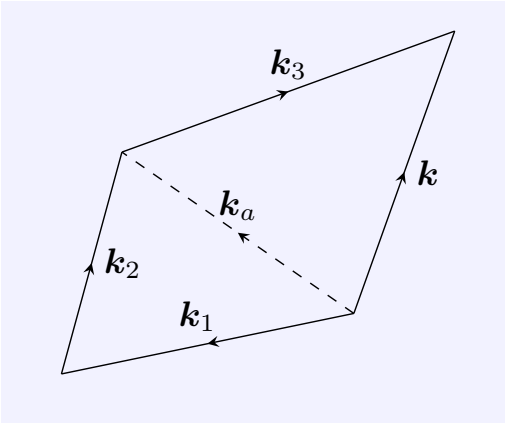

Figure 5.3: Quartet construction, as in equation (5.22). This figure is the same as figure 3.1, repeated here for convenience. The wavevector $\boldsymbol{k}_a$ takes the form of a slaved mode that can be projected onto our eigenbasis such that there are fast-like parts and a slow-like part. Each quartet has three possible slaved modes that can contribute to the quartet.

5.2.1 Continuation of the near resonant part of the expansion

Th previous section followed almost the identical analysis to the exact-resonant expansion. We now continue with the near resonant triads. To form the next 'order' of the near resonant expansion we will follow what is effectively the same process again, although there are now key differences in the mathematics, notably in the timescales. We assume that at least one of the amplitudes in the RHS of (5.12) is also a member of another near resonant triad† and substitute (5.13) in its place:

$$\frac{\partial a^{\alpha}_{\boldsymbol{k}}}{\partial t_0} = - \sum_{\substack{\boldsymbol{k}_3,\boldsymbol{k}_a \\ \alpha_3,\alpha_a \\ \boldsymbol{k}=\boldsymbol{k}_3+\boldsymbol{k}_a}} \sum_{\substack{\boldsymbol{k}_1,\boldsymbol{k}_2 \\ \alpha_1,\alpha_2 \\ \boldsymbol{k}_a=\boldsymbol{k}_1+\boldsymbol{k}_2}} \frac{C^{\alpha_3\alpha_a\alpha}_{\boldsymbol{k}_3\boldsymbol{k}_a\boldsymbol{k}} C^{\alpha_1\alpha_2\alpha_a}_{\boldsymbol{k}_1\boldsymbol{k}_2\boldsymbol{k}_a}}{i\Delta^{\alpha_1\alpha_2\alpha_a}_{\boldsymbol{k}_1\boldsymbol{k}_2\boldsymbol{k}_a}} a^{\alpha_3}_{\boldsymbol{k}_3} a^{\alpha_1}_{\boldsymbol{k}_1} a^{\alpha_2}_{\boldsymbol{k}_2} e^{i\Delta^{\alpha_1\alpha_2\alpha_a}_{\boldsymbol{k}_1\boldsymbol{k}_2\boldsymbol{k}_a} t_0} e^{i\Delta^{\alpha_3\alpha_a\alpha}_{\boldsymbol{k}_3\boldsymbol{k}_a\boldsymbol{k}} t_0}$$

$$+ \text{ above quartet terms}, \tag{5.24}$$

where the right hand term of (5.13) gets pushed into the 'above quartet terms' because the $\partial/\partial s$ terms will be functions of two or more amplitudes as shown by (5.12). The assumption † is justified provided the wavenumber spacing is sufficiently small, as discussed in the opening of chapter 1.

This again mirrors the exact resonant quartet expansion (the same interaction coefficient Q as given in (5.22), although scaled by ϵ, would be formed), except that the evolution is still on the t_0

timescale. Because of our imposed structure we should note that the near resonant triads can only form a 'higher order interaction' with other near resonant sets, and slaved modes can only form a higher order resonance by combination with each other.

The near resonant expansion (that evolves according to dynamical equation (5.12)) contains a subset of the exact quartet resonances from the analysis of chapter 3, which behave as before, but now acting on the faster t_0 timescale instead of t_1. The near resonant expansion contains the strongest of the exact quartet resonances, constructed from near resonant triads, without proceeding to a higher order.

One way to interpret this is to say that in forming the exact quartet interaction coefficient given by equation (3.32) we divide by Ω, but in the case of the near resonant component triads this causes an extremely large interaction coefficient $\sim 1/\epsilon$. The near resonant interactions pick out the cases where the higher order interaction coefficient is large enough to rearrange the asymptotic ordering.

5.3 Expansion to arbitrary order

We previously defined the general interaction coefficient (3.34):

$$\{C^{(n)}\}^{\alpha_1 \ldots \alpha_{n+2}\alpha}_{\boldsymbol{k}_1 \ldots \boldsymbol{k}_{n+1}\boldsymbol{k}} = \frac{1}{(n+1)!}\sum_{r=1}^{n}\left[\sum_{\alpha_a,\alpha_b}\frac{\{C^{(1)}\}^{\alpha_a\alpha_b\alpha}_{\boldsymbol{k}_a\boldsymbol{k}_b\boldsymbol{k}}\ \{C^{(r-1)}\}^{\alpha_{n-r+2}\ldots\alpha_{n+1}\alpha_b}_{\boldsymbol{k}_{n-r+2}\ldots\boldsymbol{k}_{n+1}\boldsymbol{k}_b}\Big|_{nr}\ \{C^{(n-r)}\}^{\alpha_1\ldots\alpha_{n-r+1}\alpha_a}_{\boldsymbol{k}_1\ldots\boldsymbol{k}_{n-r+1}\boldsymbol{k}_a}\Big|_{nr}}{-\{\Omega^{(n-r)}\}^{a}_{1,\ldots,n-r+1}\{\Omega^{(r-1)}\}^{b}_{n-r+2,\ldots,n+1}} + \textit{input wavenumber permutations}\right], \tag{5.25}$$

where: $\{\Omega^{(n)}\}^{a}_{b,\ldots,c} = \omega_a - \omega_b - \ldots - \omega_c$.

Where $C^{(n)}$ is the nonlinear interaction coefficient at the nth closure (ie $n = 1$ would be triad interactions at the first closure). We need to define the particular case of $\{C^{(0)}\}^{\alpha_a\alpha}_{\boldsymbol{k}_a\boldsymbol{k}} = 1$ such that it is simply an identity mapping with $\boldsymbol{k}_a = \boldsymbol{k}$, $\alpha_a = \alpha$. We also define separately $\Omega^{(0)} = -i$. It can be noted that the detuning terms are assumed to be large, because anywhere that they would be small they have been included with the near resonant interactions.

We will now see that the triad near resonances in fact reproduce this coefficient at all orders.

5.3.1 Near resonances

As occurred for quartets in section 5.2.1, the near resonances will expand in the same manner as the exact resonant part, except that the n-tets, for every order n are all evolving on the t_0 timescale. To show the equivalent higher order behaviour in the near resonances we will continue the expansion using integration by parts, as we did in section 5.1.2.

We take one of the right hand terms (with minor relabelling) of (5.13) and substitute into (5.12) to replace the derivative in t_0:

$$\begin{aligned}
&\sum_{\substack{\boldsymbol{k}_1,\boldsymbol{k}_a\\ \alpha_1,\alpha_a\\ \boldsymbol{k}=\boldsymbol{k}_1+\boldsymbol{k}_a}} C^{\alpha_1\alpha_a\alpha}_{\boldsymbol{k}_1\boldsymbol{k}_a\boldsymbol{k}} \int_0^{t_0} \frac{\frac{\partial}{\partial s}(a^{\alpha_a}_{\boldsymbol{k}_a}(s,t_1))a^{\alpha_1}_{\boldsymbol{k}_1}(s,t_1)}{i\Delta^{\alpha_1\alpha_a\alpha}_{\boldsymbol{k}_1\boldsymbol{k}_a\boldsymbol{k}}} e^{i\Delta^{\alpha_1\alpha_a\alpha}_{\boldsymbol{k}_1\boldsymbol{k}_a\boldsymbol{k}}s} ds \\
&= \sum_{\substack{\boldsymbol{k}_1,\boldsymbol{k}_a\\ \alpha_1,\alpha_a\\ \boldsymbol{k}=\boldsymbol{k}_1+\boldsymbol{k}_a}} \sum_{\substack{\boldsymbol{k}_2,\boldsymbol{k}_3\\ \alpha_2,\alpha_3\\ \boldsymbol{k}_a=\boldsymbol{k}_2+\boldsymbol{k}_3}} \frac{C^{\alpha_1\alpha_a\alpha}_{\boldsymbol{k}_1\boldsymbol{k}_a\boldsymbol{k}} C^{\alpha_2\alpha_3\alpha_a}_{\boldsymbol{k}_2\boldsymbol{k}_3\boldsymbol{k}_a}}{i\Delta^{\alpha_1\alpha_a\alpha}_{\boldsymbol{k}_1\boldsymbol{k}_a\boldsymbol{k}}} \int_0^{t_0} a^{\alpha_1}_{\boldsymbol{k}_1}(s,t_1)a^{\alpha_2}_{\boldsymbol{k}_2}(s,t_1)a^{\alpha_3}_{\boldsymbol{k}_3}(s,t_1) e^{i\Delta^{\alpha_1\alpha_a\alpha}_{\boldsymbol{k}_1\boldsymbol{k}_a\boldsymbol{k}}s} e^{i\Delta^{\alpha_2\alpha_3\alpha_a}_{\boldsymbol{k}_2\boldsymbol{k}_3\boldsymbol{k}_a}s} ds.
\end{aligned} \tag{5.26}$$

This process would then be continued by repeatedly expanding the integral by parts, each time the integral remainder treated similarly, forming an expansion containing all combinations of n amplitudes (for $n > 2$) that obey the n-tet condition $\sum_{i=1}^{n-1} \boldsymbol{k}_i = \boldsymbol{k}$. This expansion is then substituted back into the equation (5.13) in every place that an amplitude is involved in another near resonance. This will return, after some more relabelling, (5.24) except that we can now see the form of the previously omitted 'above quartet terms':

$$\begin{aligned}
\frac{\partial a^{\alpha}_{\boldsymbol{k}}}{\partial t_0} = &- \sum_{\substack{\boldsymbol{k}_3,\boldsymbol{k}_a\\ \alpha_3,\alpha_a\\ \boldsymbol{k}=\boldsymbol{k}_3+\boldsymbol{k}_a}} \sum_{\substack{\boldsymbol{k}_1,\boldsymbol{k}_2\\ \alpha_1,\alpha_2\\ \boldsymbol{k}_a=\boldsymbol{k}_1+\boldsymbol{k}_2}} \frac{C^{\alpha_3\alpha_a\alpha}_{\boldsymbol{k}_3\boldsymbol{k}_a\boldsymbol{k}} C^{\alpha_1\alpha_2\alpha_a}_{\boldsymbol{k}_1\boldsymbol{k}_2\boldsymbol{k}_a}}{i\Delta^{\alpha_1\alpha_2\alpha_a}_{\boldsymbol{k}_1\boldsymbol{k}_2\boldsymbol{k}_a}} a^{\alpha_3}_{\boldsymbol{k}_3} a^{\alpha_1}_{\boldsymbol{k}_1} a^{\alpha_2}_{\boldsymbol{k}_2} e^{i\Delta^{\alpha_1\alpha_2\alpha_a}_{\boldsymbol{k}_1\boldsymbol{k}_2\boldsymbol{k}_a}t_0} e^{i\Delta^{\alpha_3\alpha_a\alpha}_{\boldsymbol{k}_3\boldsymbol{k}_a\boldsymbol{k}}t_0} \\
&- \sum_{\substack{\boldsymbol{k}_b,\boldsymbol{k}_a\\ \alpha_b,\alpha_a\\ \boldsymbol{k}=\boldsymbol{k}_b+\boldsymbol{k}_a}} \sum_{\substack{\boldsymbol{k}_1,\boldsymbol{k}_2\\ \alpha_1,\alpha_2\\ \boldsymbol{k}_a=\boldsymbol{k}_1+\boldsymbol{k}_2}} \sum_{\substack{\boldsymbol{k}_3,\boldsymbol{k}_4\\ \alpha_3,\alpha_4\\ \boldsymbol{k}_b=\boldsymbol{k}_3+\boldsymbol{k}_4}} \frac{C^{\alpha_b\alpha_a\alpha}_{\boldsymbol{k}_b\boldsymbol{k}_a\boldsymbol{k}} C^{\alpha_1\alpha_2\alpha_a}_{\boldsymbol{k}_1\boldsymbol{k}_2\boldsymbol{k}_a} C^{\alpha_3\alpha_4\alpha_b}_{\boldsymbol{k}_3\boldsymbol{k}_4\boldsymbol{k}_b}}{-\Delta^{\alpha_3\alpha_4\alpha_b}_{\boldsymbol{k}_3\boldsymbol{k}_4\boldsymbol{k}_b}\Delta^{\alpha_1\alpha_2\alpha_a}_{\boldsymbol{k}_1\boldsymbol{k}_2\boldsymbol{k}_a}} a^{\alpha_1}_{\boldsymbol{k}_1} a^{\alpha_2}_{\boldsymbol{k}_2} a^{\alpha_3}_{\boldsymbol{k}_3} a^{\alpha_4}_{\boldsymbol{k}_4} e^{i\Delta^{\alpha_1\alpha_2\alpha_3\alpha_4\alpha}_{\boldsymbol{k}_1\boldsymbol{k}_2\boldsymbol{k}_3\boldsymbol{k}_4\boldsymbol{k}}t_0} \\
&- \sum_{\substack{\boldsymbol{k}_4,\boldsymbol{k}_a\\ \alpha_4,\alpha_a\\ \boldsymbol{k}=\boldsymbol{k}_4+\boldsymbol{k}_a}} \sum_{\substack{\boldsymbol{k}_1,\boldsymbol{k}_2\boldsymbol{k}_3\\ \alpha_1,\alpha_2\alpha_3\\ \boldsymbol{k}_a=\boldsymbol{k}_1+\boldsymbol{k}_2+\boldsymbol{k}_3}} \frac{C^{\alpha_4\alpha_a\alpha}_{\boldsymbol{k}_4\boldsymbol{k}_a\boldsymbol{k}} \{C^{(2)}\}^{\alpha_1\alpha_2\alpha_3\alpha_a}_{\boldsymbol{k}_1\boldsymbol{k}_2\boldsymbol{k}_3\boldsymbol{k}_a}}{i\Delta^{\alpha_1\alpha_2\alpha_3\alpha_a}_{\boldsymbol{k}_1\boldsymbol{k}_2\boldsymbol{k}_3\boldsymbol{k}_a}} a^{\alpha_1}_{\boldsymbol{k}_1} a^{\alpha_2}_{\boldsymbol{k}_2} a^{\alpha_3}_{\boldsymbol{k}_3} a^{\alpha_4}_{\boldsymbol{k}_4} e^{i\Delta^{\alpha_1\alpha_2\alpha_3\alpha_4\alpha}_{\boldsymbol{k}_1\boldsymbol{k}_2\boldsymbol{k}_3\boldsymbol{k}_4\boldsymbol{k}}t_0} + \dots .
\end{aligned} \tag{5.27}$$

This is exactly as for the general higher order coefficient (3.34), except for some ϵ scaling. If one were to continue this, always substituting in for near resonant terms, then the expansion will eventually contain only exact and super-near resonances. All of these will look identical in form to a subset of the exact resonant expansion, but will take place on the t_0 timescale.

This expansion is not necessary in the practical use of the near resonant expansion. It is simply a method to show that the near resonant triads interact exactly like the strongest parts of a

full exact expansion. All of the dynamics is captured simply by maintaining the near resonances in the triad equations given in (5.12).

5.3.2 Splitting of n-tets in the near resonant part

Interestingly, n-tets can be split between orders in the near resonant expansion. As an example, consider the rotating shallow water equations with small f (where fast modes have $\omega \sim \alpha c|\boldsymbol{k}|$) for the following quartet of modes:

$$\boldsymbol{k}_1, \qquad \alpha_1 = +, \tag{5.28a}$$

$$\boldsymbol{k}_2 = \boldsymbol{k}_1^\perp, \qquad \alpha_2 = +, \tag{5.28b}$$

$$\boldsymbol{k}_3 = -\boldsymbol{k}_1 + \epsilon^2 \boldsymbol{k}_1^\perp, \qquad \alpha_3 = -, \tag{5.28c}$$

$$\boldsymbol{k} = \boldsymbol{k}_1^\perp (1+\epsilon^2), \qquad \alpha = +. \tag{5.28d}$$

This forms a near resonant quartet. From these we calculate the slaved mode wavenumbers that would contribute to the quartet:

$$\boldsymbol{k}_a = \boldsymbol{k}_1 + \boldsymbol{k}_2 = \boldsymbol{k}_1 + \boldsymbol{k}_1^\perp, \tag{5.29a}$$

$$\boldsymbol{k}_b = \boldsymbol{k}_2 + \boldsymbol{k}_3 = -\boldsymbol{k}_1 + (1+\epsilon^2)\boldsymbol{k}_1^\perp, \tag{5.29b}$$

$$\boldsymbol{k}_c = \boldsymbol{k}_3 + \boldsymbol{k}_1 = \epsilon^2 \boldsymbol{k}_1^\perp. \tag{5.29c}$$

Calculating Ω in each case (assuming all fast modes):

$$\Omega_{12a} = \omega(\boldsymbol{k}_1 + \boldsymbol{k}_1^\perp) - \omega(\boldsymbol{k}_1) - \omega(\boldsymbol{k}_1^\perp) \approx c(\sqrt{2}-2)|\boldsymbol{k}_1|, \tag{5.30a}$$

$$\Omega_{23b} = \omega(-\boldsymbol{k}_1 + (1+\epsilon^2)\boldsymbol{k}_1^\perp) - \omega(\boldsymbol{k}_1) + \omega(-\boldsymbol{k}_1 + \epsilon^2 \boldsymbol{k}_1^\perp) \approx c(\sqrt{2})|\boldsymbol{k}_1|, \tag{5.30b}$$

$$\Omega_{13c} = \omega(\epsilon^2 \boldsymbol{k}_1^\perp) + \omega(\boldsymbol{k}_1) - \omega(-\boldsymbol{k}_1 + \epsilon^2 \boldsymbol{k}_1^\perp) \approx c\epsilon^2 |\boldsymbol{k}_1|. \tag{5.30c}$$

We see that a fast mode c will be part of a near resonant triad. However fast-like mode a or b would not be included in the near resonant triads.

5.4 Overview of expansion structure

In order to compare the two versions of the asymptotic expansion we summarise the expansions as given in chapters 3 and 5 here. We start by describing an exactly resonant expansion as

follows:

1. To first order we solve for the linear modes of the system (equation (3.6), with solution (3.11)).
2. At second order:
   - We solve to remove secular terms giving the variation of $\boldsymbol{u}_0$ on the first slow timescale t_0. Equation (3.18) (no explicit solution).
   - We solve the remaining nonlinearly forced equation (3.20) to give the slaved modes in $\boldsymbol{u}_1$ (solution in (3.22)).
3. At third order:
   - Substitution of slaved modes in $\boldsymbol{u}_1$ into nonlinear part to form quartets (Equation (3.30)).
   - Removal of secular terms to give evolution of $\boldsymbol{u}_0$ on timescale t_1 (Equation (3.29)).
   - Solution for slaved modes in $\boldsymbol{u}_2$ as particular integral of remaining $O(\epsilon)$ equation (not explicitly shown).
4. At higher orders:
   - The same process is repeated, forming n-tets in the nonlinear part and calculating the effect on $\boldsymbol{u}_0$ to timescale t_n. The interaction coefficient is given by the recurrence relation (3.34).

For the near resonant expansion this process is augmented:

1. To first order we solve for the linear modes of the system (equation (5.1), with solution (5.4)). There is no change compared to the exact expansion at this order.
2. At second order:
   - We solve to remove secular terms (these now include near resonances) giving the variation of $\boldsymbol{u}_0$ on the first slow timescale t_0. This is now equation (5.12). We can write this as (5.24), or with the inclusion of some above quartet terms: (5.27). This moves n-tet terms that were previously in the subsequent orders to act on timescale t_0, where all components were formed of near resonant triads with $\Omega \sim O(\epsilon)$.
   - We solve the remaining forced equation to give the slaved modes in $\boldsymbol{u}_1$ (solution (5.11)) as the particular integral of (5.9).
3. At third order:

- Substitution of slaved modes $\boldsymbol{u}_1$ (these are now only formed of non-near resonances) into nonlinear part to form quartets (Equation (5.17)).
- Removal of secular terms (including near resonances) to give evolution of $\boldsymbol{u}_0$ on timescale t_1 gives near resonant quartets as in equation (5.21). In (5.20) the resonant quartet condition was derived: $\Omega \sim \epsilon^2$. These are not the same as quartets formed of near resonant triads.
- Solution for slaved modes in $\boldsymbol{u}_2$ as particular integral of remaining $O(\epsilon)$ equation (not explicitly shown).

4. At higher orders:
   - The same process is repeated, forming n-tets in the nonlinear part and calculating the effect on $\boldsymbol{u}_0$ to timescale t_n.

The near resonant expansion does not require any of the stages in equations (5.24) and (5.27), these are just expressions derived from the near resonant dynamics equation, the n-tet interactions in the near resonant expansion exist just by allowing the near resonant triads to interact. The quartet near resonant expansion gives the behaviour on the next timescale, and a general n-tet near resonant expansion would also be possible.

5.4.1 Caveats

There are a few caveats to the resonant expansion, made more relevant where ϵ is considered larger.

- With small but finite ϵ the definition of what constitutes $O(\epsilon^n)$ may become problematic. For example if $\epsilon = 0.1$, then a term of size 0.2 might be considered $O(\epsilon)$ but $0.2^4 = 0.0016 \sim \epsilon^3$. This is increasingly problematic as $\epsilon \to 1$. If the 'size' of a term is not well defined making an arbitrary cut-off point - say $\Omega = O(\epsilon)$ is not rigorous.
- A key requirement for this expansion is that if ϵ is not asymptotically small it needs to be the dominant small term everywhere; it is implicitly assumed that all other terms, if not stated, are $O(1)$. Unfortunately all that is required to break the hierarchy of sizes is for one of the interaction coefficients to become $O(1/\epsilon)$ large. However above a certain wavenumber size $|\boldsymbol{k}|$ the size of the maximum size of the interaction coefficient can be approximated as a linear function of $|\boldsymbol{k}|$ ($C \sim U^2|k|$). So the separation of the hierarchy is maintained up to a given wavenumber, above this the asymptotic series can be disrupted by the strength of the interaction coefficient alone.

5.5 Chapter summary

In this chapter the main points were:

- We derived the resonant expansion but now taking into account near resonances as a source of secularity. This maintains the asymptotic ordering that would previously have broken down, in particular when the small value ϵ would take a slightly larger value.
- Any higher order resonance constructed only from near resonant triads will be 'promoted' to triad order. This effect can be considered to be due to higher order interaction coefficients being large enough to upset the asymptotic sequence.
- We defined the concept of super-near resonance to ensure that no issues were caused in the asymptotic expansion due to detuning values that are $O(\epsilon^2)$ or smaller.
- Larger ϵ values open up the possibility of other parts of the expansion reaching comparable size to $1/\epsilon$ and so we discussed some of these dangers. In particular the interaction coefficient becomes larger with larger wavenumbers, in general, and could upset the ordering of any expansion.
- An exact quartet resonance may be constructed with (three) different combinations of triads. There are cases of quartets where some of these are near resonant triads and some are non-near resonant triads. This means that the quartet resonances will be represented in the near resonant expansion, but only by some of the triad combinations, a somewhat strange behaviour when compared to the exact theory.

The combination of the outcomes of this chapter allow us a new perspective on the near resonant expansion, as a restructuring of the exact resonant asymptotics to allow promotion of certain high order terms to the triad timescale. This will be seen to lead to fundamentally different behaviour in the following chapter where we apply the near resonant theory to our example systems.

Chapter 6

Applications of the near resonant theory to rotating stratified flow

The applications presented here follow on naturally from the exactly resonant examples of chapter 4. The first section takes the one layer shallow water equations and solves them numerically. Whilst the numerical solution is far from unique in the literature, the intent of the simulation is, we evaluate the results with respect to the theory of the preceding chapter. It is shown that the near resonant expansion is a good approximation of the full resonant expansion, and hence a good approximation of the full equations, in contrast to an expansion limited to the exact resonances. In particular it was shown that a near resonance is not limited to being in the vicinity of an exact resonance - they are not simply an approximation of the exact resonant part, but something more intrinsic to the motion. It is also seen clearly in the simulation output that the modes driven only by non-resonances oscillate rapidly but these oscillations prevent a coherent direction of growth such that the amplitudes of those modes never grow on a slower timescale: demonstrating directly how the underlying theory of near resonances (due to non-cancellation of oscillations) functions.

The two layer rotating shallow water equations are not investigated numerically here. The layered equations are prone to Kelvin-Helmholtz instability, substantially increasing the numerical difficulties. Based on this, and the expectation that the outcomes for the particular behaviour being investigated would not be substantially different to the one layer case, they were not investigated numerically.

The stratified equations are considered analytically, with particular attention paid to the fast-fast-slow interaction that is not found in the layered equations. It is shown that the near resonances behave strangely in this case: the smallness of the interaction coefficient exactly balances that of

the detuning, such that these interactions cannot show a 'promotion' to higher order, but must still be considered near resonant as they can only form higher order resonant interactions when they pair with other near resonant sets. Many numerical integrations of these equations have been performed and evaluated in the literature, however numerical simulations are not explored here.

6.1 One layer rotating shallow water equations

6.1.1 Numerical method

To demonstrate the theory, the one layer equations were solved numerically. The equations were solved for periodic boundary conditions in both directions using spectral methods. Dealiasing was applied using the 2/3rds method and the time stepping used the Runge-Kutta 4th order scheme.

A 160x160 grid was used with side lengths 20x20m, giving wavenumbers of $\hat{\boldsymbol{k}} = \frac{\pi}{10}\boldsymbol{k}$ where $\boldsymbol{k} \in \mathbb{N}^2$. Parameters used were: $f = 1s^{-1}$, $g = 10ms^{-2}$, $H = 5m$, $L = 20m$. The amplitudes of the input eigenvectors were scaled by 0.1. Approximate Rossby and Froude numbers are then $\sim 0.003 - 0.05$, ~ 0.02 respectively, we can then take $\epsilon = 0.1$ as a reasonable scaling, as the largest of the 3 small numbers with all 3 greater than ϵ^2.

For discussion we will always refer to the integer valued non-dimensional wavenumber $\boldsymbol{k}$ for clarity. However quoted values of Ω are dimensional but are directly comparable to ϵ values as $f = 1$.

6.1.2 Initial conditions

Specific initial conditions (chosen to demonstrate most clearly the theory) were used, with the eigenfunctions given by the following modes:

$$\begin{aligned}
\alpha = 0, \qquad \boldsymbol{k} =& (0,1)^T, (1,1)^T, (1,0)^T, (1,-1)^T, \\
& (0,-1)^T, (-1,-1)^T, (-1,0)^T, (-1,1)^T, \\
& (0,2)^T, (0,-2)^T, (2,0)^T, (-2,0)^T, \\
\alpha = +, \qquad \boldsymbol{k} =& (15,15)^T (\omega \approx 47.13), \\
\alpha = -, \qquad \boldsymbol{k} =& (14,14)^T (\omega \approx -43.99),
\end{aligned}$$

so that there is a ring of low wavenumber slow modes and two fast modes. The formulae for the eigenfunctions can be found in (2.85). This configuration is somewhat similar to an idealised version of the simulation found in Ward and Dewar 2010, but here the focus of the analysis is on showing the role of resonant interactions as described in the theory of chapters 3 and 5.

From these initial conditions the only exact resonances available are those between the slow modes, as these are all resonant. Any triad between the two input fast modes and any other mode,for example $(15, 15, +)$, $(14, 14, -)$, and $(1, 1, \alpha)$ is non-resonant. In a non-discretised model it would be possible for there to be exact modes from fast-slow-fast triads, but here there can only exist near resonant modes, strongest of which are those with the output fast mode very close to the input fast mode, for example $(15, 15, +)$, $(1, -1, 0)$, $(16, 14, +)$.

6.1.3 Results

From the limited number of modes present it becomes possible to isolate the interaction types that must be responsible for the spread of energy amongst the wave modes. For discussion we will refer to long, medium and short waves as those with wavenumbers in the vicinity of $(0, 0)$, $(15, 15)$, and $(30+, 30+)$ respectively. By these definitions the simulation is started with short zero modes and medium fast modes at around an amplitude of 10^{-1}. We split the motion into 5 regions for discussion, as shown in figure 6.5.

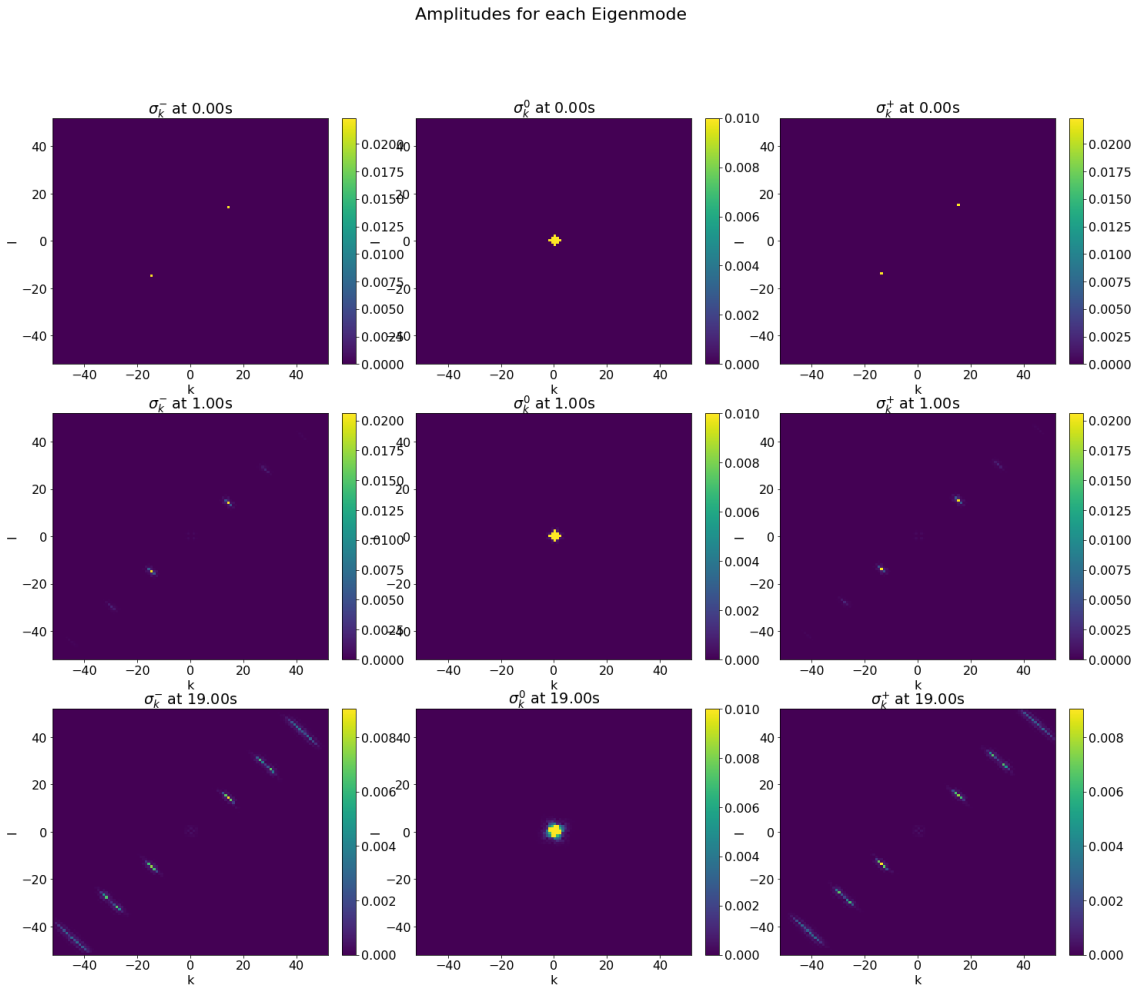

Figure 6.1: Distribution with time of the eigenmode amplitudes. Each graph shows the wavenumber $\boldsymbol{k}$ on the x and y axes, and the mode types α are $-, 0, +$ from left to right in the columns. Time increases downwards with graphs showing the distribution at 0s, 1s and 19s into the simulation. In the later times (on the triad timescale t_0) the output shows stimulated amplitudes in the zero modes close to $\boldsymbol{k} = (0, 0)$ that correspond to resonant interactions, and in the fast modes amplitudes increasing at $\boldsymbol{k} = (15n, 15n), n \in \mathbb{Z}$ that could only have been produced by near resonances as the fast-fast-fast interactions are never exactly resonant in the rotating shallow water equations.

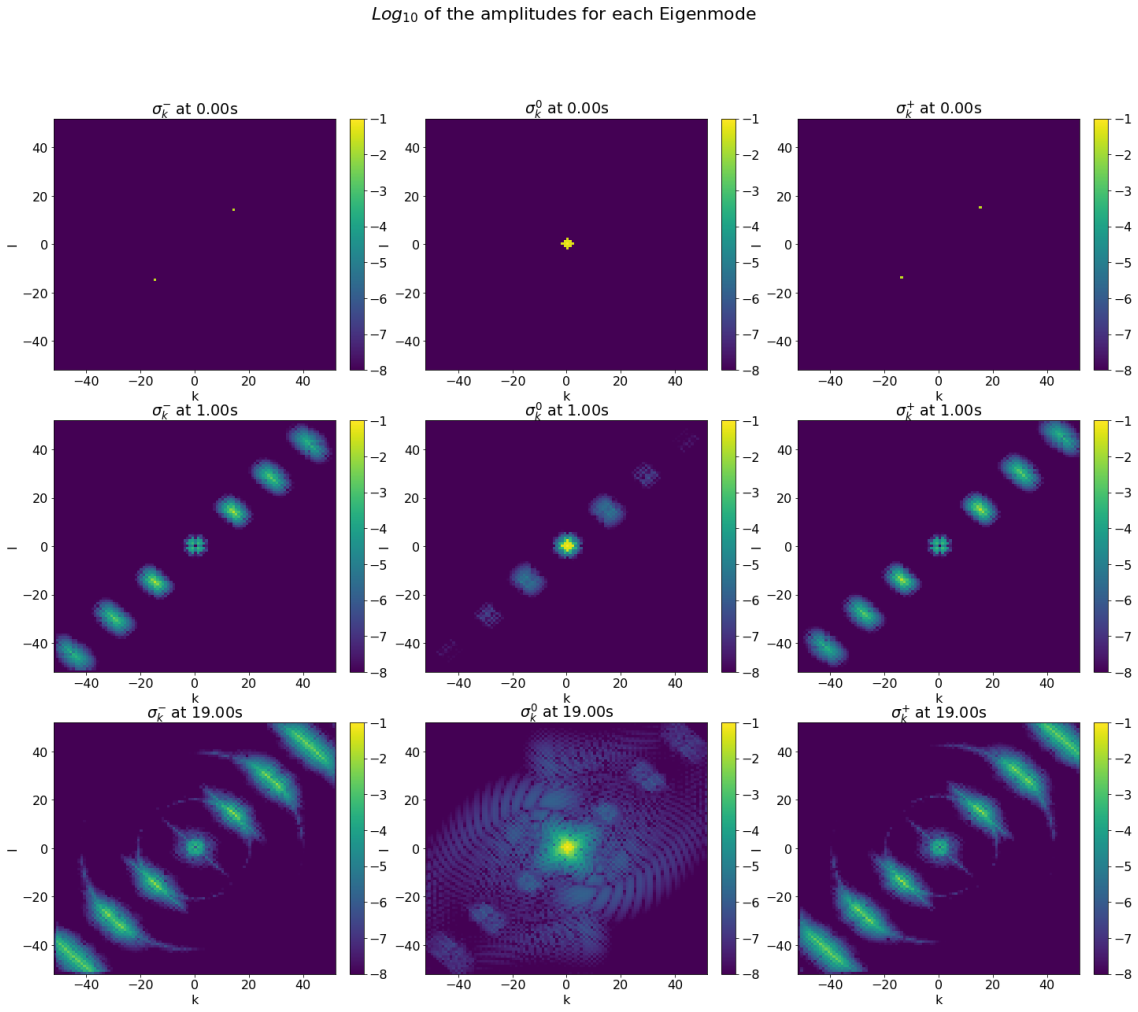

Figure 6.2: Distribution with time of the log of the eigenmode amplitudes. The log scaling shows in much greater detail the distribution of energy amongst the different modes compared to fig 6.1. Many areas can be seen to have been stimulated, although on scales that correspond to the $\boldsymbol{u}_1$ parts of the expansion. With the log scaling in addition to what was visible in figure 6.1 the resonance between a slow mode and two fast modes with equal wavenumber modulus but different direction can be seen by the arcs of the circle forming close to $\boldsymbol{k} = (\pm 15, \pm 15)$ and $\boldsymbol{k} = (\pm 30, \pm 30)$. It is also clear that there is a complicated redistribution of a small amount of energy amongst the slow modes.

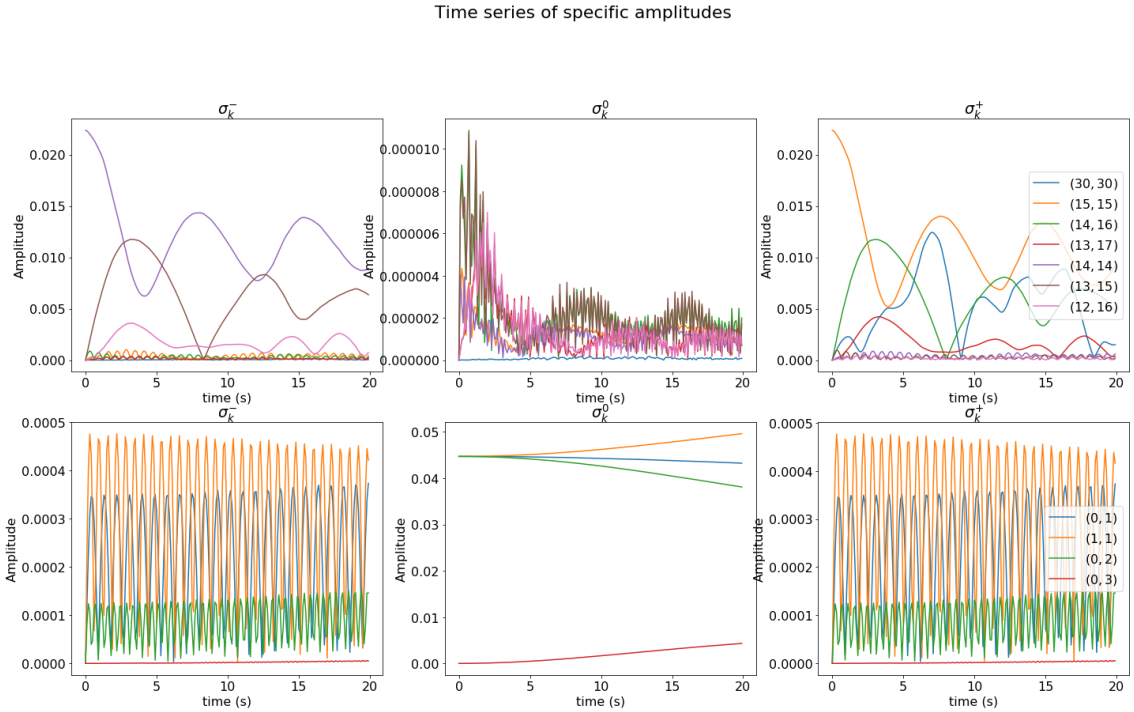

Figure 6.3: Distribution with time of specific eigenmode amplitudes. The amplitudes show how the energy of selected modes varies, with low wavenumber modes shown in the bottom row and higher wavenumbers in the top row. The left and right hand columns show the $\alpha = \pm$ fast modes respectively and the middle column shows the slow modes. In general the modes affected by the exact and near resonances show gradual changes on a slow timescale, whilst the amplitudes only involved in non-resonances show rapid oscillations but no sustained change. For example in the top right frame, the $\alpha = +$ modes, slow changes can be seen in mode $(15, 15, +)$, which is involved in a near resonant triad with several other modes, for example $(14, 16, +)$ and $(-1, 1, 0)$ (a close grid point to the exact resonance that forms the circular trace in figure 6.2), and $(15, 15, +)$ and $(30, 30, +)$ a near resonance that shows strong growth. In the bottom left frame the low wavenumber fast modes can be seen to oscillate rapidly with only minor sustained changes, a symptom of the lack of near or exact resonances affecting them.

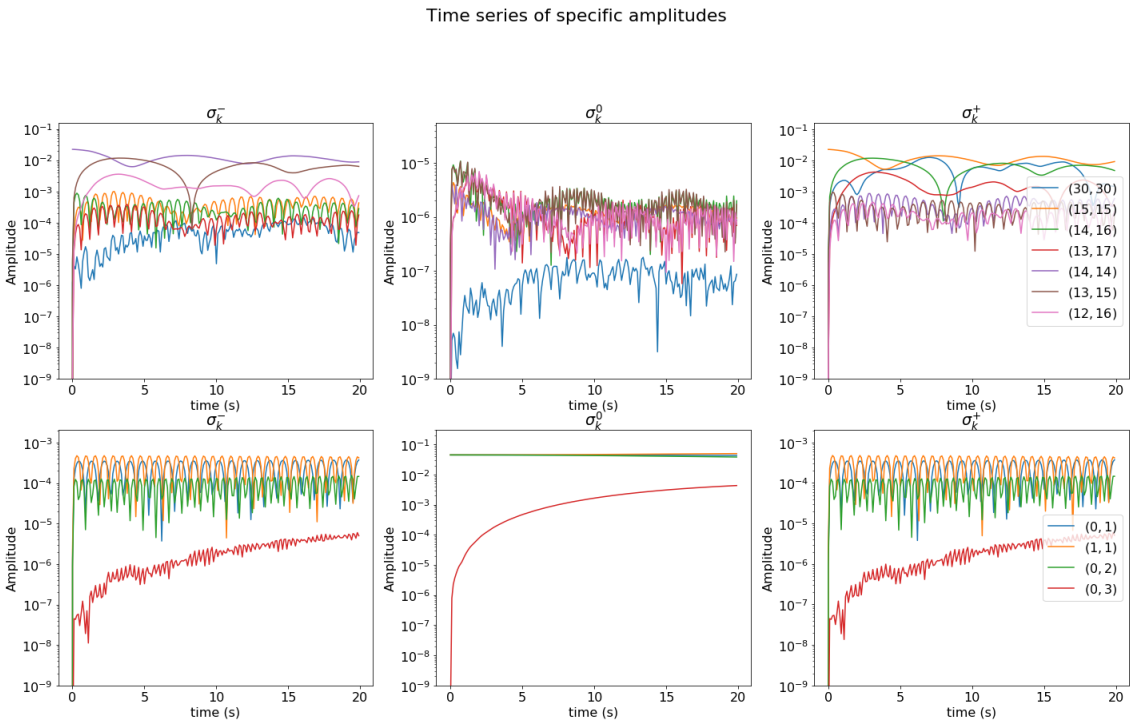

Figure 6.4: Distribution with time of the log of specific eigenmode amplitudes. This figure follows the layout of fig 6.3 but on a log scale. On the log scale it can be seen clearly that rapidly oscillating amplitudes do not grow to the scales seen for the modes that do interact resonantly.

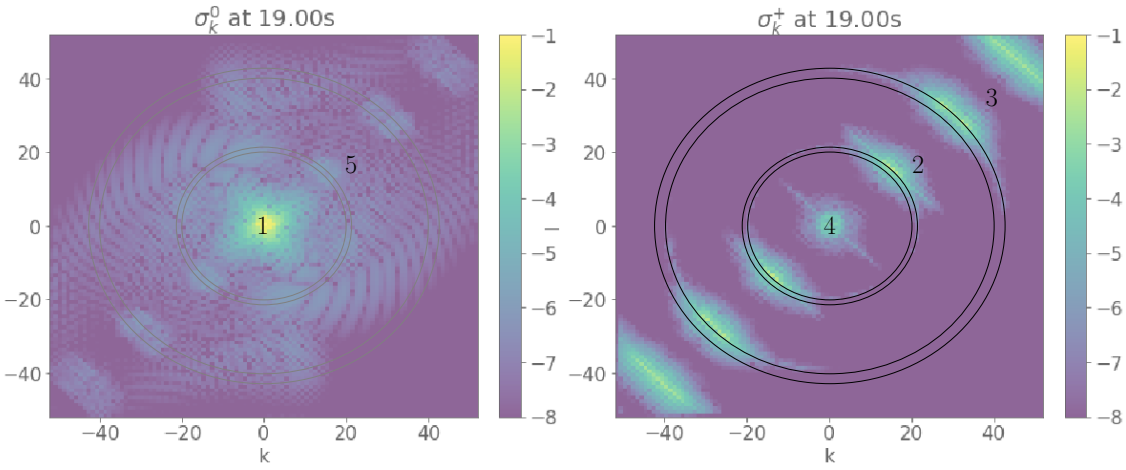

Figure 6.5: Diagram showing the regions referred to in the text, and the possible fast-slow-fast interactions of the input and double input wavelengths.

Region 1

The only exact resonances in the simulation are the slow-slow-slow resonances. These are seen to spread slowly to higher wavelengths although they have only limited change away from the long wavelengths. By comparison to figure 6.6 where the simulation was run without the initial fast modes we can see that in this region the motion is dominated by the exact resonances, as predicted by the usual resonance theory.

However figure 6.6 also makes clear that some interaction must be occurring due to slow-slow-fast interactions due to the presence of the fast mode of amplitude $\sim 10^{-3}$ after the simulation has been running for some time. The small size of the amplitudes can be attributed to the lack of near or exact resonance in the triads. These low amplitude modes would then be able to interact back onto the slow modes, and in fact the trace in the fast modes can be regarded as the fast part of the smaller amplitude $\boldsymbol{u}_1$ term of our theory, and hence what is being described is the slow-slow-slow-slow exact quartet interaction, where the transfer of energy is via the smaller amplitude $\boldsymbol{u}_1$ modes in a pathway composed of a pair of non-resonant triads. This corresponds to the interaction coefficient of the type:

$$Q^{0\ 0\ 0\ 0}_{\boldsymbol{k}_1\boldsymbol{k}_2\boldsymbol{k}_3\boldsymbol{k}} = \frac{2}{3}\left[\sum_{\alpha_a=\pm}\frac{C^{\alpha_a\ 0\ 0}_{\boldsymbol{k}_a\boldsymbol{k}_3\boldsymbol{k}}\,C^{0\ \ 0\ \alpha_a}_{\boldsymbol{k}_1\boldsymbol{k}_2\boldsymbol{k}_a}|_{nr}}{i(\omega_a-\omega_1-\omega_2)}+\sum_{\alpha_b=\pm}\frac{C^{\alpha_b 0\ 0}_{\boldsymbol{k}_b\boldsymbol{k}_1\boldsymbol{k}}\,C^{0\ \ 0\ \alpha_b}_{\boldsymbol{k}_2\boldsymbol{k}_3\boldsymbol{k}_b}|_{nr}}{i(\omega_b-\omega_2-\omega_3)}+\sum_{\alpha_c=\pm}\frac{C^{\alpha_c\ 0\ 0}_{\boldsymbol{k}_c\boldsymbol{k}_2\boldsymbol{k}}\,C^{0\ 0\ \alpha_c}_{\boldsymbol{k}_3\boldsymbol{k}_1\boldsymbol{k}_c}|_{nr}}{i(\omega_c-\omega_3-\omega_1)}\right].$$

This is the higher order interaction considered by Reznik, Zeitlin, and Ben Jelloul 2001 for the non-periodic case, with compact initial conditions.

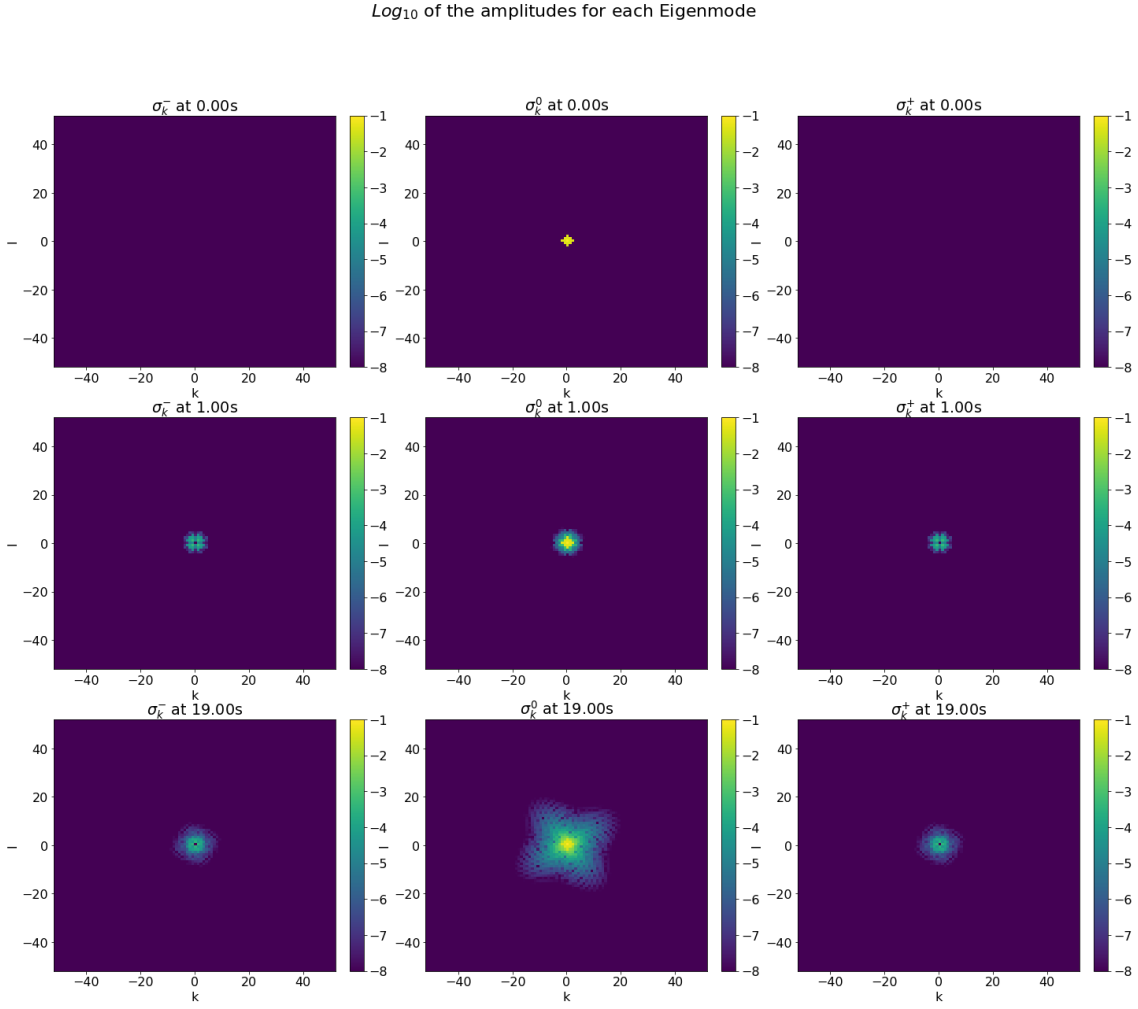

Figure 6.6: Distribution with time of the log of the eigenmode amplitudes. Time increases from top to bottom from $0s$, to $1s$, to $19s$. The central column shows the slow modes and the outside columns show the fast modes. In this simulation only the slow modes were included in the initial condition. In comparison to fig 6.2 there is no spread of energy to the higher wavenumber slow modes. It is clear that some energy has spread to the fast modes at low wavenumbers (the amplitudes close to the origin in the left and right columns). This is on a scale associated with the $\boldsymbol{u}_1$ part of the expansion, and can be associated with the $(0, 0, 0; 0)$ resonance of Reznik, Zeitlin, and Ben Jelloul 2001. Without the low energy fast modes providing a pathway via the slow-slow-fast and fast-slow-slow interactions this resonance would not be possible.

Region 2

As the simulation progresses the strongest spread of energy is seen in the vicinity of the medium length fast modes, visible even on the absolute amplitude graphs, with amplitudes in the region of 10^{-2} after a second of simulation time. These must (at least initially) be due to the fast-slow-fast interactions where the resonant condition is equivalent to $|\boldsymbol{k}_1| = |\boldsymbol{k}|$ (marked in figure 6.5). However on this discrete grid no exact resonance can exist in the region of the initial wave. This can therefore only be interpreted as either near resonant or higher order interaction. The closest points to resonances from the initial conditions are those such as:

$$(-1, 1, 0), \qquad (15, 15, \pm), \qquad (14, 16, \pm), \qquad\qquad \Omega = \mp 0.209 \sim \epsilon.$$

The exactly resonant quintet:

$$\begin{aligned} &(-1, 1, 0), \qquad (15, 15, \pm), \qquad (14, 16, \pm), \\ &\qquad\qquad\qquad\qquad (1, -1, 0), \qquad (-15, -15, \mp), \qquad (14, 16, \pm), \qquad\qquad \Omega = 0, \end{aligned}$$

would also be able to cause this behaviour, although this would require some amplitude to be present in the output mode initially, and would also be expected to interact on the t_2 timescale: around $100s$. In this case the exact resonant theory simply doesn't represent the true behaviour of the system.

Adding additional strength to the near resonance is the size of the interaction coefficient. Figure 6.7 (middle second row) shows that the strongest interaction coefficients coincide with the area of near resonance. This is important as relative sizes of the interaction coefficient can be $\sim \epsilon^{-1}$ or larger, especially for large $|\boldsymbol{k}|$, which has the potential to disrupt the asymptotic series.

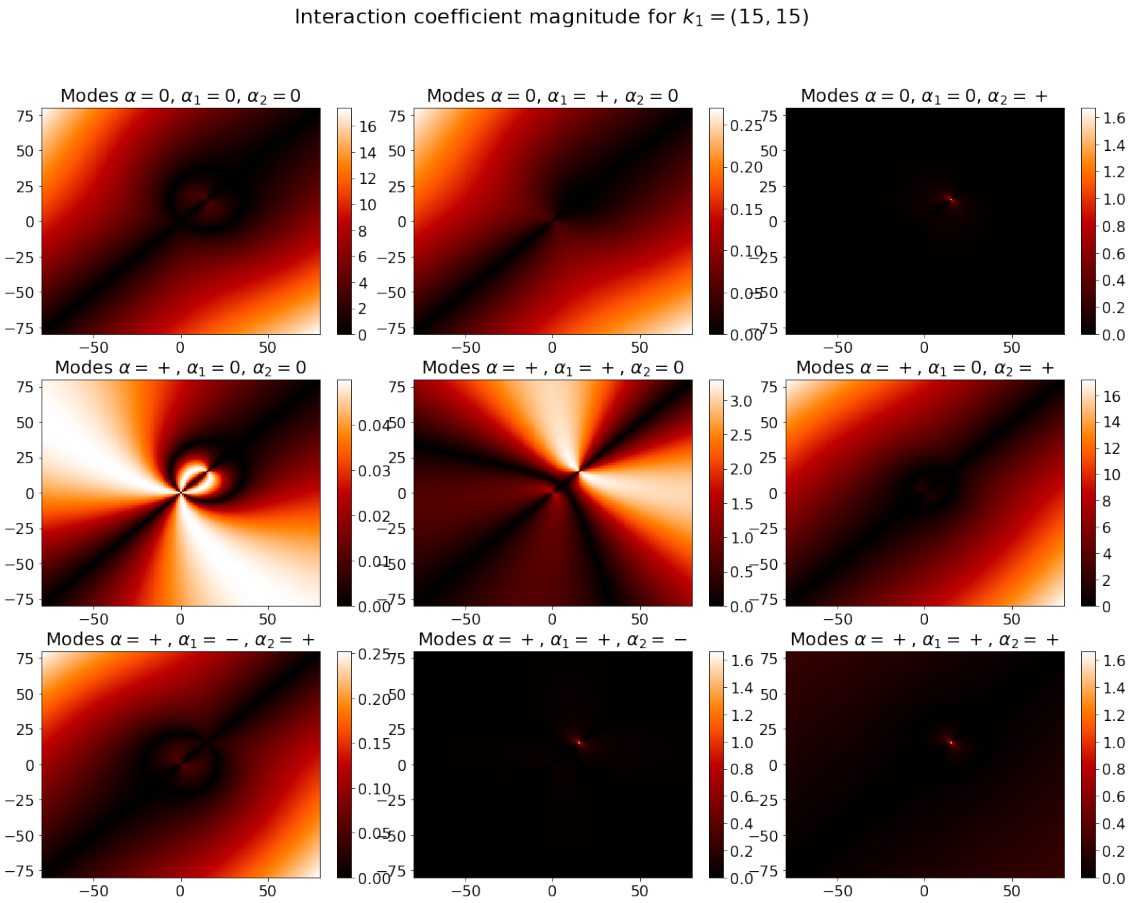

Figure 6.7: Graphs showing the relative strength of the real part of the interaction coefficients for different wavenumbers in each relevant case. The first wavenumber is fixed to (15,15), and the heat maps are given on axes corresponding to the output wavenumber $\boldsymbol{k}$, with $\boldsymbol{k}_2$ calculated from the other two wavenumbers. The top row shows the possible mode combinations outputting onto the slow mode. The middle row gives the output of mixed mode triads onto a fast mode, and the bottom row shows the possible fast mode only triads. From the differences in amplitude it is clear that some interactions will be weakened by the small size of the interaction coefficient. It should also be noted that these interactions are not necessarily resonant. For example from the central graph we can see that the fast-slow-fast interaction has O(1) interaction coefficient in the region of the resonance (the circular resonance seen in figure 6.2), this suggests that as well as forming a resonant interaction, the energy exchange between the modes will not be limited by the interaction coefficient, whereas from the centre top graph slow-fast-slow interactions between (15,15,+) and any other slow mode will not only be non-resonant, but limited by an interaction coefficient an order of magnitude smaller.

Region 3

Region three provides a good example of where near resonant theory is a much better approximation of the motion than exactly resonant theory.

Closely following the first two regions are the short fast modes that are excited to around an amplitude of $10^{-3} - 10^{-2}$ within the first second of the simulation. These can only be attributed to fast-fast-fast interactions, although these cannot be exactly resonant at triad order. Again we conclude that these must be either near resonant or higher order interactions.

Considering the possible quartets that would be almost exactly resonant we find that the dynamics must be initially governed by quartets of the form:

$$(1, 1, \pm), \qquad (14, 14, \pm), \qquad (15, 15, \pm), \qquad (30, 30, \pm), \qquad \Omega = 0.0874 \sim \epsilon.$$

By the theory in the previous section for these to be comparable with the triad resonances there would need to be at least one pairing of the constituent triads that are near resonant, and indeed there is:

$$\begin{aligned} &(1, 1, \pm), \qquad (14, 14, \pm), \qquad (15, 15, \pm), && \Omega = 0.00795 \sim \epsilon^2, \\ &(15, 15, \pm), \qquad (15, 15, \pm), \qquad (30, 30, \pm), && \Omega = 0.0795 \sim \epsilon. \end{aligned}$$

It can be noted that the other triad pair combinations within this triad do not have this behaviour, highlighting the point of section 5.3.2 that a quartet can be split between orders for a near resonant expansion.

No exact resonance is know at higher order n-tets, and running a numerical search is computationally intensive, having exponential order of operations A^n for some constant A that in practice is reasonably large. Although this problem is trivially parallelisable we have not yet done this. Due to these limitations only limited searches have been run, for possible combinations of modes in the vicinity of the starting modes, up to sextet order. The closest approach of the resonances up to these orders are the following:

$$\begin{aligned} &(-4, -4, \mp), \qquad (17, 17, \pm), \qquad (17, 17, \pm), \qquad (30, 30, \pm), && \Omega = 0.0132, \\ &(-1, -2, 0), \qquad (3, 2, \pm), \qquad (14, 16, \pm), \qquad (14, 14, \pm), \qquad (30, 30, \pm), && \Omega = -0.000219, \\ &(1, 1, \pm), \qquad (13, 14, \pm), \qquad (15, 16, \pm), \\ &\qquad\qquad (-16, -16, \pm), \qquad (17, 15, \mp), \qquad (30, 30, \pm), && \Omega = 0.000116. \end{aligned}$$

That is to say if an exact resonance exists that could explain the appearance of energy in region 3 it is operating on, at a minimum, the timescale $t_3 \sim \epsilon^3$, and so we would expect noticeable effects to occur at around 1000s of simulation time. This highlights an important point of near resonant theory. Near resonances should not be considered to exist solely in the vicinity of wavenumber space where exact resonances occur, and do not play the role of exact resonance approximation, they are more intrinsic, as this case shows, where energy is strongly transferred to higher wavenumbers in t_0 time, which is simply not the case in the exact resonant theory.

Another behaviour is also derived from the fast-fast-fast modes in this region: the radial spreading of the wave energy. This is due to near resonant triads (and super-near resonant) such as

$$\begin{aligned} &(-1,-1,\pm), \qquad (-14,-14,\pm), \qquad (-15,-15,\pm), && \Omega = 0.00795 \sim \epsilon^2, \\ &(1,1,\mp), \qquad (30,30,\pm), \qquad (29,29,\pm), && \Omega = 0.0792 \sim \epsilon. \end{aligned}$$

Both these behaviours are seen in the same simulation run with the zero modes removed, shown in figure 6.8. This confirms that these fast mode only interactions must be responsible for the behaviours seen.

Here the near resonant interactions describe the behaviour of the system much better than the exact resonances.

Region 4

Similarly to region 3 the long fast wave modes are excited, although to a lesser extent (amplitudes around 10^{-3}-10^{-4}) than the short wave modes. Here the dominant interaction is the slow-slow-fast interaction, from comparison to the simulation without initial fast modes (that shown in figure 6.6).

This can never be resonant, and the closest to resonance that it can approach is for smaller wavenumbers, giving a minimum for the interaction:

$$(1,1,0), \qquad (-1,0,0), \qquad (0,1,\pm), \qquad \Omega = 4.55 \sim 1.$$

The size of the real part of the interaction coefficient is shown in figure 6.9 in the centre left panel for one particular mode. Here the interaction coefficient is also small, and we would expect that the modes would not be able to grow to a large size, as is the case. The small amplitudes reflect this. Once there are fast modes present at the low wavenumbers the fast-slow-fast interaction can transfer energy amongst the modes, with its relatively strong coefficient (central and centre right

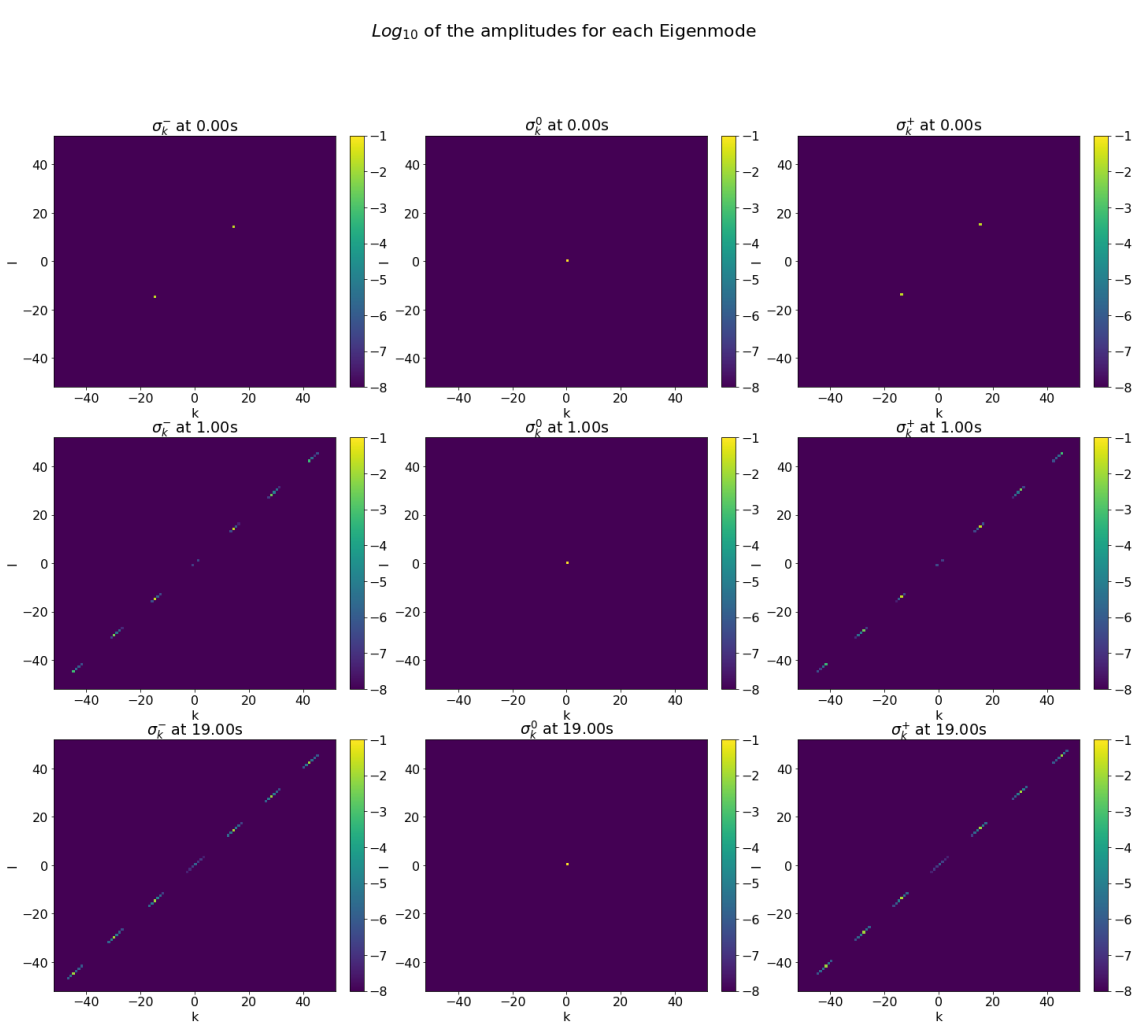

Figure 6.8: Distribution with time of the log of the eigenmode amplitudes. Time increases from top to bottom from $0s$, to $1s$, to $19s$. The central column shows the slow modes and the outside columns show the fast modes. In this simulation only the fast modes were included in the initial conditions. No energy is transferred to the slow modes, as expected from the proof in chapter 4 that the interaction coefficient for $(\pm, ..., \pm, 0)$ is always zero. It can be seen that both the self interaction and radial spreading of energy occur without the presence of slow modes, it follows that the radial spreading can be attributed to the near-resonant fast-fast-fast interactions such as mode (15,15,+) with mode (15,15,+) to form (30,30,+). It can also be seen that the spread of energy to low wavenumbers is very weak from fast mode only interactions, suggesting that the spread of energy to these modes will be mostly from interactions with slow modes.

panels) and possible near resonant interaction.

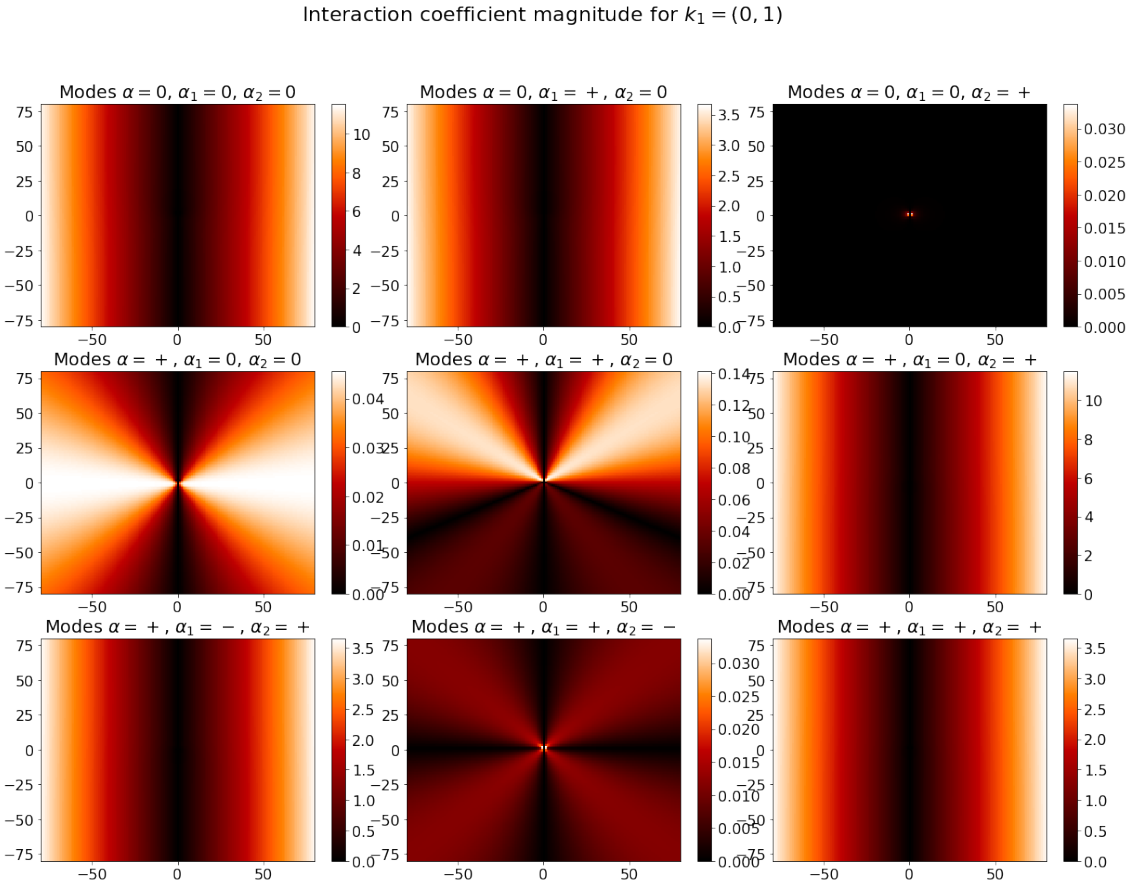

Figure 6.9: Graphs showing the relative strength of the real part of the interaction coefficients for different wavenumbers in each relevant case. The first wavenumber is fixed to (0,1), and the heat maps are given on axes corresponding to the output wavenumber $\boldsymbol{k}$, with $\boldsymbol{k}_2$ calculated from the other two wavenumbers. The top row shows the possible mode combinations outputting onto the slow mode. The middle row gives the output of mixed mode triads onto a fast mode, and the bottom row shows the possible fast mode only triads. From the differences in amplitude it is clear that some interactions will be weakened by the small size of the interaction coefficient. It should also be noted that these interactions are not necessarily resonant. For the smaller wavenumber the complexity of the graphs is contained close to the origin, and the majority of the interaction coefficient follows a radial pattern, mostly dependent only on the angle of incidence between the modes. As an example the centre-right graph shows that the fast-slow-fast interaction that would cause energy to spread to wavenumbers close to (15,15,+) has an O(1) interaction coefficient, in this region there are resonances and near resonances, and the expected spreading of energy can be observed in figure 6.2 as the region of higher amplitudes around the (15,15,+) mode.

Region 5

This region is the least stimulated of all those considered, with amplitudes of around 10^{-6}, lower for shorter wavelengths. However by comparison with figure 6.6 it is clear that the shorter waves, although low amplitude, have a very different energy distribution due to interaction with the fast modes. For the energy to have reached this region of the mode space must be, at least in part, due to the quartet interaction of Thomas 2016: slow-fast-fast-slow. However the amplitudes are even lower than might be expected for a resonant quartet interaction, and there is reason for this. Considering the full quartet interaction coefficient:

$$Q^{0\ \pm\ \mp\ 0}_{\boldsymbol{k}_1\boldsymbol{k}_2\boldsymbol{k}_3\boldsymbol{k}} = \frac{2}{3}\left[\frac{C^{0\mp\ 0}_{\boldsymbol{k}_a\boldsymbol{k}_3\boldsymbol{k}}\ C^{0\ \pm\ 0}_{\boldsymbol{k}_1\boldsymbol{k}_2\boldsymbol{k}_a}\big|_{nr}}{i(\omega_a-\omega_1-\omega_2)} + \sum_{\alpha_b=\pm}\frac{C^{\alpha_b 0\ 0}_{\boldsymbol{k}_b\boldsymbol{k}_1\boldsymbol{k}}\ C^{\pm\ \mp\ \alpha_b}_{\boldsymbol{k}_2\boldsymbol{k}_3\boldsymbol{k}_b}\big|_{nr}}{i(\omega_b-\omega_2-\omega_3)} + \frac{C^{0\pm\ 0}_{\boldsymbol{k}_c\boldsymbol{k}_2\boldsymbol{k}}\ C^{\mp\ 0\ 0}_{\boldsymbol{k}_3\boldsymbol{k}_1\boldsymbol{k}_c}\big|_{nr}}{i(\omega_c-\omega_3-\omega_1)}\right].$$

It is clear that every triad pairing must contain a fast-slow-slow triad, which can never be near resonant, and so these quartets will never be 'bumped up an order' like those considered in region 3. If we consider the exactly resonant quartet:

$$(15,15,0), \qquad (1,1,\pm), \qquad (-1,-1,\mp), \qquad (15,15,0), \qquad \Omega = 0,$$

the triad pairings give:

1. $(15,15,0), \quad (1,1,\pm), \quad (16,16,0), \quad \Omega = 6.36,$
   $(16,16,0), \quad (-1,-1,\mp), \quad (15,15,0), \quad \Omega = -6.36.$

2. $(15,15,0), \quad (-1,-1,\mp), \quad (14,14,0), \quad \Omega = -6.36,$
   $(14,14,0), \quad (1,1,\pm), \quad (15,15,0), \quad \Omega = 6.36.$

3. $(-1,-1,\mp), \quad (1,1,\pm), \quad (0,0,+), \quad \Omega = -1,$
   $(0,0,+), \quad ,(15,15,0), \quad (15,15,0) \quad \Omega = 1.$

4. $(-1,-1,\mp), \quad (1,1,\pm), \quad (0,0,-), \quad \Omega = 1,$
   $(0,0,-), \quad (15,15,0), \quad (15,15,0), \quad \Omega = -1.$

It follows that this quartet interaction is formed of non-near resonant triads, explaining the small amplitudes in the region.

The other possible quartet combination that could have moved energy to this region is the quartet $(0, 0, \pm; 0)$. It is clear that this can never be near resonant as the quartet detuning is $O(1)$.

All Regions

A feature visible in all of the time series in figures 6.3-6.4 is that the behaviour of the regions driven by non-resonances have high frequency oscillations present. This is visible in the theory: the non-resonances have an exponential term $e^{i\Omega\tau}$, which then drives them on a fast timescale, whereas the near resonances have the alternative exponential $e^{i\Delta_{(n)}t_n}$ which does not lead to these fast oscillations. We are seeing the effect of averaging: fast oscillations force the amplitudes in both directions in rapid succession causing little net change, whereas slow oscillations have a direction that is consistent for a longer time, leading to coherent growth of a mode.

A near resonant expansion

From the analysis of this section, we can conclude that limiting a simulation to only the near resonant modes of the shallow water equations would only exclude stimulation of modes that never grow to greater than 10^{-3} in amplitude during the $\sim t_0$ timescale, and so all of the strong behaviour would be captured. Conversely an exact resonant expansion would not capture some of the strongest effects of the motion. Also, misleadingly, exact resonant quartets that would be included at next order have a smaller effect on the dynamics than interactions that would be excluded until some unknown higher order (at least sextet or times of $\sim 10^6 s$ by the numerical calculation in the region 3 analysis above).

One area that complicates the theory is the size of the triad interaction coefficient, this typically varies in a manner such that at sufficiently large wavenumbers it can be of size ϵ^{-1}. This would make it necessary to include interactions in these regions further from resonance, introducing strong rapidly oscillating amplitudes.

6.2 Stratified Equations

The stratified equations are now considered analytically. This case is interesting due to the fast-fast-fast triad that was found to be 0 only when the triad interaction is exactly resonant, unlike the layered equations for which it is always 0. This is however not true for a near resonant fast-fast-slow triad, and therefore for any higher order interaction containing them.

For the stratified equations we will concentrate only on the near resonant fast-fast-slow interactions: those that could not occur in the layered equations. The interaction coefficient was given by:

$$C^{\alpha_1\alpha_2 0}_{\boldsymbol{k}_1\boldsymbol{k}_2\boldsymbol{k}} = \frac{iN(\alpha_1\omega_1+\alpha_2\omega_2)}{2\omega\omega_1\omega_2|\boldsymbol{k}||\boldsymbol{k}_1||\boldsymbol{k}_2||\boldsymbol{k}_1^h||\boldsymbol{k}_2^h|}\big[if(\boldsymbol{k}_1^h\cdot\boldsymbol{k}_2^h)(m_1^2|\boldsymbol{k}_2^h|^2+m_2^2|\boldsymbol{k}_1^h|^2) \\ -2ifm_2m_1|\boldsymbol{k}_1^h|^2|\boldsymbol{k}_2^h|^2+\frac{1}{N^2-f^2}(\alpha_1\omega_1-\alpha_2\omega_2)(\alpha_1\alpha_2\omega_2\omega_1+f^2)|\boldsymbol{k}_1|^2|\boldsymbol{k}_2|^2(\boldsymbol{k}_2\times\boldsymbol{k}_1)_z\big]. \tag{6.1}$$

In this interaction we expect the interaction coefficient to be close to 0 in the vicinity of a resonance, and so even though we might expect a near resonance it may have an ϵ small interaction coefficient. However in the specific scenario that $f/N\sim 1+\epsilon$, we must check that this cannot be broken. The largest part of the interaction coefficient would then be the last term. To $O(1)$:

$$C^{\alpha_1\alpha_2 0}_{\boldsymbol{k}_1\boldsymbol{k}_2\boldsymbol{k}} = \frac{i}{2|\boldsymbol{k}||\boldsymbol{k}_1^h||\boldsymbol{k}_2^h|}\big[(m_2|\boldsymbol{k}_1|-m_1|\boldsymbol{k}_2|)(\alpha_1\alpha_2+1)(\boldsymbol{k}_2\times\boldsymbol{k}_1)_z\big].$$

However because all near resonant interactions have $\alpha_1=-\alpha_2$ the $\alpha_1\alpha_2+1$ term makes this exactly 0, and so even in this special case the interaction coefficient is $O(\epsilon)$. So despite this term appearing in the near resonances, the interaction coefficient will ensure that the interaction is always small.

We have a situation in which including the near resonances in this particular case would result in inclusion of lower order terms in the expansion. However, in this construction, for them to interact as a component of a quartet resonance they must be grouped with the near resonances, if they were considered a slaved mode they could never resonate with the normal slaved modes as $O(1)+O(\epsilon)=O(1)$. They would then only be able to take part in quintet and higher order interactions. However for the triad interactions one could easily pair them with the slaved modes - showing that their effect is equivalent to a slower timescale quartet (or higher order) interaction.

Another compelling case for inclusion in the near resonant terms is the better approximation of enstrophy conservation. The fast-fast-slow interactions result in an $O(\epsilon)$ error in the enstrophy conservation of $\boldsymbol{u}_0$ due to the changes in the $\boldsymbol{u}_1$ terms, but in the near resonant expansion the fastest growing of these terms would be included in the $\boldsymbol{u}_0$ part of the expansion, resulting in a smaller anomaly for the largest part of the flow on the t_0 timescale.

To show how this near resonant triad behaves differently to the exactly resonant version we

consider the resonant triad set:

$$\frac{\partial a^{\pm}_{\boldsymbol{k}_1}}{\partial t_0} = C^{\mp\, 0\, \pm}_{\boldsymbol{k}_2\boldsymbol{k}_3\boldsymbol{k}_1} a^{\mp}_{\boldsymbol{k}_2} a^{0}_{\boldsymbol{k}_3}, \tag{6.2}$$

$$\frac{\partial a^{\mp}_{\boldsymbol{k}_2}}{\partial t_0} = C^{\pm\, 0\, \mp}_{\boldsymbol{k}_1\boldsymbol{k}_3\boldsymbol{k}_2} a^{\pm}_{\boldsymbol{k}_1} a^{0}_{\boldsymbol{k}_3}, \tag{6.3}$$

$$\frac{\partial a^{0}_{\boldsymbol{k}_3}}{\partial t_0} = 0. \tag{6.4}$$

From this we can derive the two energy conservation laws:

$$\frac{1}{2}\frac{\partial |a^{0}_{\boldsymbol{k}_3}|^2}{\partial t_0} = 0 \Rightarrow |a^{0}_{\boldsymbol{k}_3}(t_0)| = |a^{0}_{\boldsymbol{k}_3}(0)|, \tag{6.5}$$

$$\frac{1}{2}\frac{\partial |a^{\pm}_{\boldsymbol{k}_1}|^2}{\partial t_0} + \frac{1}{2}\frac{\partial |a^{\mp}_{\boldsymbol{k}_2}|^2}{\partial t_0} = 0, \tag{6.6}$$

and clearly no energy is exchanged with the slow mode, leaving it unaffected.

In the near resonant case however, the situation is different:

$$\frac{\partial a^{\pm}_{\boldsymbol{k}_1}}{\partial t_0} = C^{\mp\, 0\, \pm}_{\boldsymbol{k}_2\boldsymbol{k}_3\boldsymbol{k}_1} a^{\mp}_{\boldsymbol{k}_2} a^{0}_{\boldsymbol{k}_3} e^{i\Omega^{\mp\, 0\, \pm}_{\boldsymbol{k}_2\boldsymbol{k}_3\boldsymbol{k}_1}\tau}, \tag{6.7}$$

$$\frac{\partial a^{\mp}_{\boldsymbol{k}_2}}{\partial t_0} = C^{\pm\, 0\, \mp}_{\boldsymbol{k}_1\boldsymbol{k}_3\boldsymbol{k}_2} a^{\pm}_{\boldsymbol{k}_1} a^{0}_{\boldsymbol{k}_3} e^{i\Omega^{\pm\, 0\, \mp}_{\boldsymbol{k}_1\boldsymbol{k}_3\boldsymbol{k}_2}\tau}, \tag{6.8}$$

$$\frac{\partial a^{0}_{\boldsymbol{k}_3}}{\partial t_0} = C^{\pm\, \mp\, 0}_{\boldsymbol{k}_1\boldsymbol{k}_2\boldsymbol{k}_3} a^{\pm}_{\boldsymbol{k}_1} a^{\mp}_{\boldsymbol{k}_2} e^{i\Omega^{\pm\, \mp\, 0}_{\boldsymbol{k}_1\boldsymbol{k}_2\boldsymbol{k}_3}\tau}, \tag{6.9}$$

with energy conservation law:

$$\frac{1}{2}\frac{\partial |a^{0}_{\boldsymbol{k}_3}|^2}{\partial t_0} + \frac{1}{2}\frac{\partial |a^{\pm}_{\boldsymbol{k}_1}|^2}{\partial t_0} + \frac{1}{2}\frac{\partial |a^{\mp}_{\boldsymbol{k}_2}|^2}{\partial t_0} = 0. \tag{6.10}$$

In the near resonant case there is energy exchange between the slow and fast modes, and hence the near resonant interaction can't be considered just a scattering of the fast modes, as found in the shallow water equations (Ward and Dewar 2010). However this energy exchange will be constrained by the interaction coefficient of $O(\epsilon)$.

If we reconsider a resonance of the type in Thomas 2016 - slow-fast-fast-slow, unlike in the layered case we cannot rule out these fast-fast-slow resonances and so the interaction coefficient looks like:

$$Q^{0\, \pm\, \mp\, 0}_{\boldsymbol{k}_1\boldsymbol{k}_2\boldsymbol{k}_3\boldsymbol{k}} = \frac{2}{3}\left[\sum_{\alpha_a} \frac{C^{\alpha_a \mp\, 0}_{\boldsymbol{k}_a\boldsymbol{k}_3\boldsymbol{k}}\, C^{0\, \pm\, \alpha_a}_{\boldsymbol{k}_1\boldsymbol{k}_2\boldsymbol{k}_a}\big|_{nr}}{i(\omega_a - \omega_1 - \omega_2)} + \sum_{\alpha_b = \pm} \frac{C^{\alpha_b 0\, 0}_{\boldsymbol{k}_b\boldsymbol{k}_1\boldsymbol{k}}\, C^{\pm\, \mp\, \alpha_b}_{\boldsymbol{k}_2\boldsymbol{k}_3\boldsymbol{k}_b}\big|_{nr}}{i(\omega_b - \omega_2 - \omega_3)} + \sum_{\alpha_c} \frac{C^{\alpha_c \pm\, 0}_{\boldsymbol{k}_c\boldsymbol{k}_2\boldsymbol{k}}\, C^{\mp\, 0\, \alpha_c}_{\boldsymbol{k}_3\boldsymbol{k}_1\boldsymbol{k}_c}\big|_{nr}}{i(\omega_c - \omega_3 - \omega_1)}\right].$$

All the possible pairing of mode types are:

1. $(\pm, \pm; 0)^{\dagger},\ (0, \pm; \pm)$,

2. $(0,\pm;0)^*,\ (0,\pm;0)^*,$

3. $(\pm,0;0)^*,\ (\pm,\pm;\pm),$

where * marks the triads that can never be near resonant, and † marks the fast-fast-slow triads that despite being near resonant can only act mildly on the system due to the interaction coefficient size.

It is clear that these interactions will not be made up of near resonances, unless they contain the fast-fast-slow triad that limits the speed of the interaction anyway. A similar process can be applied to the $(\pm,\pm,\pm;0)$ (this interaction now exists but will always be slowed by the process described) and $(\pm,0,0;0)$ interactions. Despite the possibility of near resonant interactions, the slow mode can never be affected on the t_0 timescale by any interaction other than the usual quasigeostrophic (0,0;0) interaction, the same conclusion as found in the layered equations.

Similarly the quartets $(0,0,0;\pm)$ can never be formed of near resonances, due to the $(0,0;\pm)$ triad components. This suggests that spontaneous production of gravity waves (fast modes) will also only ever occur on timescales $\sim t_1$.

All mixed mode interactions that lead to energy exchanges between the fast and slow components can only occur on the longer t_1 timescale, even where ϵ takes larger values. This finding helps to explain the strength of the fast-slow splitting observed in quasigeostrophic systems.

6.3 Chapter Summary

The main points covered in this chapter were:

- The simple numerical example of the shallow water equations was chosen, demonstrating the theory of chapter 5. This included confirmation that near resonances can evolve on the t_0 timescale along with the exact resonances (section 5.1.2) and the formation of higher order n-tets from near resonant triads (section 5.2.1).
- The better approximation of the full equations given by the near resonances was demonstrated for the rotating shallow water equations by numerical computation.
- Specific cases were found that showed strong energy transfer in regions that can never contain exact resonances - it was found in a numeric search for resonances that this is true up to sextet order for all wave amplitudes close to those present initially.

- Energy exchange due to the resonance given in Thomas 2016 was found, but in this context it can be seen to be a weak interaction as it is not formed of near resonances. A very similar conclusion was reached for the equivalent interaction in the stratified equations.
- The amplitude of the interaction coefficient was discussed in relation to the limits of the near resonant theory. This was especially explored in the context of the fast-fast-slow interaction in the stratified equations where the near resonance condition enforces smallness of the interaction coefficient.

In general it was found that the near resonant theory, and the framework based on promotion of higher order interactions of chapter 5 is a much better approximation of the dynamics of the systems considered than the expansion in terms of the exact resonances.

Chapter 7

Wavepackets

An often neglected aspect of asymptotics is that there can be slow spatial variation of a solution. If we have variation on a range of spatial scales such that the small scales are of a size ϵ smaller than the larger ones we must consider introducing multiple scales in the spatial dimension as well. This leads to wavepacket theory, the real distinction of which emerges on infinite domains, as opposed to the finite periodic domains the previous analysis has been most relevant to.

In this chapter we introduce wavepackets and consider the implications of this extension from the expansions previously derived for periodic domains in the preceding chapters. The extra condition of the time of coincidence of wavepackets is considered in conjunction with the previous theory, with the aim of ascertaining extra limits on the feasibility of a given interaction. In particular the conclusions are related to the findings of Reznik, Zeitlin, and Ben Jelloul 2001 and Thomas 2016 where certain higher order interactions were found to exist in a periodic domain, but not in the scenario in which there is an infinite domain with compact initial conditions. It is found that the expansion of the exact resonances will agree with those findings, but that taking into account near resonances can allow interactions that would otherwise be absent to all orders to appear in the system once again. Near resonances are needed for interactions other than self interaction of a wavepacket to occur.

Wavepacket theory decreases the effectiveness of nonlinear interactions, however, isolated packets of waves cannot be considered any more representative of the reality than periodic wave trains. Reality might be expected to rest in the middle between these two extremes.

7.1 Derivation of a wavepacket

In the standard manner (see Whitham 1974 or Vallis 2006 for example), we want to consider a wavepacket (in one space dimensional for simplicity, though the equivalent results hold in higher dimensions) that is composed of wavenumbers in a small region around the main wavenumber k^*. We write:

$$A(x,t)e^{i(k^*x-\omega(k^*)t)} = \int_{-\infty}^{\infty} a(k^*+\epsilon K)e^{i((k^*+\epsilon K)x-\omega(k^*+\epsilon K)t)}dK. \tag{7.1}$$

Where ϵK is the perturbation from the main wavenumber, and the x and t coordinates are currently unscaled. It should be noted that when there are multiple branches of the dispersion relation this is still valid, with each branch given by a separate integral.

We will assume that the wavepacket is composed entirely of waves from one branch of the dispersion relation so that we can Taylor expand:

$$\omega(k^*+\epsilon K) \approx \omega(k^*) + \epsilon K\frac{\partial\omega}{\partial K}(k) + \frac{\epsilon^2}{2}K^2\frac{\partial^2\omega}{\partial K^2}(k^*) + \dots . \tag{7.2}$$

We can then isolate the part that contributes to A:

$$A(x,t) = \int_{-\infty}^{\infty} a(k^*+\epsilon K)e^{i(\epsilon Kx-(\epsilon K\omega'(k^*)+\frac{\epsilon^2}{2}K^2\omega''(k^*+\dots)t)}dK. \tag{7.3}$$

Assuming we can exchange the order of differentiation and integration we can write:

$$A_{\boldsymbol{x}} = \int_{-\infty}^{\infty} i\epsilon Ka\ dK, \tag{7.4}$$

$$A_{\boldsymbol{xx}} = \int_{-\infty}^{\infty} -\epsilon^2K^2a\ dK, \tag{7.5}$$

$$A_t = \int_{-\infty}^{\infty} -i(\epsilon K\omega'(k^*) + \frac{\epsilon^2}{2}K^2\omega''(k^*))a + \dots\ dK\ , \tag{7.6}$$

and from this we can write:

$$A_t + \epsilon\omega'(k^*)A_x - \frac{i\epsilon^2}{2}\omega''(k^*)A_{xx} + \dots = 0, \tag{7.7}$$

We can reintroduce the time scalings used in the multiple scale expansion, as well as a spatial scale $x_0 \sim \epsilon$ to split this into:

$$A_{t_0} + \omega'(k^*)A_{x_0} = 0, \tag{7.8}$$

$$A_{t_1} - \frac{i}{2}\omega''(k^*)A_{x_0x_0} = 0. \tag{7.9}$$

These two parts together form the linear Schrödinger equation. This is the behaviour of a wavepacket that is only evolving linearly, in the full equations these terms will simply replace the previous time derivatives in the nonlinear expansions. When the two parts are combined for a single wavepacket together with the nonlinear quartets (triads are assumed absent) then a change of variables into the frame moving with the group velocity returns the nonlinear Schrödinger equation, as seen in Benney and Newell 1967 or Zakharov 1967 for instance. This derivation underlies the modulational instability. With more wavepackets a similar derivation gives the three wave equations at the earlier triad order (see Kaup, Reiman, and Bers 1979 for instance). In the following we will not be making the assumption that there is only a single wavepacket, neither will it be assumed that there are no triads, or only triads.

7.2 Multiple scale expansion in time and space

We introduce multiple spatial scales (cf Newell 1969 or Benney and Roskes 1969 for example) into the analysis of chapters 3 and 5, choosing the scaling $x_0 \sim \epsilon x$ such that the triad resonances operate on the timescale at which the wave packet moves with its group velocity:

$$x \sim x, \qquad x_0 \sim \epsilon x, \qquad t \sim t, \qquad t_0 \sim \epsilon t, \tag{7.10}$$

$$\frac{\partial}{\partial x} \to \frac{\partial}{\partial x} + \epsilon \frac{\partial}{\partial x_0}, \tag{7.11}$$

$$\frac{\partial}{\partial t} \to \frac{\partial}{\partial t} + \epsilon \frac{\partial}{\partial t_0}. \tag{7.12}$$

We define the following:

$$\mathcal{L} = \mathcal{L}_0 + \epsilon \mathcal{L}_1 + \dots , \tag{7.13}$$

$$\mathcal{N} = \mathcal{N}_0 + \epsilon \mathcal{N}_1 + \dots , \tag{7.14}$$

where the new spatial variables introduce ϵ dependence into the operators.

The multiple scale expansion will now look as follows:

$$O(\epsilon^{-1}) \qquad \frac{\partial \boldsymbol{u}_0}{\partial \tau} + \mathcal{L}_0 \boldsymbol{u}_0 = 0, \tag{7.15}$$

$$O(1) \qquad \frac{\partial \boldsymbol{u}_1}{\partial \tau} + \mathcal{L}_0 \boldsymbol{u}_1 = -\left(\frac{\partial \boldsymbol{u}_0}{\partial t_0} + \mathcal{L}_1 \boldsymbol{u}_0 + \mathcal{N}_0(\boldsymbol{u}_0, \boldsymbol{u}_0) \right), \tag{7.16}$$

$$O(\epsilon) \qquad \frac{\partial \boldsymbol{u}_2}{\partial \tau} + \mathcal{L}_0 \boldsymbol{u}_2 = -\left(\frac{\partial \boldsymbol{u}_1}{\partial t_0} + \frac{\partial \boldsymbol{u}_0}{\partial t_1} + \mathcal{L}_1 \boldsymbol{u}_1 + \mathcal{L}_2 \boldsymbol{u}_0 \right.$$
$$\left. + \mathcal{N}_0(\boldsymbol{u}_0, \boldsymbol{u}_1) + \mathcal{N}_0(\boldsymbol{u}_1, \boldsymbol{u}_0) + \mathcal{N}_1(\boldsymbol{u}_0, \boldsymbol{u}_0) \right). \tag{7.17}$$

The first new term is at the triad order of interaction: $\mathcal{L}_1 \boldsymbol{u}_0$. To understand this term we consider $\mathcal{L}(\boldsymbol{k})$, the linear operator in Fourier space. We Taylor expand in $\boldsymbol{K}$ about the peak wavenumber $\boldsymbol{k}^*$ where $\mathcal{L}_0 = \mathcal{L}(\boldsymbol{k}^*) = \mathcal{L}(\boldsymbol{k} - \epsilon \boldsymbol{K})$:

$$\mathcal{L}(\boldsymbol{k}) \approx \mathcal{L}_0 + \epsilon (\nabla_{\boldsymbol{k}} \mathcal{L}(\boldsymbol{k}^*)) \cdot \boldsymbol{K} + \frac{1}{2} \epsilon^2 \boldsymbol{K} \cdot (\nabla_{\boldsymbol{k}}^T \nabla_{\boldsymbol{k}} \mathcal{L}(\boldsymbol{k}^*)) \cdot \boldsymbol{K} + \dots . \tag{7.18}$$

We then convert the vectors $\boldsymbol{K}$ back to real space using $i\boldsymbol{K} = \nabla_{x_0}$:

$$\mathcal{L} \approx \mathcal{L}_0 - i\epsilon (\nabla_{\boldsymbol{k}} \mathcal{L}(\boldsymbol{k}^*)) \cdot \nabla_{\boldsymbol{x}_0} - \frac{1}{2} \epsilon^2 \nabla_{\boldsymbol{x}_0}^T \cdot (\nabla_{\boldsymbol{k}}^T \nabla_{\boldsymbol{k}} \mathcal{L}(\boldsymbol{k}^*)) \cdot \nabla_{\boldsymbol{x}_0} + \dots . \tag{7.19}$$

By comparison to (7.13) we have:

$$\mathcal{L}_1 = -i (\nabla_{\boldsymbol{k}} \mathcal{L}(\boldsymbol{k}^*)) \cdot \nabla_{\boldsymbol{x}_0}, \tag{7.20}$$

$$\mathcal{L}_2 = -\frac{1}{2} \nabla_{\boldsymbol{x}_0}^T \cdot (\nabla_{\boldsymbol{k}}^T \nabla_{\boldsymbol{k}} \mathcal{L}(\boldsymbol{k}^*)) \cdot \nabla_{\boldsymbol{x}_0}. \tag{7.21}$$

We then apply these operators to an eigenmode multiplied by some wave envelope: $\boldsymbol{A}(\boldsymbol{x}_0, t) \boldsymbol{r}_{\boldsymbol{k}^*}^{\alpha}$, and use the fact that $\mathcal{L}_0 \boldsymbol{r}_{\boldsymbol{k}^*}^{\alpha} = i\omega_{\boldsymbol{k}^*}^{\alpha} \boldsymbol{r}_{\boldsymbol{k}^*}^{\alpha}$:

$$\mathcal{L}_1 \boldsymbol{r}_{\boldsymbol{k}^*}^{\alpha} \boldsymbol{A}(\boldsymbol{x}_0, t) = ((\nabla_{\boldsymbol{k}} \omega_{\boldsymbol{k}^*}^{\alpha}) \cdot \nabla_{\boldsymbol{x}_0}) \boldsymbol{A}(\boldsymbol{x}_0, t) \boldsymbol{r}_{\boldsymbol{k}^*}^{\alpha} \qquad = (\{\boldsymbol{c}_g\}_{\boldsymbol{k}^*}^{\alpha} \cdot \nabla_{\boldsymbol{x}_0}) \boldsymbol{A}(\boldsymbol{x}_0, t) \boldsymbol{r}_{\boldsymbol{k}^*}^{\alpha}, \tag{7.22}$$

$$\mathcal{L}_2 \boldsymbol{r}_{\boldsymbol{k}^*}^{\alpha} \boldsymbol{A}(\boldsymbol{x}_0, t) = (-\frac{i}{2} \nabla_{\boldsymbol{x}_0}^T \cdot (\nabla_{\boldsymbol{k}}^T \nabla_{\boldsymbol{k}} \omega_{\boldsymbol{k}^*}^{\alpha}) \cdot \nabla_{\boldsymbol{x}_0}) \boldsymbol{A}(\boldsymbol{x}_0, t) \boldsymbol{r}_{\boldsymbol{k}^*}^{\alpha} \quad = (-\frac{i}{2} \nabla_{\boldsymbol{x}_0}^T Q_{\boldsymbol{k}^*}^{\alpha} \nabla_{\boldsymbol{x}_0}) \boldsymbol{A}(\boldsymbol{x}_0, t) \boldsymbol{r}_{\boldsymbol{k}^*}^{\alpha}, \tag{7.23}$$

where $Q_{\boldsymbol{k}}^{\alpha} = \nabla_{\boldsymbol{k}} \boldsymbol{c}_g = \nabla_{\boldsymbol{k}}^T \nabla_{\boldsymbol{k}} \omega_{\boldsymbol{k}}^{\alpha}$ is the second moment of the wavepacket that defines its linear spreading.

The $\mathcal{L}_1 \boldsymbol{u}_1$ term represents the translation of slaved mode wavepackets by the usual group velocity. We shall see later that these terms will not affect the quartet order interactions.

7.2.1 Structure of the wave envelope for a mode

It is necessary to note that whilst in scalar equations one can arbitrarily define the wavepacket envelope as any function of the slowly varying spatial scale $\boldsymbol{x}_0$, in vector systems there are no extra degrees of freedom in wavepacket choice, and so once one has chosen the shape of the wavepacket in one field, the other fields are prescribed. To describe a well defined wavepacket each dimension must obey the polarisation relations. For slowly varying $\boldsymbol{x}_0$ probably the clearest way to do this is by considering the small changes in the wavenumber $\boldsymbol{k} = \boldsymbol{k}^* + \epsilon \boldsymbol{K}$ as defining the variation around peak wavenumber $\boldsymbol{k}^*$.

For example we consider a Gaussian wavepacket in the height field of a slow mode of the shallow water equations, with wavenumbers grouped in a range of size ϵ around $\boldsymbol{k}^*$. Using the eigenvector from (2.85) we would then have the full wavepacket shape:

$$\boldsymbol{u}^{\alpha}_{\boldsymbol{k}} = \frac{\sigma^2}{2\pi}\int_{-\infty}^{\infty}\int_{-\infty}^{\infty}\begin{pmatrix} -i(l^*+\epsilon L)c \\ i(k^*+\epsilon K)c \\ f \end{pmatrix} e^{-\frac{\sigma^2|\boldsymbol{K}|^2}{2}} e^{i(\epsilon\boldsymbol{K}+\boldsymbol{k}^*)\cdot\boldsymbol{x}}\, d\boldsymbol{K} \;=\; \frac{1}{\sqrt{2}\sigma}\begin{pmatrix} -icl^*\sigma^2 + \epsilon c y_0 \\ ick^*\sigma^2 - \epsilon c x_0 \\ f\sigma^2\sqrt{2} \end{pmatrix} e^{i\boldsymbol{k}^*\cdot\boldsymbol{x}} e^{-\frac{|\boldsymbol{x}_0|^2}{2\sigma^2}}, \tag{7.24}$$

and so the envelope for the u and v components has a correction term in the shape of a dipole. This wavepacket is illustrated in figure 7.1 where the adjusted wavepacket and the correction term are shown for a given parameter set. In other modes and equation sets it may be impossible to write the wavepacket in an explicit form and only an integral form can be found.

We need to understand the effect these correction terms will have on the nonlinear part. We write the Taylor series:

$$\mathcal{N}(\boldsymbol{u}^{\alpha_1}_{\boldsymbol{k}_1}, \boldsymbol{u}^{\alpha_2}_{\boldsymbol{k}_2}) = \mathcal{N}_0(\boldsymbol{u}^{\alpha_1}_{\boldsymbol{k}^*_1}, \boldsymbol{u}^{\alpha_2}_{\boldsymbol{k}^*_2}) + \epsilon\boldsymbol{K}\cdot\nabla_{\boldsymbol{k}}\mathcal{N}(\boldsymbol{u}^{\alpha_1}_{\boldsymbol{k}_1}, \boldsymbol{u}^{\alpha_2}_{\boldsymbol{k}_2})|_{\boldsymbol{k}^*} + O(\epsilon^2), \tag{7.25}$$

$$\boldsymbol{u}^{\alpha}_{\boldsymbol{k}} = \boldsymbol{u}^{\alpha}_{\boldsymbol{k}^*} + \epsilon\boldsymbol{K}\cdot\nabla_{\boldsymbol{k}}\boldsymbol{u}^{\alpha}_{\boldsymbol{k}}|_{\boldsymbol{k}^*} + O(\epsilon^2). \tag{7.26}$$

In (7.26) we can identify the terms as the main and correction parts of the wavepacket calculated above in (7.24). We now follow how this affects the nonlinear part. From (7.25) we consider $\mathcal{N}(\boldsymbol{u}^{\alpha_1}_{\boldsymbol{k}_1}, \boldsymbol{u}^{\alpha_2}_{\boldsymbol{k}_2})$:

$$\begin{aligned}
\mathcal{N}(\boldsymbol{u}^{\alpha_1}_{\boldsymbol{k}_1}, \boldsymbol{u}^{\alpha_2}_{\boldsymbol{k}_2}) &= \mathcal{N}_0(\boldsymbol{u}^{\alpha_1}_{\boldsymbol{k}^*_1}, \boldsymbol{u}^{\alpha_2}_{\boldsymbol{k}^*_2}) + \epsilon\boldsymbol{K}_i\cdot\nabla_{\boldsymbol{k}_i}\mathcal{N}(\boldsymbol{u}^{\alpha_1}_{\boldsymbol{k}_1}, \boldsymbol{u}^{\alpha_2}_{\boldsymbol{k}_2})|_{\boldsymbol{k}^*} + O(\epsilon^2) \\
&= \mathcal{N}_0(\boldsymbol{u}^{\alpha_1}_{\boldsymbol{k}^*_1}, \boldsymbol{u}^{\alpha_2}_{\boldsymbol{k}^*_2}) + \epsilon(\boldsymbol{K}_i\cdot\nabla_{\boldsymbol{k}_i}\mathcal{N})(\boldsymbol{u}^{\alpha_1}_{\boldsymbol{k}_1}, \boldsymbol{u}^{\alpha_2}_{\boldsymbol{k}_2})|_{\boldsymbol{k}^*} \\
&\qquad + \mathcal{N}_0(\epsilon\boldsymbol{K}_1\cdot\nabla_{\boldsymbol{k}}\boldsymbol{u}^{\alpha_1}_{\boldsymbol{k}_1}, \boldsymbol{u}^{\alpha_2}_{\boldsymbol{k}_2})|_{\boldsymbol{k}^*} + \mathcal{N}_0(\boldsymbol{u}^{\alpha_1}_{\boldsymbol{k}_1}, \epsilon\boldsymbol{K}_2\cdot\nabla_{\boldsymbol{k}}\boldsymbol{u}^{\alpha_2}_{\boldsymbol{k}_2})|_{\boldsymbol{k}^*} + O(\epsilon^2) \\
&= \mathcal{N}_0(\boldsymbol{u}^{\alpha_1}_{\boldsymbol{k}_1}, \boldsymbol{u}^{\alpha_2}_{\boldsymbol{k}_2}) + \epsilon\mathcal{N}_1(\boldsymbol{u}^{\alpha_1}_{\boldsymbol{k}^*_1}, \boldsymbol{u}^{\alpha_2}_{\boldsymbol{k}^*_2}) + O(\epsilon^2),
\end{aligned} \tag{7.27}$$

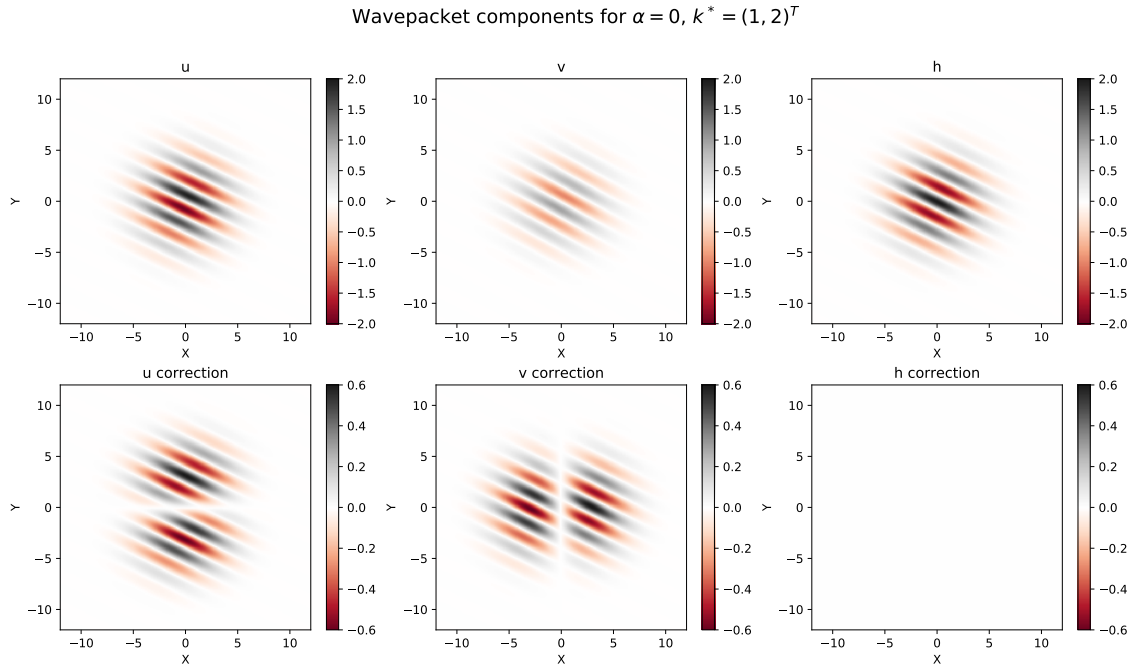

Figure 7.1: The wavepacket, in each field u, v, h for central wavenumber $\boldsymbol{k}^*$ for the case of $\alpha = 0$ in the shallow water equations with $c = 0.5$, $f = 1$ and $\epsilon = 0.35$. In the height field in the right hand frame a Gaussian wavepacket has been chosen, dictating the shape of the wavepackets in the other two fields given in the left hand and centre frames. The second row shows only the order ϵ correction term that adjusts the shape away from a simple Gaussian envelope.

where we used (7.26) to recombine the correction part of the wavepacket in the $\mathcal{N}_0$ terms. We can see that the two parts of equation (7.25) are split between the $\mathcal{N}_0$ and $\mathcal{N}_1$ terms. In a similar manner this would continue at each order with small terms re-accounted for at the next order of expansion. The key point is that the $\mathcal{N}_0$ term has the form:

$$\mathcal{N}_0(\boldsymbol{u}_{\boldsymbol{k}_1}^{\alpha_1}, \boldsymbol{u}_{\boldsymbol{k}_2}^{\alpha_2}) = \mathcal{N}_0(\boldsymbol{u}_{\boldsymbol{k}_1^*}^{\alpha_1}, \boldsymbol{u}_{\boldsymbol{k}_2^*}^{\alpha_2}) + \mathcal{N}_0(\epsilon \boldsymbol{K}_1 \cdot \nabla_{\boldsymbol{k}} \boldsymbol{u}_{\boldsymbol{k}_1}^{\alpha_1}, \boldsymbol{u}_{\boldsymbol{k}_2}^{\alpha_2})|_{\boldsymbol{k}^*} + \mathcal{N}_0(\boldsymbol{u}_{\boldsymbol{k}_1}^{\alpha_1}, \epsilon \boldsymbol{K}_2 \cdot \nabla_{\boldsymbol{k}} \boldsymbol{u}_{\boldsymbol{k}_2}^{\alpha_2})|_{\boldsymbol{k}^*} + \dots . \tag{7.28}$$

The left hand term on the right hand side is identical to the nonlinear term used in the previous chapters, but the right hand terms represent a small adjustment to this due to the correction to the wavepacket envelope in each field. This suggests that with caution the same interaction coefficients as previously (found in sections 4.2.1, 4.30, and 4.5.1) may be used, on the understanding that they are accurate to $O(\epsilon)$. This needs particular caution where the interaction coefficient is expected to be 0, as is the case for $(\pm, \pm; 0)$ triads in the layered equations for example (see section **??**). In this case, in (7.25) each term is individually 0 in the expansion. This leads to the equality:

$$\epsilon(\boldsymbol{K}_i \cdot \nabla_{\boldsymbol{k}_i} \mathcal{N})(\boldsymbol{u}_{\boldsymbol{k}_1}^{\alpha_1}, \boldsymbol{u}_{\boldsymbol{k}_2}^{\alpha_2})|_{\boldsymbol{k}^*} + \mathcal{N}_0(\epsilon \boldsymbol{K}_1 \cdot \nabla_{\boldsymbol{k}} \boldsymbol{u}_{\boldsymbol{k}_1}^{\alpha_1}, \boldsymbol{u}_{\boldsymbol{k}_2}^{\alpha_2})|_{\boldsymbol{k}^*} + \mathcal{N}_0(\boldsymbol{u}_{\boldsymbol{k}_1}^{\alpha_1}, \epsilon \boldsymbol{K}_2 \cdot \nabla_{\boldsymbol{k}} \boldsymbol{u}_{\boldsymbol{k}_2}^{\alpha_2})|_{\boldsymbol{k}^*} = 0, \tag{7.29}$$

and hence:

$$\mathcal{N}_0(\boldsymbol{u}_{\boldsymbol{k}_1}^{\alpha_1}, \boldsymbol{u}_{\boldsymbol{k}_2}^{\alpha_2}) = -\epsilon\mathcal{N}_1(\boldsymbol{u}_{\boldsymbol{k}_1^*}^{\alpha_1}, \boldsymbol{u}_{\boldsymbol{k}_2^*}^{\alpha_2}). \tag{7.30}$$

This will continue at all orders. In effect, spurious terms will appear in the expansion due to the truncation, allowing what should be a non-interaction to appear as a small error term. With this in mind one can rule out the interaction $\{\mathcal{N}_1(\{\boldsymbol{u}\}_{\boldsymbol{k}_1}^{\pm}, \{\boldsymbol{u}\}_{\boldsymbol{k}_2}^{\pm})\}_{\boldsymbol{k}}^0$ that could otherwise appear in the analysis of layered equations at timescale t_1.

7.3 Restrictions on wavepacket interactions between multiple packets

We now rework the analysis of chapters 3 and 5 to include slow spatial variation. The first new term, $\mathcal{L}_1\boldsymbol{u}_0$, appears at the removal of secular terms stage (equivalent to equation (3.14)), and so we will jump in here. Removing secular terms from the right hand side of (7.16):

$$\left\{\frac{\partial\bar{\boldsymbol{u}}}{\partial t_0} + \mathcal{L}_1\bar{\boldsymbol{u}}\right\}_{\boldsymbol{k}}^{\alpha} = -\lim_{\tau\to\infty}\frac{1}{\tau}\int_0^{\tau} e^{s\mathcal{L}_0}\mathcal{N}_0(e^{-s\mathcal{L}_0}\bar{\boldsymbol{u}}(\boldsymbol{x}_0, t_0), e^{-s\mathcal{L}_0}\bar{\boldsymbol{u}}(\boldsymbol{x}_0, t_0))ds. \tag{7.31}$$

We should here be clearer about what the limit of τ is doing. The right hand side forms an average over the fast oscillations that will affect the t_0 timescale. This can be expressed as $\sim \tau/\epsilon$ and so the limit we are interested in at this order is $\tau \to 1/\epsilon$. On this timescale we can assume that t_0 is not varying. We need to consider the coincidence time of the wavepackets: if they don't overlap for sufficient time for significant energy exchange to occur, the interaction would not appear as a secular term.

The basic premise is that the width of a wavepacket scales like $x_0 \sim 1/\epsilon$, the amplitude of each mode like ϵ and so for a significant interaction to take place the difference in group velocities $|\boldsymbol{c}_{g1} - \boldsymbol{c}_{g2}|$ cannot be more than $a_1 a_2 x_0 t_n/at \sim t_n/t$ for the timescale $t_n \sim \epsilon^n t$. This is not a problem for triad interactions on the t_0 timescale: in these cases the difference in group velocities can be $O(1)$ and the interaction will be significant whilst the wavepackets coincide. However for quartet interactions on the timescale t_1 the difference between all input group velocities is restricted to $O(\epsilon)$. If $|\boldsymbol{c}_{g1} - \boldsymbol{c}_{g2}| \sim O(1)$ the component triad interactions producing slaved modes will only output modes of order ϵ^2, belonging to $\boldsymbol{u}_2$ and demoting the quartet interaction to slower than the t_1 timescale. This constraint is accentuated in more than one dimension: if the wavepackets move perpendicularly the only way in which they can interact on the t_1 timescale is if they have group velocities $c_g \sim O(\epsilon)$. We will first consider triad interactions.

For simplicity we show this for a simple case: two wavepackets that do not form a triad resonance, that are initialised both at $x_0 = 0$ with wavepackets with shape $a(\boldsymbol{x}_0) = e^{-|\boldsymbol{x}_0|^2/2} + O(\epsilon)$. The equations of the two wavepacket amplitudes on the t_0 timescale are given by:

$$\frac{\partial a_1}{\partial t_0} + (\boldsymbol{c}_{g1} \cdot \nabla) a_1 \;\Rightarrow\; a_1 = a_1(\boldsymbol{x}_0 - \boldsymbol{c}_{g1} t_0) = a(\boldsymbol{x}_0 - \boldsymbol{c}_{g1} t_0), \tag{7.32}$$

$$\frac{\partial a_2}{\partial t_0} + (\boldsymbol{c}_{g2} \cdot \nabla) a_2 \;\Rightarrow\; a_2 = a_2(\boldsymbol{x}_0 - \boldsymbol{c}_{g2} t_0) = a(\boldsymbol{x}_0 - \boldsymbol{c}_{g2} t_0). \tag{7.33}$$

The amplitude of the nonlinear term in equation (7.31) is then $a_1 a_2$. Changing the coordinates to centre around a_1 we write:

$$a(0) a((\boldsymbol{c}_{g2} - \boldsymbol{c}_{g1}) t_0), \tag{7.34}$$

and then given a maximum $|\boldsymbol{x}_0| \sim 1/\epsilon$ value, at which the amplitude is $O(1)$ we can write the time over which the packets can interact as:

$$t = \frac{|\boldsymbol{x}_0|}{|\boldsymbol{c}_{g2} - \boldsymbol{c}_{g1}|}, \tag{7.35}$$

here we have dropped the scaling on time, the size of the right hand side will determine the timescale over which the interaction occurs, so $O(1)$ implies the t_0 timescale etc. As the scale of $|\boldsymbol{x}_0|$ is fixed, this is effectively governed by the size of $1/|\boldsymbol{c}_{g2} - \boldsymbol{c}_{g1}|$. In general we assume that this cannot take values larger than $O(1)$. For this reason we will not need to consider the coincidence of wavepackets at this timescale, however it will become important later, in the quartet order interactions.

Because the wavepackets don't separate on this timescale we can perform the integration in (7.31) as in the previous chapters to find that our resonance condition is $\Omega \sim \epsilon$. At this order the only difference is the introduction of the group velocity term.

However the $\boldsymbol{u}_1$ terms need to be considered in what is a fundamentally different manner to the periodic case. We need to solve the remainder of equation (7.16) after removing the resonant terms, as was done previously in equation (3.20):

$$\begin{aligned} &\frac{\partial \boldsymbol{u}_1}{\partial \tau} + \mathcal{L}_0 \boldsymbol{u}_1 = -\mathcal{N}_0(\boldsymbol{u}_0, \boldsymbol{u}_0)|_{nr}, \\ &\Rightarrow \boldsymbol{u}_1 = e^{-\tau \mathcal{L}_0} \int_0^\tau -e^{s\mathcal{L}_0} \mathcal{N}_0(e^{-s\mathcal{L}_0} \bar{\boldsymbol{u}}_0(\boldsymbol{x}_0, t_0), e^{-s\mathcal{L}_0} \bar{\boldsymbol{u}}_0(\boldsymbol{x}_0, t_0))|_{nr}\, ds. \end{aligned} \tag{7.36}$$

This has the same result as before, except that now the nonlinear term is only non-zero whilst the two parts of the input $\boldsymbol{u}_0$ modes coincide in the spatial direction. The wavepacket will propagate at the weighted average of the two inputs: $\boldsymbol{c}_{ga} = (\sigma_2^2 \boldsymbol{c}_{g1} + \sigma_1^2 \boldsymbol{c}_{g2})/(\sigma_1^2 + \sigma_2^2)$ where σ is the wavepacket

width. This means that $\boldsymbol{u}_1$ modes cannot be generated and then propagated away from the area of interaction. When these then participate in a quartet interaction, all three input modes must therefore be coincident for a length of time of the order of t_1. This will then impose restrictions on the possible group velocities of the components of the interaction.

We now want to calculate the t_1 variation. We take equation (7.17) and perform the same machinations as we did in chapter 3 and 5 to remove secular terms. This leads to the wavepacket version of equation (3.24):

$$\begin{aligned}\lim_{\tau\to 1/\epsilon^2}\frac{1}{\tau}\int_0^\tau & e^{s(\mathcal{L}_0-\mathcal{L}_0')}\frac{\partial\bar{\boldsymbol{u}}_1}{\partial t_0}+\frac{\partial\bar{\boldsymbol{u}}_0}{\partial t_1}\\ &+e^{s(\mathcal{L}_0-\mathcal{L}_0')}\mathcal{L}_1\bar{\boldsymbol{u}}_1+\mathcal{L}_2\bar{\boldsymbol{u}}_0+e^{s\mathcal{L}_0}\Big(\mathcal{N}_0(e^{-s\mathcal{L}_0}\bar{\boldsymbol{u}}_0,e^{-s\mathcal{L}'{}_0}\bar{\boldsymbol{u}}_1)\\ &+\mathcal{N}_0(e^{-s\mathcal{L}'{}_0}\bar{\boldsymbol{u}}_1,e^{-s\mathcal{L}_0}\bar{\boldsymbol{u}}_0)+\mathcal{N}_1(e^{-s\mathcal{L}_0}\bar{\boldsymbol{u}}_0,e^{-s\mathcal{L}_0}\bar{\boldsymbol{u}}_0)\Big)ds=0.\end{aligned} \tag{7.37}$$

Similarly to the previous chapters, we find that for large $\tau\sim t_1\sim O(1/\epsilon^2)$ the first and third terms containing $\boldsymbol{u}_1$ must disappear from the integral as they are by definition non-resonant. In addition if the underlying modes of the $\boldsymbol{u}_1$ term are only coincident on the t_0 timescale the integral will be $O(1)$ but the division by τ will make this 0 in the limit. The second and fourth terms have no τ dependence and so they are maintained after averaging. We now consider the $\mathcal{N}_0$ terms:

$$\lim_{\tau\to 1/\epsilon^2}\frac{1}{\tau}\int_0^\tau e^{s\mathcal{L}_0}\mathcal{N}_0(e^{-s\mathcal{L}_0}\bar{\boldsymbol{u}}_0(\boldsymbol{x}_0,\epsilon\tau),e^{-s\mathcal{L}'{}_0}\bar{\boldsymbol{u}}_1(\boldsymbol{x}_0,\epsilon\tau))ds. \tag{7.38}$$

We now must take into account the movement of the wavepackets. We will bound the wavepacket envelopes by a square envelope of width 1 (in $\boldsymbol{x}_0$) and height a_i. We consider a resonant quartet of wavepackets so that:

$$\begin{aligned}\lim_{\tau\to 1/\epsilon^2}\frac{1}{\tau}&\left|\int_0^\tau\mathcal{N}_0(\{\bar{\boldsymbol{u}}_0\}_{\boldsymbol{k}_1}^{\alpha_1},\{\bar{\boldsymbol{u}}_1\}_{\boldsymbol{k}_a}^{\alpha_a})+\textit{permutations}\,ds\right|\\ &<\lim_{\tau\to 1/\epsilon^2}\frac{1}{\tau}\left|\int_{\tau_{init}}^{\tau_{init}+\epsilon/|\boldsymbol{c}_{ga}-\boldsymbol{c}_{g1}|}\boldsymbol{r}_{\boldsymbol{k}}^{\alpha}Q_{\boldsymbol{k}_1\boldsymbol{k}_2\boldsymbol{k}_3\boldsymbol{k}}^{\alpha_1\alpha_2\alpha_3\alpha}a_{\boldsymbol{k}_1}^{\alpha_1}a_{\boldsymbol{k}_2}^{\alpha_2}a_{\boldsymbol{k}_3}^{\alpha_3}+\textit{permutations}\,ds\right|\\ &=\left|\frac{\epsilon}{|\boldsymbol{c}_{ga}-\boldsymbol{c}_{g1}|}\boldsymbol{r}_{\boldsymbol{k}}^{\alpha}Q_{\boldsymbol{k}_1\boldsymbol{k}_2\boldsymbol{k}_3\boldsymbol{k}}^{\alpha_1\alpha_2\alpha_3\alpha}a_{\boldsymbol{k}_1}^{\alpha_1}a_{\boldsymbol{k}_2}^{\alpha_2}a_{\boldsymbol{k}_3}^{\alpha_3}\right|,\end{aligned} \tag{7.39}$$

where Q is given by (3.32), the quartet interaction coefficient, and t_{init} is the time at the onset of coincidence. For an $O(1)$ contribution all three group velocities must be separated by an $O(\epsilon)$ amount, so that the input modes are coincident.

In a similar manner the $\mathcal{N}_1$ terms require the two input modes to be coincident on the t_1 timescale. As previously discussed in section 7.2.1, parts of the $\mathcal{N}_1$ term will effectively act to negate the small differences between the wavepacket interactions and the previously calculated

coefficients.

This leaves:

$$\frac{\partial \bar{\boldsymbol{u}}_0}{\partial t_1} + \mathcal{L}_2 \bar{\boldsymbol{u}}_0 + \mathcal{N}_0^{rc}(\bar{\boldsymbol{u}}_0, \bar{\boldsymbol{u}}_1) + \mathcal{N}_0^{rc}(\bar{\boldsymbol{u}}_1, \bar{\boldsymbol{u}}_0) + \mathcal{N}_1^{rc}(\bar{\boldsymbol{u}}_0, \bar{\boldsymbol{u}}_0) = 0, \tag{7.40}$$

where $\mathcal{N}^{rc}$ are the resonant parts of the nonlinearity where the modes are coincident for t_1 time. The remainder of the terms will then become the 'forcing' on the $\boldsymbol{u}_2$ equation:

$$\frac{\partial \boldsymbol{u}_2}{\partial \tau} + \mathcal{L}_0 \boldsymbol{u}_2 = -\left(\frac{\partial \boldsymbol{u}_1}{\partial t_0} + \mathcal{L}_1 \boldsymbol{u}_1 + \mathcal{N}_0^{nrc}(\boldsymbol{u}_0, \boldsymbol{u}_1) + \mathcal{N}_0^{nrc}(\boldsymbol{u}_1, \boldsymbol{u}_0) + \mathcal{N}_1^{nrc}(\boldsymbol{u}_0, \boldsymbol{u}_0) \right), \tag{7.41}$$

and so the non-coincident, and/or non-resonant triads will affect only the smaller scale $\boldsymbol{u}_2$ part of the expansion.

However for the quartets formed of near resonant triads, as shown in chapter 5, the interaction is promoted to the faster t_0 timescale, and so these can occur between group velocities separated by $O(1)$ amounts. In the following we are considering only n-tets formed of non-near resonant $\boldsymbol{u}_1$ modes, for each possibility of mode type combinations. We also assume that the initial conditions are such that either the wavepackets are initially coincident or will cross each other during the time considered.

7.3.1 Slow mode input interactions

The simple case of n-tets involving only slow mode inputs has the simple property that all of the component triads have zero group velocity and so provided that they are initially coincident they are able to continuously interact to produce higher order slow mode interactions and higher order spontaneous fast wave emission interactions $(0, ..., 0; \pm)$. In these cases the slow only interactions will always be exactly resonant, whilst the fast wave emission interactions will never resonate. This suggests that slow mode interactions will appear in the expansion while spontaneous emission will only occur on slower timescales.

7.3.2 Mixed mode input interactions

For mixed modes with the usual quasigeostrophic assumptions all fast modes will have greater than $O(\epsilon)$ group velocity and will therefore never coincide with fast modes for sufficient time to cause an interaction. In this case, despite the possibility of resonant interactions, they would be severely limited in a wavepacket expansion due to the amount of time for which the wavepackets

interact, they would therefore not appear in an expansion in the continuous domain.

However for different scaling assumptions it could be possible for the group velocity of certain fast modes to be of $O(\epsilon)$, allowing for interactions, notably for those very close to $\boldsymbol{k} = 0$.

7.3.3 Fast mode input interactions

For the fast mode input interactions the condition will be $\boldsymbol{c}_{g1} \sim \boldsymbol{c}_{g2} \sim \boldsymbol{c}_{g3}$. which in many circumstances can be severely limiting to the possible quartet interactions: generally the possibility of interaction only occurs for wavenumbers ϵ close to one another, which can therefore only be considered to belong to the same wavepacket. This just allows for the appearance of modulational instability, although in more than the original 1 dimension.

However depending on the form of the group velocity function in the vicinity of the wavenumbers considered it may be possible to consider interactions with a greater separation. Writing the Taylor expansion of the group velocity:

$$\begin{aligned} &\boldsymbol{c}_g(\boldsymbol{k} + \delta\boldsymbol{k}) \approx \boldsymbol{c}_g(\boldsymbol{k}) + \delta\boldsymbol{k} \cdot \nabla \boldsymbol{c}_g(\boldsymbol{k}) + ... \\ \Rightarrow \qquad &\boldsymbol{c}_g(\boldsymbol{k} + \delta\boldsymbol{k}) - \boldsymbol{c}_g(\boldsymbol{k}) \approx \delta\boldsymbol{k} \cdot \nabla \boldsymbol{c}_g(\boldsymbol{k}). \end{aligned} \tag{7.42}$$

For an $O(\epsilon)$ difference between the group velocities but with $\delta\boldsymbol{k} \sim O(1)$ we require $\nabla \boldsymbol{c}_g(\boldsymbol{k}) \sim O(\epsilon)$.

In this case it is possible to have larger differences between the input wave modes. In general this occurs for large values of $|\boldsymbol{k}|$, close to the non-dispersive limit. These wavepackets also maintain coherency for a longer time (longer than the timescale of the quartet interaction) as the linear spreading term $\nabla^T_{\boldsymbol{x}_0} Q \nabla_{\boldsymbol{x}_0}$ will be small.

These resonances might be expected to appear in an expansion. It should also be noted that the 1 dimensional case is in fact integrable (Kaup, Reiman, and Bers 1979), whereas this is not true in more dimensions.

7.3.4 A special case

We now analyse a special case of the fast input interactions. We consider the case where $\Omega \sim \sqrt{\epsilon}$. This will not be resonant as it does not meet the resonance criterion $\Omega \sim \epsilon$, and so it will form a

slaved mode. From (3.22):

$$\{\boldsymbol{u}_1\}^{\alpha_a}_{\boldsymbol{k}_a} = \sum_{\substack{\boldsymbol{k}_1,\boldsymbol{k}_2\\ \alpha_1,\alpha_2}} \frac{C^{\alpha_1\alpha_2\alpha_a}_{\boldsymbol{k}_1\boldsymbol{k}_2\boldsymbol{k}_a}\big|_{nr}\, a^{\alpha_1}_{\boldsymbol{k}_1} a^{\alpha_2}_{\boldsymbol{k}_2}}{i\Omega_{12a}} \boldsymbol{r}^{\alpha_a}_{\boldsymbol{k}_a} e^{-i(\omega_1+\omega_2)\tau}\, \delta_{\boldsymbol{k}_a-\boldsymbol{k}_1-\boldsymbol{k}_2} \sim \frac{1}{\sqrt{\epsilon}}.$$

Then when this mode goes on to form a quartet, as in (7.38) above, we can alter the scaling of (7.39) to get:

$$\frac{\sqrt{\epsilon}}{|\boldsymbol{c}_{ga}-\boldsymbol{c}_{g1}|} \boldsymbol{r}^{\alpha}_{\boldsymbol{k}} Q^{\alpha_1\alpha_2\alpha_3\alpha}_{\boldsymbol{k}_1\boldsymbol{k}_2\boldsymbol{k}_3\boldsymbol{k}} a^{\alpha_1}_{\boldsymbol{k}_1} a^{\alpha_2}_{\boldsymbol{k}_2} a^{\alpha_3}_{\boldsymbol{k}_3}.$$

This reduces the restriction on the group velocity difference to:

$$|\boldsymbol{c}_{ga}-\boldsymbol{c}_{g1}| \sim \sqrt{\epsilon}. \tag{7.43}$$

In these special conditions the non-resonant, non-coincident wavepackets are able to form a quartet resonance that evolves on the t_1 timescale.

Further there is a specific situation in which the detuning and the group velocities are both small: when a near resonance occurs that is not close to an exact resonance. In this case we have:

$$\min(\omega-\omega_1-\omega_2) \sim \epsilon \neq 0, \tag{7.44}$$

and so, given that each branch of the dispersion relation is continuous, the closest approach is given by the stationary point of Ω. We fix the output wavenumber ($\boldsymbol{k}=\boldsymbol{k}_1+\boldsymbol{k}_2$) such that by chain rule:

$$\frac{\partial}{\partial \boldsymbol{k}_1} = -\frac{\partial}{\partial \boldsymbol{k}_2}, \tag{7.45}$$

and then:

$$\frac{\partial \Omega}{\partial \boldsymbol{k}_1} = \boldsymbol{c}_{g2}-\boldsymbol{c}_{g1}. \tag{7.46}$$

It follows that at the closest approach where $\Omega \sim \epsilon$, the group velocities are identical. On the assumption that group velocities are $O(1)$ we find that $\Omega \sim \sqrt{\epsilon}$ then implies that $|\boldsymbol{c}_{g2}-\boldsymbol{c}_{g1}| \sim \sqrt{\epsilon}$. This will always occur for triads corresponding to self interaction of a wavepacket.

7.4 Applications

Some effects of these interaction limitations will now be discussed in the context of the geophysical examples we have considered throughout.

7.4.1 Shallow water equations

Here we compare our conclusions for wavepacket interactions to the work in Reznik, Zeitlin, and Ben Jelloul 2001 on the shallow water equations where it was found in the case of compact initial conditions that slow-slow-slow-slow interactions were the only permissible ones affecting the slow mode.

By the theory of section 7.3 the only possible quartet interactions would be subsets of the $(0,0,0;0)$, $(0,0,0;\pm)$, $(\pm,\pm,\pm;0)$ and $(\pm,\pm,\pm;\pm)$ interactions. In the case of exact resonances the $(0,0,0;\pm)$ interaction is easily ruled out. We can then use the theory of chapter 3 to ignore the $(\pm,\pm,\pm;0)$ interaction, as only fast wave inputs cannot cause a slow mode output.

The remaining (fast-only and slow-only) interactions are all that were found to exist in Reznik, Zeitlin, and Ben Jelloul 2001. The main difference to the case with a doubly-periodic domain is the $(0,\pm,\pm;0)$ that is removed by the inability of the quartet interaction to take place before the slow and fast wavepackets have propagated apart.

The effect of near resonant interactions changes these conclusions. Because the near resonant triads interact on a timescale for which the group velocity differences can be $O(1)$, any quartet that can be formed by a combination of near resonant $(\pm,0;\pm)$ and $(\pm,\pm;\pm)$ triads will be present in the expansion. This includes $(0,\pm,\pm;\pm)$, $(0,0,\pm;\pm)$, and $(\pm,\pm,\pm;\pm)$ quartets. However it is still not possible to affect the slow part.

7.4.2 Two layer rotating shallow water equations

Many of the results for the two layer case follow exactly as for the one layer. However we now evaluate the new resonance between sets of fast modes from section 4.3.2, in the context of wavepackets. The resonance in fig 4.1d can now exactly fit the criteria described in section 7.3.4, allowing the relaxing of the resonance and coincidence conditions for the quartet resonances to appear so that interactions may occur when $|\boldsymbol{c}_{ga}-\boldsymbol{c}_1| \sim \sqrt{\epsilon}$ and $\Omega \sim \sqrt{\epsilon}$. This allows this particular interaction to be one of the component triads in a dominant t_1 order energy exchange.

7.4.3 Stratified equations

In the stratified equations the situation is somewhat similar to the layered equations. Although the near resonant $(\pm, \pm; 0)$ interaction exists, it does not act fast enough that the group velocities can be markedly different to one another.

However the fact that these interactions are non-zero does allow the $(\pm, \pm, \pm; 0)$ quartets to occur, even in the non-periodic case. This means that a combination of wavepackets at larger wavenumbers should be able to interact to spontaneously produce a zero mode, on a quartet timescale. The relevant interaction coefficient is the following:

$$Q^{\pm\,\pm\,\pm\,0}_{\boldsymbol{k}_1\boldsymbol{k}_2\boldsymbol{k}_3\boldsymbol{k}} = \frac{2}{3}\left[\frac{C^{\pm\pm\,0}_{\boldsymbol{k}_a\boldsymbol{k}_3\boldsymbol{k}}\, C^{\pm\,\pm\,\pm}_{\boldsymbol{k}_1\boldsymbol{k}_2\boldsymbol{k}_a}\big|_{nr}}{i(\omega_a - \omega_1 - \omega_2)} + \frac{C^{\pm\pm\,0}_{\boldsymbol{k}_b\boldsymbol{k}_1\boldsymbol{k}}\, C^{\pm\,\pm\,\pm}_{\boldsymbol{k}_2\boldsymbol{k}_3\boldsymbol{k}_b}\big|_{nr}}{i(\omega_b - \omega_2 - \omega_3)} + \frac{C^{\pm\pm\,0}_{\boldsymbol{k}_c\boldsymbol{k}_2\boldsymbol{k}}\, C^{\pm\,\pm\,\pm}_{\boldsymbol{k}_3\boldsymbol{k}_1\boldsymbol{k}_c}\big|_{nr}}{i(\omega_c - \omega_3 - \omega_1)}\right].$$

7.5 Chapter summary

In this chapter:

- Wavepackets were incorporated into the multiple scale theory.
- The restriction of wavepacket shape for systems of equations was discussed.
- The conditions in which wavepackets are concurrent for sufficient time to interact on a quartet order were discussed. It was found that in the wavepacket context near resonances have a substantial effect on the behaviour of a system, allowing interactions to take place that would otherwise not appear until a much higher order of the expansion.
- A special case was discussed that allows the quartet order interaction to occur on timescale t_1 with the weaker pair of conditions $|\boldsymbol{c}_{ga} - \boldsymbol{c}_1| \sim \sqrt{\epsilon}$ and $\Omega \sim \sqrt{\epsilon}$

Chapter 8

Conclusions

8.1 Summary

In this thesis we formulated a general framework for calculating higher order exact resonant expansions (chapter 3), including the general form of the interaction coefficient for all orders given in (3.34). In chapter 4, we then formed particular conclusions for the application of this to fast-slow systems, which occur frequently in atmospheric and oceanic contexts. This allowed the reappraisal of several papers in the literature concerned with the rotating shallow water equations (eg Thomas 2016, Reznik, Zeitlin, and Ben Jelloul 2001). We saw that the higher order effects of these papers can be considered more generally to belong to any layered equation and, more generally still, any equation with a pointwise conserved potential vorticity of the form:

$$q = \frac{\boldsymbol{\zeta}' + \boldsymbol{f}}{H + \eta'},$$

where variables marked with a ‘ are $O(\epsilon)$ to leading order and f is constant.

For the more general form of Ertel PV:

$$q = (\boldsymbol{\zeta}' + \boldsymbol{f}) \cdot \nabla\theta,$$

we have shown that in the weakly nonlinear approximation the fast-slow interactions are still limited to no higher than the quartet order timescale t_1. However this is still an interesting fundamental difference between the layered and stratified equations: above triad order the n-layer equations would not approximate the nonlinear part of the stratified equations, regardless of how large a value of n one might choose.

The particular case of the two-layer rotating shallow water equations (work originally published in Owen, Grimshaw, and Wingate 2018) contained newly derived resonant triad interactions that allow the exchange of energy between gravity waves in different vertical modes: the barotropic and baroclinic parts. We investigated this thoroughly, including the unusual feature of a set of resonances that can exist in some parameter ranges but not others, and in many cases are highly directional in nature. We found that in a discretisation of the system this resonance could be entirely absent, prompting the need to consider near resonant interactions.

In both the two layer shallow water and stratified equations we derived the interaction coefficients in full (for the first time to the best of the author's knowledge). This allowed detailed examination of possible interactions.

We then extended the theory (chapter 5) in a general manner to include the near resonant interactions. We have shown that near resonant interactions are a simple method for picking out all of the higher order interactions that happen fast enough that they can skip to the faster t_0 timescale in the expansion. Where the n-tets of the interactions are formed entirely of near resonant triads their dynamics will be on the t_0 triad timescale, regardless of the order they would have occurred at in the exact resonant expansion. Here we have also shown that for layered type equations the fast-fast-slow interactions cannot occur at all, and for the more general form of Ertel PV found in other equations we have shown that they can never occur significantly at the faster time due to the small size of the interaction coefficient. From this and the earlier theory on triad combinations we can conclude that the non-near resonance of the slow-slow-fast triads is single-handedly responsible for the strength of the fast-slow splitting of any zero-mode system. Other than the scattering fast-slow-fast resonance of eg Ward and Dewar 2010, there can be no fast-slow interaction that generates slow modes until quartet order (t_1 time) interactions, and we have now shown that this is true in the more general near resonant expansion, for any system with potential vorticity conservation in an f-plane.

We analysed a numerical simulation of the rotating shallow water equations in terms of the possible near and exact resonances, and we found that the near resonant theory was a much more accurate description of the system's behaviour. This included near resonances that exist in regions that do not contain exact resonances, demonstrating clearly that near resonant theory cannot be understood as an approximation of exact resonances: the near resonances are important in their own right. This is a point that is easily lost on the reader in the existing literature, where terminology such as detuning suggest an adjustment to an exact resonance.

In chapter 7 we extended the theory further to include multiple spatial scales and the assumption of wavepackets. We then showed that consideration of the interaction times was sufficient to

explain the difference between the periodic and continuous results found in Thomas 2016, and Reznik, Zeitlin, and Ben Jelloul 2001. Further, we have shown that for the more general near resonant case extra interactions may be allowed that would be prevented by the exact theory for wavepackets. This theory was also formulated in a manner that makes it applicable to wavepacket interactions in multiple dimensions, something that is less commonly found in the literature and can be seen in the near resonant context to require more consideration. We also found a special case where the resonance and coincidence conditions were weaker, and made an argument that this is an important consideration where near resonances exist that are not in the vicinity of an exact resonance.

To summarise, the theory of this thesis is a method of multiscale expansion that allows the simultaneous usage of effects from conservation laws and the usual timescale analysis to determine some very general properties of flow timescales. The extension to near resonances increases the applicability of the theory to a greater range of ϵ values. The extension to wavepacket theory shows that the near resonances can fundamentally change the behaviour that would be predicted when one expands using the exact resonances.

8.2 Discussion and Future work

Some possible limitations of the work were highlighted through the thesis. One of the most major of these was the implications for using a range of wavenumbers such that the ratio of smallest to largest is comparable to ϵ. In this case the interaction coefficient, which scales like $U^2|\boldsymbol{k}|$ could become sufficiently large as to disrupt the asymptotic ordering, rendering the expansion invalid. This can be considered equivalent to taking the non-dispersive limit of the equations, and would result in qualitatively different behaviour.

We have everywhere been implicitly assuming that no shocks will form. However in hyperbolic equations dissipative effects have been ignored. Whilst neglecting viscosity is a useful assumption, in order to be able to use results from conservative systems, it is not particularly realistic. As dissipative effects (including wave breaking) are considered to be one of the major ways in which the gravity waves can act on the balanced flow, inclusion may significantly affect the theory. For discussion of the applicability of higher order asymptotic expansions in shallow water one may refer to Bühler 2000. The implications of wave breaking and dissipation on the near resonant expansion could be the subject of future work.

Two of the major underlying assumptions of all the work presented here were that the system does not consider internal energy/entropy, and the rotating frame obeys the f-plane assumption.

This led to the exact pointwise conservation of potential vorticity and to the quadratic nature of the nonlinearity. However, if both of these assumptions are slackened slightly, the resulting range of systems includes many more common geophysical fluid models, those on a sphere or on a beta-plane, and those which allow for temperature/salinity variation and compressibility. Relaxation of the f-plane assumption might allow analysis of a linear PV of the form found in the f-plane but only conserved up to $O(\epsilon)$. For compressible systems we might expect an order $2+\epsilon$ nonlinearity. In both cases, an $O(\epsilon)$ adjustment to the theory we have discussed in the thesis. It may therefore be possible to extend the theory of this thesis to a more general class of systems. The exact algebra may be significantly more complicated, particularly where Fourier transforms would not be valid and more complicated basis functions are needed, but exploiting the asymptotic similarity with the work here may make it a tractable problem.

Of particular interest would be if the conclusions on the interactions between fast and slow modes remained relatively similar, such that zero modes become 'ϵ modes', and fast-fast-slow interactions are still at least approximately inaccessible. It seems likely that this may be true in the extension to the beta-plane. At mid latitudes this would give an ϵ-order adjustment to the propagation speed of the slow modes. This same approximation is used in Bühler and McIntyre 1998 to consider beta-plane effects at a later order of interaction than the first order part of the rotation.

The conclusion that strong fast-slow splitting derives from the non-near resonance of the slow-slow-fast triads could then be challenged by any fast terms with small ω interacting with the largest of the ϵ modes. This could theoretically provide a pathway by which to evaluate the specific situations in which quasigeostrophy is least applicable, and hence conversion of energy between slow and fast waves is strongest. This could be invaluable in considerations of the ocean's energy budget for instance, where it is thought that energy is dissipated by the large wavenumber gravity waves, as well as work on parametrising gravity waves in numerical simulations.

To conclude, this thesis has explored the weakly nonlinear limit of a common class of fluid equations: those with quadratic linearity and a conserved potential vorticity. The resonant analysis finds its use in a wide range of geophysical fluid systems and has been extended here to high order, near resonance and to multidimensional wavepackets, exploring the effects that might occur due to the interactions of fast and slow parts of the flow. This analysis could form the building blocks for analysis of the more detailed systems that occur in atmospheric and oceanic study.

Appendix A

Appendix

A.1 Big and Little O notation

Big-o and little-o notation are defined (in the specific limit for small ϵ) as:

$$f(\epsilon) = O(g(\epsilon)) \qquad \text{iff} \qquad \left|\lim_{\epsilon\to 0} \frac{f(\epsilon)}{g(\epsilon)}\right| \leq A, \qquad \text{where } A \text{ is a finite constant,} \tag{A.1}$$

$$f(\epsilon) = o(g(\epsilon)) \qquad \text{iff} \qquad \lim_{\epsilon\to 0} \frac{f(\epsilon)}{g(\epsilon)} = 0. \tag{A.2}$$

In words $O(\epsilon)$ refers to something that has variation of maximum size $\sim \epsilon$ and $o(\epsilon)$ means anything with variation of maximum size smaller than ϵ.

A.2 Matrix Exponential

In this thesis the matrix exponential is used to reduce the notation and so a brief description is included here.

The matrix exponential is defined similarly to the scalar exponential function as follows:

$$e^{\boldsymbol{A}} = \boldsymbol{I} + \boldsymbol{A} + \frac{1}{2}\boldsymbol{A}^2 + \dots . \tag{A.3}$$

There is much theory on the matrix exponential, particularly on its efficient computation, for example in Moler and Van Loan 2003. However thanks to the conservative systems we intend to consider we will find that we will always be able to diagonalise (i.e. put into its eigenbasis) the

matrix that we wish to exponentiate:

$$\boldsymbol{D} = \boldsymbol{T}^{-1}\boldsymbol{A}\boldsymbol{T}. \tag{A.4}$$

Where $\boldsymbol{T}$ is the transform matrix to the space in which the matrix is diagonal.

We note that:

$$\begin{aligned}\boldsymbol{D}^n &= \boldsymbol{T}^{-1}\boldsymbol{A}\boldsymbol{T}\boldsymbol{T}^{-1}\boldsymbol{A}\boldsymbol{T}...\boldsymbol{T}^{-1}\boldsymbol{A}\boldsymbol{T}, \\ &= \boldsymbol{T}^{-1}\boldsymbol{A}^n\boldsymbol{T},\end{aligned} \tag{A.5}$$

and hence:

$$\boldsymbol{T}^{-1}e^{\boldsymbol{A}}\boldsymbol{T} = \boldsymbol{I} + \boldsymbol{D} + \frac{1}{2}\boldsymbol{D}^2 + ... = e^{\boldsymbol{D}}. \tag{A.6}$$

We then use that $\{\boldsymbol{D}^n\}_{ii} = \{\boldsymbol{D}_{ii}\}^n$ for a diagonal matrix. From this it follows that:

$$\{e^{\boldsymbol{D}}\}_{ii} = e^{\boldsymbol{D}_{ii}}, \tag{A.7}$$

and what we effectively have is element by element exponentiation.

Physically we have a linear system of $rank(\boldsymbol{D})$ equations that are all decoupled and are therefore soluble separately. The power of the matrix exponential in our case is in fact just notational as it allows us to write any of the different linear equations from our system in the same manner.

In the thesis the elements D_{ii} are $i\omega_i\tau$ where ω_i is the frequency from the ith branch of the dispersion relation.

Bibliography

Ablowitz, MJ (2011). *Nonlinear dispersive waves: asymptotic analysis and solitons*. Vol. 47. Cambridge University Press.

Ablowitz, MJ et al. (1974). “The inverse scattering transform-Fourier analysis for nonlinear problems”. In: *Studies in Applied Mathematics* 53.4, pp. 249–315.

Alber, MS et al. (1998). “Geometric phases, reduction and Lie-Poisson structure for the resonant three-wave interaction”. In: *Physica D: Nonlinear Phenomena* 123.1-4, pp. 271–290.

Babin, A, A Mahalov, and B Nicolaenko (1997). “Regularity and integrability of rotating shallow-water equations”. In: *Comptes Rendus de l’Académie des Sciences-Series I-Mathematics* 324.5, pp. 593–598.

Ball, FK (1964). “Energy transfer between external and internal gravity waves”. In: *Journal of Fluid Mechanics* 19.03, pp. 465–478.

Bartello, P (1995). “Geostrophic adjustment and inverse cascades in rotating stratified turbulence”. In: *Journal of the atmospheric sciences* 52.24, pp. 4410–4428.

Benjamin, TB and JE Feir (1967). “The disintegration of wave trains on deep water Part 1. Theory”. In: *Journal of Fluid Mechanics* 27.03, pp. 417–430.

Benney, DJ (1962). “Non-linear gravity wave interactions”. In: *Journal of Fluid Mechanics* 14.4, pp. 577–584.

Benney, DJ and AC Newell (1967). “The propagation of nonlinear wave envelopes”. In: *Journal of mathematics and Physics* 46.1, pp. 133–139.

Benney, DJ and GJ Roskes (1969). “Wave instabilities”. In: *Studies in Applied Mathematics* 48.4, pp. 377–385.

Benney, DJ and PG Saffman (1966). “Nonlinear interactions of random waves in a dispersive medium”. In: *Proc. R. Soc. Lond. A* 289.1418, pp. 301–320.

Boussinesq, J (1877). *Essai sur la théorie des eaux courantes*. Impr. nationale.

Bretherton, FP (1964). “Resonant interactions between waves. The case of discrete oscillations”. In: *Journal of Fluid Mechanics* 20.3, pp. 457–479.

Bühler, O (2000). “On the vorticity transport due to dissipating or breaking waves in shallow-water flow”. In: *Journal of Fluid Mechanics* 407, pp. 235–263.

Bühler, O and ME McIntyre (1998). “On non-dissipative wave–mean interactions in the atmosphere or oceans”. In: *Journal of Fluid Mechanics* 354, pp. 301–343.

Bustamante, MD, B Quinn, and D Lucas (2014). “Robust energy transfer mechanism via precession resonance in nonlinear turbulent wave systems”. In: *Physical review letters* 113.8, p. 084502.

Charney, JG (1948). *On the scale of atmospheric motions*. Cammermeyer in Komm.

Craik, ADD (1988). *Wave interactions and fluid flows*. Cambridge University Press.

— (2004). “The origins of water wave theory”. In: *Annu. Rev. Fluid Mech.* 36, pp. 1–28.

Embid, PF and AJ Majda (1996). “Averaging over fast gravity waves for geophysical flows with arbitary”. In: *Communications in Partial Differential Equations* 21.3-4, pp. 619–658.

Franklin, B, W Brownrigg, et al. (1774). “XLIV. Of the stilling of waves by means of oil. Extracted from sundry letters between Benjamin Franklin, LL. DFRS William Brownrigg, MDFRS and the Reverend Mr. Farish”. In: *Philosophical Transactions* 64, pp. 445–460.

Gardner, CS et al. (1967). “Method for solving the Korteweg-deVries equation”. In: *Physical Review Letters* 19.19, p. 1095.

Gill, AE (1982). *Atmosphere-Ocean dynamics (International Geophysics Series)*. Academic press.

Harper, KL, MD Bustamante, and SV Nazarenko (2013). “Quadratic invariants for discrete clusters of weakly interacting waves”. In: *Journal of Physics A: Mathematical and Theoretical* 46.24, p. 245501.

Hasselmann, K (1962). “On the non-linear energy transfer in a gravity-wave spectrum”. In: *J. Fluid Mech* 12.15, pp. 481–500.

— (1967). “Nonlinear interactions treated by the methods of theoretical physics (with application to the generation of waves by wind)”. In: *Proc. R. Soc. Lond. A* 299.1456, pp. 77–103.

Hasselmann, K and PG Saffman (1967). “Nonlinear Interactions Treated by the Methods of Theoretical Physics (with Application to the Generation of Waves by Wind)”. In: *Proceedings of the Royal Society of London. Series A, Mathematical and Physical Sciences*, pp. 77–103.

Haurwitz, B (1937). “The oscillations of the atmosphere”. In: *Gerlands Beitr. Geophys* 51, pp. 195–233.

— (1940). “The motion of atmospheric disturbances on the spherical earth”. In: *J. mar. Res.* 3, pp. 254–267.

Haut, T and B Wingate (2014). “An asymptotic parallel-in-time method for highly oscillatory PDEs”. In: *SIAM Journal on Scientific Computing* 36.2, A693–A713.

Haut, TS et al. (2015). “A high-order time-parallel scheme for solving wave propagation problems via the direct construction of an approximate time-evolution operator”. In: *IMA Journal of Numerical Analysis* 36.2, pp. 688–716.

Hough, SS (1898). “On the application of harmonic analysis to the dynamical theory of the tides. Part II: On the general integration of Laplace’s dynamical equations”. In: *Philosophical Transactions of the Royal Society of London. Series A, Containing Papers of a Mathematical or Physical Character* 191, pp. 139–185.

Kartashova, E (1998). “Wave resonances in systems with discrete spectra”. In: *AMERICAN MATHEMATICAL SOCIETY TRANSLATIONS*, pp. 95–130.

— (2010). *Nonlinear resonance analysis: theory, computation, applications*. Cambridge University Press.

Kartashova, E and G Mayrhofer (2007). “Cluster formation in mesoscopic systems”. In: *Physica A: Statistical Mechanics and its Applications* 385.2, pp. 527–542.

Kartashova, E, S Nazarenko, and O Rudenko (2008). “Resonant interactions of nonlinear water waves in a finite basin”. In: *Physical Review E* 78.1, p. 016304.

Kartashova, EA (1990). “Partitioning of ensembles of weakly interacting dispersing waves in resonators into disjoint classes”. In: *Physica D: Nonlinear Phenomena* 46.1, pp. 43–56.

Kaup, DJ, A Reiman, and A Bers (1979). “Space-time evolution of nonlinear three-wave interactions. I. Interaction in a homogeneous medium”. In: *Reviews of Modern Physics* 51.2, p. 275.

Korteweg, DJ and G De Vries (1895). “XLI. On the change of form of long waves advancing in a rectangular canal, and on a new type of long stationary waves”. In: *The London, Edinburgh, and Dublin Philosophical Magazine and Journal of Science* 39.240, pp. 422–443.

Lelong, M-P and JJ Riley (1991). “Internal wave—vortical mode interactions in strongly stratified flows”. In: *Journal of Fluid Mechanics* 232, pp. 1–19.

Lighthill, MJ (1965). “Contributions to the theory of waves in non-linear dispersive systems”. In: *IMA Journal of Applied Mathematics* 1.3, pp. 269–306.

Longuet-Higgins, MS and ND Smith (1966). “An experiment on third-order resonant wave interactions”. In: *Journal of Fluid Mechanics* 25.03, pp. 417–435.

McComas, CH and FP Bretherton (1977). “Resonant interaction of oceanic internal waves”. In: *Journal of Geophysical Research* 82.9, pp. 1397–1412.

McGoldrick, LF (1965). “Resonant interactions among capillary-gravity waves”. In: *Journal of Fluid Mechanics* 21.02, pp. 305–331.

McGoldrick, LF et al. (1966). “Measurements of third-order resonant wave interactions”. In: *Journal of Fluid Mechanics* 25.3, pp. 437–456.

Miura, RM, CS Gardner, and MD Kruskal (1968). “Korteweg-de Vries equation and generalizations. II. Existence of conservation laws and constants of motion”. In: *Journal of Mathematical physics* 9.8, pp. 1204–1209.

Moler, C and C Van Loan (2003). “Nineteen dubious ways to compute the exponential of a matrix, twenty-five years later”. In: *SIAM review* 45.1, pp. 3–49.

Morrison, PJ (1998). “Hamiltonian description of the ideal fluid”. In: *Reviews of modern physics* 70.2, p. 467.

Müller, P (1995). “Ertel’s potential vorticity theorem in physical oceanography”. In: *Reviews of Geophysics* 33.1, pp. 67–97.

Nazarenko, S (2011). *Wave turbulence*. Vol. 825. Springer Science & Business Media.

Newell, AC (1968). “The closure problem in a system of random gravity waves”. In: *Reviews of Geophysics* 6.1, pp. 1–31.

— (1969). “Rossby wave packet interactions”. In: *Journal of Fluid Mechanics* 35.02, pp. 255–271.

Owen, A, R Grimshaw, and B Wingate (2018). “Fast and slow resonant triads in the two layer rotating shallow water equations”. In: *arXiv preprint arXiv:1803.01736*.

Peddle, A (2018). “Components of Nonlinear Oscillation and Optimal Averaging for Stiff PDEs”. In:

Peierls, R (1929). “Zur kinetischen theorie der wärmeleitung in kristallen”. In: *Annalen der Physik* 395.8, pp. 1055–1101.

Phillips, OM (1960). “On the dynamics of unsteady gravity waves of finite amplitude Part 1. The elementary interactions”. In: *Journal of Fluid Mechanics* 9.02, pp. 193–217.

— (1981). “Wave interactions-the evolution of an idea”. In: *Journal of Fluid Mechanics* 106, pp. 215–227.

Rees, EL (1922). “Graphical discussion of the roots of a quartic equation”. In: *The American Mathematical Monthly* 29.2, pp. 51–55.

Reznik, GM, V Zeitlin, and M Ben Jelloul (2001). “Nonlinear theory of geostrophic adjustment. Part 1. Rotating shallow-water model”. In: *Journal of Fluid Mechanics* 445, pp. 93–120.

Ripa, P (1981). “On the theory of nonlinear wave-wave interactions among geophysical waves”. In: *Journal of Fluid Mechanics* 103, pp. 87–115.

Rossby, CG (1939a). “Planetary flow patterns in the atmosphere”. In: *Quart. J. Roy. Met. Soc* 66, p. 68.

— (1939b). “Relation between variations in the intensity of the zonal circulation of the atmosphere and the displacements of the semi-permanent centers of action”. In: *J. Marine Res.* 2, pp. 38–55.

Russell, JS (1845). *Report on Waves: Made to the Meetings of the British Association in 1842-43*.

Salmon, R (1998). *Lectures on geophysical fluid dynamics*. Oxford University Press.

Schochet, S (1994). “Fast singular limits of hyperbolic PDEs”. In: *Journal of differential equations* 114.2, pp. 476–512.

Shabat, A and V Zakharov (1972). “Exact theory of two-dimensional self-focusing and one-dimensional self-modulation of waves in nonlinear media”. In: *Soviet physics JETP* 34.1, p. 62.

Shepherd, Theodore G (1990). “Symmetries, conservation laws, and Hamiltonian structure in geophysical fluid dynamics”. In: *Advances in Geophysics*. Vol. 32. Elsevier, pp. 287–338.

Smith, LM and Y Lee (2005). “On near resonances and symmetry breaking in forced rotating flows at moderate Rossby number”. In: *Journal of Fluid Mechanics* 535, pp. 111–142.

Smith, LM and F Waleffe (1999). “Transfer of energy to two-dimensional large scales in forced, rotating three-dimensional turbulence”. In: *Physics of fluids* 11.6, pp. 1608–1622.

Stokes, GG (1847). “GG Stokes, On the theory of oscillatory waves, Camb. Trans. 8, 441 (1847); see also”. In: *Camb. Trans.* 8, p. 441.

— (1880). “On the theory of oscillatory waves”. In: *Transactions of the Cambridge Philosophical Society*.

Thomas, J (2016). “Resonant fast–slow interactions and breakdown of quasi-geostrophy in rotating shallow water”. In: *Journal of Fluid Mechanics* 788, pp. 492–520.

Thorpe, SA (1966). “On wave interactions in a stratified fluid”. In: *Journal of Fluid Mechanics* 24.4, pp. 737–751.

Vallis, GK (2006). *Atmospheric and oceanic fluid dynamics: fundamentals and large-scale circulation*. Cambridge University Press.

Vanneste, J (2007). *Wave Interactions in Nonlinear waves in fluids: recent advances and modern applications*. Vol. 483. Springer Science & Business Media.

Vanneste, J and F Vial (1994). “On the nonlinear interactions of geophysical waves in shear flows”. In: *Geophysical & Astrophysical Fluid Dynamics* 78.1-4, pp. 115–141.

Ward, ML and WK Dewar (2010). “Scattering of gravity waves by potential vorticity in a shallow-water fluid”. In: *Journal of Fluid Mechanics* 663, pp. 478–506.

Warn, T (1986). “Statistical mechanical equilibria of the shallow water equations”. In: *Tellus A* 38.1.

Whitham, GB (1965). “Non-linear dispersive waves”. In: *Proceedings of the Royal Society of London A: Mathematical, Physical and Engineering Sciences*. Vol. 283. 1393. The Royal Society, pp. 238–261.

— (1974). “Linear and nonlinear waves”. In:

Zabusky, NJ and MD Kruskal (1965). “Interaction of” solitons” in a collisionless plasma and the recurrence of initial states”. In: *Physical review letters* 15.6, p. 240.

Zakharov, VE (1967). “The instability of waves in nonlinear dispersive media”. In: *Sov. Phys. JETP* 24.4, pp. 740–744.

— (1968). “Stability of periodic waves of finite amplitude on the surface of a deep fluid”. In: *Journal of Applied Mechanics and Technical Physics* 9.2, pp. 190–194.

Zakharov, VE and SV Manakov (1976). “The theory of resonance interaction of wave packets in nonlinear media”. In: *Soviet Journal of Experimental and Theoretical Physics* 42, p. 842.

Zakharov, VE and LA Ostrovsky (2009). “Modulation instability: the beginning”. In: *Physica D: Nonlinear Phenomena* 238.5, pp. 540–548.

Zeitlin, V (2013). “Resonant excitation of coastal Kelvin waves in the two-layer rotating shallow water model”. In: *Nonlinear Processes in Geophysics* 20.6, pp. 993–999.

Zeitlin, V, GM Reznik, and M Ben Jelloul (2003). “Nonlinear theory of geostrophic adjustment. Part 2. Two-layer and continuously stratified primitive equations”. In: *Journal of Fluid Mechanics* 491, pp. 207–228.

Ziman, JM (1960). *Electrons and phonons: the theory of transport phenomena in solids*. Oxford university press.